The development of targeting nanosystems for the treatment of glioblastoma and neuroblastoma tumours

by

Taahirah Boltman

UNIVERSITY *of the* **WESTERN CAPE**

A thesis submitted in fulfilment of the requirements for the degree
Doctor of Philosophy (PhD)

Department of Medical Biosciences
Faculty of Natural Sciences
University of the Western Cape

Supervisor: Professor Okobi Ekpo
Co-Supervisor: Professor Mervin Meyer

September 2022

ABSTRACT

Chlorotoxin (CTX) peptide selectively targets glioblastoma multiforme (GB) and neuroblastoma (NB) and has excellent blood-brain barrier permeability. Therefore, CTX is a promising targeting molecule for nanoparticle (NP) based diagnostic and therapeutic applications. Bimetallic gold-platinum nanoparticles (AuPtNPs) have recently attracted great attention for anti-cancer and catalysis applications due to the synergistic effects of combined metal atoms which enhance NP properties when compared to their monometallic NP counterparts. Therefore, the aim of this study was to develop gold NPs (AuNPs) and AuPtNPs, both conjugated to CTX for treatment in GB and NB cancer cells *in vitro*.

This was achieved by synthesizing two novel CTX-NPs through the preparation of citrate capped AuNPs and AuPtNPs which was modified using two different types of polyethylene glycol (PEG) molecules, which allowed for conjugation of CTX onto the NPs. The physicochemical properties of the NPs were characterized, and ultraviolet-visible absorbance spectroscopy analysis demonstrated an increase in the absorption maxima (λ max) of all AuNPs, while the absence of an λ max for all AuPtNPs confirmed the formation of bimetallic NPs. Dynamic light scattering analysis for both citrate capped NPs showed a hydrodynamic size of approximately 7 nm, which doubled after surface functionalization with PEG and slightly increased following CTX surface functionalization. The zeta-potential revealed highly stable citrate NPs and decreased to more neutral charges following PEG and CTX surface functionalization confirming surface modification of NPs which was further supported by fourier transform infra-red spectroscopy analysis. Transmission electron microscopy (TEM) measurements revealed roughly spherical and monodispersed NPs with a core size of approximately 5 nm for all NPs. NPs were stable in biological media over 48-hours and CTX-NPs demonstrated binding and uptake to U87 human GB and SH-SY5Y human NB cancer cell lines.

NP-induced toxicity was investigated using the WST-1 cell viability assay at concentrations of 75-300 µg/ml for 48 hours in U87 and SH-SY5Y cells, while the non-cancerous KMST-6 human fibroblast cells served as a control cell line. The maximal inhibitory concentrations (IC_{50} values) for all NPs in U87 and SH-SY-5Y cells was generally similar, however the most promising results was revealed in U87 cells with CTX-AuPtNPs treatment and was further

investigated and showed the induction of apoptosis (using the APOPercentage™ apoptosis assay), the production of reactive oxygen species (using the CM-H$_2$DCFDA probe), and decrease in mitochondrial activity (using the Tetramethylrhodamine ethyl ester, perchlorate probe) using flow cytometry. KMST-6 cell line highlighted selective toxicity towards the cancerous cell lines. CTX-NPs demonstrated significant decrease in cell survival through the inhibition of colony formation (using clonogenic assay) and inhibitory effects on cell migration (using wound healing assay) in U87 cell line. Gene expression analysis using real-time polymerase chain reaction (using the Human Molecular Toxicology Pathway RT² PCR Array) for investigating early cytotoxic effects of CTX-AuPtNPs, showed that genes involved in cellular stress responses were more significant, suggesting that U87 cells activated cytoprotective responses.

In addition to the anti-cancer applications, AuPtNPs successfully reduced the 4-nitrophenol to 4-aminophenol at a catalytic rate constant (k_{cat}) of 3.2 x 10^{-3}/sec, demonstrating potential applications in catalysis.

KEYWORDS:

Chlorotoxin (CTX)

Chlorotoxin gold nanoparticles (CTX-AuNPs)

Chlorotoxin gold platinum nanoparticles (CTX-AuPtNPs)

Glioblastoma multiforme (GB)

Gold platinum nanoparticles (AuPtNPs)

Nanoparticles (NPs)

Neuroblastoma (NB)

DECLARATION

I, <u>Taahirah Boltman</u>, declare that "The development of targeting nanosystems for the treatment of glioblastoma and neuroblastoma tumours" is my own work that has not been submitted for any degree or examination in any other university and that all the resources I have used or quoted have been indicated and acknowledged by means of references.

UNIVERSITY *of the*
WESTERN CAPE

Signature..

Date...........23-09-2022..................

ACKNOWLEDGMENTS

DEDICATION

For my dearest family...

"If we can reduce the cost and improve the quality of medical technology through advances in nanotechnology, we can more widely address the medical conditions that are prevalent and reduce the level of human suffering"-Ralph Merkle (Turney, 2008)

v

LIST OF CONFERENCES

- Authors: **Boltman, T.**, Ekpo, O. and Meyer, M. Title: "Preliminary investigation of metallic nanosystems against glioblastoma and neuroblastoma cell lines" at The International Conference On Nanomedicine And Nanobiotechnology 2018 (ICONAN-2018), Rome, Italy-September 2018.

UNIVERSITY *of the* WESTERN CAPE

LIST OF ABBREVIATIONS

AuNPs	Gold nanoparticles
AuPtNPs	Gold platinum nanoparticles
BBB	Blood brain barrier
Biotin-CTX	Biotinylated-chlorotoxin
BMNPs	Bimetallic nanoparticles
ClC-3	Chloride channel 3
CTX	Chlorotoxin
CTX-AuNPs	Chlorotoxin gold nanoparticles
CTX-AuPtNPs	Chlorotoxin gold platinum nanoparticles
DEGs	Differentially expressed genes
DLS	Dynamic light scattering
DMEM	Dulbecco's modified eagle medium
EDX	Energy dispersive X-ray spectra
FBS	Foetal bovine serum
Fcc	Face centred cubic
FITC	Fluorescein isothiocyanate
FIT-CTX	Fluorescein isothiocyanate chlorotoxin
FTIR	Fourier transform infra-red spectroscopy
GB	Glioblastoma
GCC	Glioma-specific chloride channel
TEM	Transmission Electron Microscopy
KMST-6	Human Immortalized fibroblast cell line
MMP-2	Matrix metalloproteinase-2
MNPs	Metallic nanoparticles

NB	Neuroblastoma
NPs	Nanoparticles
PEG	Poly(ethylene glycol)
PEG-AuNPs	Poly(ethylene glycol) gold nanoparticles
PEG-AuPtNPs	Poly(ethylene glycol) gold platinum nanoparticles
PEG-Biotin	poly(ethylene glycol)- Biotin
PEG-OH	poly(ethylene glycol)- Hydroxyl
PDI	Polydispersity index
PTT	Photothermal therapy
ROS	Reactive oxygen species
SAED	Selected area electron diffraction
SEM	Standard error of means
SD	Standard deviation
SH-SY5Y	Human neuroblastoma cell line
StrepA	Streptavidin
TEM	Transmission Electron Microscopy
TMRE	Tetramethylrhodamine, ethyl ester
U87	Human malignant glioblastoma cell line
UV-Vis	UV-Vis absorbance example
WST-1	Water Soluble Tetrazolium-1
Z-average	Average size distribution by intensity
ζ-potential	Zeta potential

LIST OF FIGURES

x

LIST OF TABLES

Table 3. Table 3. Summary of the catalytic rate constants (k_{cat}) obtained from AuPtNPs from the current work compared to k_{cat} of similar studies reported in literature

TABLE OF CONTENTS

CHAPTER ONE: INTRODUCTION

CHAPTER TWO: Diagnostic and therapeutic approaches for glioblastoma and neuroblastoma cancers using chlorotoxin nanoparticles

.

CHAPTER THREE: The synthesis and characterization of chlorotoxin functionalised metallic nanoparticles

CHAPTER FOUR: The toxicity and anti-cancer properties of chlorotoxin peptide-functionalized gold and gold platinum nanoparticles in neuroblastoma and glioblastoma cells

CHAPTER FIVE: Investigating the early cytotoxic molecular effects of chlorotoxin functionalized bimetallic gold platinum nanoparticles in U87 human glioblastoma cells

CHAPTER SIX: Catalytic reduction of 4-nitrophenol to 4-aminophenol with bimetallic gold platinum nanoparticles

CHAPTER SEVEN: CONCLUSION

CHAPTER ONE: INTRODUCTION

1.1. Background

Cancer remains the leading cause of death and shortened life-expectancy worldwide, imposing a significant socio and economic burden on societies (Sung *et al.*, 2021). While major advancements have been made in the diagnosis and treatment of numerous prominent cancers, less attention is directed towards rare cancers such as tumours of the nervous system (NS). These tumours are some of the most aggressive cancers occurring in both children and adults.

Glioblastoma (GB), also known as glioblastoma multiforme, is the most aggressive and devastating primary brain tumours diagnosed in adults, with a median survival time predicted at 12-15 months and a 5-year survival rate of less than 7 % (Miller *et al.*, 2021; Wu *et al.*, 2021). GB are characterized by highly heterogeneous cytogenetic nature of cells which infiltrate deep within the brain parenchyma obscuring the complete surgical removal of the tumour and tumour relapse is therefore unavoidable (Bastiancich, Da Silva and Estève, 2021). Neuroblastoma (NB) are the most frequently occurring childhood cancers of the sympathetic NS and presents a challenge in paediatric oncology as the five-year survival rate for patients presenting with high-risk NB tumours is still below 40 % (Smith and Foster, 2018). Standard treatment for both these NS tumours consists of maximal surgical resection, followed by chemotherapy and radiation therapy, which is plagued with systemic toxicity causing adverse side effects (Stupp *et al.*, 2017; Tan *et al.*, 2020).

The current first-line of chemotherapeutic treatment for GB is temozolomide (TMZ) (Tan *et al.*, 2020). TMZ is employed because it is one of the few chemotherapeutic drugs that can permeate the blood brain barrier (BBB), however TMZ induces damage to hematopoietic stem cells in patients resulting in dose-limiting haematological toxicity (Sawai *et al.*, 2001). Additionally, TMZ is weakly soluble under physiological conditions and is involved in rapid hydrolysis that further limits its antitumor efficacy (Fang *et al.*, 2015). Chemotherapy and radiation side effects on the brain include loss of physical ability and cognitive decline (Ahles, 2012; Lawrie *et al.*, 2018). Many patients with metastatic tumours eventually develop drug resistance as is often observed in GB and NB patients. NB cells are prone to spread and invade to other tissues such as bone marrow, lymph nodes, skin, lung, liver and central nervous system (Stupp *et al*., 2017). More than half of children diagnosed with

https://etd.uwc.ac.za/

high-risk NB will either not respond to standard treatments or relapse after treatment (Smith and Foster, 2018). Some of the adverse side effects as a result of high-dose chemotherapy experienced by children, include renal toxicity, cardiotoxicity and toxicity to reproductive organs which may affect fertility later in life (Emadi, Jones and Brodsky, 2009; Schacht, Talaska and Rybak, 2012). The long-term toxic side effects include cognitive deficits, epilepsy, growth reduction, thyroid function disorders, learning difficulties and an increased risk of developing secondary cancers in survivors of high-risk NB (Applebaum *et al.*, 2017; Speckhart, Antony and Fernandez, 2017). Although improvements have been achieved in the management of NB, the overall cure rate for high-risk patients is still 50 % (Smith and Foster, 2018).

The blood-brain barrier (BBB) is considered the brain's first line of defence from harmful substances in the blood stream. The arrangement of capillary endothelial cells held together by complex tight junction proteins, surrounding pericytes, the basal membrane and astrocytic endfeet all contribute to the highly selective nature of the BBB (Castro Dias *et al.*, 2019). This barrier is approximately 200 nm thick and only allow molecules with a mass lower than 400–600 Da and hydrophilic molecules with a mass lower than 150 Da across via passive diffusion (Pardridge, 2012). Most molecules cannot cross the BBB due to these factors, rendering the vast majority of chemotherapeutics and targeted agents ineffective (Angeli *et al.*, 2019). In addition, capillary endothelial cells are known to have a high concentration of drug efflux transporter proteins such as P-glycoprotein (P-gp) and multidrug resistance-associated proteins which further prevent therapeutic agents into the brain (Calatozzolo *et al.*, 2005). Depending on the grade classification, GB may disrupt the integrity of the blood brain barrier (BBB) but peripheral areas of brain tumours have regions with an intact BBB causing formation of favourable niches of cancer cell invasion and treatment resistance (Dong, 2018). When tumour cells reach a specific size, the BBB is damaged. This causes the formation of the blood-brain tumour barrier (BBTB) through new blood vessels (brain tumour capillary) and is distinct from the BBB (Arvanitis, Ferraro and Jain, 2020). BBTB permeability in GBs is high in bulk tumour areas, but less in peripheral regions (Dong, 2018). Thus, the combination of the BBB and the BBTB presents unique challenges in effective drug delivery to brain tumour sites.

Tumour migration and invasion adds to the failure of many treatment options for these tumours (Welch and Hurst, 2019). Numerous studies propose that tumorigenesis is associated with the expression or increased expression of certain cell surface proteins in cancer cells. Matrix

metalloproteinases (MMPs) are a family of secreted, zinc-dependent endopeptidases that have functions in tissue-remodelling processes, including embryo implantation, wound healing, tumour invasion, metastasis, and angiogenesis (Visse and Nagase 2003; Latifi *et al.*, 2018; Quintero-Fabián *et al.*, 2019; Tardáguila-García *et al.*, 2019; Cabral-Pacheco *et al.*, 2020). During the development of tumours, the activation of MMPs promotes tumour invasion and metastasis through the degradation of the basement membrane and either invasion into surrounding tissue or intravasation through endothelial cells into the blood stream (Stamenkovic, 2000). Thus, MMPs are considered one of the important driving factors in cancer invasion and metastasis (Gonzalez-Avila *et al.*, 2019). The over-expression of matrix metalloproteinase-2 (MMP-2) has been reported as an active contributor for the progression of GB (Guo *et al.*, 2005; Zhou *et al.*, 2019) and NB (Ribatti *et al.*, 2001; Hall *et al.*, 2020) and the level of invasiveness of these tumours can be linked to the increased expression levels of MMP-2 (Ribatti *et al.*, 2001; Yu *et al.*, 2017). In addition to the overexpression of MMP-2 on the cell surface of gliomas, chloride ion channel 3 (ClC-3) has been suggested to affect the invasion and migration of glioma cells by forming protein complexes with MMP-2 (Cheng *et al.*, 2014; Turner and Sontheimer, 2014). Annexin A2 is a calcium-binding cytoskeletal protein that is expressed on the extracellular surface of different cancer cells including GB and NB cells and also plays a role in tumour progression through cell migration and invasion (Chen *et al.*, 2019; Li *et al.*, 2021). Annexin A2 has been reported to increase multi-drug resistance in NB (Wang *et al.*, 2017). These surface proteins are not overexpressed or upregulated in normal cells and therefore provide an alternative method for targeting GB and NB for anti-cancer therapy. One such targeting molecule of great potential for NS tumours is the chlorotoxin (CTX) peptide.

CTX is a 36-amino acid peptide, derived from the venom of the Deathstalker Scorpion (*Leiurus quinquestriatus)* and has been shown to be a promising tumour-targeting ligand owing to its strong affinity for a host of tumours, including GB, NB, medulloblastoma, breast cancer, ovarian cancer, prostate cancer, lung cancer, sarcoma, skin cancer and intestinal cancer (Soroceanu *et al.*, 1998; Lyons, O'Neal and Sontheimer, 2002; Deshane, Garner and Sontheimer, 2003; Veiseh *et al.*, 2007; Kesavan *et al.*, 2010; Kievit *et al.*, 2010; McGonigle *et al.*, 2019; Wang *et al.*, 2019). However, CTX demonstrates the highest binding affinity for gliomas. The formed protein complex of ClC-3 and MMP-2 is targeted by the CTX-peptide and this action is reported to inhibit glioma cell migration and invasion (Deshane, Garner and Sontheimer, 2003; Lui *et al.*, 2010; Cheng *et al.*, 2014; Qin *et al.*, 2014). CTX has also been shown to bind to Annexin A2 in various cancer cell lines including glioma

3

cells (Kesavan *et al.*, 2010; Wang, Luo and Guo, 2013). Additionally, CTX has been observed to permeate the intact BBB in both animal models and humans with brain tumours, with no reported toxicity to healthy cells (Ojeda, Wang and Craik, 2016; Khanyile *et al.*, 2019). Therefore, the CTX peptide has been widely investigated as a favourable targeting molecule in recent years in the development of improved diagnostic and therapeutic applications primarily for GB tumours but holds promise for other types of tumours such as NB (Kievit *et al.*, 2010; Dardevet *et al.*, 2015; Ojeda, Wang and Craik, 2016; Khanyile *et al.*, 2019).

Given the advancement of nanotechnology for biomedical applications, nanoparticles (NPs) are attractive for the development of precise targeting based diagnostic and therapeutic platforms for cancer. Due to extensive abnormal angiogenesis in the vicinity of tumours, NPs (1-100 nm) have the ability to exit blood vessels and accumulate within tumours through processes referred to as the enhanced permeability and retention effect and this is exploited for passive targeting of NPs to tumours (Prabhakar *et al.*, 2013). While NPs of sizes ranging from 5-200 nm in diameter have been reported to penetrate the BBB, NPs less than 15 nm may cross the BBB through the transmembrane or the paracellular pathway even more readily (Sokolova *et al.*, 2020). Surface functionalization of NPs with the synthetic molecule, polyethylene glycol (PEG), or "PEGylation", is a commonly used approach to improve NP stability which prevents NP aggregation, opsonization and phagocytosis, which all contribute to improved biocompatibility and prolong the systemic circulation times of the NPs *in vivo* (Hoang Thi *et al.*, 2020). PEG also enables the attachment of targeting molecules onto the NPs for active targeting through terminal modification with various functional groups (Shi *et al.*, 2021). While the ability of some NPs to penetrate the BBB may be improved through attaching PEG or charged/lipophilic groups (Shakeri *et al.*, 2020; Kahana *et al.*, 2021), the attachment of an active targeting moiety may be even more promising (Rabiei *et al.*, 2020; Wu *et al.*, 2020). In addition to the BBB crossing potential of small NPs, these NPs are also advantageous for active targeting strategies due to their larger surface area which allows for increased surface loading of different targeting and/or therapeutic agents, while also permitting entry through cells and small membrane passageways and increasing drug bioavailability and delivery (Yetisgin *et al.*, 2020). Active targeting strategies using NPs for cancer treatment is possible through surface modification of NPs with targeting molecules which includes antibodies, peptides and aptamers etc. that bind to specific recognition binding sites which could be cell surface proteins that are overexpressed on the surface of cancer cells (Rabiei *et al.*, 2020). This decreases delivery or binding to healthy cells and thereby

4

reduces toxicity to healthy cells and increases the anti-cancer activity in diseased cells specifically, thus addressing systemic toxicity with current cancer treatments, while also protecting and prolonging the circulation times of drugs (Yao *et al.*, 2020).

Gold NPs (AuNPs) remains the most extensively used metal-based NP for biomedical applications based on many favourable characteristics. Their perceived biocompatibility is based on their small size and both their *in vivo* and *in vitro* characteristics (Sani, Cao and Cui, 2021). The types of AuNPs that have been designed and fabricated for anti-cancer applications may act as a multifunctional platform for combinational cancer therapy, especially for a type of hyperthermia treatment called photothermal therapy (PTT). Metallic NPs (MNPs) constructed of noble metals such as gold (AuNPs) and platinum (PtNPs) demonstrate local surface plasmon resonance (SPR) and upon exposure to external sources such as light, these MNPs can absorb photon energy which is then converted into photothermal energy which can be harnessed as a PTT (Kim and Lee, 2018; Norouzi, Khoshgard and Akbarzadeh, 2018; Samadi *et al.*, 2018). Targeted NP-mediated PTT can be an efficient method of inducing localized hyperthermia in diseased cells resulting in the ablation of such cells. Hyperthermia treatments involves the induction of intracellular heat stress (i.e. the localised increase in temperature to between 40-46 ºC) resulting in mitochondrial swelling, protein denaturation, alteration in signal transduction, cellular structure rupturing and induction of necrosis or apoptosis (Rajan and Sahu, 2020). The disadvantages of conventional hyperthermia treatments includes procedures that are invasive, incomplete tumour destruction, low penetration of heat in the tumour region (lesions > 4-5 cm in diameter), excessive heating of surrounding healthy tissues as the treatment is non-specific, thermal under-dosage in the target region and dissipation of heat by blood flow (Chang *et al.*, 2018). AuNPs and PtNPs have been used in both *in vitro* and *in vivo* studies to demonstrate PTT induced thermal cytotoxicity, mostly through exposure to near-infrared (NIR) light (650–950 nm) (Norouzi, Khoshgard and Akbarzadeh, 2018; Samadi *et al.*, 2018; Moros *et al.*, 2020; Rajan and Sahu, 2020). Combining metals to produce bimetallic NPs (BNPs) is a simple way of developing new materials that can produce enhanced technological usefulness when compared to their starting substances (Medina-Cruz *et al.*, 2020). BNPs exhibit a wide range of excellent electronic, chemical, biological, mechanical and thermal properties due to the synergistic effects of combined metal atoms (Sharma *et al.*, 2019). BNPs constructed of Au and Pt metals to produce AuPtNPs have elicited much interest in recent years for improved catalytic performances when compared to monometallic NPs, due to the strong synergistic effects between metals (Zaleska-Medynska *et al.*, 2016). However, these materials

5

have also started to find applications in PTT. Recent studies reported that bimetallic gold platinum NPs (AuPtNPs) of different sizes and shapes may exhibit better PTT and radiation effects than their monometallic AuNPs and PtNPs (Tang *et al.*, 2014; Liu *et al.*, 2017; Song *et al.*, 2017, 2021; Yang *et al.*, 2018; Depciuch *et al.*, 2019; Salado-Leza *et al.*, 2019; Fathima and Mujeeb, 2021).

The widely studied NIR-induced PTT using traditional organic PTT agents is limited to subcutaneous malignant tumours because of the minimal tissue penetration depth (~3 cm depth) and may therefore not be ideal for deep seated brain tumours such as GB (Henderson and Morries, 2015). Here, other applications for NP-mediated hyperthermia treatments such as radiofrequency (RF) ablation is recommended as radio wave energy has been shown to penetrate tissues much deeper (7-17 cm) and may hold promise for the treatment of brain tumours (Röschmann, 1987; Raoof and Curley, 2011). Radio waves are low-frequency electromagnetic waves that have low tissue-specific absorption rate and therefore great whole-body tissue penetration that is considered safe for humans (Raoof and Curley, 2011). While the heating properties of AuNP and PtNPs have been investigated using RF waves, with some demonstrating promising non-invasive RF anti-cancer applications, research using AuPtNPs for this application is still limited (Porcel *et al.*, 2010; Raoof and Curley, 2011; Manikandan, Hasan and Wu, 2013; San, Moh and Kim, 2013; Liu *et al.*, 2015; Nasseri *et al.*, 2016; Chakaravarthi *et al.*, 2019).

Although monometallic NPs such as AuNPs show promise as a therapeutic option for various cancers, there remains a discrepancy between preclinical results and clinical outcomes (Sani, Cao and Cui, 2021). Given that most tumours are known to be heterogeneous in nature, BNPs may be more effective for the management of tumours due to the synergistic effects of the combined metals (Katifelis *et al.*, 2018). Size, shape, concentrations, time, synthesis method, surface functionalization and cell type are factors that influence the cytotoxicity of metallic NPs (Sani, Cao and Cui, 2021). It has been reported that AuPtNPs larger than 30 nm demonstrated no significant toxicity towards various cancer cell lines at low concentrations (Tang *et al.*, 2014; Oladipo *et al.*, 2020). No acute cytotoxicity was observed when AuPtNPs were PEGylated (Liu *et al.*, 2017). However smaller AuPtNPs (< 20 nm) are reported to significantly decrease cell viability and induced cell death through apoptosis in cancer cell lines (Boomi *et al.*, 2019; Chaturvedi *et al.*, 2021). Research describing the use of AuPtNPs for anti-cancer applications is relatively novel, including for the development of treatments for NS tumours. Moreover, the use of AuPtNP for the targeted destruction of NS tumours

using RF ablation has not been described before. This treatment strategy has immense potential for the development of target specific NP-mediated hyperthermia.

1.2.   Problem statement and rationale

Despite the remarkable advances in neuro-oncology, the treatment of GB and NB remains a challenge for clinical oncology and research as it constitutes some of the most challenging types of tumours to treat. Patient mortality due to brain cancers is one of the highest among all cancers, as these types of cancers have complex morphology and are usually resistant to current treatments (Aldape *et al.*, 2019). The current treatment options for advanced stage GB and NB are largely unsatisfactory and there has been little significant improvement in effective therapeutic strategies for these cancers in recent years, as both remain incurable. Treatment remains a challenge due to the rapid growth and the highly infiltrative nature of GB cells that penetrate deep within brain parenchyma, impeding complete surgical resection, therefore tumour relapse is inevitable (King and Benhabbour, 2021).

Chemotherapy and radiotherapy are known to have severe side effects, poor target drug delivery efficiency, drug resistance and the highly selective BBB which impedes the distribution of most drugs at the target site, limiting the available treatment options (King and Benhabbour, 2021). Toxicity as a result of treatments for GB is a serious concern, as it is important to preserve healthy neurons within the brain as these cells lack regenerative capacity (Stone and DeAngelis, 2016). Side effects of chemotherapeutic drugs for children diagnosed with NB are prone to short and long-term toxic side effects with an increased risk of secondary cancers affecting survivors in adulthood (Applebaum *et al.*, 2017). Therefore, these challenges require a unique multidiscplinary approach with the emphasis on the developemnt of novel target specific delivery systems for GB and NB which are cell specific inducing anti-cancer activity within diseased cells only while preserving normal cells and show the potential to cross the BBB.

A variety of sophisticated NPs have been developed and investigated for anti-cancer applications often presenting as multifunctional nano systems with combined targeting, imaging, and therapeutic applications. NPs ranging from 5-200 nm have been reported in literature to cross the BBB, however NPs less than 15 nm in diameter may easily cross the BBB through the transmembrane or the

7

paracellular pathway (Ohta *et al.*, 2020; Sokolova *et al.*, 2020). NPs of 20 nm or less can permeate through capillary walls and filtering organs and NPs in a size range of 3-50 nm or less can be endocytosed by cells (Shang, Nienhaus and Nienhaus, 2014; Foroozandeh and Aziz, 2018). Owing to their very small size, NPs have a very large surface area to volume ratio when compared to bulk material. This characteristic is highly favoured for active targeting strategies due to their larger surface area which allows for increased surface loading of targeting and/or therapeutic agents with the additional advantage of being able to deposit large quantities of drugs at target sites (Yetisgin *et al.*, 2020). Active targeting of NP delivery systems in cancer allows the anti-cancer activity to be specifically directed to cancer cells only, through targeting specific recognition binding sites that are either overexpressed on the surface of cancer cells or expressed at low levels in normal cells. Targeted delivery using NPs avoids toxicity towards normal cells while promoting anti-cancer activity in diseased cells, thus addressing the lack of specificity with current cancer treatments, while also protecting drugs from degradation and increasing the circulation time of drugs (Ali *et al.*, 2021). Active targeting for NPs can occur through conjugating NPs with molecules such as antibodies, peptides, and aptamers. Although monoclonal antibodies (mAbs) are commonly used as targeting molecules for the targeted delivery of NPs, they are also associated with limitations such as their large size and the difficulty in conjugating mAbs to NPs. When compared to antibodies, peptides are more appealing targeting molecules due to advantages such as their smaller size, lower immunogenicity, lower production cost, similar binding affinities to mAbs and easier synthesis and modification routes (Sasikumar and Ramachandra, 2018). In comparison to smaller molecule ligands, peptides are more diverse and show higher specificity, and targeting capabilities (Sasikumar and Ramachandra, 2018). Due to these factors, peptides are usually more widely investigated as targeting agents for NP-based drug delivery development. One such peptide that has generated much interest as a targeting molecule for GB is CTX.

CTX selectively binds to gliomas and other tumours of the neuroectodermal origin without any effect on normal glial cells or neurons (Soroceanu *et al.*, 1998; Lyons, O'Neal and Sontheimer, 2002; McFerrin and Sontheimer, 2006). Molecular targets of CTX such as the overexpressed MMP-2, ClC-3 and Annexin A2 present on the surface of GB and NB cancer cells all participate in cell migration and invasion and therefore provide a different method for targeting and anti-cancer therapy. In addition, CTX has been observed to permeate intact BBBs in both animal models and humans with brain tumours, possibly through Annexin A2 expression in BBB vascular endothelial cells, while

having no effect on normal brain tissues (Kesavan *et al.*, 2010). Therefore, CTX peptide has been widely investigated as a promising targeting molecule in recent years for NS tumours (Deshane, Garner and Sontheimer, 2003; Fu *et al.*, 2012; Dardevet *et al.*, 2015; Ojeda, Wang and Craik, 2016; Khanyile *et al.*, 2019).

To address the challenges associated with NB and GB, the cancer targeting and BBB penetrating properties of CTX can be combined with NPs to develop effective multifunctional cancer targeting nano-systems. In recent years, a variety of different types of CTX-conjugated NPs (CTX-NP) has emerged with imaging and therapeutic functionalities (Cohen-Inbar and Zaaroor, 2016; Ojeda, Wang and Craik, 2016; Khanyile *et al.*, 2019). Currently, CTX covalently attached to fluorescent molecules are on trial and are yielding promising results for real-time guidance during surgical tumour resections (Cohen-Inbar and Zaaroor, 2016; Patil *et al.*, 2019; Yamada *et al.*, 2021). CTX-conjugated NPs reported in literature include iron oxides, liposomes, dendrimers, quantum dots, and rare-earth up-conversion NPs (Sun *et al.*, 2008; Veiseh *et al.*, 2009; Fang *et al.*, 2010; Deng *et al.*, 2014; Zhao, Shi and Zhao, 2015; Khanyile *et al.*, 2019). Few research groups also reported on the synthesis of CTX-conjugated to noble metals such as gold NPs (Locatelli *et al.*, 2014a; Zhao *et al.*, 2019, 2020) and silver NPs (AgNPs) (Locatelli *et al.*, 2012; Locatelli *et al.*, 2014b; Tamborini *et al.*, 2016) for applications in cancer diagnosis and treatment. However, no reports exist for the synthesis of CTX-bimetallic NPs constructed of noble metals such as Au and Pt.

Recently, bimetallic AuPtNPs has generated much interest in anti-cancer applications due to improved features based on the synergistic effects of combined metal atoms in contrast to their monometallic counterparts. AuPtNPs are effective nano-drug carriers for chemotherapeutic drugs and possess significant computed tomography (CT) imaging signal enhancement, which demonstrates their potential for use in image-guided tumour therapy (Liu *et al.*, 2017; Yang *et al.*, 2018; Song *et al.*, 2021; Oladipo *et al.*, 2020). AuPtNPs of different sizes and shapes demonstrated improved PTT and radiation therapy when compared to some of its monometallic counterparts (AuNP and PtNPs) (Tang *et al.*, 2014; Liu *et al.*, 2017; Song *et al.*, 2017, 2021; Yang *et al.*, 2018; Depciuch *et al.*, 2019; Fathima and Mujeeb, 2021). Non-invasive targeted radiofrequency (RF) thermal ablation using NPs may be more effective than NIR PTT for inducing hyperthermia in GB as it can penetrate tumours more deeply located (Raoof and Curley, 2011). AuNP and PtNPs show promise for non-invasive RF anti-cancer thermal therapy but there are no reports on the use of AuPtNPs for this treatment in NS

tumours and should be further investigated as they may prove to be more effective than AuNPs and PtNPs (Porcel *et al.*, 2010; Manikandan, Hasan and Wu, 2013; San, Moh and Kim, 2013). Hyperthermia treatments also have the added benefit of sensitizing cells to other forms of standard therapy, including radiation and chemotherapy having a potential in combination treatments (Oei *et al.*, 2020).

The use of bimetallic NPs as multi-functional nano-systems has recently gained momentum in cancer nanotechnology research but has not been fully exploited for brain and other NS tumours. Therefore, combining the cancer targeting and BBB penetrating properties of CTX with AuNP and AuPtNPs that can be used for RF-induced targeted NP hyperthermia may contribute to novel nano-systems for effective management of GB and NB tumours and address the major concerns of current treatments. Furthermore, CTX is known to bind to a broad list of cancer cell lines and therefore this approach could be further expanded and investigated for other tumours (Zhao, Shi and Zhao, 2015).

1.3.   Hypothesis

We hypothesized that CTX-AuNPs and CTX-AuPtNPs will demonstrate target specific uptake by the cancerous U87 human GB cells and SH-SY5Y human NB cells more efficiently than the non-cancerous KMST-6 human fibroblast cells. This is expected since CTX targets MMP-2, ClC-3 and Annexin A2, which is overexpressed in U87 and SH-SY5Y cells. These NPs, CTX-AuPtNPs in particular, can be activated by RF waves to induce hyperthermia treatment through non-invasive RF targeted hyperthermia of cancer cells. The target specific delivery of CTX-AuNPs and CTX-AuPtNPs will enhance the thermal ablation to cells that overexpress the targets of CTX.

1.4.   Research aims and objectives

The principle aim of this study was to develop two novel CTX- NPs for targeting GB and NB cancer cells and investigate their anti-cancer effects through *in vitro* studies. The CTX-NPs are designed for the potential use for future non-invasive RF targeted thermal therapy.

The aim was achieved through the following objectives:

1) The optimization of NP synthesis:

1.1) Synthesis of sub 10 nm citrate capped metallic nanoparticles (MNPs): Gold nanoparticles (AuNPs) and bimetallic gold platinum nanoparticles (AuPtNPs)

1.2) PEGylation with a ratio of two types of polyethylene glycol (PEG) molecules with different terminal ends, PEG-biotin and PEG-OH in order to produce PEG-AuNPs and PEG-AuPtNP

1.3) Biofunctionalization with streptavidin and biomolecular immobilization of CTX onto PEG-AuNPs and PEG-AuPtNP to produce CTX-AuNPs and CTX-AuPtNPs, respectively

2) Physiochemical characterization of synthesised NPs using ultraviolet-visible spectroscopy (UV-Vis), dynamic light scattering (DLS) analysis, transmission electron microscopy (TEM), selected area electron diffraction (SAED) pattern analysis, energy-dispersive X-ray spectroscopy (EDX) and fourier-transform infrared spectroscopy (FTIR)

3) Evaluating the stability of NPs in growth media and the targeting, *in vitro* binding of CTX and uptake of NPs in U87 human GB cell line and SH-SY5Y human NB cell line

4) *In vitro* investigation of the effects of all NPs on the cell viability of U87, SH-SY5Y and non-cancerous KMST-6 cells. The evaluation of CTX-NPs on cell survival and anti-migratory properties in U87 cells

5) Investigation of the mechanisms involved in CTX-AuPtNPs induced cell death in U87 human cells by assessing the induction of apoptosis, oxidative stress and mitochondrial depolarization.

6) Investigation of the early cytotoxic effects of CTX-AuPtNPs in U87 human cells using gene expression analysis.

11

7) The investigation of the catalytic activity of AuPtNPs by assessing the reduction of 4-nitrophenol to 4-aminophenol using aqueous NaBH₄.

1.5. Thesis outline

The thesis is divided into 7 chapters, each results chapter is presented as a research paper while the literature review is presented as a review article. Chapter 1 is an overall introduction to the scope of the study, hypothesis, research aims and objectives. Chapter 2 is a literature review paper tilted '*Diagnostic and therapeutic approaches for glioblastoma and neuroblastoma cancers using chlorotoxin nanoparticles*' and provides an extensive and updated review on the use of CTX-NPs for the diagnosis and treatment of GB, highlighting the challenges associated with GB and NB and presenting CTX as promising targeting peptide for both cancers. This chapter also offer some areas where CTX-NPs may be implemented in developing novel CTX-based diagnostic and therapeutic applications for both GB and NB. Chapters 3, titled '*The synthesis and characterization of chlorotoxin functionalised metallic nanoparticles*' describes the synthesis and characterization of two novel different metallic CTX functionalized NPs (CTX-AuNP and CTX-AuPtNP) and the stability testing of these NPs. This chapter also demonstrates CTX binding to U87 and SH-SY5Y cell lines known to express molecular targets of interest and shows uptake of NPs by the cells. Chapter 4 titled '*The toxicity and anti-cancer properties of chlorotoxin peptide-functionalized gold and gold platinum nanoparticles in neuroblastoma and glioblastoma cells*' presents the investigation of both CTX-functionalized nanoparticles in U87, SH-SY5Y and KMST-6 cell lines by investigating cytotoxicity, cell survival and anti-migratory effects of the NPs. This chapter also reports on the effects of CTX-AuPtNPs on the induction of apoptosis, oxidative stress and mitochondrial depolarization in U87 cells treated with the established half maximal inhibitory concentration (IC₅₀) values. Chapter 5 titled '*Investigating the early cytotoxic molecular effects of chlorotoxin functionalized bimetallic gold platinum nanoparticles in U87 human glioblastoma cells*' describes an investigation into the early cytotoxicity effects of CTX-AuPtNPs in U87 cells by analysing the impact of CTX-AuPtNP-treatment on the expression of 86 genes that are known to be involved in cytotoxicity. Chapter 6 deviates away from the main theme of the thesis and is tilted '*Catalytic reduction of 4-nitrophenol to 4-aminophenol with bimetallic gold platinum nanoparticles*'. This chapter demonstrates the catalytic

12

properties of AuPtNPs. Finally, Chapter 7 includes the general conclusions that summarizes the main findings found in each research chapter and provides brief recommendations for future work.

1.6. References

Ahles, T.A. (2012). Brain Vulnerability to Chemotherapy Toxicities. *Psycho-oncology*, 21(11): 1141–1148.

Aldape, K., Brindle, K.M., Chesler, L., Chopra, R., Gajjar, A., Gilbert, M.R., Gottardo, N., Gutmann, D.H., Hargrave, D., Holland, E.C., Jones, D.T.W., Joyce, J.A., Kearns, P., Kieran, M.W., Mellinghoff, I.K., Merchant, M., Pfister, S.M., Pollard, S.M., Ramaswamy, V., Rich, J.N., Robinson, G.W., Rowitch, D.H., Sampson, J.H., Taylor, M.D., Workman, P. and Gilbertson, R.J.(2019). Challenges to curing primary brain tumours. *Nature Reviews Clinical Oncology*, 16(8): 509–520.

Ali, E.S., Sharker, S.M., Islam, M.T., Khan, I.N., Shaw, S., Rahman, M.A., Uddin, S.J., Shill, M.C., Rehman, S., Das, N., Ahmad, S., Shilpi, J.A., Tripathi, S., Mishra, S.K. and Mubarak, M.S. (2021). Targeting cancer cells with nanotherapeutics and nanodiagnostics: Current status and future perspectives. *Seminars in cancer biology*, 69: 52–68.

Angeli, E., Nguyen, T.T., Janin, A. and Bousquet, G. (2019). How to Make Anticancer Drugs Cross the Blood–Brain Barrier to Treat Brain Metastases. *International Journal of Molecular Sciences*, 21(1): 22.

Applebaum, M.A., Vaksman, Z., Lee, S.M., Hungate, E.A., Henderson, T.O., London, W.B., Pinto, N., Volchenboum, S.L., Park, J.R., Naranjo, A., Hero, B., Pearson, A.D., Stranger, B.E., Cohn, S.L. and Diskin, S.J. (2017). Neuroblastoma survivors are at increased risk for second malignancies: A report from the International Neuroblastoma Risk Group Project. *European Journal of Cancer*, 72: 177–185.

Arvanitis, C.D., Ferraro, G.B. and Jain, R.K. (2020). The blood-brain barrier and blood-tumour barrier in brain tumours and metastases. *Nature Reviews. Cancer*, 20(1): 26–41.

Bastiancich, C., Da Silva, A. and Estève, M.-A. (2021). Photothermal Therapy for the Treatment of Glioblastoma: Potential and Preclinical Challenges. *Frontiers in Oncology*, 10: 610356.

Boomi, P., Poorani, G.P., Palanisamy, S., Selvam, S., Ramanathan, G., Ravikumar, S., Barabadi, H., Prabu, H.G., Jeyakanthan, J. and Saravanan, M. (2019). Evaluation of Antibacterial and Anticancer Potential of Polyaniline-Bimetal Nanocomposites Synthesized from Chemical Reduction Method. *Journal of Cluster Science*, 30(3): 715–726.

Cabral-Pacheco, G.A., Garza-Veloz, I., Castruita-De la Rosa, C., Ramirez-Acuña, J.M., Perez-Romero, B.A., Guerrero-Rodriguez, J.F., Martinez-Avila, N. and Martinez-Fierro, M.L. (2020). The Roles of Matrix Metalloproteinases and Their Inhibitors in Human Diseases. *International Journal of Molecular Sciences*, 21(24): 9739.

Calatozzolo, C., Gelati, M., Ciusani, E., Sciacca, F.L., Pollo, B., Cajola, L., Marras, C., Silvani, A., Vitellaro-Zuccarello, L., Croci, D., Boiardi, A. and Salmaggi, A. (2005). Expression of drug resistance proteins Pgp, MRP1, MRP3, MRP5 and GST-pi in human glioma. *Journal of Neuro-Oncology*, 74(2): 113–121.

Castro Dias, M., Mapunda, J.A., Vladymyrov, M. and Engelhardt, B. (2019). Structure and Junctional Complexes of Endothelial, Epithelial and Glial Brain Barriers. *International Journal of Molecular Sciences*, 20(21): E5372.

Chakaravarthi, G., Narasimhan, A.K., Ramachandra Rao, M.S. and Arunachalam, K. (2019). Influence of Gold Nanoparticles (GNPs) on Radiofrequency Tissue Heating, in: 2019 URSI Asia-Pacific Radio Science Conference (AP-RASC). *Presented at the 2019 URSI Asia-Pacific Radio Science Conference (AP-RASC),* 1–3.

Chang, D., Lim, M., Goos, J.A.C.M., Qiao, R., Ng, Y.Y., Mansfeld, F.M., Jackson, M., Davis, T.P. and Kavallaris, M. (2018). Biologically Targeted Magnetic Hyperthermia: Potential and Limitations. *Frontiers in Pharmacology*, 9: 831.

Chaturvedi, V.K., Yadav, N., Rai, N.K., Bohara, R.A., Rai, S.N., Aleya, L. and Singh, M.P. (2021). Two birds with one stone: oyster mushroom mediated bimetallic Au-Pt nanoparticles for agro-waste management and anticancer activity. *Environmental Science and Pollution Research International*, 28(11): 13761–13775.

Chen, L., Lin, L., Xian, N. and Zheng, Z. (2019). Annexin A2 regulates glioma cell proliferation through the STAT3-cyclin D1 pathway. *Oncology Reports*, 42(1): 399–413.

Cheng, Y., Zhao, J., Qiao, W. and Chen, K. (2014). Recent advances in diagnosis and treatment of gliomas using chlorotoxin-based bioconjugates. *American Journal of Nuclear Medicine and Molecular Imaging*, 4(5): 385–405.

Cohen-Inbar, O. and Zaaroor, M. (2016). Glioblastoma multiforme targeted therapy: The Chlorotoxin story. *Journal of Clinical Neuroscience: Official Journal of the Neurosurgical Society of Australasia*, 33: 52–58.

Dardevet, L., Rani, D., Abd El Aziz, T., Bazin, I., Sabatier, J.-M., Fadl, M., Brambilla, E. and De Waard, M. (2015). Chlorotoxin: A Helpful Natural Scorpion Peptide to Diagnose Glioma and Fight Tumor Invasion. *Toxins*, 7(4): 1079–1101.

Deng, Y., Wang, H., Gu, W., Li, S., Xiao, N., Shao, C., Xu, Q. and Ye, L. (2014). Ho3+ doped NaGdF4 nanoparticles as MRI/optical probes for brain glioma imaging. *Journal of Materials Chemistry B*, 2(11): 1521–1529.

Depciuch, J., Stec, M., Klebowski, B., Baran, J. and Parlinska-Wojtan, M. (2019). Platinum–gold nanoraspberries as effective photosensitizer in anticancer photothermal therapy. *Journal of Nanobiotechnology*, 17(1): 107.

Deshane, J., Garner, C.C. and Sontheimer, H. (2003). Chlorotoxin Inhibits Glioma Cell Invasion via Matrix Metalloproteinase-2. *Journal of Biological Chemistry*, 278(6): 4135–4144.

14

Dong, X. (2018). Current Strategies for Brain Drug Delivery. *Theranostics*, 8(6): 1481–1493.

Emadi, A., Jones, R.J. and Brodsky, R.A. (2009). Cyclophosphamide and cancer: golden anniversary. *Nature Reviews. Clinical Oncology*, 6(11): 638–647.

Fang, C., Veiseh, O., Kievit, F., Bhattarai, N., Wang, F., Stephen, Z., Li, C., Lee, D., Ellenbogen, R.G. and Zhang, M. (2010). Functionalization of iron oxide magnetic nanoparticles with targeting ligands: their physicochemical properties and in vivo behavior. *Nanomedicine (London, England)*, 5(9): 1357–1369.

Fang, C., Wang, K., Stephen, Z.R., Mu, Q., Kievit, F.M., Chiu, D.T., Press, O.W. and Zhang, M. (2015). Temozolomide nanoparticles for targeted glioblastoma therapy. *ACS applied materials & interfaces*, 7(12): 6674–6682.

Fathima, R. and Mujeeb, A. (2021). Enhanced nonlinear and thermo optical properties of laser synthesized surfactant-free Au-Pt bimetallic nanoparticles. *Journal of Molecular Liquids*, 343: 117711.

Foroozandeh, P. and Aziz, A.A. (2018). Insight into Cellular Uptake and Intracellular Trafficking of Nanoparticles. *Nanoscale Research Letters*, 13(1): 339.

Fu, Y., An, N., Li, K., Zheng, Y. and Liang, A. (2012). Chlorotoxin-conjugated nanoparticles as potential glioma-targeted drugs. *Journal of Neuro-Oncology*, 107(3): 457–462.

Gonzalez-Avila, G., Sommer, B., Mendoza-Posada, D.A., Ramos, C., Garcia-Hernandez, A.A. and Falfan-Valencia, R. (2019). Matrix metalloproteinases participation in the metastatic process and their diagnostic and therapeutic applications in cancer*Critical Reviews in Oncology/Hematology*, 137: 57–83.

Guo, P., Imanishi, Y., Cackowski, F.C., Jarzynka, M.J., Tao, H.-Q., Nishikawa, R., Hirose, T., Hu, B. and Cheng, S.-Y. (2005). Up-regulation of angiopoietin-2, matrix metalloprotease-2, membrane type 1 metalloprotease, and laminin 5 gamma 2 correlates with the invasiveness of human glioma. *The American Journal of Pathology*, 166(3): 877–890.

Hall, M.K., Whitman, A.A., Weidner, D.A. and Schwalbe, R.A. (2020). Knockdown of N-Acetylglucosaminyltransferase-II Reduces Matrix Metalloproteinase 2 Activity and Suppresses Tumorigenicity in Neuroblastoma Cell Line. *Biology*, 9(4): 71.

Henderson, T.A. and Morries, L.D. (2015). Near-infrared photonic energy penetration: can infrared phototherapy effectively reach the human brain?. *Neuropsychiatric Disease and Treatment*, 11: 2191–2208.

Hoang Thi, T.T., Pilkington, E.H., Nguyen, D.H., Lee, J.S., Park, K.D. and Truong, N.P. (2020). The Importance of Poly(ethylene glycol) Alternatives for Overcoming PEG Immunogenicity in Drug Delivery and Bioconjugation. *Polymers*, 12(2): E298.

Kahana, M., Weizman, A., Gabay, M., Loboda, Y., Segal-Gavish, H., Gavish, A., Barhum, Y., Offen, D., Finberg, J., Allon, N. and Gavish, M. (2021). Liposome-based targeting of dopamine to the brain: a novel approach for the treatment of Parkinson's disease. *Molecular Psychiatry*, 26(6): 2626–2632.

15

Katifelis, H., Lyberopoulou, A., Mukha, I., Vityuk, N., Grodzyuk, G., Theodoropoulos, G.E., Efstathopoulos, E.P. and Gazouli, M. (2018). Ag/Au bimetallic nanoparticles induce apoptosis in human cancer cell lines via P53, CASPASE-3 and BAX/BCL-2 pathways. *Artificial Cells, Nanomedicine, and Biotechnology*, 46(sup3): S389–S398.

Kesavan, K., Ratliff, J., Johnson, E.W., Dahlberg, W., Asara, J.M., Misra, P., Frangioni, J.V. and Jacoby, D.B. (2010). Annexin A2 is a molecular target for TM601, a peptide with tumor-targeting and anti-angiogenic effects. *The Journal of Biological Chemistry*, 285(7): 4366–4374.

Khanyile, S., Masamba, P., Oyinloye, B.E., Mbatha, L.S. and Kappo, A.P. (2019). Current Biochemical Applications and Future Prospects of Chlorotoxin in Cancer Diagnostics and Therapeutics. *Advanced Pharmaceutical Bulletin*, 9(4): 510–520.

Kievit, F.M., Veiseh, O., Fang, C., Bhattarai, N., Lee, D., Ellenbogen, R.G. and Zhang, M. (2010). Chlorotoxin Labeled Magnetic Nanovectors for Targeted Gene Delivery to Glioma. *ACS Nano*, 4(8): 4587–4594.

Kim, H.S. and Lee, D.Y. (2018). Near-Infrared-Responsive Cancer Photothermal and Photodynamic Therapy Using Gold Nanoparticles. *Polymers*, 10(9): 961.

King, J.L. and Benhabbour, S.R. (2021). Glioblastoma Multiforme—A Look at the Past and a Glance at the Future. *Pharmaceutics*, 13(7): 1053.

Latifi, Z., Fattahi, A., Ranjbaran, A., Nejabati, H.R. and Imakawa, K. (2018). Potential roles of metalloproteinases of endometrium-derived exosomes in embryo-maternal crosstalk during implantation. *Journal of Cellular Physiology*, 233(6): 4530–4545.

Lawrie, T.A., Evans, J., Gillespie, D., Erridge, S., Vale, L., Kernohan, A. and Grant, R. (2018). Long-term side effects of radiotherapy, with or without chemotherapy, for glioma. *The Cochrane Database of Systematic Reviews*, 2018(6): CD013047.

Li, X., Nie, S., Lv, Z., Ma, L., Song, Y., Hu, Z., Hu, X., Liu, Z., Zhou, G., Dai, Z., Song, T., Liu, J. and Wang, S. (2021). Overexpression of Annexin A2 promotes proliferation by forming a Glypican 1/c-Myc positive feedback loop: prognostic significance in human glioma. *Cell Death & Disease*, 12(3): 1–13.

Liu, X., Chen, H., Chen, X., Alfadhl, Y., Yu, J. and Wen, D. (2015). Radiofrequency heating of nanomaterials for cancer treatment: Progress, controversies, and future development. *Applied Physics Reviews*, 2(1): 011103.

Liu, X., Zhang, X., Zhu, M., Lin, G., Liu, J., Zhou, Z., Tian, X. and Pan, Y. (2017). PEGylated Au@Pt Nanodendrites as Novel Theranostic Agents for Computed Tomography Imaging and Photothermal/Radiation Synergistic Therapy. *ACS Applied Materials & Interfaces*, 9(1): 279–285.

Locatelli, E., Bost, W., Fournelle, M., Llop, J., Gil, L., Arena, F., Lorusso, V. and Comes Franchini, M. (2014a). Targeted polymeric nanoparticles containing gold nanorods: a therapeutic approach against glioblastoma. *Journal of Nanoparticle Research*, 16(3): 2304.

Locatelli, E., Broggi, F., Ponti, J., Marmorato, P., Franchini, F., Lena, S. and Franchini, M.C. (2012). Lipophilic silver nanoparticles and their polymeric entrapment into targeted-PEG-based micelles for the treatment of glioblastoma. *Advanced Healthcare Materials*, 1(3): 342–347.

Locatelli, E., Naddaka, M., Uboldi, C., Loudos, G., Fragogeorgi, E., Molinari, V., Pucci, A., Tsotakos, T., Psimadas, D., Ponti, J. and Franchini, M.C. (2014b). Targeted delivery of silver nanoparticles and alisertib: in vitro and in vivo synergistic effect against glioblastoma. *Nanomedicine (London, England)*, 9(6), pp. 839–849.

Lui, V.C.H., Lung, S.S.S., Pu, J.K.S., Hung, K.N. and Leung, G.K.K. (2010). Invasion of human glioma cells is regulated by multiple chloride channels including ClC-3. *Anticancer Research*, 30(11): 4515–4524.

Lyons, S.A., O'Neal, J. and Sontheimer, H. (2002). Chlorotoxin, a scorpion-derived peptide, specifically binds to gliomas and tumors of neuroectodermal origin. *Glia*, 39(2): 162–173.

Manikandan, M., Hasan, N. and Wu, H.-F. (2013). Platinum nanoparticles for the photothermal treatment of Neuro 2A cancer cells. *Biomaterials*, 34(23): 5833–5842.

McFerrin, M.B. and Sontheimer, H. (2006). A role for ion channels in glioma cell invasion. *Neuron Glia Biology*, 2(1): 39–49.

McGonigle, S., Majumder, U., Kolber-Simonds, D., Wu, J., Hart, A., Noland, T., TenDyke, K., Custar, D., Li, D., Du, H., Postema, M.H.D., Lai, W.G., Twine, N.C., Woodall-Jappe, M. and Nomoto, K. (2019). Neuropilin-1 drives tumor-specific uptake of chlorotoxin', *Cell communication and signaling: CCS*, 17(1): 67.

Medina-Cruz, D., Saleh, B., Vernet-Crua, A., Nieto-Argüello, A., Lomelí-Marroquín, D., Vélez-Escamilla, L.Y., Cholula-Díaz, J.L., García-Martín, J.M. and Webster, T. (2020). Bimetallic Nanoparticles for Biomedical Applications: A Review in Li, B., Moriarty, T., Webster, T., Xing, M. (eds). *Racing for the Surface: Antimicrobial and Interface Tissue Engineering*. Cham: Springer International Publishing: 397–434.

Miller, K.D., Ostrom, Q.T., Kruchko, C., Patil, N., Tihan, T., Cioffi, G., Fuchs, H.E., Waite, K.A., Jemal, A., Siegel, R.L. and Barnholtz-Sloan, J.S. (2021). Brain and other central nervous system tumor statistics, 2021. *CA: A Cancer Journal for Clinicians*, 71(5): 381–406.

Mora, J. (2016). Dinutuximab for the treatment of pediatric patients with high-risk neuroblastoma. *Expert Review of Clinical Pharmacology*, 9(5): 647–653.

Moros, M., Lewinska, A., Merola, F., Ferraro, P., Wnuk, M., Tino, A. and Tortiglione, C. (2020). Gold Nanorods and Nanoprisms Mediate Different Photothermal Cell Death Mechanisms In Vitro and In Vivo. *ACS applied materials & interfaces*, 12(12): 13718–13730.

Nasseri, B., Yilmaz, M., Turk, M., Kocum, I.C. and Piskin, E. (2016). Antenna-type radiofrequency generator in nanoparticle-mediated hyperthermia. *RSC Advances*, 6(54): 48427–48434.

Norouzi, H., Khoshgard, K. and Akbarzadeh, F. (2018). In vitro outlook of gold nanoparticles in photo-thermal therapy: a literature review. *Lasers in Medical Science*, 33(4): 917–926.

Oei, A.L., Kok, H.P., Oei, S.B., Horsman, M.R., Stalpers, L.J.A., Franken, N.A.P. and Crezee, J. (2020). Molecular and biological rationale of hyperthermia as radio- and chemosensitizer. *Advanced Drug Delivery Reviews*, 163–164: 84–97.

Ohta, S., Kikuchi, E., Ishijima, A., Azuma, T., Sakuma, I. and Ito, T. (2020). Investigating the optimum size of nanoparticles for their delivery into the brain assisted by focused ultrasound-induced blood–brain barrier opening. *Scientific Reports*, 10(1): 18220.

Ojeda, P.G., Wang, C.K. and Craik, D.J. (2016). Chlorotoxin: Structure, activity, and potential uses in cancer therapy. *Biopolymers*, 106(1): 25–36.

Oladipo, A.O., Iku, S.I.I., Ntwasa, M., Nkambule, T.T.I., Mamba, B.B. and Msagati, T.A.M. (2020). Doxorubicin conjugated hydrophilic AuPt bimetallic nanoparticles fabricated from Phragmites australis: Characterization and cytotoxic activity against human cancer cells. *Journal of Drug Delivery Science and Technology*, 57: 101749.

Pardridge, W.M. (2012). Drug transport across the blood–brain barrier. *Journal of Cerebral Blood Flow & Metabolism*, 32(11): 1959–1972.

Patil, C.G., Walker, D.G., Miller, D.M., Butte, P., Morrison, B., Kittle, D.S., Hansen, S.J., Nufer, K.L., Byrnes-Blake, K.A., Yamada, M., Lin, L.L., Pham, K., Perry, J., Parrish-Novak, J., Ishak, L., Prow, T., Black, K. and Mamelak, A.N. (2019). Phase 1 Safety, Pharmacokinetics, and Fluorescence Imaging Study of Tozuleristide (BLZ-100) in Adults With Newly Diagnosed or Recurrent Gliomas. *Neurosurgery*, 85(4): E641–E649.

Porcel, E., Liehn, S., Remita, H., Usami, N., Kobayashi, K., Furusawa, Y., Le Sech, C. and Lacombe, S. (2010). Platinum nanoparticles: a promising material for future cancer therapy?. *Nanotechnology*, 21(8): 85103.

Prabhakar, U., Maeda, H., Jain, R.K., Sevick-Muraca, E.M., Zamboni, W., Farokhzad, O.C., Barry, S.T., Gabizon, A., Grodzinski, P. and Blakey, D.C. (2013). Challenges and Key Considerations of the Enhanced Permeability and Retention Effect for Nanomedicine Drug Delivery in Oncology. *Cancer Research*, 73(8): 2412–2417.

Qin, C., He, B., Dai, W., Lin, Z., Zhang, H., Wang, X., Wang, J., Zhang, X., Wang, G., Yin, L. and Zhang, Q. (2014). The impact of a chlorotoxin-modified liposome system on receptor MMP-2 and the receptor-associated protein ClC-3. *Biomaterials*, 35(22): 5908–5920.

Quintero-Fabián, S., Arreola, R., Becerril-Villanueva, E., Torres-Romero, J.C., Arana-Argáez, V., Lara-Riegos, J., Ramírez-Camacho, M.A. and Alvarez-Sánchez, M.E. (2019). Role of Matrix Metalloproteinases in Angiogenesis and Cancer. *Frontiers in Oncology*, 9: 1370.

Rabiei, M., Kashanian, S., Samavati, S.S., Jamasb, S. and McInnes, S.J.P. (2020). Active Targeting Towards and Inside the Brain based on Nanoparticles: A Review. *Current Pharmaceutical Biotechnology*, 21(5): 374–383.

Rajan, A. and Sahu, N.K. (2020). Review on magnetic nanoparticle-mediated hyperthermia for cancer therapy. *Journal of Nanoparticle Research*, 22(11): 319.

Raoof, M. and Curley, S.A. (2011). Non-invasive radiofrequency-induced targeted hyperthermia for the treatment of hepatocellular carcinoma. *International Journal of Hepatology*, 2011: 676957.

Ribatti, D., Surico, G., Vacca, A., De Leonardis, F., Lastilla, G., Montaldo, P.G., Rigillo, N. and Ponzoni, M. (2001). Angiogenesis extent and expression of matrix metalloproteinase-2 and -9 correlate with progression in human neuroblastoma. *Life Sciences*, 68(10): 1161–1168.

Röschmann, P. (1987). Radiofrequency penetration and absorption in the human body: limitations to high-field whole-body nuclear magnetic resonance imaging. *Medical Physics*, 14(6): 922–931.

Salado-Leza, D., Traore, A., Porcel, E., Dragoe, D., Muñoz, A., Remita, H., García, G. and Lacombe, S. (2019). Radio-Enhancing Properties of Bimetallic Au:Pt Nanoparticles: Experimental and Theoretical Evidence', *International Journal of Molecular Sciences*, 20(22): E5648.

Samadi, A., Klingberg, H., Jauffred, L., Kjær, A., Bendix, P.M. and Oddershede, L.B. (2018). Platinum nanoparticles: a non-toxic, effective and thermally stable alternative plasmonic material for cancer therapy and bioengineering. *Nanoscale*, 10(19): 9097–9107.

San, B.H., Moh, S.H. and Kim, K.K. (2013). Investigation of the heating properties of platinum nanoparticles under a radiofrequency current. *International Journal of Hyperthermia: The Official Journal of European Society for Hyperthermic Oncology, North American Hyperthermia Group*, 29(2): 99–105.

Sani, A., Cao, C. and Cui, D. (2021). Toxicity of gold nanoparticles (AuNPs): A review. *Biochemistry and Biophysics Reports*, 26: 100991.

Sasikumar, P.G. and Ramachandra, M. (2018). Small-Molecule Immune Checkpoint Inhibitors Targeting PD-1/PD-L1 and Other Emerging Checkpoint Pathways. *BioDrugs: Clinical Immunotherapeutics, Biopharmaceuticals and Gene Therapy*, 32(5): 481–497.

Sawai, N., Zhou, S., Vanin, E.F., Houghton, P., Brent, T.P. and Sorrentino, B.P. (2001). Protection and in Vivo Selection of Hematopoietic Stem Cells Using Temozolomide, O6-Benzylguanine, and an Alkyltransferase-Expressing Retroviral Vector. *Molecular Therapy*, 3(1): 78–87.

Schacht, J., Talaska, A.E. and Rybak, L.P. (2012). Cisplatin and Aminoglycoside Antibiotics: Hearing Loss and Its Prevention. *Anatomical record (Hoboken, N.J.: 2007)*, 295(11): 1837–1850.

Shakeri, S., Ashrafizadeh, M., Zarrabi, A., Roghanian, R., Afshar, E.G., Pardakhty, A., Mohammadinejad, R., Kumar, A. and Thakur, V.K. (2020). Multifunctional Polymeric Nanoplatforms for Brain Diseases Diagnosis, Therapy and Theranostics. *Biomedicines*, 8(1): E13.

Shang, L., Nienhaus, K. and Nienhaus, G.U. (2014). Engineered nanoparticles interacting with cells: size matters. *Journal of Nanobiotechnology*, 12(1): p. 5.

Sharma, G., Kumar, A., Sharma, S., Naushad, Mu., Prakash Dwivedi, R., ALOthman, Z.A. and Mola, G.T. (2019). Novel development of nanoparticles to bimetallic nanoparticles and their composites: A review. *Journal of King Saud University - Science*, 31(2): 257–269.

Shi, L., Zhang, J., Zhao, M., Tang, S., Cheng, X., Zhang, W., Li, W., Liu, X., Peng, H. and Wang, Q. (2021). Effects of polyethylene glycol on the surface of nanoparticles for targeted drug delivery. *Nanoscale*, 13(24): 10748–10764.

Smith, V. and Foster, J. (2018). High-Risk Neuroblastoma Treatment Review. *Children*, 5(9): 114.

Sokolova, V., Mekky, G., van der Meer, S.B., Seeds, M.C., Atala, A.J. and Epple, M. (2020). Transport of ultrasmall gold nanoparticles (2 nm) across the blood–brain barrier in a six-cell brain spheroid model. *Scientific Reports*, 10(1): 18033.

Song, Y., Qu, Z., Li, J., Shi, L., Zhao, W., Wang, H., Sun, T., Jia, T. and Sun, Y. (2021). Fabrication of the biomimetic DOX/Au@Pt nanoparticles hybrid nanostructures for the combinational chemo/photothermal cancer therapy. *Journal of Alloys and Compounds*, 881: 160592.

Song, Y., Shi, Q., Zhu, C., Luo, Y., Lu, Q., Li, H., Ye, R., Du, D. and Lin, Y. (2017). Mitochondrial Reactive Oxygen Species Burst for Cancer Therapy Triggered by Near-Infrared Light. *Nanoscale*, 2017.

Soroceanu, L., Gillespie, Y., Khazaeli, M.B. and Sontheimer, H. (1998). Use of chlorotoxin for targeting of primary brain tumors. *Cancer Research*, 58(21): 4871–4879.

Speckhart, B., Antony, R. and Fernandez, K.S. (2017). Long-term side effects of high-risk neuroblastoma survivors in a referral center in central Illinois. *Journal of Clinical Oncology*, 35(5_suppl): 129–129.

Stamenkovic, I. (2000). Matrix metalloproteinases in tumor invasion and metastasis. *Seminars in Cancer Biology*, 10(6): 415–433.

Stone, J.B. and DeAngelis, L.M. (2016). Cancer Treatment-Induced Neurotoxicity: A Focus on Newer Treatments. *Nature reviews. Clinical oncology*, 13(2): 92–105.

Stupp, R., Taillibert, S., Kanner, A., Read, W., Steinberg, D.M., Lhermitte, B., Toms, S., Idbaih, A., Ahluwalia, M.S., Fink, K., Di Meco, F., Lieberman, F., Zhu, J.-J., Stragliotto, G., Tran, D.D., Brem, S., Hottinger, A.F., Kirson, E.D., Lavy-Shahaf, G., Weinberg, U., Kim, C.-Y., Paek, S.-H., Nicholas, G., Bruna, J., Hirte, H., Weller, M., Palti, Y., Hegi, M.E. and Ram, Z. (2017). Effect of Tumor-Treating Fields Plus Maintenance Temozolomide vs Maintenance Temozolomide Alone on Survival in Patients With Glioblastoma: A Randomized Clinical Trial', *JAMA*, 318(23): 2306–2316.

Sun, C., Fang, C., Stephen, Z., Veiseh, O., Hansen, S., Lee, D., Ellenbogen, R.G., Olson, J. and Zhang, M. (2008). Tumor-targeted drug delivery and MRI contrast enhancement by chlorotoxin-conjugated iron oxide nanoparticles. *Nanomedicine (London, England)*, 3(4): 495–505.

Sung, H., Ferlay, J., Siegel, R.L., Laversanne, M., Soerjomataram, I., Jemal, A. and Bray, F. (2021). Global Cancer Statistics 2020: GLOBOCAN Estimates of Incidence and Mortality Worldwide for 36 Cancers in 185 Countries. *CA: A Cancer Journal for Clinicians*, 71(3): 209–249.

Tamborini, M., Locatelli, E., Rasile, M., Monaco, I., Rodighiero, S., Corradini, I., Franchini, M.C., Passoni, L. and Matteoli, M. (2016). A Combined Approach Employing Chlorotoxin-Nanovectors

and Low Dose Radiation To Reach Infiltrating Tumor Niches in Glioblastoma. *ACS nano*, 10(2): 2509–2520.

Tan, A.C., Ashley, D.M., López, G.Y., Malinzak, M., Friedman, H.S. and Khasraw, M. (2020). Management of glioblastoma: State of the art and future directions. *CA: a cancer journal for clinicians*, 70(4): 299–312.

Tang, J., Jiang, X., Wang, L., Zhang, H., Hu, Z., Liu, Y., Wu, X. and Chen, C. (2014). Au@Pt nanostructures: a novel photothermal conversion agent for cancer therapy. *Nanoscale*, 6(7): 3670–3678.

Tardáguila-García, A., García-Morales, E., García-Alamino, J.M., Álvaro-Afonso, F.J., Molines-Barroso, R.J. and Lázaro-Martínez, J.L. (2019). Metalloproteinases in chronic and acute wounds: A systematic review and meta-analysis. *Wound Repair and Regeneration*, 27(4): 415–420.

Turner, K.L. and Sontheimer, H. (2014). Cl- and K+ channels and their role in primary brain tumour biology. *Philosophical Transactions of the Royal Society of London. Series B, Biological Sciences*, 369(1638): 20130095.

Turney, J. (2008). Technology - Ethical Debates about the Application of Science. *Evans Brothers*: 29.

Veiseh, M., Gabikian, P., Bahrami, S.-B., Veiseh, O., Zhang, M., Hackman, R.C., Ravanpay, A.C., Stroud, M.R., Kusuma, Y., Hansen, S.J., Kwok, D., Munoz, N.M., Sze, R.W., Grady, W.M., Greenberg, N.M., Ellenbogen, R.G. and Olson, J.M. (2007). Tumor Paint: A Chlorotoxin:Cy5.5 Bioconjugate for Intraoperative Visualization of Cancer Foci. *Cancer Research*, 67(14): 6882–6888.

Veiseh, O., Gunn, J.W., Kievit, F.M., Sun, C., Fang, C., Lee, J.S.H. and Zhang, M. (2009). Inhibition of tumor-cell invasion with chlorotoxin-bound superparamagnetic nanoparticles. *Small (Weinheim an Der Bergstrasse, Germany)*, 5(2): 256–264.

Veschi, V., Verona, F. and Thiele, C.J. (2019). Cancer Stem Cells and Neuroblastoma: Characteristics and Therapeutic Targeting Options. *Frontiers in Endocrinology*, 10: 782.

Visse, R. and Nagase, H. (2003). Matrix Metalloproteinases and Tissue Inhibitors of Metalloproteinases. *Circulation Research*, 92 (8): 827–39.

Wang, X.-M., Luo, X. and Guo, Z.-Y. (2013). Recombinant expression and downstream processing of the disulfide-rich tumor-targeting peptide chlorotoxin. *Experimental and Therapeutic Medicine*, 6(4): 1049–1053.

Wang, Y., Chen, K., Cai, Yihong, Cai, Yuanxia, Yuan, X., Wang, L., Wu, Z. and Wu, Y. (2017). Annexin A2 could enhance multidrug resistance by regulating NF-κB signaling pathway in pediatric neuroblastoma. *Journal of Experimental & Clinical Cancer Research*, 36(1): 111.

Wang, Y., Li, K., Han, S., Tian, Y., Hu, P., Xu, X., He, Y., Pan, W., Gao, Y., Zhang, Z., Zhang, J. and Wei, L. (2019). Chlorotoxin targets ERα/VASP signaling pathway to combat breast cancer. *Cancer Medicine*, 8(4): 1679–1693.

Welch, D.R. and Hurst, D.R. (2019). Defining the Hallmarks of Metastasis. *Cancer Research*, 79(12): 3011–3027.

Wu, W., Klockow, J.L., Zhang, M., Lafortune, F., Chang, E., Jin, L., Wu, Y. and Daldrup-Link, H.E. (2021). Glioblastoma multiforme (GBM): An overview of current therapies and mechanisms of resistance. *Pharmacological Research*, 171: 105780.

Wu, Y., Lu, Z., Li, Y., Yang, J. and Zhang, X. (2020). Surface Modification of Iron Oxide-Based Magnetic Nanoparticles for Cerebral Theranostics: Application and Prospection. *Nanomaterials*, 10(8): 1441.

Yamada, M., Miller, D.M., Lowe, M., Rowe, C., Wood, D., Soyer, H.P., Byrnes-Blake, K., Parrish-Novak, J., Ishak, L., Olson, J.M., Brandt, G., Griffin, P., Spelman, L. and Prow, T.W. (2021). A first-in-human study of BLZ-100 (tozuleristide) demonstrates tolerability and safety in skin cancer patients. *Contemporary Clinical Trials Communications*, 23: 100830.

Yang, Q., Peng, J., Xiao, Y., Li, W., Tan, L., Xu, X. and Qian, Z. (2018). Porous Au@Pt Nanoparticles: Therapeutic Platform for Tumor Chemo-Photothermal Co-Therapy and Alleviating Doxorubicin-Induced Oxidative Damage. *ACS Applied Materials & Interfaces*, 10(1): 150–164.

Yao, Y., Zhou, Y., Liu, L., Xu, Y., Chen, Q., Wang, Y., Wu, S., Deng, Y., Zhang, J. and Shao, A. (2020). Nanoparticle-Based Drug Delivery in Cancer Therapy and Its Role in Overcoming Drug Resistance. *Frontiers in Molecular Biosciences*, 7: 193.

Yetisgin, A.A., Cetinel, S., Zuvin, M., Kosar, A. and Kutlu, O. (2020). Therapeutic Nanoparticles and Their Targeted Delivery Applications. *Molecules (Basel, Switzerland)*, 25(9): E2193.

Yu, C.-F., Chen, F.-H., Lu, M.-H., Hong, J.-H. and Chiang, C.-S. (2017). Dual roles of tumour cells-derived matrix metalloproteinase 2 on brain tumour growth and invasion. *British Journal of Cancer*, 117(12): 1828–1836.

Zaleska-Medynska, A., Marchelek, M., Diak, M. and Grabowska, E. (2016). Noble metal-based bimetallic nanoparticles: the effect of the structure on the optical, catalytic and photocatalytic properties. *Advances in Colloid and Interface Science*, 229, pp. 80–107.

Zhao, L., Li, Y., Zhu, J., Sun, N., Song, N., Xing, Y., Huang, H. and Zhao, J. (2019). Chlorotoxin peptide-functionalized polyethylenimine-entrapped gold nanoparticles for glioma SPECT/CT imaging and radionuclide therapy. *Journal of Nanobiotechnology*, 17(1): 30.

Zhao, L., Shi, X. and Zhao, J. (2015). Chlorotoxin-conjugated nanoparticles for targeted imaging and therapy of glioma. *Current Topics in Medicinal Chemistry*, 15(13):1196–1208.

Zhao, M., van Straten, D., Broekman, M.L.D., Préat, V. and Schiffelers, R.M. (2020). Nanocarrier-based drug combination therapy for glioblastoma. *Theranostics*, 10(3):1355–1372.

Zhou, W., Yu, X., Sun, S., Zhang, Xuehai, Yang, W., Zhang, J., Zhang, Xin and Jiang, Z. (2019). Increased expression of MMP-2 and MMP-9 indicates poor prognosis in glioma recurrence. *Biomedicine & Pharmacotherapy*, 118: 109369.

CHAPTER TWO:

Diagnostic and therapeutic approaches for glioblastoma and neuroblastoma cancers using chlorotoxin nanoparticles

Taahirah Boltman[1], Okobi Ekpo[1], Mervin Meyer[2]*

[1] Department of Medical Biosciences, University of the Western Cape, Cape Town, Robert Sobukwe Road, Bellville 7535, South Africa; 2917424@myuwc.ac.za (T.B.)

[2] DSI/Mintek Nanotechnology Innovation Centre, Biolabels Node, Department of Biotechnology, University of the Western Cape, Cape Town, Robert Sobukwe Road, Bellville 7535, South Africa

*Correspondence: memeyer@uwc.ac.za (M.M.); Tel.: +27-21-5952032 (M.M.)

Abstract

Glioblastoma multiforme (GB) and high-risk neuroblastoma (NB) are known to have poor therapeutic outcomes and as for most cancers, chemotherapy and radiotherapy are the current mainstay treatments. However, the known limitations of systemic toxicity, drug resistance, poor targeted delivery, and inability to access the blood-brain barrier (BBB), make these treatments less satisfactory. Other treatment options have been investigated in many studies in literature, especially nutraceutical and naturopathic products, most of which have also been reported to be poorly effective against these cancer types. This necessitates the development of treatment strategies with the potential to cross the BBB and specifically target cancer cells. Compounds that target the endopeptidase, matrix metalloproteinase 2 (MMP-2), have been reported to offer therapeutic insights for GB and NB, since MMP-2 is known to be over-expressed in these cancers and plays significant roles in such physiological processes as angiogenesis, metastasis and cellular invasion. Chlorotoxin (CTX) is a promising 36-amino acid peptide isolated from the venom of the deathstalker scorpion, *Leiurus quinquestriatus*, demonstrating high selectivity and binding affinity to a broad-spectrum of cancers, especially GB and NB through specific molecular targets including MMP-2. The favourable characteristics of nanoparticles (NPs) such as their small sizes, large surface area for active targeting, as well as BBB permeability, make CTX-functionalized NPs (CTX-NPs) promising diagnostic and therapeutic applications for addressing the many challenges associated with these cancers. CTX-NPs

may function by improving diffusion through the BBB, enabling increased localization of chemotherapeutic and genotherapeutic drugs to diseased cells specifically, enhancing imaging modalities like magnetic resonance imaging (MRI), single-photon emission computed tomography (SPECT), optical imaging techniques and image-guided surgery, as well as improving the sensitization of radio-resistant cells to radiotherapy treatment. This review discusses the characteristics of GB and NB cancers, related treatment challenges as well as the potential of CTX and its functionalized NP formulations, as targeting systems for diagnostic, therapeutic and theranostic purposes. It also provides insights into the potential mechanisms through which CTX crosses the BBB to bind cancer cells and provides suggestions for the development and application of novel CTX-based applications for future diagnosis and treatment of GB and NB.

Keywords: blood-brain-barrier (BBB), chlorotoxin (CTX), glioblastoma multiforme (GB), matrix metalloproteinase 2 (MMP-2), nanoparticles (NPs) and neuroblastoma (NB).

1. Introduction

Cancer is the leading cause of low life expectancy and death worldwide (Sung *et al.*, 2021). Nervous system (NS) tumours include a broad spectrum of brain and spinal cord malignancies that contribute to global economic burden and are often associated with short- and long-term disabilities (Feigin *et al.*, 2021). The treatment of malignant tumours of the NS remains a challenge due to the BBB, with about 330,000 new central nervous system (CNS) cancer cases reported globally (Mohammadi *et al.*, 2021). High grade glioblastoma, also known as glioblastoma multiforme (GB) (Sevastre *et al.*, 2021), is the most aggressive and consistently debilitating primary brain tumours in adults, with a dismal median survival time of 12-15 months and a 5-year survival rate of less than 7% (Miller *et al.*, 2021). Standard treatments are ineffective due to the diffuse invasion and infiltrative overgrowth of heterogeneous glioma cells contributing to the development of irregular and indistinct tumour margins, thereby hindering complete surgical resection (Thon, Tonn and Kreth, 2019). The location of deep-seated GB also makes it difficult to treat without damaging healthy brain cells, hence radiotherapy and chemotherapeutic drugs have the treatment limitations of non-specificity and systemic toxicity (Jain, 2018), in addition to the most important challenge of effective delivery into the brain, i.e. BBB permeability (Ferraris *et al.*, 2020).

Neuroblastoma (NB) are amongst the most frequent childhood cancers of the sympathetic NS and remain one of the major challenges in paediatric oncology (Southgate *et al.*, 2020). The progression of NB is associated with hematogenous metastasis, common relapses, with a fast declining survival timeline and drug resistance (Aravindan *et al.*, 2019). Like for GB, conventional treatment for NB is limited by systemic toxicity and more than half of children diagnosed with high-risk NB do not respond to high-dose chemotherapy and often demonstrate multi-drug resistance (Smith and Foster, 2018). Some of the reported adverse side effects of high-dose chemotherapy include nephrotoxicity, cardiotoxicity and gonadotoxicity leading to infertility in later life (Emadi, Jones and Brodsky, 2009; Schacht, Talaska and Rybak, 2012). Specific long-term toxic side effects include cognitive deficits, epilepsy, growth reduction, thyroid function disorders, learning difficulties and an increased risk of secondary cancers in survivors of high-risk NB (Trahair *et al.*, 2007; Applebaum *et al.*, 2017; Speckhart, Antony and Fernandez, 2017). Although there have been improvements in the management of NB during the past two decades, the overall cure rate remains at approximately 50 % for high-risk patients (Smith and Foster, 2018). Tumour migration and invasion have been identified as the major causes of treatment failure in patients with malignant tumours (Welch and Hurst, 2019).

Metastasis is a multistep process that consists of cancer cell migration and invasion (Tahtamouni *et al.*, 2019) and most NS tumours are known to undergo metastasis like other cancer types (Lah, Novak and Breznik, 2020). Tumour metastasis comprises of neovascularization as well as cell adhesion, invasion, migration, and proliferation, with the degradation of the extracellular matrix (ECM) and the basement membrane playing an important role (Jiang *et al.*, 2015; Walker, Mojares and del Río Hernández, 2018). The overexpression of matrix metalloproteinases (MMPs) in tumour cells has been implicated in tumour progression (Winer, Adams and Mignatti, 2018). Metalloproteinases (MPs) are a family of secreted, zinc-dependent endopeptidases involved in such processes as tissue-remodelling, wound healing, embryo implantation, tumour invasion, metastasis and angiogenesis (Latifi *et al.*, 2018; Quintero-Fabián *et al.*, 2019; Tardáguila-García *et al.*, 2019). MMPs are reported to contribute to the degradation of extracellular matrix (ECM), stromal connective tissue, and the BBB tight junctions, which are some of the driving factors of cancer invasion and metastasis, the progression of neurodegenerative diseases, and other pathological disorders (Raeeszadeh-Sarmazdeh, Do and Hritz, 2020).

There are over 20 matrix metalloproteinase (MMP) family members, and the subset MMP-2s, released from neurons and glia, is known to be present in the CNS (Conant, Allen and Lim, 2015;

Allen *et al.*, 2016). Literature evidence suggests that the over-expression of MMP2 is an active contributor to the progression of malignant GB (Forsyth *et al.*, 1999; Guo *et al.*, 2005; Zhou *et al.*, 2019) and NB (Sugiura *et al.*, 1998; Ribatti *et al.*, 2001; Hall *et al.*, 2020) via increased cancer-cell growth, migration, invasion, and angiogenesis. The degree of invasiveness of GB and NB tumours is related to increased levels of MMP-2 expression (Ribatti *et al.*, 2001; Yu *et al.*, 2017). In addition to the overexpression of MMP-2 on the cell surface, the chloride ion channel 3 (ClC-3) is specifically upregulated in human GB cells but not in normal glial cells and neurons (Habela, Olsen and Sontheimer, 2008; B. Wang *et al.*, 2017). ClC-3 is involved in cell cytoskeletal rearrangements as well as cell shape and movements during cell migration (McFerrin and Sontheimer, 2006; Habela, Olsen and Sontheimer, 2008).

The annexin protein family is a group of calcium-dependent phospholipid-binding proteins that contribute to such cellular functions as angiogenesis, apoptosis, cell migration, proliferation, invasion, and cohesion (Staquicini *et al.*, 2017; Valls *et al.*, 2021). The surface protein annexin A2, a calcium-binding cytoskeletal protein located at the extracellular surface of various tumour cell types, including glioma, is involved in tumour progression through cell migration and invasion (Chen *et al.*, 2019; Li *et al.*, 2021). Annexin A2 is also implicated in enhanced multidrug resistance in NB (Y. Wang *et al.*, 2017).

Thus, MMP-2, chloride channels and Annexin 2 are all involved in malignant cell migration and invasion and provide therapeutic opportunities for targeting GB and NB cancers. One promising molecule for achieving such targeting is the peptide, chlorotoxin (CTX) which is a 36-amino acid peptide isolated from the venom of the deathstalker scorpion, *Leiurus quinquestriatus*, known to specifically bind to gliomas and many other tumours of neuroectodermal origin like NB (Khanyile *et al.*, 2019). Although the precise mechanism of CTX targeting has yet to be fully elucidated, a number of studies have suggested the presence of many targeting receptors for CTX on the surfaces of different cancer cells, including chloride channels (Soroceanu *et al.*, 1998; Soroceanu, Manning and Sontheimer, 1999; Cheng *et al.*, 2014), MMP-2 (Deshane, Garner and Sontheimer, 2003; El-Ghlban *et al.*, 2014; Ayomide *et al.*, 2018), annexin A2 (Kesavan *et al.*, 2010; Wang, Luo and Guo, 2013), estrogen receptor alpha (ERα) (Y. Wang *et al.*, 2019) and neuropilin-1 receptor (NRP-1) (McGonigle *et al.*, 2019; Sharma *et al.*, 2021). In gliomas, it is reported that MMP-2 and CIC-3 form a protein complex located within the same membrane domain targeted by CTX and could potentially inhibit

glioma cell invasion through the induction of MMP-2/ClC-3 protein complex endocytosis (Deshane, Garner and Sontheimer, 2003). Additionally, CTX has been observed to permeate intact BBBs in both animal models and human brain tumours, with no cross-reactivity reported in non-malignant cells in the brain and other parts of the body (Khanyile *et al.*, 2019). Thus, CTX could be considered as a promising targeting molecule for the development of novel diagnostic and therapeutic applications for GB and NB tumours.

The use of nanoparticle-based systems is attractive in biomedical research for the development of improved cancer-targeting diagnostic and therapeutic applications. Nanoparticles (NPs) improve the targeting of tumour cells by enhancing drug diffusion through the BBB and the specific targeting of diseased tumour cells, thereby limiting systemic toxicity (Sokolova *et al.*, 2020; Mitchell *et al.*, 2021). NPs that are surface-functionalized with CTX as a targeting molecule, have been widely investigated and demonstrate BBB-penetrating properties to reach GB tumours *in vivo*. These molecules are also useful for imaging-guided maximal surgical resection, drug delivery and therapy monitoring (Costa *et al.*, 2013; Dardevet *et al.*, 2015; Ojeda, Wang and Craik, 2016; Cohen, Burks and Frank, 2018; Khanyile *et al.*, 2019). Fluorescent-labelled CTX molecules and CTX-NP formulations for the delivery of chemotherapeutics and small interfering RNAs (siRNAs) have entered early clinical trials and preliminary results are promising (Kievit *et al.*, 2010; Zhao *et al.*, 2015a; Khanyile *et al.*, 2019; C. G. Patil *et al.*, 2019; Yamada *et al.*, 2021).

This review highlights the challenges associated with GB and NB cancers, describes the characteristics of CTX as a promising targeting peptide for these cancers, explores the mechanisms of action of CTX and discusses CTX-based nanotechnology applications that have been mostly investigated for diagnostic and therapeutic purposes in the management of GB, but may be expanded for potential applications for NB. The potential therapeutic, diagnostic and theranostic applications of CTX-NP formulations as well as the properties of some CTX-like peptides will also be discussed.

2. Glioblastoma multiforme (GB): Standard treatments and challenges

Glioblastoma multiforme (GB) is the most highly invasive and aggressive, intracranial brain tumour diagnosed in adults, with a poor median survival time of 12−15 months and a 5-year survival rate of less than 7 % (Miller *et al.*, 2021; Rabab'h *et al*., 2021). There are many challenges associated with the treatment of GB, as highlighted in Figure 1, a major one being the blood-brain barrier (BBB) which diminishes the therapeutic value of most drugs for brain tumours due to its unique

characteristics. GB is characterized by high inter-tumour and intra-tumour heterogeneity at cellular, molecular, histological, and clinical levels, resulting in poor and unchanged prognosis despite advancements in drug delivery strategies (Bastiancich, Da Silva and Estève, 2021). Standard treatment for GB follows the Stupp protocol which has been employed for the past 2 decades and involves maximal surgical resection, followed by radiotherapy and chemotherapy with temozolomide (TMZ) (Stupp *et al.*, 2017; Tan *et al.*, 2020). TMZ initiates DNA double-strand breaks, cell cycle arrest, and eventually cell death; however, it is associated with dose-limiting haematological toxicity (Singh *et al.*, 2021). Furthermore, TMZ is poorly soluble under physiological conditions and is prone to rapid hydrolysis that restricts its antitumour efficacy (Fang *et al.*, 2015). Drug resistance to TMZ is also often reported (Chien *et al.*, 2021). The size and anatomical location of GB tumours are major challenges to effective treatment as GB cells tend to overgrow rapidly, become highly invasive and migrate deep into fragile brain regions, leading to incomplete tumour resection and tumour relapse (Hatoum, Mohammed and Zakieh, 2019). In addition, a subpopulation of highly tumorigenic glioma stem cells (GSCs) with high plasticity and self-renewal properties add to tumour malignancy through their continued proliferation, invasion, stimulation of angiogenesis, reduction of anti-tumour immune responses and chemo-resistance (Wang *et al.*, 2018). Though not curative, extensive surgical resection is required to reduce the tumour size and relieve the intracranial pressure associated with GB symptoms and therefore presents a high risk of damaging healthy brain regions leading to further side effects.

Radiotherapy utilizes x-rays, gamma rays or other charged particles to induce DNA damage in cells (Baskar *et al.*, 2012). The main disadvantage of radiotherapy is the non-specificity as normal cell DNA is also damaged, leading to permanent neuronal damage and radio-resistance of tumours and its attendant relapses following high dose radiation treatment or even combination therapy (Mohan *et al.*, 2013). Although the Stupp protocol may extend survival times, it does not cure GB, hence without treatment, the survival time is usually 3 months (Harrison *et al.*, 2016). In 2015, a medical

device based on tumour treating fields was introduced and applied on GB patients. However, this device did not significantly improve the median overall survival rates (Stupp *et al.*, 2017).
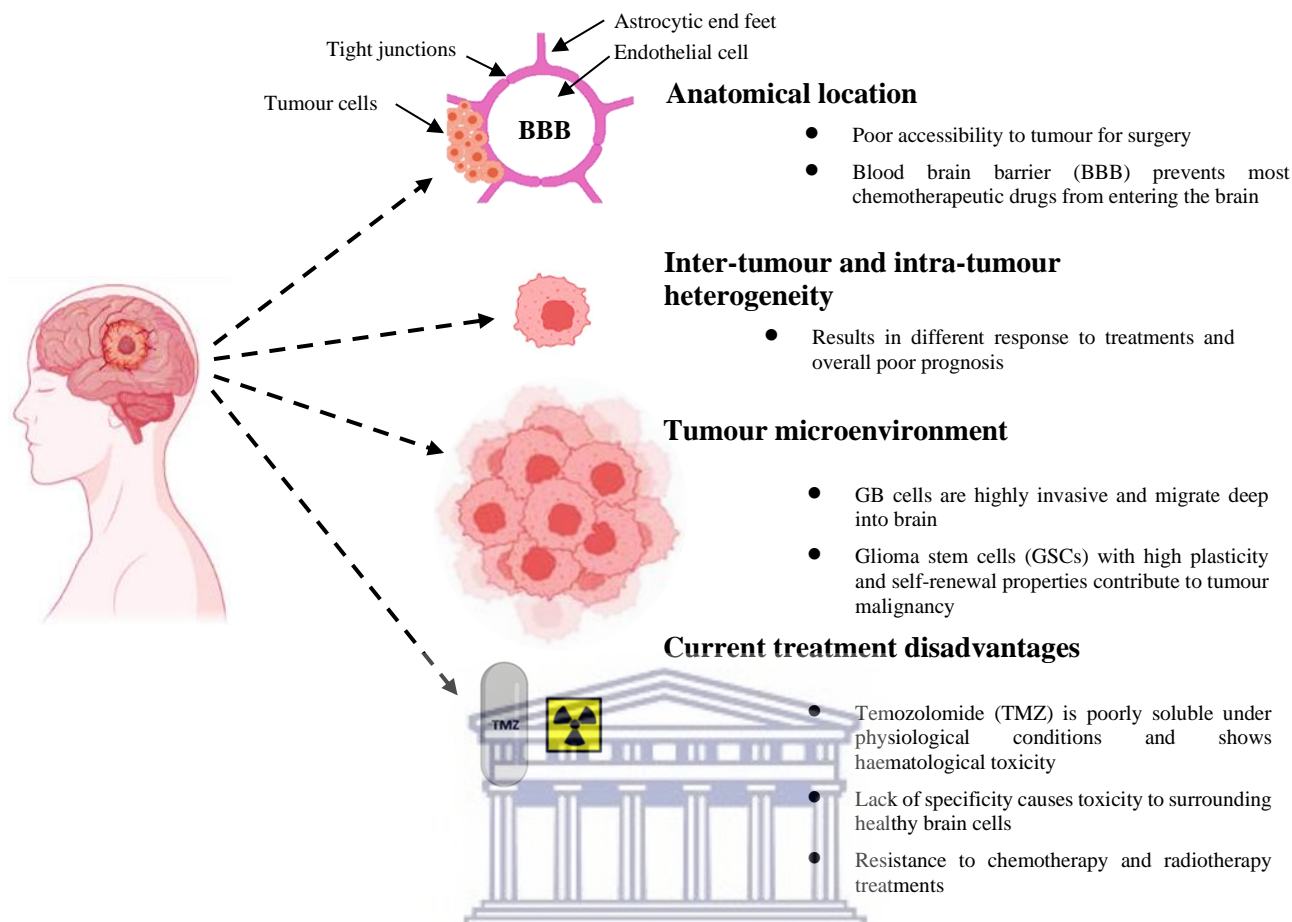
Figure 1. The characteristics and therapeutic challenges associated with glioblastoma (Figure adapted with permission from Bastiancich, Da Silva, and Estève 2021, Frontiers in Oncology, image created using BioRender.com)

3. Neuroblastomas (NBs): Standard treatments and challenges

Neuroblastomas (NBs) are the most frequent extracranial solid brain tumours diagnosed in childhood and one of the major challenges in paediatric oncology, with a 5-year survival rate for patients presenting with high-risk NB tumours being below 40 % (Smith and Foster, 2018). A NB is an embryonal tumour of the sympathetic NS that arises because of disturbances within the migratory route of primitive neural crest cells along the sympathoadrenal lineage and normally originates in the adrenal glands or the paravertebral ganglia (Luksch *et al.*, 2016). Thus, most tumours may be present in the neck, thorax, abdomen, and pelvis, as localized or metastatic tumours, while others may be

secondary to such mental disorders as Hirschsprung's disease or conditions like congenital central hypoventilation syndrome and neurofibromatosis type 1 (Rohrer *et al.*, 2002; Swift *et al.*, 2018; Pudela, Balyasny and Applebaum, 2020). NB cells may invade other tissues and metastasize to bone marrow, bones, lymph nodes, skin, liver, lung and the brain (Chu *et al.*, 2011; Rifatbegovic *et al.*, 2018). Studies have shown that overexpression of the MYCN oncogene, which is known to be involved in embryogenesis, is one of the predominant factors implicated in NB (Luksch *et al.*, 2016). On the other hand, the downregulation of the tyrosine kinase receptors (Trk), CD44 and overexpression of anaplastic lymphoma kinase (ALK) are the other molecular mechanisms that could lead to tumorigenesis or tumour expansion (Zhu *et al.*, 2012).

The standard treatment for NB consists of a coordinated sequence of chemotherapy, radiation therapy, surgical tumour resection, and combinations thereof, as well as myeloablative consolidation therapy with stem cell rescue and transplantation, 13-cis retinoic acid and immunotherapy (Mallepalli, Gupta and Vadde, 2019; Fati *et al.*, 2021). Surgery for low-risk NB may be sufficient support for chemotherapy with carboplatin, etoposide, cyclophosphamide and doxorubicin (Strother *et al.*, 2012). However, surgical interventions are invasive and incomplete tumour resection may require further chemotherapy, radiotherapy and possibly stem cell transplantation (Veschi, Verona and Thiele, 2019). For high-risk NB, long-term treatment with cisplatin, carboplatin, etoposide, vincristine, cyclophosphamide and doxorubicin may be effective, but causes systemic toxicity in the form of ototoxicity, thyroid function complications, cardiotoxicity, renal toxicity, future infertility complications and secondary malignancies (Emadi, Jones and Brodsky, 2009; Kumar *et al.*, 2012; Schacht, Talaska and Rybak, 2012; Shohet and Foster, 2017). The major long-term toxic side effects present as hearing loss, cognitive deficits, epilepsy, learning difficulties, endocrinopathies, growth reduction, thyroid function disorders, ovarian failure, and increased risks of secondary cancers (Trahair *et al.*, 2007; Hudson, 2010; Speckhart, Antony and Fernandez, 2017; Applebaum *et al.*, 2017; Friedman and Henderson, 2018). Despite available treatment options, NB remains a major challenge in paediatric oncology and most survivors of high-risk NB often show spontaneous tumour regression after treatment (Brodeur, 2018), with more than half of the survivors not responding to high-dose chemotherapy and demonstrating multi-drug resistance (Wang, Yao and Li, 2020). The overall cure rate for high-risk NB is approximately 50 % during the past two decades (Smith and Foster, 2018), and the lack of specificity of anticancer drugs to NB indicates that only low amounts of administered drugs can ultimately reach the tumour, with long lasting side effects.

4. Current challenges associated with drug delivery to the brain

A major challenge in the development of novel drugs for the treatment of NS tumours and other CNS diseases is the limitations posed by the BBB, which is the first line of defence from harmful substances in the blood that enters the brain circulation (Lampron, Elali and Rivest, 2013). The highly selective nature of the BBB is attributed to the combination of capillary endothelial cells that is held together by tight junction proteins, surrounding pericytes, the basal membrane and astrocytic end-feet (Castro Dias *et al.*, 2019). The BBB is approximately 200 nm thick, permitting the passage of small molecules (atomic mass < 400-600 Da) and hydrophilic molecules (atomic masses < 150 Da) via lipid-mediated diffusion, carrier-mediated transport systems and receptor-mediated transport systems, while strictly preventing the paracellular entry of most chemotherapeutic drugs (Pardridge, 2012; Belykh *et al.*, 2020). In addition, capillary endothelial cells in BBBs have a high concentration of drug efflux transporter proteins such as P-glycoprotein (P-gp) and multidrug resistance-associated proteins, resulting in reduced drug bioavailability (Thuerauf and Fromm, 2006).

As tumour cells invade the CNS and reach > 0.2 mm^3 of volume, the BBB is damaged and new blood vessels are formed through angiogenesis, leading to the formation of the blood-brain tumour barrier (BBTB) (Groothuis, 2000; Ferraris *et al.*, 2020). The newly formed capillaries are fenestrated, allowing the entry of approximately 12 nm-sized molecules through the BBTB (Sarin *et al.*, 2008). With cancer progression, there is the depletion of tight junction proteins and the capillary fenestrations become even more enlarged to allow for the passage of molecules of approximately 48 nm size and eventually 1μm size, at which stage the BBB integrity is considered completely compromised (Dubois *et al.*, 2014). The resultant leaky vasculature of most parts of the affected CNS tissue renders some chemotherapeutic drugs ineffective but peripheral areas of these tumours may have regions with an intact BBB resulting in the formation of favourable niches of cancer cell invasion and treatment resistance (Tamborini *et al.*, 2016). Thus, the combination of the BBB and the BBTB presents a unique challenge for brain tumour drug delivery.

The lack of specificity, poor drug delivery, drug resistance and severe toxic side effects associated with standard treatments for GB and NB, are limitations to the effective management of these tumours. The avoidance of the systemic toxicity induced by chemotherapy and radiation treatments is crucial especially within the paediatric age group associated with NB patients because this can cause permanent changes to the developing body and increased risk of secondary cancers later in life

(Q. Zhao, Liu, Zhang, *et al.*, 2020). Although there are many advances in research on GB and NB tumours in the past two decades, no effective treatments has been developed (Tan *et al.*, 2020; Wang, Yao and Li, 2020) as the current treatment options appear to be largely unsatisfactory and inconsistent results have been reported for their effects on prolonging the median survival time of patients. In addition, significant remission is reported for early-diagnosed tumours but not for advanced disease stages (Lombardi *et al.*, 2020; Sbeih *et al.*, 2020).

Improvements in all treatment modalities is required for successful management of cancers, and for GB and other CNS tumours, improved surgical resection techniques would result in fewer neurological side-effects and overall improvement in patient outcomes (McCutcheon and Preul, 2021). A better understanding of the exact mechanisms involved in drug delivery across dynamic biological barriers and the specific targeting of cancerous cells for treatment will foster novel and effective therapeutic strategies. Chlorotoxin (CTX) is one peptide that has recently generated interests in cancer research especially for the targeted treatment of most CNS tumours (Cohen-Inbar and Zaaroor, 2016; Cohen, Burks and Frank, 2018; Khanyile *et al.*, 2019), hence the development of CTX-based nanoparticle treatments could offer promising outcomes for CNS tumours as discussed below.

5. **Chlorotoxin (CTX): A promising natural targeting peptide for cancers**

In recent years, interests in exploiting the beneficial properties of venoms through the isolation of their peptides and investigating their efficacy as targeting molecules, have increased (Pennington, Czerwinski and Norton, 2018). CTX is derived from the venom of the deathstalker scorpion (*Leiurus quinquestriatus*) and is a 36-amino acid peptide stabilized by four disulfide bonds, used as a potent targeting moiety due to its ability to bind to cancerous tissues, with a high binding specificity for gliomas and NBs, and not to normal tissues (Soroceanu *et al.*, 1998; Lyons, O'Neal and Sontheimer, 2002). CTX has emerged as a promising targeting agent for brain tumours due to its ability to specifically bind to 74 of the 79 World Health Organization (WHO) brain tumour classifications (Lyons, O'Neal and Sontheimer, 2002). More than 15 normal human tissues have been shown to demonstrate negative CTX-binding properties (Soroceanu *et al.*, 1998; Lyons, O'Neal and Sontheimer, 2002).

CTX is considered safe and has been observed to permeate intact BBBs in both animal models and humans with brain tumours (Sun *et al.*, 2008a; Veiseh *et al.*, 2009a; Xiang *et al.*, 2011). It is also a promising agent for the imaging and treatment of gliomas as demonstrated in clinical trials (C. G. Patil *et al.*, 2019; Yamada *et al.*, 2021). A synthetic CTX peptide labelled with [131]I (commercial name ^{131}I-TM-601) has already undergone early phase clinical trials and received Food and Drug Administration (FDA) approval for a phase III trial in patients with newly diagnosed gliomas (Jacoby *et al.*, 2010). In addition to its high selectivity for targeting and binding of GB tumours, CTX has been shown to bind to a broad-spectrum of cancer cells including NB, medulloblastoma, breast cancer, ovarian cancer, prostate cancer, sarcoma, intestinal cancer, lung cancer and pancreatic cancer (Soroceanu *et al.*, 1998; Lyons, O'Neal and Sontheimer, 2002; Deshane, Garner and Sontheimer, 2003; Veiseh *et al.*, 2007; Kesavan *et al.*, 2010; Kievit *et al.*, 2010; El-Ghlban *et al.*, 2014; Qin *et al.*, 2014a; Ayomide *et al.*, 2018; McGonigle *et al.*, 2019; Y. Wang *et al.*, 2019). For peptides to be considered useful in therapeutics, they should normally possess the following characteristics: a small molecular size, contain at least three disulfide bonds and demonstrate clear activity on ion channels (Ojeda, Wang and Craik, 2016). In addition, receptors present on cancer cells for these peptides should be uniquely or highly overexpressed in comparison to non-malignant cells, and a tumour-to-normal-cell expression ratio of 3:1 or higher is usually preferred to achieve the desired therapeutic effects (Worm, Els-Heindl and Beck-Sickinger, 2020). Based on the above information, CTX meets all the important characteristics of a therapeutic peptide and is therefore a useful candidate in medical research considering its bioavailability and ability to induce target selectivity, which in turn reduces the side effects of drug resistance and systemic toxicity due to lack of specificity (Khanyile *et al.*, 2019). The selective binding of CTX to GB tumour cells has made its application as a targeting molecule for brain cancer therapy as well as a contrast agent for tumour optical imaging, very plausible (Cohen, Burks and Frank, 2018).

5.1. Molecular targets of CTX:

The exact mechanisms by which CTX targeting occurs is not completely understood but potential primary cell surface targets have been identified over the years (Figure 2). Some studies have shown that CTX is an effective blocker of small conductance epithelial chloride channels (DeBin and Strichartz, 1991; DeBin, Maggio and Strichartz, 1993) and mainly binds to overexpressed cancer cell surface receptors involved in the progression of tumours such as ClC-3 (chloride channel-3) in GB

cells (DeBin, Maggio and Strichartz, 1993; Ullrich and Sontheimer, 1996, 1997; Ullrich, Gillespie and Sontheimer, 1996; Ullrich *et al.*, 1998; Lyons, O'Neal and Sontheimer, 2002; McFerrin and Sontheimer, 2006; Lui *et al.*, 2010; B. Wang *et al.*, 2017) which forms a protein complex with matrix metalloprotease-2 receptor (MMP-2) (Deshane, Garner and Sontheimer, 2003; El-Ghlban *et al.*, 2014; Qin *et al.*, 2014a; Ayomide *et al.*, 2018; Pandey *et al.*, 2020); annexin A2 which is present in various cell lines (Kesavan *et al.*, 2010; Wang, Luo and Guo, 2013) and has since been shown to be a potential target of CTX, and more recently estrogen receptor alpha (ERα) (Y. Wang *et al.*, 2019) and the Neuropilin-1 (NRP-1) (McGonigle *et al.*, 2019; Sharma *et al.*, 2021) which is a vascular endothelial growth factor receptor responsible for tumour uptake. These molecules provide alternative methods for CTX targeting of tumours in cancer diagnosis and therapy.
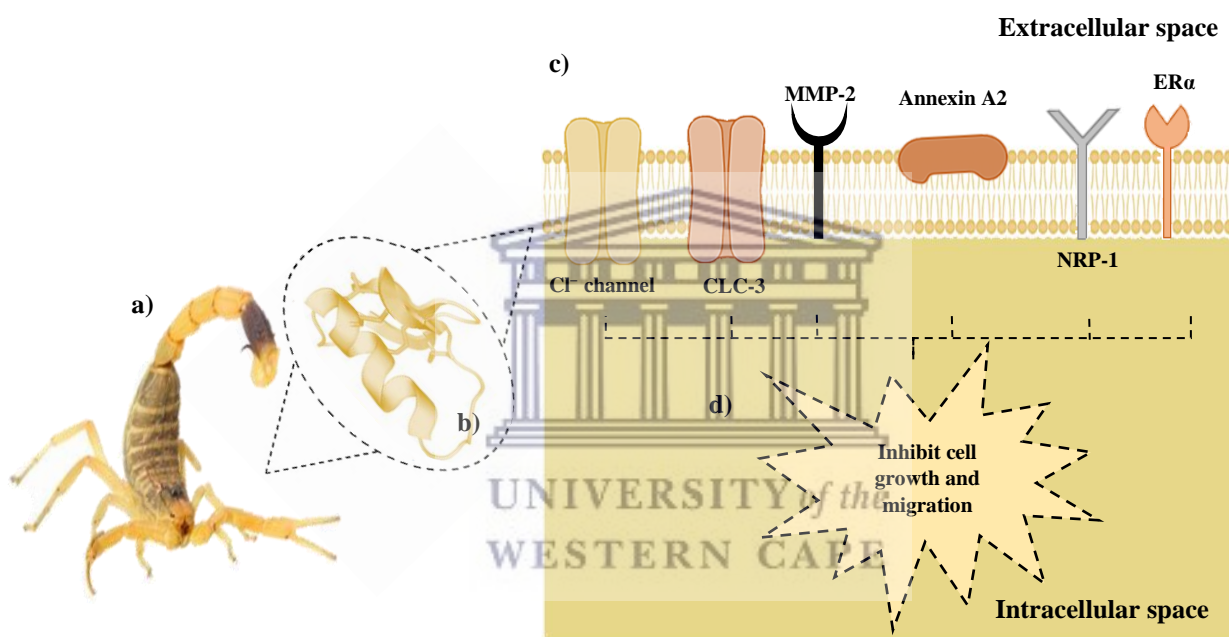
Figure 2. Proposed molecular targets for CTX. CTX is isolated from the venom of the deathstalker scorpion (*Leiurus quinquestriatus*) **(a)** and is composed of a 36-amino acid peptide stabilized by four disulfide bonds **(b)**. CTX has been shown to block Cl- channels, bind to overexpressed cell surface receptors found in various tumours such as: ClC-3, MMP-2, Annexin A2, NRP-1 and ERα **(c)**, all these receptors interact with CTX and ultimately contribute to an overall inhibition/suppression of cellular growth and migration **(d)** (image created with BioRender.com).

5.1.1. Chloride channels

Voltage-gated chloride (Cl-) channels are associated with the cell migration and proliferation of primary brain tumour cells (Soroceanu, Manning and Sontheimer, 1999; Ransom, O'Neal and Sontheimer, 2001). Glioma cell shrinkage can be inhibited by Cl- channel blockers leading to reduced cell invasion (Soroceanu *et al.*, 1998; Soroceanu, Manning and Sontheimer, 1999; Ransom, O'Neal and Sontheimer, 2001). Intracellular Ca^{2+} can be considered as a main regulator of cell motility due to Ca^{2+}-activated ion channels (Wei *et al.*, 2012) such as Ca^{2+}-activated K^+ channels which are known to increase glioma migration (Turner *et al.*, 2014). Among the chloride channel protein family, chloride channel-2 and 3 (ClC-2 and ClC-3) are upregulated in glioma and are involved in changes occurring in cellular size and shape that can be observed in dividing cells which rapidly invade extracellular brain spaces (Olsen *et al.*, 2003). ClC-3 has been suggested to affect the invasion and migration of glioma cells by forming protein complexes with membrane type-I matrix metalloproteinase (MMP), MMP-2, tissue inhibitor of metaloprotein-2, and αvβ3 integrin, co-localizing with Ca^{2+}-activated K^+ channel to lipid raft domains of invadopodia (Cheng *et al.*, 2014; Turner and Sontheimer, 2014).

The tumour-binding activity of a radioisotope ^{125}I-labeled CTX (^{125}I -CTX) was described by Soroceanu *et al*. (1998) who showed its accumulation in tumour cells of GB-bearing mice, sparing normal neurons and astrocytes. Similarly, melanoma, neuroblastomas, meduloblastomas, and small cell lung carcinomas in over 200 human surgical biopsy samples have shown CTX binding possibly because of their common neuro-ectodermal embryonic origin with glial cells (Lyons, O'Neal and Sontheimer, 2002). Normal human brain and other tissues have also been shown to be consistently negative for CTX immunostaining (Soroceanu, Manning and Sontheimer, 1999).

The inhibitory effect of CTX on human GB-associated chloride channels was described by Ullrich *et al*. (1996) and they also discovered the existence of specific CTX-sensitive glioma chloride currents in acute slices of human gliomas (Ullrich *et al.*, 1998). Cheng *et al*. (2014) described the blocking activity of CTX on a single Cl specific peptide blocker, a glioma-specific chloride channel (GCC) while Turner and Sontheimer (2014) reported high-grade tumours expressing GCC more than low-grade tumours, while healthy tissues or tumours of non-glial origin poorly expressed these channels. GCC activity has also been suggested to regulate apoptosis and to be linked to changes in cellular

35

cytoskeleton (Ullrich and Sontheimer, 1997) as well as glioma cell morphology, proliferation and migration (Ullrich and Sontheimer, 1997; Habela *et al.*, 2009).

CTX was found not to inhibit volume-regulated, calcium-activated and cyclic AMP-activated chloride channels expressed in different human, bovine and monkey cells using concentrations of up to 1.2 µM (Maertens *et al.*, 2000). However, Dalton and colleagues evaluated astrocytes found in injured adult rat brains and showed that CTX could inhibit calcium-activated chloride currents with an EC50 of ~50 nM (Dalton *et al.*, 2003). It remains unclear if CTX may inhibit calcium-activated Cl⁻ channels; therefore, further research is required.

From the literature, it can be inferred that chloride channels may act as one of the markers of interest for targeting cancers, because of their role in tumour migration and growth, however the findings reviewed above suggest the involvement of more than one type of chloride channel as GBs present with CTX being highly sensitive to ClC-3.

5.1.2. *Matrix Metalloproteinase-2 (MMP-2)*

Matrix metalloproteinases (MMPs) are a family of calcium-dependent, zinc-containing endopeptidases, which are responsible for tissue remodelling and the degradation of the extracellular matrix (ECM), thus releasing several proteolytic and growth factors which contribute to tumorigenesis (Gonzalez-Avila *et al.*, 2019; Siddhartha and Garg, 2021). Thus, MMPs have invasive properties to tumour cells, regulate angiogenesis, trigger cell proliferation and are upregulated in most cancer types, making them very important biomarkers for tumour detection (Quintero-Fabián *et al.*, 2019). High levels of MMP-2 and MMP-9 have been observed in patients with high-grade GB and high-risk NB and associated with tumour progression (Ara *et al.*, 1998; Sugiura *et al.*, 1998; Noujaim *et al.*, 2002; Roomi *et al.*, 2017; Pullen *et al.*, 2018; Zhou *et al.*, 2019). MMP-2 appears to be a more promising molecular target of CTX (Deshane, Garner and Sontheimer, 2003), as its activation is a vital process required by GB for the degradation of the ECM during cell invasion and migration (Roomi *et al.*, 2007).

Although some researchers have suggested that MMP-1 plays a more important role than MMP-2 in the migration, remodelling and invasiveness of GB (Lu *et al.*, 2011), it has been shown that high levels of MMP-2 play a more important role in the virulent progression of cancer through its contribution to three vital processes: angiogenesis, metastasis and invasion (Chintala, Tonn and Rao,

1999; Haas and Madri, 1999; Quintero-Fabián *et al.*, 2019). MMP-2 is specifically upregulated in gliomas as well as in other tumours of neuroectodermal origin such as NB, but not in the normal cells of the CNS (Lyons, O'Neal and Sontheimer, 2002; Deshane, Garner and Sontheimer, 2003). In addition, MMP-2 expression is related to tumour aggressiveness and grade (Ullrich and Sontheimer, 1997; Olsen *et al.*, 2003) and is reduced by CTX binding (Deshane, Garner and Sontheimer, 2003). The reduced binding efficiency of CTX to GB cells in the presence of an MMP-2 inhibitor was demonstrated in a study by Veiseh *et al.* (2007). Jacoby *et al.* (2010) proposed that CTX interacts with a cell surface protein complex that consists of MMP-2, membrane type-I MMP, a transmembrane inhibitor of metalloproteinase-2 as well as αvβ3, an integrin suggested to play an important role in angiogenesis and neural tumour invasion (Dearling *et al.*, 2013).

The structure of CTX is stabilized by 4 disulfide bonds and contains β-sheet and helical structure. A computational study which predicted the binding of CTX with MMP-2 suggested that the β-sheet of CTX interacts in a region between the collagen binding domain and the catalytic domain of MMP-2, whereas the α-helix of CTX does not appear to be involved in the interaction (Othman *et al.*, 2017). CTX has also been shown to inhibit MMP2 activity through fluorescence resonance energy transfer (FRET) substrate assay and gelatin zymography (Alam *et al.*, 2012). From the literature, it is proposed that ClC-3 and MMP-2 form a protein complex which is targeted by the CTX-peptide and this action is thought to inhibit glioma cell migration and invasion through the induction of endocytosis of the MMP-2/ClC-3 protein complex (Deshane, Garner and Sontheimer, 2003; McFerrin and Sontheimer, 2006; Lui *et al.*, 2010). Hence, CTX targeting to MMP-2 has been widely investigated and proposed as one of the main molecular mechanisms for the development of CTX-based treatments for gliomas (Deshane, Garner and Sontheimer, 2003; Veiseh *et al.*, 2007; 2009a; Jacoby *et al.*, 2010; Kovar *et al.*, 2013; El-Ghlban *et al.*, 2014; Qin *et al.*, 2014a; Ayomide *et al.*, 2018; Y. Wang *et al.*, 2019).

5.1.3. *Annexin A2*

The Annexin protein family is a group of calcium-dependent phospholipid-binding proteins, involved in the repair of plasma membrane lesions triggered by different stimuli (Lizarbe *et al.*, 2013) as well as the control of various cellular functions including vesicle trafficking, vesicle fusion, and membrane segregation in a Ca^{2+}-dependent manner through the binding of anionic phospholipids (Miwa, Uebi and Kawamura, 2008). Other roles in cellular functions include angiogenesis, apoptosis, cell migration, proliferation, invasion and cohesion (Zhang *et al.*, 2012; Staquicini *et al.*, 2017; Valls *et*

37

al., 2021). In addition, annexins and their binding partners (the S100 proteins) are recognized regulators of the cellular actin cytoskeleton (Lauritzen, Boye and Nylandsted, 2015). The surface protein annexin A2, a calcium-binding cytoskeletal protein localized on various tumour cells, has been shown to be a receptor for CTX on the surface of human cancer cell lines (Kesavan *et al.*, 2010; Wang, Luo and Guo, 2013) and to be involved in cell migration, invasion and adhesion (Staquicini *et al.*, 2017; J. Wang *et al.*, 2019; Ma and Wang, 2021). Annexin A2 cell surface receptors have been implicated as molecular targets for CTX, based on studies on the effects of the commercially available CTX (TM-601) in human umbilical vein endothelial cells and human tumour cell lines (Kesavan *et al.*, 2010). The A2-complex comprises annexin-A2 and the protein p11, shown to be overexpressed on the surfaces of GB and is associated with poor prognosis (Seckinger *et al.*, 2012; Li *et al.*, 2021). TM-601 specifically binds to glioma cells but not normal brain tissues (Hockaday *et al.*, 2005) and found to bind the surfaces of Panc-1 cells as well, depending on the level of annexin A2 expression (Kesavan *et al.*, 2010). A small interfering ribonucleic acid (siRNA) knockout of annexin A2 was found to result in reduced binding of a technetium-99m-labelled-TM601 in cell lines expressing annexin A2 (Tatenhorst *et al.*, 2006). A recent study demonstrated CTX binding to Hela cells known to overexpress Annexin A2 (Díaz *et al.*, 2019).

5.1.4. Estrogen receptor alpha (ERα)-mediated signalling pathway

Estrogen activates the estrogenic receptor (ER) signalling pathway and stimulates the expression of different genes that are involved in cell proliferation, causing breast cancer and related malignancies (Rothenberger, Somasundaram and Stabile, 2018). Studies have shown that ER can regulate the invasion and metastasis of tumour cells (Saha Roy and Vadlamudi, 2012; Hua *et al.*, 2018; Lombardi *et al.*, 2021), hence targeting of ER signalling pathways is one of the important strategies for breast cancer treatment. A recent study by Wang *et al*. (2019) found that CTX significantly inhibited breast cancer cell proliferation, migration and invasion through binding to estrogen receptor alpha (ERα) to inhibit the expression of ERα, which inhibits the ERα/vasodilator stimulated phosphoprotein (VASP) signalling pathway.

5.1.5. Neuropilin-1 (NRP-1)

The most recent molecular target suggested for CTX is Neuropilin-1 (NRP-1), a vascular endothelial growth factor (VEGF) (Kolber-Simonds et al. 2018; McGonigle et al. 2019; Sharma et al. 2021),

known to be overexpressed in many cancers but naturally upregulated in normal lung and heart tissues (Roche, Drabkin and Brambilla, 2013; Roy *et al.*, 2017; Dumond and Pagès, 2020; S.-D. Liu *et al.*, 2021). Using nuclear magnetic resonance (NMR) spectroscopy and isothermal titration calorimetry (ITC), Sharma *et al.* (2021) characterized the binding of CTX to the b1-domain of NRP1 (NRP1-b1) via a non-canonical primary sequence that satisfies the receptor binding motif through its tertiary fold. A novel peptide drug conjugate called ER-472, comprised of CTX linked to a cryptophycin analog, was found to possess antitumor activity related to NRP1 expression levels in xenografts, and its potency was significantly reduced following treatment with NRP-1 blocking antibodies or following knockout in tumour cells, confirming a role for NRP1-binding in ER-472 activity (McGonigle et al. 2019).

All the potential CTX molecular targets and receptors described above, appear to be over-expressed in diverse tumours, with MMP-2, Cl- channels and Annexin A2 being the most widely investigated receptor targets; these are also known to be present in GB and NB. A recent study showed that neither CTX-CONH$_2$ nor CTX-COOH affected cytotoxicity in a variety of Human tumour cell lines (U87MG, MCF-7, PC3 and A549) suggesting that terminal arginine amidation may not play an important role in the cytotoxic properties of CTX (Ayed *et al.*, 2021). Other studies suggested that the C-terminal region plays a critical role in the bioactivity of CTX and inhibition of cancer growth and migration (Jacoby *et al.*, 2010; Dastpeyman *et al.*, 2019; McGonigle *et al.*, 2019). The exact mechanisms of CTX targeting action on cancer cells requires further investigation, perhaps through more detailed analysis that specifically identifies the structural determinants of CTX that are involved in binding to the respective potential receptors.

5.2. The blood–brain barrier crossing potential of CTX

In addition to drug delivery for GB, the use of CTX as a carrier for delivering levodopa has been shown to result in increased distribution of dopamine in the brains of Parkinson's disease mice (Xiang *et al.*, 2012). Thus, CTX has been shown in several studies to demonstrate considerable potential for crossing the BBB to bind specifically to malignant brain tissue (Fu *et al.*, 2012; Dardevet *et al.*, 2015; Cohen-Inbar and Zaaroor, 2016; Ojeda, Wang and Craik, 2016; Cohen, Burks and Frank, 2018), and further diffuse deeply into the tumour environment, unlike other targeting agents like antibodies (Mamelak *et al.*, 2006; Cohen, Burks and Frank, 2018). CTX conjugated to fluorescent imaging

agents and dyes such as Cy5.5 and 800CW, were shown to bind to GB tumours in mice when delivered via tail injection (Veiseh *et al.*, 2007; Kovar *et al.*, 2013).

Blaze Bioscience, Inc. has developed a fluorescent imaging agent composed of CTX covalently attached to the near-infrared fluorophore indocyanine green, commercially known as BLZ-100 (other names include: tozuleristide or Tumor Paint®) which is known to target tumour tissue for a complete and more precise surgical resection of brain tumours (Yamada *et al.*, 2021). In addition, BLZ-100 demonstrated success in the preclinical resection of glioma (Butte *et al.*, 2014), head and neck carcinoma (Baik *et al.*, 2016), and soft-tissue sarcoma (Fidel *et al.*, 2015). It has passed Phase I clinical trial and does not demonstrate any toxicity for doses up to 30 mg (C. G. Patil *et al.*, 2019; Yamada *et al.*, 2021). Presently, BLZ-100 is going through a joint Phase II/III trial for fluorescence-guided resection of paediatric CNS tumours (NCT03579602) (C. G. Patil et al., 2019; Belykh *et al.*, 2020). The mechanism by which CTX crosses the BBB is not fully understood, however Annexin A2 expression in BBB vascular endothelial cells has been suggested (Kesavan *et al.*, 2010).

6.   Nanotechnology for cancer applications

The development of novel diagnostic and therapeutic tools for the treatment of cancer requires innovations within the field of nanotechnology involving nanoparticles (NPs) (1-100 nm) which possess unique chemical, physical and biological properties that render them attractive for biomedical applications, including in neuroscience research (Saeedi *et al.*, 2019; Opris *et al.*, 2020). NPs that deliver therapeutic drugs along with an imaging moiety may provide multiple functions like targeting, tracking, imaging and treatment and are commonly referred to as "theranostic approaches" (Mendes *et al.*, 2018). NPs are comprised of polymers, lipids, or metals, among other materials, that allow for encapsulation or surface conjugation with multiple therapeutic agents like small molecules, peptides, or nucleic acids (Mitchell *et al.*, 2021), with better therapeutic outcomes for many antitumour compounds (Bayón-Cordero, Alkorta and Arana, 2019). Based on their sizes, NPs are naturally attracted to tumour sites with extensive abnormal angiogenesis, a phenomenon known as the enhanced permeability and retention effect (EPR) and often explored for passive targeting (Prabhakar *et al.*, 2013; Huang *et al.*, 2021; Wu, 2021). Passive targeting allows for the efficient localization of NPs within the tumour microenvironment, while active targeting facilitates the uptake of NPs by the tumour cells (Attia *et al.*, 2019). One main disadvantage of passive targeting is that it cannot be used

for all tumours due to varied phenotypes (Moreno-Sánchez *et al.*, 2016), hence active targeting approaches are preferred.

In normal vasculature, endothelial junctions are ~ 5-10 nm in width but in tumour tissues, sizes of 100-780 nm have been reported, depending on the tumour type (Hashizume *et al.*, 2000; Haley and Frenkel, 2008). Thus, NPs of 15 > 50 nm diameter size easily cross the intact BBB (Ohta *et al.*, 2020; Sokolova *et al.*, 2020) but in large and advanced brain tumours with extensive angiogenesis, the disrupted BBB allows NPs of size ranges of 5-200 nm to cross (Ohta *et al.*, 2020; Sokolova *et al.*, 2020). Other factors like size, specificity for target sites, biocompatibility, stability in blood, evasion of the reticulo-endothelial system (RES), site-specific drug release, etc. may also play a role (Agarwal *et al.*, 2018). Smaller NPs have larger surface areas which permit increased surface loading of therapeutic agents, while also promoting entry through tiny membrane passageways and increased drug bioavailability (Yetisgin *et al.*, 2020). Thus, low doses or concentrations of therapeutic agents can be used, and systemic toxicity may be avoided (Yetisgin *et al.*, 2020). The ideal size for maximum effect is 15-100 nm diameter as NPs below 10 nm can be cleared by the kidneys and those > 150 nm will be removed by the RES (Li and Huang, 2009; Choi *et al.*, 2011), whereas NPs > 200 nm are usually considered undesirable for *in vivo* biomedical applications (Hoshyar *et al.*, 2016).

Active targeting of NP drug delivery systems in cancer therapy allows the drug effects to be specifically directed to cancer cells, facilitated by specific recognition binding sites that are either overexpressed on the surfaces of cancer cells or expressed at lower levels in normal cells (Fu *et al.*, 2020). Active targeting strategies have been accomplished by conjugating NPs with antibodies, peptides and aptamers; however, for monoclonal antibodies (mAbs) that are generally used as targeting molecules for the targeted delivery of NPs, their large size, limited tissue penetration, cellular uptake and conjugation difficulty to NPs, present significant challenges (Haggag, El-Gizawy and Osman, 2018; M. Liu *et al.*, 2021).

Peptides are considered more attractive targeting molecules based on their smaller size, lower immunogenicity, lower production costs, similar binding affinities to mAbs, easier synthesis and modification methods (Accardo, Tesauro and Morelli, 2013; Jeong *et al.*, 2018; Goddard *et al.*, 2020). In addition, peptides have a higher diversity, specificity, and targeting capability compared to other small molecule ligands (Haggag, El-Gizawy and Osman *et al*., 2018; Sasikumar and Ramachandra, 2018). Surface modification of NPs with synthetic polymers such as the FDA approved polyethylene

41

glycol (PEG) and other synthetic polymers such as polyvinyl alcohol (PVA), polyethylenimine (PEI) or chitosan, act to enhance the solubility of hydrophobic materials and improve biocompatibility of NPs through decreasing nonspecific binding and prolonging circulation durations *in vivo* (Suk *et al.*, 2016; Hoang Thi *et al.*, 2020). These synthetic polymers also allow for the attachment of targeting molecules onto NPs for active targeting through modification of terminal ends with various functional groups (Suk *et al.*, 2016).

In nearly two decades, many CTX NP-based applications have proven to be novel diagnostic and targeting treatment agents for GB considering the many beneficial characteristics they possess, including their ability to penetrate the BBB, their high binding specificity for gliomas and other neuroectoderm-derived cancers, their ease of being internalized into tumour cells leading to prolonged retention time. Other reported characteristics include their low toxicity or immunoreactivity profiles in human trials as well as the ease at which their structure can be modified to conjugate a variety of imaging or therapeutic agents without compromising the functionality of the peptide (Cohen, Burks and Frank, 2018). Thus, CTX-based NPs may be considered as highly promising platforms for diagnostic imaging and targeted drug delivery for NS tumours.

7. CTX-NPs with diagnostic potential

Advances in nanotechnology innovation have resulted in the development of less invasive diagnostic and therapeutic approaches with high precision and specificity. Thus, there are many nano-based applications which incorporate CTX to improve the visualization of GB tumours, as summarized in Table 1. Some of the CTX-conjugated NPs with diagnostic potential for GB have been used in magnetic resonance imaging (MRI), optical imaging and single-photon emission computed tomography (SPECT) (Dardevet *et al.*, 2015; Ojeda, Wang and Craik, 2016; Cohen, Burks and Frank, 2018). CTX-NPs delivered to target tumour tissues serve as MRI contrast molecules, while fluorophores or fluorescent probes that bind to molecular targets in tumours have been detected by optical imaging (Cohen, Burks and Frank, 2018). These techniques allow for precision-guided surgery without affecting normal tissues, based on the targeting function of CTX and the physicochemical characteristics of NPs. The conjugation of CTX to a fluorescent molecular probe, Cy5.5, described as ''tumour paint'' was first used for intraoperative imaging (Veiseh *et al.*, 2007) while a CTX functionalized iron oxide multifunctional nanoprobe (IONP-PEG-CTX) which could

42

target glioma cells, was detectable by MRI (Veiseh *et al.,* 2005) although superparamagnetic iron oxide NPs (SPIONPs) have now replaced these nanoprobes because they better enhance MRI.

The application of CTX-functionalized SPIONPs for MRI/Optical imaging remains an area of active research (Veiseh *et al.*, 2005; Sun *et al.*, 2008a; 2008b; Veiseh *et al.*, 2009a; Kievit *et al.*, 2010; Lee *et al.*, 2010; Wan *et al.*, 2010; Cheng *et al.*, 2016). Iron oxide NPs (IONPs) are composed of solid iron oxide cores (typically magnetite, Fe_3O_4, or its oxidized form maghemite, γ-Fe_2O_3) usually coated with synthetic polymers like PEG, polyvinyl alcohol (PVA), polyethylenimine (PEI), or chitosan to enhance the solubility of hydrophobic materials, limit the non-specific binding (thus prolonging circulation time), and enhancing tumour-specific targeting (Sangaiya and Jayaprakash, 2018). SPIONPs in a size range of 60-150 nm can possess different magnetic properties and functions differently in various applications (Thorek *et al.*, 2006). Local interactions between iron and water protons accelerate the dephasing of protons to shorten transverse T2 relaxation times and enhance MRI contrast upon T2* imaging (Liu *et al.*, 2016).

Some studies have shown that CTX functionalization onto the surface of IONPs using PEG or a copolymer of PEG and chitosan resulted in high targeting and the ability to cross the BBB (Veiseh *et al.*, 2005; Sun *et al.*, 2008b; Veiseh *et al.*, 2009a; 2009c; Wan *et al.*, 2010). The addition of Cy5.5 to CTX-IONPs in genetically engineered mice with no systemic toxicity, was found to improve the targeting of glioma cells, the inhibition of glioma cells, easy crossing of the BBB and prolonged detection of tumour cells by optical imaging and MRI (Veiseh *et al.*, 2007; 2009c; Li *et al.*, 2015; Ai *et al.*, 2017). The precise real-time detection of small foci of cancer cells with tumour margins could be achieved by optical imaging without affecting the BBB using CTX-NPs (Sun *et al.*, 2008b).

Fluorescence-based nano-imaging probes such as quantum dots (QDs) that provide excitation/emission wavelengths ranging from ultraviolet (UV) to near infrared (NIR) light, have also been used with CTX. QDs are composed of metals such as cadmium (Cd), zinc (Zn), selenium (Se), indium (In), tellurium (Te), and have several significant advantages over fluorescent dyes and molecules (Jha *et al*., 2018; Tarantini *et al*., 2019). QDs exhibit broad absorption and narrow emission spectra which makes them produce brighter emissions and have a higher signal-to-noise ratio compared with other fluorescent dyes (Chou and Dennis, 2015), and resistant to photo-bleaching (Liang *et al.*, 2021). Cadmium-free silver-indium-sulfide QDs conjugated to CTX [QD(Ag-In-S/ZnS)-CTX] were developed by Chen *et al*. (2015) for cellular imaging studies and showed specific

internalization into U87 human brain cancer cells while a stable polymer-blend dots CTX conjugate (PBdot-CTX) capable of crossing the BBB and specifically targeting tumour tissue in the ND2:SmoA1 medulloblastoma mouse model, was also developed (Wu *et al.*, 2011). The 15 nm PBdot-CTX conjugate was unaffected by photo-bleaching and was 15 times brighter than QDs (Wu *et al.*, 2011). The use of QDs may offer great advantages in experimental drug targeting and imaging but limited for clinical use due to reported toxicity (Reshma and Mohanan, 2019; Liu and Tang, 2020).

A class of NPs called up-converting NPs (UCNPs) have been reported as fluorescent imaging agents due to their ability to absorb low energy near infra-red light (NIR) and "up-convert" to emit in the visible spectrum (Yu *et al.*, 2010). This characteristic allows tissue penetration of excitation light and minimizes auto-fluorescence, with the added benefit of photo-stability and prolonged fluorescing (Stroud, Hansen and Olson, 2011). This allows UCNPs to be exploited for bio-imaging, bio-detection, and photodynamic therapy (Gao *et al.*, 2021). UCNPs composed of polyethylenimine-coated hexagonal-phase thulium doped sodium yttrium fluoride (NaYF(4):Yb), co-doped with erbium and cerium (NaYF4:Yb, Er/Ce) nanorods functionalized with CTX (PEI-NaYF(4):Yb, Er/Ce-CTX) have been shown to target C6 glioma-xenograft tumours *in vivo* without toxicity (Yu *et al.*, 2010).

Deng *et al*. (2014) showed that CTX-conjugated lanthanide-ion doped sodium gadolinium fluoride NPs (NaGdF4-Ho^{3+}-CTX) demonstrated targeting towards glioma cells *in vitro* and *in vivo*, using MRI and fluorescence imaging techniques. Gu *et al*. (2014) developed a glioma-targeted contrast agent by conjugating CTX to PEG-coated gadolinium oxide NPs (CTX-PEG-Gd$_2$O$_3$ NPs). The r1 value of CTX-PEG-Gd$_2$O$_3$ NPs (8.41 mM^{-1} s^{-1}) was higher than that of commercially available Gd-DTPA (4.57 mM^{-1} s^{-1}) and the enhancement of T1 contrast with a prolonged retention period up to 24 hours within the brain glioma was observed due to CTX conjugation with low cytotoxicity. Similarly, europium-doped gadolinium oxide nanorods (Eu-Gd$_2$O$_3$ NRs) with paramagnetic and fluorescent properties were conjugated with doxorubicin (DOX) and CTX via PEGylation (CTX-PEG-Dox-Eu-Gd$_2$O$_3$ NRs) and found to target glioblastoma, deliver significant amounts of DOX to tumour sites and enhance MRI of the intracranial tumours in *in vivo* mouse models (Zhang *et al.*, 2020). Dendrimer-based NPs are highly branched spherical structures that offer multifunctional applications in diagnosis and therapeutics (Sk and Kojima, 2015). Huang *et al*. (2011) developed CTX-modified dendrimer-based conjugates that incorporated the MRI contrast molecule gadolinium (Gd(III)) which was composed of a L-lysine dendritic macromolecule conjugated to CTX either with

44

Gd chelates or distyryl-substituted boradiazaindacene (BODIPY) fluorophore, resulting in enhanced uptake and retention time in tumour cells without toxicity. Many other CTX-dendrimer NPs have since been developed (Wu *et al.*, 2010; Cheng *et al.*, 2016; Sun *et al.*, 2017; Zhao *et al.*, 2019). NIR fluorescent moieties are well suited for intraoperative CTX-based conjugates used for the identification of pre-malignant lesions and to improve the visualization of tumour boundaries. These moieties are poorly absorbed by water or haemoglobin, and this decreases the interference from auto-fluorescence and optimizes signal intensity. Studies have shown that NIR fluorescent molecules modified with CTX such as Cy5.5 and IR Dye 800CW or indocyanine green (ICG) increased specificity and targeting with no impact on the efficacy of CTX for optical imaging (Kovar *et al.*, 2013; Butte *et al.*, 2014; Chen *et al.*, 2015; Staderini *et al.*, 2018; C. G. Patil *et al.*, 2019; Belykh *et al.*, 2020; Yamada *et al.*, 2021). A few studies have reported the use of NIR fluorescent molecules modified with CTX as well for MRI and other forms of imaging (Lee *et al.*, 2010; Li *et al.*, 2015; Ai *et al.*, 2017).

CTX has also been used in nuclear-based imaging techniques such as positron emission tomography (PET) and single photon emission computed tomography (SPECT) both of which have been exploited for dual imaging and treatment. Zhao *et al.* (2015b) first developed CTX multifunctional dendrimers labelled with radioactive ^{131}I for SPECT imaging and radiotherapy of gliomas, followed by ^{131}I-labeled CTX-functionalized gold NP entrapped in polyethylene naphthalate (poly(ethylene 2,6-naphthalate) (^{131}I-labeled CTX- Au-PENPs) which was used as a nanoprobe for targeted SPECT/CT imaging in *in vitro* and *in vivo* radionuclide therapy of gliomas in a subcutaneous tumour model that also demonstrated BBB permeability (Sun *et al.*, 2019; Zhao *et al.*, 2019). Other theranostic NP formulations developed, include a polyethylenimine (PEI), a methoxypolyethylene glycol (mPEG) CTX targeting, and a diethylenetriaminepentaacetic acid (DTPA) for ^{99m}Tc radiolabeling DOX-loaded NPs (mPEI-CTX-^{99m}Tc/DOX) (Zhao *et al.*, 2020). These authors also found that the theranostic nanocomplex demonstrated enhanced BBB permeability and tumour-targeting efficiency for gliomas using SPECT imaging and *in vivo* DOX drug delivery. CTX silver NPs (CTX-AgNP) was first studied in U87 human GB cell line (Locatelli *et al.*, 2012) but a novel CTX-based polymeric NP radiolabelled with ^{99m}Tc containing alisertib and silver NPs (Ag/Ali-PNPs-CTX-^{99m}mTc), was later developed as a theranostic agent (Locatelli *et al.*, 2014b) and its targeting ability was tested on the U87 GB cell line and found to allow for *in vivo* visualization of bio-distribution in U87 tumour-bearing mice (Locatelli *et al.*, 2014b).

Table 1. Summary of CTX-NPs for diagnostic applications

Name of Nanoparticle (NP) formulation	Imaging Modality	Size in nm (hydrodynamic size/ core size)	References
mPEI-CTX-^{99m}Tc/DOX	SPECT	394.77 nm	(L. Zhao *et al.*, 2020a)
CTX-PEG-Dox-Eu-Gd$_2$O$_3$ NRs	MRI	116.3 nm	(Zhang *et al.*, 2020)
^{131}I-labeled BmK-Au-PENPs	SPECT/CT	147 nm	(Sun *et al.*, 2019)
^{131}I-labeled CTX-Au-PENPs	SPECT/CT imaging	151 nm	(Zhao *et al.*, 2019)
Fe$_3$O$_4$/PEG-FA–Cy5.5-CTX	MRI	< 20 nm	(Ai *et al.*, 2017)
^{131}I-G5.NHAc-HPAO-(PEG-BmK CT)-(mPEG)	SPECT imaging	N/A	(Cheng *et al.*, 2016)
SPIONP-PEG-CTX	MRI	< 100 nm	(Chen *et al.*, 2016)
QD(Ag-In-S/ZnS)-CTX	Optical imaging	126 nm	(Chen *et al.*, 2015)
Fe$_3$O$_4$/MnO–Cy5.5-CTX	MRI	25 nm	(Li *et al.*, 2015)
Ag/Ali-PNPs-CTX-^{99m}Tc	Optical imaging	199 nm	(Locatelli *et al.*, 2014b)
NaGdF4-Ho^{3+}-CTX	MRI/Optical imaging	44.2 nm	(Deng *et al.*, 2014)
CTX-PEG-Gd$_2$O$_3$	MRI	3.46 nm	(Gu *et al.*, 2014)
Pdot-CTX	Optical imaging	~ 15 nm	(Wu *et al.*, 2011)
Gd-DTPA/BODIPY-dendrigraft poly-L-lysines-PEG-CTX	MRI	N/A	(Huang *et al.*, 2011)
SPIONP-PEG-PEI-siRNA-CTX	Optical imaging	7.5 nm	(O. Veiseh et al. 2010)
IONP-PEG-Chitosan-DNA-CTX	MRI	48.8 nm	(Kievit *et al.*, 2010)
MFNP–CTX	MRI/Optical imaging	< 100 nm	(Wan *et al.*, 2010)
IONP-PEG-Chitosan-Cy5.5-CTX	MRI/Optical imaging	7 nm	(Lee *et al.*, 2010)
PEI-NaYF(4):Yb, Er/Ce-CTX	Optical imaging	Width: 55 nm; length: 25 nm	(Yu *et al.*, 2010)
NP-MTX-CTX	MRI	5-8 nm	(Sun *et al.*, 2008a)
IONP-PEG-CTX	MRI	10-15 nm	(Sun *et al.*, 2008b)
SPIONP-FITC-CTX	MRI/Optical imaging	80 nm	(Meng *et al.*, 2007)
IONP-PEG-CTX	MRI/Optical imaging	10.5 nm	(Veiseh *et al.*, 2005)

Abbreviations: MRI: Magnetic resonance imaging; SPECT: Single-photon emission computed tomography; CTX: Chlorotoxin; mPEI-CTX-^{99m}Tc/DOX: methoxypolyethylene glycol (m), polyethylenimine (PEI) ^{99m}Tc radiolabelling NP loaded with doxorubicin (DOX); CTX-PEG-Dox-Eu-Gd$_2$O$_3$ NRs: Doxorubicin and CTX conjugated to polyethylene glycol coated gadolinium oxide NPs; ^{131}I-labeled BmK-Au-PENPs: iodine-131 (^{131}I-labeled) PEI-entrapped gold nanoparticles (Au PENPs) surfaced functionalized with Buthus martensii Karsch CTX like peptide (BmK); ^{131}I-labeled CTX-Au-PENPs: iodine-131 (^{131}I-labeled) PEI-entrapped gold nanoparticles (Au PENPs) surfaced functionalized with CTX; Fe$_3$O$_4$/PEG-FA–Cy5.5-CTX: IONPs functionalized with polyethylene glycol and PEGylated folic acid (FA) labeled with Cy5.5 and CTX; ^{131}I-G5.NHAc-HPAO-(PEG-BmK CT)-(mPEG): Bmk-CT: Buthus martensii Karsch CTX like peptide conjugated to amine-terminated poly(amidoamine) dendrimers of generation 5 (G5.NHAc-HPAO) and ^{131}I-labeled; SPIONP-PEG-CTX: superparamagnetic iron oxide coated NPs with polyethylene glycol and CTX; QD(Ag-In-S/ZnS)-CTX: Cadmium-free silver-indium-sulfide Zinc shell (Ag-In-S/ZnS) Quantum dots functionalized with CTX; Ag/Ali-PNPs-CTX-^{99m}Tc: Silver and alisertib polymeric NPs with ^{99m}Tc radiolabelling and CTX surface functionalization; Fe$_3$O$_4$/MnO–Cy5.5: oleic acid-capped iron oxide manganese oxide with conjugation Cy5.5 dye and CTX; NaGdF4-Ho^{3+}-CTX: Holmium doped dsodium gadolinium fluoride (NaGdF4-Ho^{3+}) nanoparticles conjugated with CTX; CTX-PEG-Gd$_2$O$_3$: CTX) to poly(ethylene glycol) (PEG) coated Gadolinium(III) oxide (Gd$_2$O$_3$)nanoparticles; Pdot-CTX: Polymer-blend dots conjugated with CTX; Gd-DTPA/BODIPY-dendrigraft poly-L-lysines-PEG-CTX: dendrigraft poly-L-lysines-PEG containing gadolinium ion diethylenetriamine pentaacetate NPs reacted with BODIPY dye; SPIONP-PEG-PEI-siRNA-CTX: superparamagnetic iron oxide NPs coated with polyethylene glycol and polyethylenimine (PEI) conjugated with small/short interfering ribonucleic acid and CTX; IONP-PEG-Chitosan-DNA-CTX: iron oxide coated with polyethylene glycol and chitosan conjugated with deoxyribonucleic acid and CTX; MFNP–CTX: Magnetite and fluorescent silica nanoparticles functionalized with CTX; IONP-PEG-Chitosan-Cy5.5-CTX: iron oxide coated with polyethylene glycol and chitosan conjugated with fluorescent molecule Cy5.5-CTX; PEI-NaYF(4):Yb, Er/Ce-CTX: Polyethylenimine-coated hexagonal-phase Ytterbium and Thulium Doped Sodium Yttrium Fluoride (NaYF(4):Yb), erbium and cerium co-doped nanoparticles; NP-MTX-CTX: IONPs conjugated to methotrexate (MTX), and CTX; SPIONP-FITC-CTX: superparamagnetic iron oxide NPs conjugated with fluorescein isothiocyanate (FITC) and CTX and IONP-PEG-CTX: Pegylated IONPs functionalized with CTX.

8.   Therapeutic and targeting applications of CTX-NPs for GB tumours

Many studies have reported the use of CTX-conjugated NPs and CTX-attached to fluorescent imaging agents for targeted precise surgical resection, drug delivery of anti-cancer drugs/ applications for the treatment of GB tumours and other tumours with no danger to normal cells (Cohen-Inbar and Zaaroor, 2016; Khanyile *et al.*, 2019). Most of these formulations serve diagnostic, therapeutic or theranostic functions in both *in vitro* and *in vivo* models of glioma as well as in clinical trials (Cohen-Inbar and Zaaroor, 2016; Cohen, Burks and Frank, 2018; Khanyile *et al.*, 2019; C. G. Patil *et al.*, 2019; Yamada *et al.*, 2021). Table 2 provides a summary of CTX-based NP therapeutics used for the treatment of GB, but some applications overlap with diagnosis through the imaging techniques mentioned above. Many studies have shown that CTX-modified polymer or lipid-based NPs such as liposomes could be used as drug and gene delivery systems for glioma-targeted chemotherapy in brain tumours (Xiang *et al.*, 2011; Qin *et al.*, 2014b; Wang and Guo, 2015; Mahmud *et al.*, 2018; Agarwal *et al.*, 2019; Formicola *et al.*, 2019).

47

In gliomas, CTX inhibits the expression of MMP-2 and to achieve maximal inhibition, a dual system which employs an anti-cancer drug entrapped in or conjugated to a nano-carrier, together with the conjugation of CTX is used. Such a system makes use of the acidic environment inside the tumour environment to down-regulate MMP expression thus allowing for further treatment with chemotherapeutic agents (Agarwal *et al.*, 2019). In a study by Fang *et al*. (2010), biocompatible polymer-coated IONPs conjugated to CTX or arginine-glycine-aspartic acid (RGD) were found to demonstrate that both NP-CTX and NP-RGD were target-specific to MMP-2 and αvβ3 integrin, respectively. Yue *et al*. (2014) developed a transferrin receptor (TfR) monoclonal antibody (mAb) of rats (OX26) and CTX conjugated PEGylated liposome as a dual-targeting gene delivery system for GB which was found to significantly promote cell transfection, increase transportation of plasmid DNA across the BBB and target the brain glioma cells *in vitro* and *in vivo*. Qin *et al*. (2014b) demonstrated that CTX-liposomes specifically interact with MMP-2 present on brain cancer cells, which demonstrates targeting. Xiang *et al*. (2011) first developed CTX-modified DOX-loaded liposomes (CTX-DoX-Lip) for glioma cells, but other studies have improved on this NP-based system for theranostic approaches by incorporating fluorescent molecules onto the liposomes in addition to CTX and chemotherapeutic drugs (Xiang *et al.*, 2012; Mahmud *et al*., 2018; Formicola *et al.*, 2019; M. Zhao, van Straten, Broekman, *et al.*, 2020).

Other studies have reported on the encapsulation of small interfering RNAs in CTX liposomes (Veiseh *et al.*, 2009b; Costa *et al.*, 2013) and antisense oligonucleotides (Kievit *et al.*, 2010; Cheng *et al.*, 2014) used as combination therapy for GB. CTX-functionalized NPs have been investigated for glioma gene therapy which has the potential to treat drug resistant tissues, reduce unwanted toxicity to healthy cells, and provide a platform for therapy against multiple forms of cancer (Roma-Rodrigues *et al.*, 2020; Alavian and Ghasemi, 2021). The first small interfering RNA (siRNA) magnetic nanovector (named NP-siRNA-CTX) with dual glioma targeting-specificity and dual therapeutic effect, was developed in 2010 for targeted cancer imaging and therapy (Veiseh *et al.*, 2010). These small 6-10 nm NPs demonstrated both increased small interfering RNA (siRNA) internalization by target tumour cells and intracellular trafficking towards enhanced knockdown of targeted gene expression. Mok *et al*. (2010) reported that the multifunctional nanovector core coated with three different functional molecules [highly amine blocked PEI (PEIb), siRNA, and CTX] exhibited both significant cytotoxic and gene silencing effects for C6 glioma cells at acidic pH

48

conditions, but not at physiological pH conditions. The NP-siRNA-CTX could also serve as an imaging tool for real-time monitoring of the delivery of therapeutic payload (Veiseh *et al.*, 2010).

CTX has been functionalized to other noble metallic NPs such as silver (Ag) NPs and gold (Au) NPs and used for both detection and therapeutic applications (Table 1 and 2). Tamborini *et al.* (2016) reported on AgNPs entrapped in Poly (lactic–co-glycolic acid) (PLGA) nanoparticles (PNP) conjugated to CTX (Ag-PNP-CTX). These NPs allowed the detection and quantification of cellular uptake by confocal microscopy, in both *in vitro* and *in vivo* experiments and a higher uptake of Ag-PNP-CTX was reported in *in vitro* studies. Using a single whole-brain X-irradiation performed 20 hours before NP injection, the expression of the CTX targets, MMP-2 and ClC-3 was enhanced as evidenced by the BBB permeabilization and increased internalization of Ag-PNP-CTX at tumour site *in vivo* (Tamborini *et al.*, 2016). Locatelli *et al.* (2012) first described CTX-functionalized on noble metallic NPs and developed a simple method for the synthesis of lipophilic AgNPs entrapped in a PEG-based polymeric NP conjugated with CTX (AgNPs-PNS-CTX). These NPs demonstrated significant cell-specific uptake in the U87 cell line in comparison to the Balb/3T3 cell line. The authors subsequently reported on the synthesis of multifunctional nanocomposites formed by polymeric NPs (PNPs) containing the anti-cancer drug alisertib, as well as AgNPs-conjugated with CTX and ^{99m}Tc-radiolabeling (Ag/Ali-PNPs-CTX-^{99m}Tc) (Table 1 and 2), which allowed significant tumour reduction as the result of *synergistic* effects of drug and NPs in U87 tumour-bearing mice (Locatelli *et al.*, 2014b). The authors were also the first to later report on CTX and Cy5.5 functionalized gold nanorods (AuNRs-PNPs-Cltx/Cy5.5) for optoacoustic microscopy and photothermal therapy (PTT) using laser irradiation in U87 cells which consequently led to cell damage (Locatelli *et al.*, 2014a).

A recent study developed a nano drug delivery system composed of methoxypolyethylene glycol loaded with AuNPs, chemotherapeutic drug DOX and functionalized with CTX (mPEI-CTX/DOX). This product was found to have a higher IC$_{50}$ value in human glioma cells than the free DOX, possibly due to the gradual release of the DOX from the mPEI-CTX/DOX NPs (L. Zhao *et al.*, 2020a). In addition to the MRI and fluorescence imaging properties of CTX-PEG-Dox-Eu-Gd$_2$O$_3$ NRs (Table 1 and 2), these NPs allowed for higher cytotoxicity in U251 human GB cells *in vitro* and no significant toxicity in HUVEC cells. In the *in vivo* experiments after tail-vein injection demonstrated no significant toxicity to normal organs, NPs accumulated in the brain tumours and appeared to inhibit tumour growth and metastasis (L. Zhao *et al.*, 2020a). Temozolomide (TMZ) has also been

incorporated into CTX-NPs for improving target-specific drug delivery. A study by Fang *et al*. (2015) reported on TMZ bound to chitosan-based NPs (NP-TMZ-CTX) exhibiting higher stability at physiological pH, with a half-life 7-fold longer compared with free TMZ. Thus, the NP-TMZ-CTX was able to target GB cells and achieved 2-6-fold higher uptake and 50-90 % reduction of half maximal inhibitory concentration (IC_{50}) at 72 hours post-treatment compared with NPs with TMZ but no CTX.

Niosomes are nano-based drug delivery vesicles composed of non-ionic surfactants with or without cholesterol that are similar to liposomes, but could be synthesized smaller, are more stable and cheaper to manufacture in comparison to liposomes (Bartelds *et al.*, 2018; Duan *et al.*, 2020; Su and M. Kang, 2020). Niosomes coated with CTX and loaded with TMZ with an entrapment efficiency of 79.09 ± 1.56 % were developed by De *et al*. (2018) and found to have enhanced solubility and permeation into the brain in *in vivo* models due to CTX-conjugation, with less accumulation in other organs. TMZ drug resistance for GB is mediated by a DNA repair protein, O6-methylguanine-DNA methyltransferase (MGMT), which eliminates the TMZ-induced DNA lesions (Yi *et al.*, 2019). Other studies report on combination treatments with small interfering RNA (siRNA)-based MGMT (siMGMT) inhibitors incorporated into CTX-NPs for targeting GB and sensitizing cells to TMZ for more effective therapeutic potential than free TMZ (Yoo *et al.*, 2014; Wang *et al.*, 2021). In another study, Mu *et al*. (2016) developed a CTX-IONP conjugated with the drug gemcitabine (GEM) using hyaluronic acid (HA) as a cross linker (IONP-HA-GEM-CTX) for GB therapy. This conjugate NP effectively killed GB cells without losing potency when compared to the free drug and showed a prolonged blood half-life and the ability to cross the BBB in wild-type mice (Mu *et al.*, 2016). Similarly, the chemotherapeutic agent, methotrexate (MTX) conjugated to CTX-NPs (NP–MTX–CTX) demonstrated increased uptake in 9L rat glioma and significant cytotoxicity in tumour cells with prolonged retention of NPs observed within tumours *in vivo* (Sun *et al.*, 2008a). Other studies by Agarwal *et al*. (2019) showed that treatment with CTX-conjugated morusin-loaded PLGA NPs (PLGA–MOR–CTX) resulted in enhanced inhibitory effects and cell death in U87 and GI-1 glioma cells. The cytocompatibility observed with normal human neuronal cells (HCN-1A) together with enhanced lethal effects in GB cells, highlighted the potential of PLGA-MOR-CTX NPs as promising therapeutic nanocarriers for GB. In another study involving the drug sunitinib conjugated to CTX-coupled stable nucleic acid lipid NPs (CTX-SNALPs-miR-21 NPs), NPs showed preferential accumulation in brain tumours, promotion of efficient miR-21 silencing and enhanced antitumor

activity, through decreased tumour cell proliferation, reduced tumour size as well as increased apoptosis activation (Costa *et al.*, 2015).

Some earlier studies have reported on CTX-fluorescent NPs with effective targeting, BBB permeability and high therapeutic effects both *in vitro* and *in vivo* (Veiseh *et al.*, 2009b; 2009c; Lee *et al.*, 2010). Two recombinant versions of CTX named CTX-KRKRK-GFP-H6 and CTX-GFP-H6, were developed by Díaz *et al*. (2019) and investigated in two Human cancer cell lines previously identified as targets for CTX, namely HeLa (overexpressing Annexin A2) and U87 (overexpressing MMP2). CTX-GFPH6 was found to have a significant cytotoxic effect on both cell lines, while CTX-KRKRK-GFP-H6 was more cytotoxic, and U87 cells were more sensitive than HeLa cells. In a recent study, a fluorescent nano-imaging agent (NIA) synthesized with polymalic acid with CTX, indocyanine green for fluorescence and tri-leucin peptide for fluorescence enhancement (CTX-PMLA-LLL-ICG), was found to exhibit high specificity for U87 glioma cells (R. Patil *et al.*, 2019). This method involves the fluorescence-guided resection of GB using NIR light and has been shown to significantly improve the precision of tumour removal by 98 % (R. Patil *et al.*, 2019).

The efficacy of the respective NP conjugate products discussed above appears to be linked to apoptosis-mediated cell death mechanisms, possibly induced by CTX functionalization of the NPs. Wu *et al*. (2017) reported on multifunctional Eu-doped Gd_2O_3 nanorods (Eu-Gd_2O_3 NRs) surface-functionalized with PEG to serve both as a hydrophilic coating and linkage molecule. This resulted in the covalent conjugation of the functional peptides RGD and CTX (RGD-Eu-Gd_2O_3 NRs-CTX) as a targeting nanovector for the detection and inhibition/therapy of early GB; these NPs could specifically target and adhere to U251 human GB cells, leading to cellular apoptosis. Pandey *et al*. (2020) reported on a sophisticated multifunctional CTX-NP based on pH responsive poly-l-lysine-coated Fe_3O_4@FePt core shell NPs with CTX for mitochondrial targeted therapy of GB. The multifunctional NPs were efficiently localized inside mitochondria, induced oxidative stress by Fe, DNA strand breakage by Pt and demonstrated the ability to disrupt mitochondrial function and induced apoptosis (Pandey *et al*., 2020). The authors also reported on effective PTT using NIR with these NPs (Pandey *et al*., 2020).

Table 2. Summary of CTX-NPs for therapeutic applications

Name	Therapeutic effect	Theranostic application	Size in nm (hydrodynamic size/ core size)	References
NP–siMGMT–CTX	Effective number of siRNAs (MGMT) delivered to tumours to sensitize both GB cells and GB stem-like cells (GSCs) to TMZ *in vivo* via CTX targeting	Yes	60.97 nm	(Wang et al. 2021)
CTX/DOTA/LND-PANPs Lf/CTX/TPP/DOTA /LND-PANPs	Increased localization of NPs in mitochondria both *in vitro* and *in vivo*, resulting in apoptosis. Photothermal therapy (PTT) with NPs occurred using NIR	Yes	< 20 nm	(Pandey *et al.*, 2020)
mPEI-CTX-^{99m}Tc/DOX	*In vivo* targeted delivery of DOX	Yes	394.77 nm	(L. Zhao *et al.*, 2020a)
CTX-PEG-Dox-Eu-Gd_2O_3 NRs	No significant toxicity reported in HUVEC cells, while toxicity was reported in U251 cells owing to CTX targeting MMP-2. *In vivo* experiments showed the inhibition of brain tumours with no significant toxicity to normal organs.	Yes	116.3 nm	(Zhang *et al.*, 2020)
CTX-KRKRK-GFP-H6 and CTX-GFP-H6	Two recombinant CTX-fluorescent protein NPs that demonstrated significant cytotoxicity in cell lines U87 (over expressing MMP2) and Hela (overexpressing Annexin 2)	No	~ 12 nm	(Díaz *et al.*, 2019)

52

CTX-PMLA-LLL-ICG	Systemic IV injection into xenogeneic mouse model carrying human U87 GB cells indicated tumour cell binding and internalization of NPs resulting in long-lasting tumour fluorescence which guided resection of GB and significantly improved the precision of tumour removal	Yes	11.82 nm	(R. Patil *et al.*, 2019)
CTX and mApoE-Dox-Lip	Enhanced DOX across the BBB via CTX-liposomes	No	184 nm	(Formicola *et al.*, 2019)
CTX-PLGA-Morusin	NPs resulted in enhanced inhibitory effects on U87 and GI-1 glioma cells	No	242.9 nm	(Agarwal *et al.*, 2019)
CTX-TMZ niosome	Enhanced TMZ delivery into the brain *in vivo* with less deposition in the highly perfused organs	No	220 nm	(De *et al.*, 2018)
M-CTX-Fc-L-Dox	Significant cytotoxicity observed with DOX loaded CTX- liposomes in U251 cells *in vitro* and tumour suppression in BALB/c mice bearing tumours of transplanted U251 cells *in vivo*	No	100-150 nm	(Mahmud *et al.*, 2018)
RGD-Eu-Gd$_2$O$_3$ NRs-CTX	Nanorods specifically target U251 cells, leading to cellular apoptosis. *In vivo* results show NPs could effectively inhibit early tumour growth, without	Yes	~ 78nm	(Wu *et al.*, 2017)

53

	any damages to normal tissues/organ			
IONP-HA-GEM-CTX	NPs effectively crossed BBB and killed GB cells, had prolonged blood circulation duration, and was excreted from renal system	Yes	~ 32 nm	(Mu *et al.*, 2016)
Ag-PNP-CTX	*In vitro* experiments performed with different human GB cell lines showed higher uptake of Ag-PNP-CTX, with respect to non-functionalized Ag-PNP NPs and i*n vivo* experiments showed that Ag-NP-CTX efficiently targets the tumours	Yes	114 nm	(Tamborini *et al.*, 2016)
CTX-SNALPs-miR-21	MiRNA-21 silencing because of tumour-targeted CTX-NPs and decreased tumour cell proliferation and enhanced apoptosis in combination with Sunitinib	No	< 190 nm	(Costa *et al.*, 2015)
NP-TMZ-CTX	CTX-NPs demonstrated targeting of GB cells and 2-6-fold higher uptake and 50-90 % reduction of IC_{50} at 72 hours post-treatment as compared to NPs without CTX	Yes	< 100 nm	(Fang *et al.*, 2015)
Ag/Ali-PNPs-CTX-^{99m}Tc	Significant tumour reduction was achieved *in vivo* as the result of synergistic effects of Alisertib and NPs	Yes	199.1 nm	(Locatelli *et al.*, 2014b

54

AuNRs-PNPs-Cltx/Cy5.5	NPs showed enhanced binding affinity toward GB cells *in vitro* using optoacoustic microscopy and PTT using laser irradiation of the cells led to cell damage	Yes	122.5 nm	(Locatelli *et al.*, 2014a)
CTX- Lip	CTX was attached to the surface of liposomes which interacts with the MMP-2 on the surface of U87 and A549 cells, demonstrating targeting	No	103.4 nm	(Qin *et al.*, 2014b)
CTX-IONP-siMGMT	Combination treatment of mice bearing orthotopic tumours with CTX-NP-siMGMT and TMZ led to significant reduction of tumour growth	Yes	37.3 nm	(Yoo *et al.*, 2014)
CTX-SNALPs	Targeted NP-mediated miR-21 silencing in U87 and GL261 cells resulted in increased levels of the tumour suppressors PTEN and PDCD4, caspase 3/7 activation and decreased tumour cell proliferation	No	< 180 nm	(Costa *et al.*, 2013)
AgNPs-PNS-CTX	Significantly higher uptake of Ag into U87 cells compared to the non-targeted NPs. Cytotoxic effect in glioma cell lines was also reported	No	130 nm	(Locatelli *et al.*, 2012)
CTX-DoX-Lip	Increased cytotoxicity against U87 and U251 glioma and significant tumour growth inhibition *in vivo*	No	128 nm	(Xiang *et al.*, 2011)

55

NP–DNA– CTX	Enhanced uptake specifically into glioma cells *in vivo*	Yes	48.8 nm	(Kievit *et al.*, 2010)
IONPs-PEG-CTX and IONS-PEG-RDG	NP-CTX and NP-RGD were target-specific to integrin MMP-2 and αvβ3 integrin, respectively	Yes	~ 12 nm,	(Fang *et al.*, 2010)
NP(ION/ PEG)–CTX– Cy5.5	NPs showed tumour-specific accumulation *in vivo* and no toxicity effects	Yes	13.5 nm	(Sun *et al.*, 2010)
NP–CTX– chitosan–Cy5.5	NPs showed optimal serum half-life, good biodistribution and stability *in vivo*	Yes	7 nm	(Lee *et al.*, 2010)
MFNP-CTX	CTX-NPs demonstrated high specific cellular uptake	Yes	<100 nm	(Wan *et al.*, 2010)
NP–siRNA– CTX	Increased small interfering RNA (siRNA) internalization by targeting glioma cells and intracellular trafficking towards enhanced knockdown of targeted gene expression	Yes	6–10 nm	(Veiseh *et al.*, 2010)
NP–PEIb– siRNA–CTX	CTX-NPs showed long-term stability and good magnetic properties, significant cytotoxic effects, and gene silencing effects at acidic pH conditions for C6 glioma cells	Yes	~ 60 nm	(Mok *et al.*, 2010)
NP–AF647– CTX–DNA	Results showed low cytotoxicity because of CTX targeting and excellent gene transfection efficiency	Yes	134.8 nm	(Veiseh *et al.*, 2009b)

56

NP–CTX– AF680	The NPs enhanced cellular uptake via MMP-2	Yes	~11 nm	(Veiseh *et al.*, 2009a)
NPCP– Cy5.5– CTX	NPs showed cytotoxicity, sustained retention in tumours, and the ability to cross the BBB and specifically target brain tumours *in vivo*	Yes	33 nm	(Veiseh *et al.*, 2009c
NP–MTX– CTX	Increased cytotoxicity of methotrexate (MTX) in GB cells and prolonged retention of NPs was observed within tumours *in vivo* NPs	Yes	5-8 nm	(Sun *et al.*, 2008a).

Abbreviations: NP: nanoparticles; CTX: Chlorotoxin; NP–siMGMT–CTX:IONPS small interfering RNA (siRNA)-based MGMT (siMGMT) inhibitors and CTX conjugated to IONPs; CTX/DOTA/LND-PANPs Lf/CTX/TPP/DOTA/LND-PANPs: pH responsive poly-l-lysine coated Fe3O4@FePt core shell NPs with CTX for mitochondria targeted (Mito-PANPs); mPEI-CTX-^{99m}Tc/DOX: methoxypolyethylene glycol (m), polyethylenimine (PEI) ^{99m}Tc radiolabelling NP loaded with doxorubicin (DOX); CTX-PEG-Dox-Eu-Gd$_2$O$_3$ NRs: Doxorubicin and CTX conjugated to polyethylene glycol (PEG) coated gadolinium oxide NPs; CTX-KRKRK-GFP-H6 and CTX-GFP-H6: 2 different fluorescent protein NPs conjugated to CTX named CTX-KRKRK-GFP-H6 and CTX-GFP-H6; CTX-PMLA-LLL-ICG: Polymalic acid (PMLA) conjugated with CTX, tri-leucine peptide (LLL) and indocyanine green (ICG); CTX and mApoE- Dox-Lip: liposomes entrapped with DOX and dually functionalized with ApoE-derived peptide (mApoE) and CTX; CTX-TMZ noisome: Noisome entrapping Temozolomide (TMZ) surface functionalized with CTX; RGD-Eu-Gd$_2$O$_3$-CTX coated europium dopped gadolinium oxide nanorods, functionalized with arginine-glycine-aspartic acid (RGD) and CTX; CTX-PLGA-Morusin: CTX conjugated to poly(lactic-co-glycolic acid) (PLGA) NPs loaded with morusin; M-CTX-Fc-L-Dox: liposome loaded with DOX and modified with CTX fused to human IgG Fc domain without hinge region in monomeric form (M-CTX-Fc); IONP-HA-GEM-CTX: Iron oxide NPs conjugated with chemotherapeutic drug gemcitabine (GEM) and CTX using hyaluronic acid (HA) as a crosslinker; Ag-PNP-CTX: silver NPs (AgNPs) entrapped in poly(lactic-co-glycolic acid) (PLGA) nanoparticles (PNP) conjugated to chlorotoxin (CTX); AuNRs-PNPs-Cltx/Cy5.5: Gold nanorods entrapped in poly(lactic-co-glycolic acid) (PLGA) nanoparticles (PNP) conjugated to CTX and Cy5.5; CTX-SNALPs-miR-21: CTX-coupled stable nucleic acid lipid particles (SNALPs) for miR-21 silencing; NP-TMZ-CTX: chitosan-based NPs with TMZ, conjugated with CTX; NP:DNA-CTX: IONPs coated with PEG and PEI, DNA was encapsulated into NP and CTX was conjugated on the surface; Ag/Ali-PNPs-CTX-^{99m}Tc: Silver and alisertib polymeric NPs with ^{99m}Tc radiolabelling and CTX surface functionalization; AgNPs-PNS-CTX: Silver polymeric NPs with CTX surface functionalization; CTX- Lip: CTX liposomes; CTX-IONP-siMGMT: small interfering RNA (siRNA)-based MGMT

(siMGMT) inhibitors incorporated into CTX-IONPs; CTX-SNALPs: CTX-coupled stable nucleic acid lipid particles; CTX-DoX-Lip: CTX functionalized liposomes entrapping DOX; NP–DNA– CTX: IONPa conjugated with DNA and CTX; IONPs-PEG-CTX and IONS-PEG-RDG: IONPs coated with PEG conjugated with CTX or RDG; NP(ION/ PEG)–CTX– Cy5.5: IONPs surface functionalized with CTX and Cy5.5; NP–CTX– chitosan– Cy5.5: IONPs coated with chitosan and conjugated to CTX and Cy5.5; MFNP–CTX: Magnetite and fluorescent silica nanoparticles functionalized with CTX; NP–siRNA– CTX: IONPs coated with PEG and conjugated to siRNA and CTX; NP–PEIb–siRNA–CTX: IONPs coated with polyethylene glycol (PEG)-grafted chitosan, and polyethylenimine (PEI) with polyethylenimine (PEI) and conjugated to siRNA and CTX; NP–AF647– CTX–DNA: IONPs conjugated with Alexa Fluor 647 dye (AF647) and DNA; CTX; NP–CTX– AF680: IONPs conjugated with Alexa Fluor 680 dye (AF680); NPCP– Cy5.5– CTX: PEGylated-chitosan branched copolymer (CP) NPs conjugated with Cy5.5 and CTX and NP–MTX– CTX: IONPs conjugated to CTX and methotrexate (MTX).

9. Prospective applications of CTX-NP formulations

9.1. Optoacoustic imaging using CTX-NPs

CTX-NPs could also be used in other diagnosis and treatment applications for both GB and NB. For instance, optoacoustic imaging is one area of interest that has been investigated preclinically and involves the use of acoustic emissions from pulsed light energy to visualise biological structures at high optical contrast and acoustical resolution (Bost and Fournelle, 2013). Commonly used acoustic imaging contrast agents are microbubbles (MBs), nanobubbles (NBs) and nanodroplets (NDs) that can be used with photo-acoustic and ultrasound imaging (Kim *et al.*, 2010). Stable oscillations of MBs are caused by exposure to low acoustic pressure, a process termed stable cavitation (Endo-Takahashi and Negishi, 2020). MBs were initially developed as diagnostic ultrasound contrast agents but have since been explored for targeted drug delivery by enhancing vascular permeability through cavitation when bubbles occur in ultrasound fields (Goertz, 2015). MBs may have difficulty in penetrating the deep tissue layers, whereas NBs hold the potential for extensive delivery into tissues through blood vessels and NDs can pass through the leaky microvasculature and reach the perivascular space, such as a tumour's interstitial space (Endo-Takahashi and Negishi, 2020). Modifications of bubble surfaces allow targeting of diseased tissues, reduced immunogenicity, and prolonged circulation times. Various bubble formulations are used for ultrasound imaging (Rapoport *et al.*, 2011) targeted drug delivery (Bull, 2007; Hernot and Klibanov, 2008; Kooiman *et al.*, 2020; Su *et al.*, 2021), gene delivery (Sirsi and Borden, 2012; Wu and Li, 2017) and hyperthermia treatment (Yildirim, Blum and Goodwin, 2019), however research in this field incorporating CTX as a targeting

molecule has not been explored but has been previously suggested as a promising diagnostic application for GB (Cohen, Burks and Frank, 2018), and should also be considered for NB.

9.2. Hyperthermia treatment using CTX-NPs

So far, the therapeutic applications of CTX have focused on conjugating the peptide to NPs to allow for targeted delivery of drugs and therapeutic agents or for the visualization of tumours or both, with very few applications involving hyperthermia treatment (HPT) (Locatelli *et al.*, 2014a; Pandey *et al.*, 2020), which is one of the oldest treatments for cancer and a promising minimally invasive thermal therapy (Pinel *et al.*, 2019). This is an effective treatment modality which utilizes heat energy to destroy cancer cells that are more prone to generate heat, owing to their overall increased metabolic rates (Rajan and Sahu, 2020). A prospective hyperthermia treatment application of CTX-NPs for GB and NB is to induce intracellular heat stress with the use of NPs (at a temperature range of 41-47 ºC), resulting in mitochondrial swelling, protein denaturation, alteration in signal transduction, cell rupturing and induction of necrosis/apoptosis (Bettaieb and Averill-Bates, 2015; Lin, Hsu and Lin, 2018; Rajan and Sahu, 2020). Some of the common drawbacks of hyperthermia treatment include its invasiveness, incomplete tumour destruction, low heat penetration in the tumour region (lesions > 4-5cm in diameter), excessive heating of surrounding healthy tissues (non-specificity), thermal under-dosage in the target region, heat dissipation by the blood as well as the development of thermotolerance (Datta *et al.*, 2015; Rajan and Sahu, 2020). The use of magnetic and metallic NPs (MNPs) to induce localized NP-mediated hyperthermia within cancer cells, as illustrated in Figure 3, has recently gained considerable interest in cancer nanotechnology research but this has yet to be fully exploited for brain and other CNS tumours. Recent studies have reported on the promise of deep intracranial thermotherapy with MNPs for brain tumours (Mahmoudi *et al.*, 2018; Srinivasan *et al.*, 2020; Habra *et al.*, 2021) with some entering clinical trials (Skandalakis *et al.*, 2020). In general, both whole-body and regional hyperthermia treatments result in poor tumour specificity and constitute a strong limitation to the clinical application of this technique (Datta *et al.*, 2015; Rajan and Sahu, 2020).
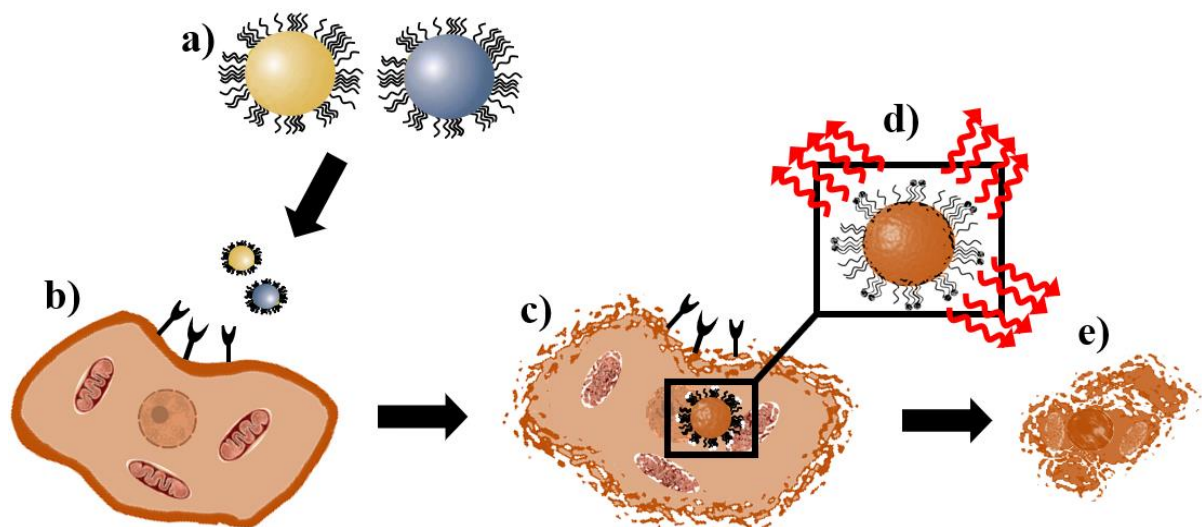
Figure 3. Principle of localized nanoparticle-mediated hyperthermia in cancer cells. Metallic NPs (e.g., AuNPs, PtNPs or bimetallic NPs) or magnetic NPs (e.g., IONPs/SIONPs) **(a)** are designed to be target specific for cancer cells that overexpress specific cell surface receptors and allow intracellular uptake of NPs through receptor-mediated endocytosis **(b)**. Cells are exposed to an external heating source (e.g., NIR light, AMF, and RF-fields) **(c)** which induces local heating (41-47 °C) **(d)** and results in thermal destruction of cells through mitochondrial swelling, protein denaturation, alteration in signal transduction, cell rupturing and induction of necrosis/apoptosis **(e)**.

Some of the most explored magnetic NPs for HPT based on their superior magnetic properties include iron, cobalt, nickel, manganese, zinc, gadolinium, as well as their alloys and oxides - $CoFe_2O_4$, $NiFe_2O_4$, $ZnFe_2O_4$, $CuFe_2O_4$, $MnFe_2O_4$, Gd-doped Zn-Mn and Zn-Mn-doped iron oxides (Sharifi, Shokrollahi and Amiri, 2012; Chen, Christiansen and Anikeeva, 2013; Mazario *et al.*, 2013; Abenojar *et al.*, 2016; Bauer *et al.*, 2016; Dalal *et al.*, 2017; Hirosawa, Iwasaki and Watano, 2017; Kotoulas *et al.*, 2017). However, the use of most of these metals and alloys is mostly limited by potential toxicity and chemical instability (Sengul and Asmatulu, 2020). Interestingly, IONPs have excellent self-heating properties and have been licensed for use in clinical applications by the FDA and the European Medicines Agency (EMA) (Martinelli, Pucci and Ciofani, 2019). External alternating magnetic field (AMF) is used with IONPs/SPIONPs to produce heat energy for the thermal ablation of cancer cells (Armijo *et al.*, 2012) at controlled environments (Estelrich *et al.*, 2015). Increasing the strength of the AMF field may result in inductive tissue heating from eddy current losses, which is independent of the presence of IONPs/SIONs; this may restrict the extent to which the AMF field can be increased (Chatterjee, Diagaradjane and Krishnan, 2011; Stigliano *et al.*, 2016).

Noble MNPs are excellent conductors of thermal energy that offer a non-invasive and effective therapeutic strategy for intracellular hyperthermia (Zhao *et al.*, 2022). Some MNPs have strong local surface plasmon resonance (SPR) effect, hence upon exposure to light, can absorb sufficient photon energy to generate photothermal properties (Boldoo *et al.*, 2020). AuNPs and platinum NPs (PtNPs) have been used in both *in vivo* and *in vitro* studies to demonstrate photothermal therapy (PTT)-induced cytotoxicity through exposure to specialized lasers, usually in near infra-red (NIR) (650-950 nm) or second near-infrared (NIR-II) (1000–1350 nm) ranges (Gobin *et al.*, 2007; Norouzi, Khoshgard and Akbarzadeh, 2018; Ma *et al*., 2020; Moros *et al.*, 2020). Interest in bimetallic NPs as anti-cancer applications has increased due to their value in enhancing drug delivery strategies and NP-mediated hyperthermia treatments (Loza, Heggen and Epple, 2020). A number of studies reported that bimetallic gold-platinum NPs (AuPtNPs) of different sizes and shapes exhibit better photothermal effects and higher radiation-enhancing properties than the respective monometallic NPs, AuNP and platinum NPs (PtNP), possibly due to the *synergistic* effects of the two composite metallic atoms and new surface properties that are different in the their monometallic NPs (Tang *et al.*, 2014; Liu *et al.*, 2017; Song *et al.*, 2017, 2021; Yang *et al.*, 2018; Depciuch *et al.*, 2019; Salado-Leza *et al.*, 2019; Fathima and Mujeeb, 2021).

The use of NIR PTT is limited to subcutaneous/superficial malignant tumours because of minimal tissue penetration (~ 3 cm depth) by NIR light which may not be suitable for deep-seated brain tumours (Henderson and Morries, 2015). Hence, other applications such as external radiofrequency (RF) ablation are suggested as radio wave energy has been shown to penetrate more deeply located tumours than NIR light (Erdreich and Klauenberg 2001; Raoof and Curley 2011; Raoof et al. 2012; Nasseri et al. 2016). At 220 MHz, RF penetration is 7 cm and increases with a decrease in frequency, whereas RF penetration is 17 cm at 85 MHz (Röschmann, 1987; Day, Morton and West, 2009). Radio waves are safe, low-frequency electromagnetic waves with low tissue-specific absorption rate (SAR) and are therefore excellent for applications involving whole-body tissue penetration (Erdreich and Klauenberg, 2001). The heating properties of AuNPs and PtNPs have been investigated using RF currents and shown to offer some promise for non-invasive RF anti-cancer therapy; however, reports on targeted bimetallic AuPtNPs for this application is limited in the literature (Porcel *et al.*, 2010; Manikandan, Hasan and Wu, 2013; San, Moh and Kim, 2013). CTX-conjugated AuPtNPs and other bimetallic NPs need further investigation as potential heating agents for RF-based hyperthermia for

61

the treatment of such deep-seated tumours as GB, as they target only tumour cells with minimal adverse effects on surrounding healthy cells.

Hyperthermia treatments are also known to sensitize cells to other forms of standard therapy, including radiation and chemotherapy having a potential in combination treatments (Datta *et al.*, 2015, 2016; Oei *et al.*, 2020). Another example of the use of nanoparticle-mediated hyperthermia treatments is in thermosensitive controlled drug release (Estelrich and Busquets, 2018; Moros *et al.*, 2019, 2020). This concept was recently explored by Pandey *et al.* (2020) using CTX-functionalized bimetallic NPs (Table 2) for mitochondria targeting and chemo-photothermal therapy with NIR. Research into multimodal CTX-NPs incorporating RF-hyperthermia for GB and NB treatment is required as this may yield results that could offer new hope for the effective treatment and management of these tumours.

10. CTX-like peptides

Another group of molecules with prospective applications for targeted cancer diagnosis and therapy is 'CTX-like peptides'. Since the discovery of CTX from the venom of the *Leiurus quinquestriatus* scorpion, a few CTX-like peptides with similar primary features and functions as CTX, have been isolated and identified (DeBin and Strichartz, 1991; Arzamasov, Vasilevskiĭ and Grishin, 2014; Dardevet *et al.*, 2015; Cohen, Burks and Frank, 2018; L. Zhao *et al.*, 2020b; Yamada *et al.*, 2021). CTX-like peptides are considered as ion channel blockers and MMP-2 inhibitors because they interact with MMP-2 on cell membrane surfaces, resulting in anti-metastasis or antitumor effects with minimal-to-no effects on normal cells (Mamelak *et al.*, 2006). Other scorpion venom peptides with similar primary structure as CTX include AaCTX, ClTx-a, -b, -c, -d, BmKCTa, BmKCL1, Lqh-8:6, Be I5A, BeI1, AmmP2, GaTx1 and GaTx2 (Rosso and Rochat, 1985; Ali *et al.*, 1998; Dardevet *et al.*, 2015). AaCTX isolated from *Androctonus australis* scorpion, has 61 % identity with CTX and was suggested to have inhibitory effects on invasion and migration through chloride channels (Rjeibi *et al.*, 2011). Sequence alignment showed that BmKCTa (isolated from *Buthus martensii Karsch* venom), GaTx1 and GaTx2 (isolated from *Leiurus quinquestriatus* venom) have 67 %, 64 % and 38 % similarity with CTX respectively, and show some activity on chloride and other ion channels (Fu *et al.*, 2005; Fan *et al.*, 2010; Dardevet *et al.*, 2015; Ojeda, Wang and Craik, 2016; Khanyile *et al.*, 2019). GaTx1 is a highly specific blocker for the cystic fibrosis transmembrane conductance regulator

(CFTR) channel, a receptor belonging to the ABC family, with intrinsic Cl− channel activity (Fuller *et al.*, 2007).

ClC-2, another member of the ABC family of chloride channels like ClC-3, is also upregulated on the surfaces of glioma cells, but its physiological role is not completely understood; it has been suggested to play a similar role as ClC-3 in glioma cell invasion and migration (Lui *et al.*, 2010). GaTx2 inhibits ClC-2 by slowing down its activation (Thompson *et al.*, 2009), and the resulting inhibition is voltage-dependent. BmKCTa, the most common CTX-like peptide investigated, also demonstrated the inhibition of glioma cell proliferation, migration and invasion in a fashion similar to CTX with MMP-2 as the potential target (Fu *et al.*, 2005, 2007, 2011; Gobin *et al.*, 2007; Cheng *et al.*, 2016; Qiao *et al.*, 2017; Sun *et al.*, 2017; L. Zhao *et al.*, 2020b). The CTX-like peptide, Bs-Tx7, from the venom of *Buthus sindicus* scorpion, has a scissile peptide bond (i.e., Gly-Ile) for MMP2 and demonstrated 66 % sequence identity with CTX and 82 % sequence identity with GaTx1 (Ali *et al*. 2016). In another study, Xu *et al*. (2016) identified the CTX-derivatives CA4 and CTX-23, which showed high selective binding to malignant glioma cells and inhibited rodent and human glioma cell growth at low concentrations, with minimal-to-no toxicity to primary astrocytes and neurons. Furthermore, these authors also found that CA4 and CTX could normalize tumour vessel morphology and vessel density in the peritumoral brain areas (Xu *et al.*, 2016). Thus, more research is required to understand the specific mechanisms of action of these CTX-like peptides, as well as the plausibility of their use as potential targeting agents for the treatment of GB and NB tumours.

11. Conclusions and future directions

The rising incidence of GB and NB imposes major global health challenges, with a substantial economic burden for patients, health insurance providers and health authorities alike. The pathophysiology of these tumours involves the elevation of many surface proteins like MMPs which contribute to proliferation and metastasis. Therefore, strategies that inhibit the over-expression of MMPs may reduce cancer progression. CTX is a peptide that holds great promise for use as a theranostic agent for NB, GB and other solid tumours, with many CTX-NPs applications constantly being investigated. CTX easily penetrates the BBB, has a high binding affinity for gliomas and other cancers including NB, but not normal tissues and is reported to be readily retained for longer periods in cancer tissue with little or no toxicity or immunoreactivity. There is substantial evidence to show that the efficacy of CTX is related to its ability to cross the BBB as well as its high tumour-binding

function mediated by the molecular targets namely, chloride channels, MMP-2, annexin A2 and recently, ERα and NRP-1. However, more research is required to fully elucidate the mechanisms involved in the binding of CTX to tumour molecular targets as well in its crossing of the BBB. Noble bimetallic NPs have recently demonstrated superior anti-cancer activity when compared to monometallic NPs, especially for hyperthermia-based treatments; however, only a few studies have reported on CTX functionalized NPs and bimetallic NPs for hyperthermia treatments, thus requiring further investigation. Finally, only a few studies have reported on the use of CTX-NPs in NIR photothermal therapy and to the best of our knowledge, no radiofrequency-based hyperthermia studies involving CTX-NPs exist in the literature, necessitating more studies on these applications, since they may be highly advantageous for deep seated tumours such as GB. Overall, this review highlights the potential of CTX and CTX-NPs as safe and effective diagnostic and therapeutic applications for GB and NB tumours.

12. References

Abenojar, E.C., Wickramasinghe, S., Bas-Concepcion, J. and Samia, A.C.S. (2016). Structural effects on the magnetic hyperthermia properties of iron oxide nanoparticles. *Progress in Natural Science: Materials International*, 26(5): 440–448.

Accardo, A., Tesauro, D. and Morelli, G. (2013). Peptide-based targeting strategies for simultaneous imaging and therapy with nanovectors. *Polymer Journal*, 45(5): 481–493.

Agarwal, S., Mohamed, M.S., Mizuki, T., Maekawa, T. and Kumar, D.S. (2019). Chlorotoxin modified morusin–PLGA nanoparticles for targeted glioblastoma therapy. *Journal of Materials Chemistry B*, 7(39): 5896–5919.

Agarwal, S., Muniyandi, P., Maekawa, T. and Kumar, D.S. (2018). Vesicular systems employing natural substances as promising drug candidates for MMP inhibition in glioblastoma: A nanotechnological approach. *International Journal of Pharmaceutics*, 551(1–2): 339–361.

Ai, P., Wang, H., Liu, K., Wang, T., Gu, W., Ye, L. and Yan, C. (2017). The relative length of dual-target conjugated on iron oxide nanoparticles plays a role in brain glioma targeting. *RSC Advances*, 7(32): 19954–19959.

Alam, M., Ali, S.A., Abbasi, A., Kalbacher, H. and Voelter, W. (2012). Design and Synthesis of a Peptidyl-FRET Substrate for Tumor Marker Enzyme human Matrix Metalloprotease-2 (hMMP-2). *International Journal of Peptide Research and Therapeutics*, 18(3): 207–215.

Alavian, F. and Ghasemi, S. (2021). The Effectiveness of Nanoparticles on Gene Therapy for Glioblastoma Cells Apoptosis: A Systematic Review. *Current Gene Therapy*, 21(3): 230–245.

Ali, S.A., Alam, M., Abbasi, A., Undheim, E.A.B., Fry, B.G., Kalbacher, H. and Voelter, W. (2016). Structure-Activity Relationship of Chlorotoxin-Like Peptides. *Toxins*, 8(2): 36.

Ali, S.A., Stoeva, S., Schütz, J., Kayed, R., Abassi, A., Zaidi, Z.H. and Voelter, W. (1998). Purification and primary structure of low molecular mass peptides from scorpion (Buthus sindicus) venom. *Comparative Biochemistry and Physiology. Part A, Molecular & Integrative Physiology*, 121(4): 323–332.

Allen, M., Ghosh, S., Ahern, G.P., Villapol, S., Maguire-Zeiss, K.A. and Conant, K. (2016). Protease induced plasticity: matrix metalloproteinase-1 promotes neurostructural changes through activation of protease activated receptor 1. *Scientific Reports*, 6(1): 35497

Applebaum, M.A., Vaksman, Z., Lee, S.M., Hungate, E.A., Henderson, T.O., London, W.B., Pinto, N., Volchenboum, S.L., Park, J.R., Naranjo, A., Hero, B., Pearson, A.D., Stranger, B.E., Cohn, S.L. and Diskin, S.J. (2017). Neuroblastoma survivors are at increased risk for second malignancies: A report from the International Neuroblastoma Risk Group Project. *European Journal of Cancer*, 72: 177–185.

Ara, T., Fukuzawa, M., Kusafuka, T., Komoto, Y., Oue, T., Inoue, M. and Okada, A. (1998). Immunohistochemical expression of MMP-2, MMP-9, and TIMP-2 in neuroblastoma: association with tumor progression and clinical outcome. *Journal of Pediatric Surgery*, 33(8): 1272–1278.

Aravindan, N., Jain, D., Somasundaram, D.B., Herman, T.S. and Aravindan, S. (2019). Cancer stem cells in neuroblastoma therapy resistance. *Cancer Drug Resistance*, 2(4): 948–967.

Armijo, L.M., Brandt, Y.I., Mathew, D., Yadav, S., Maestas, S., Rivera, A.C., Cook, N.C., Withers, N.J., Smolyakov, G.A., Adolphi, N.L., Monson, T.C., Huber, D.L., Smyth, H.D.C. and Osiński, M. (2012). Iron Oxide Nanocrystals for Magnetic Hyperthermia Applications. *Nanomaterials*, 2(2): 134–146.

Arzamasov, A.A., Vasilevskiĭ, A.A. and Grishin, E.V. (2014). Chlorotoxin and related peptides are short insect toxins from scorpion venom. *Bioorganicheskaia Khimiia*, 40(4): 387–398.

Attia, M.F., Anton, N., Wallyn, J., Omran, Z. and Vandamme, T.F. (2019). An overview of active and passive targeting strategies to improve the nanocarriers efficiency to tumour sites. *Journal of Pharmacy and Pharmacology*, 71(8): 1185–1198.

Ayed, A.S., Omran, M.A.A.A., Nabil, Z., Strong, P., Newton, K. and Abdel Rahman, M. A. (2021). C-Terminal Amidation of Chlorotoxin Does Not Affect Tumour Cell Proliferation and Has No Effect on Toxin Cytotoxicity. *International Journal of Peptide Research and Therapeutics*, 27(1): 659–667.

Ayomide, S.O., Oko, G.E., Chukwu, C.C., Vo, K.T.K. and Okoi, E.P. (2018). Effects of Chlorotoxin on Matrix Metalloproteinase-2 (MMP-2) in Melanoma and Breast Cancer Cell Lines. *Journal of Advances in Medical and Pharmaceutical Sciences*, 7(2): 1–11.

Baik, F.M., Hansen, S., Knoblaugh, S.E., Sahetya, D., Mitchell, R.M., Xu, C., Olson, J.M., Parrish-Novak, J. and Méndez, E. (2016). Fluorescence Identification of Head and Neck Squamous Cell Carcinoma and High-Risk Oral Dysplasia With BLZ-100, a Chlorotoxin-Indocyanine Green Conjugate. *JAMA otolaryngology-- head & neck surgery*, 142(4): 330–338.

Bartelds, R., Nematollahi, M.H., Pols, T., Stuart, M.C.A., Pardakhty, A., Asadikaram, G. and Poolman, B. (2018). Niosomes, an alternative for liposomal delivery. *PLoS ONE*, 13(4): e0194179.

Baskar, R., Lee, K.A., Yeo, R. and Yeoh, K.-W. (2012). Cancer and Radiation Therapy: Current Advances and Future Directions. *International Journal of Medical Sciences*, 9(3): 193–199.

Bastiancich, C., Da Silva, A. and Estève, M.-A. (2021). Photothermal Therapy for the Treatment of Glioblastoma: Potential and Preclinical Challenges. *Frontiers in Oncology*, 10: 610356.

Bauer, L.M., Situ, S.F., Griswold, M.A. and Samia, A.C.S. (2016). High-performance iron oxide nanoparticles for magnetic particle imaging – guided hyperthermia (hMPI). *Nanoscale*, 8(24): 12162–12169.

Bayón-Cordero, L., Alkorta, I. and Arana, L. (2019). Application of Solid Lipid Nanoparticles to Improve the Efficiency of Anticancer Drugs. *Nanomaterials*, 9(3): 474.

Belykh, E., Shaffer, K.V., Lin, C., Byvaltsev, V.A., Preul, M.C. and Chen, L. (2020). Blood-Brain Barrier, Blood-Brain Tumor Barrier, and Fluorescence-Guided Neurosurgical Oncology: Delivering Optical Labels to Brain Tumors. *Frontiers in Oncology*, 10: 739.

Bettaieb, A. and Averill-Bates, D.A. (2015). Thermotolerance induced at a mild temperature of 40°C alleviates heat shock-induced ER stress and apoptosis in HeLa cells. *Biochimica Et Biophysica Acta*, 1853(1): 52–62.

Boldoo, T., Ham, J., Kim, E. and Cho, H. (2020). Review of the Photothermal Energy Conversion Performance of Nanofluids, Their Applications, and Recent Advances. *Energies*, 13(21): 5748.

Bost, W. and Fournelle, M. (2013). Molecular imaging of glioblastoma cells using functionalized nanorods and a high resolution optoacoustic microscope. *2013 IEEE International Ultrasonics Symposium (IUS). 2013 IEEE International Ultrasonics Symposium (IUS)*: 120–123.

Brodeur, G.M. (2018). Spontaneous regression of neuroblastoma. *Cell and Tissue Research*, 372(2): 277–286.

Bull, J.L. (2007). The application of microbubbles for targeted drug delivery. *Expert Opinion on Drug Delivery*, 4(5): 475–493.

Butte, P.V., Mamelak, A., Parrish-Novak, J., Drazin, D., Shweikeh, F., Gangalum, P.R., Chesnokova, A., Ljubimova, J.Y. and Black, K. (2014). Near-infrared imaging of brain tumors using the Tumor Paint BLZ-100 to achieve near-complete resection of brain tumors. *Neurosurgical Focus*, 36(2): E1.

Castro Dias, M., Mapunda, J.A., Vladymyrov, M. and Engelhardt, B. (2019). Structure and Junctional Complexes of Endothelial, Epithelial and Glial Brain Barriers. *International Journal of Molecular Sciences*, 20(21): E5372.

Chatterjee, D.K., Diagaradjane, P. and Krishnan, S. (2011). Nanoparticle-mediated hyperthermia in cancer therapy. *Therapeutic Delivery*, 2(8): 1001–1014.

Chen, L., Lin, L., Xian, N. and Zheng, Z. (2019). Annexin A2 regulates glioma cell proliferation through the STAT3-cyclin D1 pathway. *Oncology Reports*, 42(1): 399–413.

Chen, R., Christiansen, M.G. and Anikeeva, P. (2013). Maximizing Hysteretic Losses in Magnetic Ferrite Nanoparticles via Model-Driven Synthesis and Materials Optimization. *ACS Nano*, 7(10): 8990–9000.

Chen, S., Ahmadiantehrani, M., Publicover, N.G., Hunter, K.W. and Zhu, X. (2015). Thermal decomposition based synthesis of Ag-In-S/ZnS quantum dots and their chlorotoxin-modified micelles for brain tumor cell targeting. *RSC Advances*, 5(74): 60612–60620.

Chen, Z., Xiao, E.-H., Kang, Z., Zeng, W.-B., Tan, H.-L., Li, H.-B., Bian, D.-J. and Shang, Q.-L. (2016). In vitro and in vivo magnetic resonance imaging with chlorotoxin-conjugated superparamagnetic nanoprobes for targeting hepatocarcinoma. *Oncology Reports*, 35(5): 3059–3067.

Cheng, Y., Zhao, J., Qiao, W. and Chen, K. (2014). Recent advances in diagnosis and treatment of gliomas using chlorotoxin-based bioconjugates. *American Journal of Nuclear Medicine and Molecular Imaging*, 4(5): 385–405.

Cheng, Y., Zhao, J., Qiao, W. and Chen, K., J. (2016). (131)I-labeled multifunctional dendrimers modified with BmK CT for targeted SPECT imaging and radiotherapy of gliomas. *Nanomedicine*, 11(10): 1253–1266.

Chien, C.-H., Hsueh, W.-T., Chuang, J.-Y. and Chang, K.-Y. (2021). Dissecting the mechanism of temozolomide resistance and its association with the regulatory roles of intracellular reactive oxygen species in glioblastoma. *Journal of Biomedical Science*, 28(1): 18.

Chintala, S.K., Tonn, J.C. and Rao, J.S. (1999). Matrix metalloproteinases and their biological function in human gliomas. *International Journal of Developmental Neuroscience*, 17(5): 495–502.

Choi, C.H.J., Zuckerman, J.E., Webster, P. and Davis, M.E. (2011). Targeting kidney mesangium by nanoparticles of defined size. *Proceedings of the National Academy of Sciences*, 108(16): 6656–6661.

Chou, K.F. and Dennis, A.M. (2015). Förster Resonance Energy Transfer between Quantum Dot Donors and Quantum Dot Acceptors. *Sensors (Basel, Switzerland)*, 15(6):13288–13325.

Chu, C.M., Rasalkar, D.D., Hu, Y.J., Cheng, F.W.T., Li, C.K. and Chu, W.C.W. (2011). Clinical presentations and imaging findings of neuroblastoma beyond abdominal mass and a review of imaging algorithm. *The British Journal of Radiology*, 84(997): 81–91.

Cohen, G., Burks, S.R. and Frank, J.A. (2018). Chlorotoxin-A Multimodal Imaging Platform for Targeting Glioma Tumors. *Toxins*, 10(12): E496.

Cohen-Inbar, O. and Zaaroor, M. (2016). Glioblastoma multiforme targeted therapy: The Chlorotoxin story. *Journal of Clinical Neuroscience: Official Journal of the Neurosurgical Society of Australasia*, 33: 52–58.

Conant, K., Allen, M. and Lim, S.T. (2015). Activity dependent CAM cleavage and neurotransmission. *Frontiers in Cellular Neuroscience*, 9: 305.

Costa, P.M., Cardoso, A.L., Custódia, C., Cunha, P., Pereira de Almeida, L. and Pedroso de Lima, M.C. (2015). MiRNA-21 silencing mediated by tumor-targeted nanoparticles combined with sunitinib: A new multimodal gene therapy approach for glioblastoma. *Journal of Controlled Release*, 207: 31–39.

Costa, P.M., Cardoso, A.L., Mendonça, L.S., Serani, A., Custódia, C., Conceição, M., Simões, S., Moreira, J.N., Pereira de Almeida, L. and Pedroso de Lima, M.C, P.M. (2013). Tumor-targeted Chlorotoxin-coupled Nanoparticles for Nucleic Acid Delivery to Glioblastoma Cells: A Promising System for Glioblastoma Treatment. *Molecular Therapy. Nucleic Acids*, 2(6): e100.

Dalal, M., Greneche, J.-M., Satpati, B., Ghzaiel, T.B., Mazaleyrat, F., Ningthoujam, R.S. and Chakrabarti, P.K. (2017). Microwave Absorption and the Magnetic Hyperthermia Applications of Li0.3Zn0.3Co0.1Fe2.3O4 Nanoparticles in Multiwalled Carbon Nanotube Matrix. *ACS Applied Materials & Interfaces*, 9(46): 40831–40845.

Dalton, S., Gerzanich, V., Chen, M., Dong, Y., Shuba, Y. and Simard, J.M. (2003). Chlorotoxin-sensitive Ca2+-activated Cl- channel in type R2 reactive astrocytes from adult rat brain. *Glia*, 42(4): 325–339.

Dardevet, L., Rani, D., Abd El Aziz, T., Bazin, I., Sabatier, J.-M., Fadl, M., Brambilla, E. and De Waard, M. (2015). Chlorotoxin: A Helpful Natural Scorpion Peptide to Diagnose Glioma and Fight Tumor Invasion. *Toxins*, 7(4): 1079–1101.

Dastpeyman, M., Giacomin, P., Wilson, D., Nolan, M.J., Bansal, P.S. and Daly, N.L (2019). A C-Terminal Fragment of Chlorotoxin Retains Bioactivity and Inhibits Cell Migration. *Frontiers in Pharmacology*, 10: 250.

Datta, N.R., Ordóñez, S.G., Gaipl, U.S., Paulides, M.M., Crezee, H., Gellermann, J., Marder, D., Puric, E. and Bodis, S. (2015). Local hyperthermia combined with radiotherapy and-/or chemotherapy: recent advances and promises for the future. *Cancer Treatment Reviews*, 41(9): 742–753.

Datta, N.R., Rogers, S., Ordóñez, S.G., Puric, E. and Bodis, S. (2016). Hyperthermia and radiotherapy in the management of head and neck cancers: A systematic review and meta-analysis. *International Journal of Hyperthermia*, 32(1): 31–40.

Day, E.S., Morton, J.G. and West, J.L. (2009). Nanoparticles for thermal cancer therapy. *Journal of Biomechanical Engineering*, 131(7): 074001.

De, A., Venkatesh, N., Senthil, M., Sanapalli, B.K.R., Shanmugham, R. and Karri, V.V.S.R. (2018). Smart niosomes of temozolomide for enhancement of brain targeting. *Nanobiomedicine*, 5: 1849543518805355.

Dearling, J.L.J., Barnes, J.W., Panigrahy, D., Zimmerman, R.E., Fahey, F., Treves, S.T., Morrison, M.S., Kieran, M.W. and Packard, A.B. (2013). Specific uptake of 99mTc-NC100692, an αvβ3-targeted imaging probe, in subcutaneous and orthotopic tumors. *Nuclear Medicine and Biology*, 40(6): 788–794.

DeBin, J.A., Maggio, J.E. and Strichartz, G.R. (1993). Purification and characterization of chlorotoxin, a chloride channel ligand from the venom of the scorpion. *The American Journal of Physiology*, 264(2 Pt 1): C361-369.

DeBin, J.A. and Strichartz, G.R. (1991). Chloride channel inhibition by the venom of the scorpion Leiurus quinquestriatus. *Toxicon*, 29(11):1403–1408.

Deng, Y., Wang, H., Gu, W., Li, S., Xiao, N., Shao, C., Xu, Q. and Ye, L. (2014). Ho3+ doped NaGdF4 nanoparticles as MRI/optical probes for brain glioma imaging. *Journal of Materials Chemistry B*, 2(11): 1521–1529.

Depciuch, J., Stec, M., Klebowski, B., Baran, J. and Parlinska-Wojtan, M. (2019). Platinum–gold nanoraspberries as effective photosensitizer in anticancer photothermal therapy. *Journal of Nanobiotechnology*, 17(1): 107.

Deshane, J., Garner, C.C. and Sontheimer, H. (2003). Chlorotoxin Inhibits Glioma Cell Invasion via Matrix Metalloproteinase-2. *Journal of Biological Chemistry*, 278(6): 4135–4144.

Díaz, R., Sachez-Garcia, L., Serna, N., Sánchez-Chardi, A., Cano Garrido, O., Sanchez, J., Unzueta, U., Vazquez, E. and Villaverde, A. (2019). Engineering a recombinant chlorotoxin as cell-targeted cytotoxic nanoparticles. *Science China Materials*, 62(6): 892–898.

Duan, Y., Dhar, A., Patel, C., Khimani, M., Neogi, S., Sharma, P., Kumar, N.S., L. and Vekariya, R. (2020). A brief review on solid lipid nanoparticles: part and parcel of contemporary drug delivery systems. *RSC Advances*, 10(45): 26777–26791.

Dubois, L.G., Campanati, L., Righy, C., D'Andrea-Meira, I., Spohr, T.C.L. de S.E., Porto-Carreiro, I., Pereira, C.M., Balça-Silva, J., Kahn, S.A., DosSantos, M.F., Oliveira, M. de A.R., Ximenes-da-Silva, A., Lopes, M.C., Faveret, E., Gasparetto, E.L. and Moura-Neto, V. (2014). Gliomas and the vascular fragility of the blood brain barrier. *Frontiers in Cellular Neuroscience*, 8: 418.

Dumond, A. and Pagès, G. (2020). Neuropilins, as Relevant Oncology Target: Their Role in the Tumoral Microenvironment. *Frontiers in Cell and Developmental Biology*, 8: 662.

El-Ghlban, S., Kasai, T., Shigehiro, T., Yin, H.X., Sekhar, S., Ida, M., Sanchez, A., Mizutani, A., Kudoh, T., Murakami, H. and Seno, M. (2014). Chlorotoxin-Fc Fusion Inhibits Release of MMP-2 from Pancreatic Cancer Cells. *BioMed Research International*, 2014: e152659.

Emadi, A., Jones, R.J. and Brodsky, R.A. (2009). Cyclophosphamide and cancer: golden anniversary. *Nature Reviews. Clinical Oncology*, 6(11): 638–647.

Endo-Takahashi, Y. and Negishi, Y. (2020). Microbubbles and Nanobubbles with Ultrasound for Systemic Gene Delivery. *Pharmaceutics*, 12(10): 964.

Erdreich, L.S. and Klauenberg, B.J. (2001). Radio frequency radiation exposure standards: considerations for harmonization. *Health Physics*, 80(5): 430–439.

Estelrich, J. and Busquets, M.A. (2018). Iron Oxide Nanoparticles in Photothermal Therapy. *Molecules : A Journal of Synthetic Chemistry and Natural Product Chemistry*, 23(7): 1567.

Estelrich, J., Escribano, E., Queralt, J. and Busquets, M.A. (2015). Iron oxide nanoparticles for magnetically-guided and magnetically-responsive drug delivery. *International Journal of Molecular Sciences*, 16(4): 8070–8101.

Fan, S., Sun, Z., Jiang, D., Dai, C., Ma, Y., Zhao, Z., Liu, H., Wu, Y., Cao, Z. and Li, W. (2010). BmKCT toxin inhibits glioma proliferation and tumor metastasis. *Cancer Letters*, 291(2): 158–166.

Fang, C., Veiseh, O., Kievit, F., Bhattarai, N., Wang, F., Stephen, Z., Li, C., Lee, D., Ellenbogen, R.G. and Zhang, M. (2010). Functionalization of iron oxide magnetic nanoparticles with targeting ligands: their physicochemical properties and in vivo behavior. *Nanomedicine (London, England)*, 5(9): 1357–1369.

Fang, C., Wang, K., Stephen, Z.R., Mu, Q., Kievit, F.M., Chiu, D.T., Press, O.W. and Zhang, M. (2015). Temozolomide nanoparticles for targeted glioblastoma therapy. *ACS applied materials & interfaces*, 7(12): 6674–6682.

Fathima, R. and Mujeeb, A. (2021). Enhanced nonlinear and thermo optical properties of laser synthesized surfactant-free Au-Pt bimetallic nanoparticles. *Journal of Molecular Liquids*, 343: 117711.

Fati, F., Pulvirenti, R., Paraboschi, I. and Martucciello, G. (2021). Surgical Approaches to Neuroblastoma: Review of the Operative Techniques. *Children*, 8(6): 446.

Feigin, V.L., Vos, T., Alahdab, F., Amit, A.M.L., Bärnighausen, T.W., Beghi, E., Beheshti, M., Chavan, P.P., Criqui, M.H., Desai, R., Dhamminda Dharmaratne, S., Dorsey, E.R., Wilder Eagan, A., Elgendy, I.Y., Filip, I., Giampaoli, S., Giussani, G., Hafezi-Nejad, N., Hole, M.K., Ikeda, T., Owens Johnson, C., Kalani, R., Khatab, K., Khubchandani, J., Kim, D., Koroshetz, W.J., Krishnamoorthy, V., Krishnamurthi, R.V., Liu, X., Lo, W.D., Logroscino, G., Mensah, G.A., Miller, T.R., Mohammed, S., Mokdad, A.H., Moradi-Lakeh, M., Morrison, S.D., Shivamurthy, V.K.N., Naghavi, M., Nichols, E., Norrving, B., Odell, C.M., Pupillo, E., Radfar, A., Roth, G.A., Shafieesabet, A., Sheikh, A., Sheikhbahaei, S., Shin, J.I., Singh, J.A., Steiner, T.J., Stovner, L.J., Wallin, M.T., Weiss, J., Wu, C., Zunt, J.R., Adelson, J.D. and Murray, C.J.L. (2021). Burden of Neurological Disorders Across the US From 1990-2017. *JAMA Neurology*, 78(2): 165–176.

Ferraris, C., Cavalli, R., Panciani, P.P. and Battaglia, L. (2020). Overcoming the Blood-Brain Barrier: Successes and Challenges in Developing Nanoparticle-Mediated Drug Delivery Systems for the Treatment of Brain Tumours. *International Journal of Nanomedicine*, 15: 2999–3022.

Fidel, J., Kennedy, K.C., Dernell, W.S., Hansen, S., Wiss, V., Stroud, M.R., Molho, J.I., Knoblaugh, S.E., Meganck, J., Olson, J.M., Rice, B. and Parrish-Novak, J. (2015). Preclinical validation of the utility of BLZ-100 in providing fluorescence contrast for imaging canine spontaneous solid tumors. *Cancer research*, 75(20): 4283–4291.

Formicola, B., Dal Magro, R., Montefusco-Pereira, C.V., Lehr, C.-M., Koch, M., Russo, L., Grasso, G., Deriu, M.A., Danani, A., Bourdoulous, S. and Re, F. (2019). The synergistic effect of chlorotoxin-mApoE in boosting drug-loaded liposomes across the BBB. *Journal of Nanobiotechnology*, 17(1): 115.

Forsyth, P.A., Wong, H., Laing, T.D., Rewcastle, N.B., Morris, D.G., Muzik, H., Leco, K.J., Johnston, R.N., Brasher, P.M., Sutherland, G. and Edwards, D.R. (1999). Gelatinase-A (MMP-2), gelatinase-B (MMP-9) and membrane type matrix metalloproteinase-1 (MT1-MMP) are involved in different aspects of the pathophysiology of malignant gliomas. *British Journal of Cancer*, 79(11–12): 1828–1835.

Friedman, D.N. and Henderson, T.O. (2018). Late Effects and Survivorship Issues in Patients with Neuroblastoma. *Children*, 5(8): 107.

Fu, X., Shi, Y., Qi, T., Qiu, S., Huang, Y., Zhao, X., Sun, Q. and Lin, G. (2020). Precise design strategies of nanomedicine for improving cancer therapeutic efficacy using subcellular targeting. *Signal Transduction and Targeted Therapy*, 5(1): 1–15.

Fu, Y., Yin, L., Wang, W., Chai, B. and Liang, A. (2005). Synthesis, Expression and Purification of a Type of Chlorotoxin-like Peptide from the Scorpion, Buthus martensii Karsch, and its Acute Toxicity Analysis. *Biotechnology Letters*, 27(20): 1597–1603.

Fu, Y., An, N., Li, K., Zheng, Y., Liang, A. (2012). Chlorotoxin-conjugated nanoparticles as potential glioma-targeted drugs. *Journal of Neuro-Oncology*, 107(3): 457–462.

Fu, Y.-J., An, N., Chan, K.-G., Wu, Y.-B., Zheng, S.-H. and Liang, A.-H. (2011). A model of BmK CT in inhibiting glioma cell migration via matrix metalloproteinase-2 from experimental and molecular dynamics simulation study. *Biotechnology Letters*, 33(7): 1309–1317.

Fu, Y.-J., Yin, L.-T., Liang, A.-H., Zhang, C.-F., Wang, W., Chai, B.-F., Yang, J.-Y. and Fan, X.-J. (2007). Therapeutic potential of chlorotoxin-like neurotoxin from the Chinese scorpion for human gliomas. *Neuroscience Letters*, 412(1): 62–67.

Fuller, M.D., Thompson, C.H., Zhang, Z.-R., Freeman, C.S., Schay, E., Szakács, G., Bakos, E., Sarkadi, B., McMaster, D., French, R.J., Pohl, J., Kubanek, J. and McCarty, N.A. (2007). State-dependent inhibition of cystic fibrosis transmembrane conductance regulator chloride channels by a novel peptide toxin. *The Journal of Biological Chemistry*, 282(52): 37545–37555.

Gao, Z., Shi, L., Ling, X., Chen, Z., Mei, Q. and Wang, F. (2021). Near-infrared photon-excited energy transfer in platinum(II)-based supramolecular polymers assisted by upconverting nanoparticles. *Chemical Communications*, 57(15): 1927–1930.

Gobin, A.M., Lee, M.H., Halas, N.J., James, W.D., Drezek, R.A. and West, J.L. (2007). Near-infrared resonant nanoshells for combined optical imaging and photothermal cancer therapy. *Nano Letters*, 7(7): 1929–1934.

Goddard, Z.R., Marín, M.J., Russell, D.A. and Searcey, M. (2020). Active targeting of gold nanoparticles as cancer therapeutics. *Chemical Society Reviews*, 49(23): 8774–8789.

Goertz, D.E. (2015). An overview of the influence of therapeutic ultrasound exposures on the vasculature: high intensity ultrasound and microbubble-mediated bioeffects. *International Journal of Hyperthermia: The Official Journal of European Society for Hyperthermic Oncology, North American Hyperthermia Group*, 31(2): 134–144.

Gonzalez-Avila, G., Sommer, B., Mendoza-Posada, D.A., Ramos, C., Garcia-Hernandez, A.A. and Falfan-Valencia, R. (2019). Matrix metalloproteinases participation in the metastatic process and their diagnostic and therapeutic applications in cancer. *Critical Reviews in Oncology/Hematology*, 137: 57–83.

Groothuis, D.R. (2000). The blood-brain and blood-tumor barriers: a review of strategies for increasing drug delivery. *Neuro-Oncology*, 2(1): 45–59.

Gu, W., Song, G., Li, S., Shao, C. and Yan, C., Ye, L. (2014). Chlorotoxin-conjugated, PEGylated Gd2O3 nanoparticles as a glioma-specific magnetic resonance imaging contrast agent. *RSC Advances*, 4(91): 50254–50260.

Guo, P., Imanishi, Y., Cackowski, F.C., Jarzynka, M.J., Tao, H.-Q., Nishikawa, R., Hirose, T., Hu, B. and Cheng, S.-Y. (2005). Up-regulation of angiopoietin-2, matrix metalloprotease-2, membrane type 1 metalloprotease, and laminin 5 gamma 2 correlates with the invasiveness of human glioma. *The American Journal of Pathology*, 166(3): 877–890.

Haas, T.L. and Madri, J.A. (1999). Extracellular Matrix-Driven Matrix Metalloproteinase Production in Endothelial Cells: Implications for Angiogenesis. *Trends in Cardiovascular Medicine*, 9(3): 70–77.

Habela, C.W., Ernest, N.J., Swindall, A.F. and Sontheimer, H. (2009). Chloride accumulation drives volume dynamics underlying cell proliferation and migration. *Journal of Neurophysiology*, 101(2): 750–757.

Habela, C.W., Olsen, M.L. and Sontheimer, H. (2008). ClC3 is a critical regulator of the cell cycle in normal and malignant glial cells. *The Journal of Neuroscience: The Official Journal of the Society for Neuroscience*, 28(37): 9205–9217.

Habra, K., McArdle, S.E.B., Morris, R.H. and Cave, G.W.V. (2021). Synthesis and Functionalisation of Superparamagnetic Nano-Rods towards the Treatment of Glioblastoma Brain Tumours', *Nanomaterials*, 11(9): 2157.

Haggag, Y., El-Gizawy, S. and Osman, M. (2018). Peptides as Drug Candidates: Limitations and Recent Development Perspectives. *BioMed Research International*, 8(4): 6659-6662.

Haley, B. and Frenkel, E. (2008). Nanoparticles for drug delivery in cancer treatment. *Urologic Oncology*, 26(1): 57–64.

Hall, M.K., Whitman, A.A., Weidner, D.A. and Schwalbe, R.A. (2020). Knockdown of N-Acetylglucosaminyltransferase-II Reduces Matrix Metalloproteinase 2 Activity and Suppresses Tumorigenicity in Neuroblastoma Cell Line. *Biology*, 9(4): 71.

Harrison, E., Nicol, J.R., Macias-Montero, M., Burke, G.A., Coulter, J.A., Meenan, B.J. and Dixon, D. (2016). A comparison of gold nanoparticle surface co-functionalization approaches using Polyethylene Glycol (PEG) and the effect on stability, non-specific protein adsorption and internalization. *Materials Science & Engineering. C, Materials for Biological Applications*, 62: 710–718.

Hashizume, H., Baluk, P., Morikawa, S., McLean, J.W., Thurston, G., Roberge, S., Jain, R.K. and McDonald, D.M. (2000). Openings between Defective Endothelial Cells Explain Tumor Vessel Leakiness. *The American Journal of Pathology*, 156(4): 1363–1380.

Hatoum, A., Mohammed, R. and Zakieh, O. (2019). The unique invasiveness of glioblastoma and possible drug targets on extracellular matrix. *Cancer Management and Research*, 11: 1843–1855.

Henderson, T.A. and Morries, L.D. (2015). Near-infrared photonic energy penetration: can infrared phototherapy effectively reach the human brain?. *Neuropsychiatric Disease and Treatment*, 11: 2191–2208.

Hernot, S. and Klibanov, A.L. (2008). Microbubbles in ultrasound-triggered drug and gene delivery. *Advanced Drug Delivery Reviews*, 60(10): 1153–1166.

Hirosawa, F., Iwasaki, T. and Watano, S. (2017). Synthesis and magnetic induction heating properties of Gd-substituted Mg–Zn ferrite nanoparticles. *Applied Nanoscience*, 7(5): 209–214.

Hoang Thi, T.T., Pilkington, E.H., Nguyen, D.H., Lee, J.S., Park, K.D. and Truong, N.P. (2020). The Importance of Poly(ethylene glycol) Alternatives for Overcoming PEG Immunogenicity in Drug Delivery and Bioconjugation. *Polymers*, 12(2): 298.

Hockaday, D.C., Shen, S., Fiveash, J., Raubitschek, A., Colcher, D., Liu, A., Alvarez, V. and Mamelak, A.N. (2005). Imaging glioma extent with 131I-TM-601. *Journal of Nuclear Medicine: Official Publication, Society of Nuclear Medicine*, 46(4): 580–586.

Hoshyar, N., Gray, S., Han, H. and Bao, G. (2016). The effect of nanoparticle size on in vivo pharmacokinetics and cellular interaction. *Nanomedicine (London, England)*, 11(6): 673–692.

Hua, H., Zhang, H., Kong, Q. and Jiang, Y. (2018). Mechanisms for estrogen receptor expression in human cancer. *Experimental Hematology & Oncology*, 7(1): 24.

Huang, D., Sun, L., Huang, L. and Chen, Y. (2021). Nanodrug Delivery Systems Modulate Tumor Vessels to Increase the Enhanced Permeability and Retention Effect. *Journal of Personalized Medicine*, 11(2): 124.

Huang, R., Han, L., Li, J., Liu, S., Shao, K., Kuang, Y., Hu, X., Wang, X., Lei, H. and Jiang, C. (2011). Chlorotoxin-modified macromolecular contrast agent for MRI tumor diagnosis. *Biomaterials*, 32(22): 5177–5186.

Hudson, M.M. (2010). Reproductive Outcomes for Survivors of Childhood Cancer. *Obstetrics and gynecology*, 116(5): 1171–1183.

Jacoby, D.B., Dyskin, E., Yalcin, M., Kesavan, K., Dahlberg, W., Ratliff, J., Johnson, E.W. and Mousa, S.A. (2010). Potent Pleiotropic Anti-angiogenic Effects of TM601, a Synthetic Chlorotoxin Peptide. *Anticancer Research*, 30(1): 39–46.

Jain, K.K. (2018). A Critical Overview of Targeted Therapies for Glioblastoma. *Frontiers in Oncology*, 8: 419.

Jeong, W., Bu, J., Kubiatowicz, L.J., Chen, S.S., Kim, Y. and Hong, S. (2018). Peptide–nanoparticle conjugates: a next generation of diagnostic and therapeutic platforms?. *Nano Convergence*, 5: 38.

Jha, S., Mathur, P., Ramteke, S. and Jain, N.K. (2018). Pharmaceutical potential of quantum dots. *Artificial Cells, Nanomedicine, and Biotechnology*, 46(sup1): 57–65.

Jiang, W.G., Sanders, A.J., Katoh, M., Ungefroren, H., Gieseler, F., Prince, M., Thompson, S.K., Zollo, M., Spano, D., Dhawan, P., Sliva, D., Subbarayan, P.R., Sarkar, M., Honoki, K., Fujii, H., Georgakilas, A.G., Amedei, A., Niccolai, E., Amin, A., Ashraf, S.S., Ye, L., Helferich, W.G., Yang, X., Boosani, C.S., Guha, G., Ciriolo, M.R., Aquilano, K., Chen, S., Azmi, A.S., Keith, W.N., Bilsland, A., Bhakta, D., Halicka, D., Nowsheen, S., Pantano, F. and Santini, D. (2015). Tissue invasion and metastasis: Molecular, biological and clinical perspectives. *Seminars in Cancer Biology*, 35: S244–S275.

Kesavan, K., Ratliff, J., Johnson, E.W., Dahlberg, W., Asara, J.M., Misra, P., Frangioni, J.V. and Jacoby, D.B. (2010). Annexin A2 is a molecular target for TM601, a peptide with tumor-targeting and anti-angiogenic effects. *The Journal of Biological Chemistry*, 285(7): 4366–4374.

Khanyile, S., Masamba, P., Oyinloye, B.E., Mbatha, L.S. and Kappo, A.P. (2019). Current Biochemical Applications and Future Prospects of Chlorotoxin in Cancer Diagnostics and Therapeutics. *Advanced Pharmaceutical Bulletin*, 9(4): 510–520.

Kievit, F.M., Veiseh, O., Fang, C., Bhattarai, N., Lee, D., Ellenbogen, R.G. and Zhang, M. (2010). Chlorotoxin Labeled Magnetic Nanovectors for Targeted Gene Delivery to Glioma. *ACS Nano*, 4(8): 4587–4594.

Kim, C., Qin, R., Xu, J.S., Wang, L.V. and Xu, R. (2010). Multifunctional microbubbles and nanobubbles for photoacoustic and ultrasound imaging. *Journal of Biomedical Optics*, 15(1): 010510.

Kolber-Simonds, D., Wu, J., Majumder, U., Custar, D., Li, D., Du, H., Postema, M.H., Noland, T., Hart, A., Lai, G., Eckley, S., Dixit, V., Tendyke, K., Nomoto, K., Woodall-Jappe, M. and McGonigle, S. (2018). Abstract 3961: Role for neuropilin1 in mode of action of chlorotoxin. *Cancer Research*, 78(13 Supplement): 3961–3961.

Kooiman, K., Roovers, S., Langeveld, S.A.G., Kleven, R.T., Dewitte, H., O'Reilly, M.A., Escoffre, J.-M., Bouakaz, A., Verweij, M.D., Hynynen, K., Lentacker, I., Stride, E. and Holland, C.K. (2020). Ultrasound-Responsive Cavitation Nuclei for Therapy and Drug Delivery. *Ultrasound in Medicine & Biology*, 46(6): 1296–1325.

Kotoulas, A., Dendrinou-Samara, C., Sarafidis, C., Kehagias, T., Arvanitidis, J., Vourlias, G., Angelakeris, M. and Kalogirou, O. (2017). Carbon-encapsulated cobalt nanoparticles: synthesis, properties, and magnetic particle hyperthermia efficiency. *Journal of Nanoparticle Research*, 19(12): 399.

Kovar, J.L., Curtis, E., Othman, S.F., Simpson, M.A. and Olive, M.D. (2013). Characterization of IRDye 800CW chlorotoxin as a targeting agent for brain tumors. *Analytical Biochemistry*, 440(2): 212–219.

Kumar, S.K., Lacy, M.Q., Dispenzieri, A., Buadi, F.K., Hayman, S.R., Dingli, D., Gay, F., Sinha, S., Leung, N., Hogan, W., Rajkumar, S.V. and Gertz, M.A. (2012). Early versus delayed autologous transplantation after immunomodulatory agents-based induction therapy in patients with newly diagnosed multiple myeloma. *Cancer*, 118(6): 1585–1592.

Lah, T.T., Novak, M. and Breznik, B. (2020). Brain malignancies: Glioblastoma and brain metastases. *Seminars in Cancer Biology*, 60: 262–273.

Lampron, A., Elali, A. and Rivest, S. (2013). Innate immunity in the CNS: redefining the relationship between the CNS and Its environment. *Neuron*, 78(2): 214–232.

Latifi, Z., Fattahi, A., Ranjbaran, A., Nejabati, H.R. and Imakawa, K. (2018). Potential roles of metalloproteinases of endometrium-derived exosomes in embryo-maternal crosstalk during implantation. *Journal of Cellular Physiology*, 233(6): 4530–4545.

Lauritzen, S.P., Boye, T.L. and Nylandsted, J. (2015). Annexins are instrumental for efficient plasma membrane repair in cancer cells. *Seminars in Cell & Developmental Biology*, 45: 32–38.

Lee, M.J.-E., Veiseh, O., Bhattarai, N., Sun, C., Hansen, S.J., Ditzler, S., Knoblaugh, S., Lee, D., Ellenbogen, R., Zhang, M. and Olson, J.M. (2010). Rapid pharmacokinetic and biodistribution studies using cholorotoxin-conjugated iron oxide nanoparticles: a novel non-radioactive method. *PloS One*, 5(3): e9536.

Li, S., Shao, C., Gu, W., Wang, R., Zhang, J., Lai, J., Li, H. and Ye, L. (2015). Targeted imaging of brain gliomas using multifunctional Fe_3O_4/MnO nanoparticles. *RSC Advances*, 5(42): 33639–33645.

Li, S.-D. and Huang, L. (2009). Nanoparticles evading the reticuloendothelial system: Role of the supported bilayer. *Biochimica et Biophysica Acta (BBA) - Biomembranes*, 1788(10): 2259–2266.

Li, X., Nie, S., Lv, Z., Ma, L., Song, Y., Hu, Z., Hu, X., Liu, Z., Zhou, G., Dai, Z., Song, T., Liu, J. and Wang, S. (2021). Overexpression of Annexin A2 promotes proliferation by forming a Glypican 1/c-Myc positive feedback loop: prognostic significance in human glioma *Cell Death & Disease*, 12(3): 1–13.

Liang, Z., Khawar, M.B., Liang, J. and Sun, H. (2021). Bio-Conjugated Quantum Dots for Cancer Research: Detection and Imaging. *Frontiers in Oncology*, 11: 4300.

Lin, F.-C., Hsu, C.-H. and Lin, Y.-Y. (2018). Nano-therapeutic cancer immunotherapy using hyperthermia-induced heat shock proteins: insights from mathematical modeling. *International Journal of Nanomedicine*, 13: 3529–3539.

Liu, H., Zhang, J., Chen, X., Du, X.-S., Zhang, J.-L., Liu, G. and Zhang, W.-G. (2016). Application of iron oxide nanoparticles in glioma imaging and therapy: from bench to bedside. *Nanoscale*, 8(15): 7808–7826.

Liu, M., Fang, X., Yang, Y. and Wang, C.(2021). Peptide-Enabled Targeted Delivery Systems for Therapeutic Applications. *Frontiers in Bioengineering and Biotechnology*, 9: 577.

Liu, N. and Tang, M. (2020). Toxicity of different types of quantum dots to mammalian cells in vitro: An update review. *Journal of Hazardous Materials*, 399: 122606.

Liu, S.-D., Zhong, L.-P., He, J. and Zhao, Y.-X. (2021). Targeting neuropilin-1 interactions is a promising anti-tumor strategy. *Chinese Medical Journal*, 134(5): 508–517.

Liu, X., Zhang, X., Zhu, M., Lin, G., Liu, J., Zhou, Z., Tian, X. and Pan, Y. (2017). PEGylated Au@Pt Nanodendrites as Novel Theranostic Agents for Computed Tomography Imaging and Photothermal/Radiation Synergistic Therapy. *ACS Applied Materials & Interfaces*, 9(1): 279–285.

Lizarbe, M.A., Barrasa, J.I., Olmo, N., Gavilanes, F. and Turnay, J. (2013). Annexin-Phospholipid Interactions. Functional Implications. *International Journal of Molecular Sciences*, 14(2): 2652–2683.

Locatelli, E., Bost, W., Fournelle, M., Llop, J., Gil, L., Arena, F., Lorusso, V. and Comes Franchini, M. (2014a). Targeted polymeric nanoparticles containing gold nanorods: a therapeutic approach against glioblastoma. *Journal of Nanoparticle Research*, 16(3): 2304.

Locatelli, E., Broggi, F., Ponti, J., Marmorato, P., Franchini, F., Lena, S. and Franchini, M.C. (2012). Lipophilic silver nanoparticles and their polymeric entrapment into targeted-PEG-based micelles for the treatment of glioblastoma. *Advanced Healthcare Materials*, 1(3): 342–347.

Locatelli, E., Naddaka, M., Uboldi, C., Loudos, G., Fragogeorgi, E., Molinari, V., Pucci, A., Tsotakos, T., Psimadas, D., Ponti, J. and Franchini, M.C. (2014b). Targeted delivery of silver nanoparticles and alisertib: in vitro and in vivo synergistic effect against glioblastoma. *Nanomedicine (London, England)*, 9(6): 839–849.

Lombardi, A.P.G., Cavalheiro, R.P., Porto, C.S. and Vicente, C.M. (2021). Estrogen Receptor Signaling Pathways Involved in Invasion and Colony Formation of Androgen-Independent Prostate Cancer Cells PC-3. *International Journal of Molecular Sciences*, 22(3): 1153.

Lombardi, G., Barresi, V., Castellano, A., Tabouret, E., Pasqualetti, F., Salvalaggio, A., Cerretti, G., Caccese, M., Padovan, M., Zagonel, V. and Ius, T. (2020). Clinical Management of Diffuse Low-Grade Gliomas. *Cancers*, 12(10): 3008.

Loza, K., Heggen, M. and Epple, M. (2020). Synthesis, Structure, Properties, and Applications of Bimetallic Nanoparticles of Noble Metals. *Advanced Functional Materials*, 30(21): 1909260.

Lu, P., Takai, K., Weaver, V.M. and Werb, Z. (2011). Extracellular Matrix Degradation and Remodeling in Development and Disease. *Cold Spring Harbor Perspectives in Biology*, 3(12): a005058.

Lui, V.C.H., Lung, S.S.S., Pu, J.K.S., Hung, K.N., and Leung, G.K.K. (2010). Invasion of human glioma cells is regulated by multiple chloride channels including ClC-3. *Anticancer Research*, 30(11): 4515–4524.

Luksch, R., Castellani, M.R., Collini, P., De Bernardi, B., Conte, M., Gambini, C., Gandola, L., Garaventa, A., Biasoni, D., Podda, M., Sementa, A.R., Gatta, G. and Tonini, G.P. (2016).

Neuroblastoma (Peripheral neuroblastic tumours). *Critical Reviews in Oncology/Hematology*, 107: 163–181.

Lyons, S.A., O'Neal, J. and Sontheimer, H. (2002). Chlorotoxin, a scorpion-derived peptide, specifically binds to gliomas and tumors of neuroectodermal origin. *Glia*, 39(2): 162–173.

Ma, Y. and Wang, H. (2021). Clinical significance of Annexin A2 expression in oral squamous cell carcinoma and its influence on cell proliferation, migration and invasion. *Scientific Reports*, 11(1): 5033.

Ma, Z., Zhang, Y., Zhang, J., Zhang, W., Foda, M.F., Dai, X. and Han, H. (2020). Ultrasmall Peptide-Coated Platinum Nanoparticles for Precise NIR-II Photothermal Therapy by Mitochondrial Targeting. *ACS Applied Materials & Interfaces* 12 (35): 39434–43.

Maertens, C., Wei, L., Tytgat, J., Droogmans, G. and Nilius, B. (2000). Chlorotoxin does not inhibit volume-regulated, calcium-activated and cyclic AMP-activated chloride channels. *British Journal of Pharmacology*, 129(4): 791–801.

Mahmud, H., Kasai, T., Khayrani, A.C., Asakura, M., Oo, A.K.K., Du, J., Vaidyanath, A., El-Ghlban, S., Mizutani, A., Seno, A., Murakami, H., Masuda, J. and Seno, M. (2018). Targeting Glioblastoma Cells Expressing CD44 with Liposomes Encapsulating Doxorubicin and Displaying Chlorotoxin-IgG Fc Fusion Protein. *International Journal of Molecular Sciences*, 19(3): 659.

Mahmoudi, K., Bouras, A., Bozec, D., Ivkov, R. and Hadjipanayis, C. (2018). Magnetic hyperthermia therapy for the treatment of glioblastoma: a review of the therapy's history, efficacy and application in humans. *International Journal of Hyperthermia*, 34(8): 1316–1328.

Mallepalli, S., Gupta, M.K. and Vadde, R. (2019). Neuroblastoma: An Updated Review on Biology and Treatment. *Current Drug Metabolism*, 20(13): 1014–1022.

Mamelak, A.N., Rosenfeld, S., Bucholz, R., Raubitschek, A., Nabors, L.B., Fiveash, J.B., Shen, S., Khazaeli, M.B., Colcher, D., Liu, A., Osman, M., Guthrie, B., Schade-Bijur, S., Hablitz, D.M., Alvarez, V.L. and Gonda, M.A. (2006). Phase I single-dose study of intracavitary-administered iodine-131-TM-601 in adults with recurrent high-grade glioma. *Journal of Clinical Oncology: Official Journal of the American Society of Clinical Oncology*, 24(22): 3644–3650.

Manikandan, M., Hasan, N. and Wu, H.-F. (2013). Platinum nanoparticles for the photothermal treatment of Neuro 2A cancer cells. *Biomaterials*, 34(23): 5833–5842.

Martinelli, C., Pucci, C. and Ciofani, G. (2019). Nanostructured carriers as innovative tools for cancer diagnosis and therapy. *APL Bioengineering*, 3(1): 011502.

Mazario, E., Menéndez, N., Herrasti, P., Cañete, M., Connord, V. and Carrey, J. (2013). Magnetic Hyperthermia Properties of Electrosynthesized Cobalt Ferrite Nanoparticles. *The Journal of Physical Chemistry C*, 117(21):11405–11411.

McCutcheon, I.E. and Preul, M.C. (2021). Historical Perspective on Surgery and Survival with Glioblastoma: How Far Have We Come?. *World Neurosurgery*, 149: 148–168.

McFerrin, M.B. and Sontheimer, H. (2006). A role for ion channels in glioma cell invasion. *Neuron Glia Biology*, 2(1): 39–49.

McGonigle, S., Majumder, U., Kolber-Simonds, D., Wu, J., Hart, A., Noland, T., TenDyke, K., Custar, D., Li, D., Du, H., Postema, M.H.D., Lai, W.G., Twine, N.C., Woodall-Jappe, M. and Nomoto, K. (2019). Neuropilin-1 drives tumor-specific uptake of chlorotoxin. *Cell communication and signaling: CCS*, 17(1): 67.

Mendes, M., Sousa, J.J., Pais, A. and Vitorino, C. (2018). Targeted Theranostic Nanoparticles for Brain Tumor Treatment. *Pharmaceutics*, 10(4): 181.

Meng, X., Wan, J., Jing, M., Zhao, S., Cai, W. and Liu, E. (2007). Specific targeting of gliomas with multifunctional superparamagnetic iron oxide nanoparticle optical and magnetic resonance imaging contrast agents. *Acta Pharmacologica Sinica*, 28(12): 2019–2026.

Miller, K.D., Ostrom, Q.T., Kruchko, C., Patil, N., Tihan, T., Cioffi, G., Fuchs, H.E., Waite, K.A., Jemal, A., Siegel, R.L. and Barnholtz-Sloan, J.S. (2021). Brain and other central nervous system tumor statistics, 2021. *CA: A Cancer Journal for Clinicians*, 71(5): 381–406.

Mitchell, M.J., Billingsley, M.M., Haley, R.M., Wechsler, M.E., Peppas, N.A. and Langer, R. (2021). Engineering precision nanoparticles for drug delivery. *Nature Reviews Drug Discovery*, 20(2): 101–124.

Miwa, N., Uebi, T. and Kawamura, S. (2008). S100–annexin complexes – biology of conditional association. *The FEBS Journal*, 275(20): 4945–4955.

Mohammadi, E., Ghasemi, E., Azadnajafabad, S., Rezaei, N., Moghaddam, S.S., Meimand, S.E., Fattahi, N., Habibi, Z., Yarandi, K.K., Amirjamshidi, A., Nejat, F., Kompani, F., Mokdad, A.H., Larijani, B. and Farzadfar, F. (2021). A global, regional, and national survey on burden and Quality of Care Index (QCI) of brain and other central nervous system cancers: global burden of disease systematic analysis 1990-2017. *PLOS ONE*, 16(2): e0247120.

Mohan, J.C., Praveen, G., Chennazhi, K.P., Jayakumar, R. and Nair, S.V. (2013). Functionalised gold nanoparticles for selective induction of in vitro apoptosis among human cancer cell lines. *Journal of Experimental Nanoscience*, 8(1): 32–45.

Mok, H., Veiseh, O., Fang, C., Kievit, F.M., Wang, F.Y., Park, J.O. and Zhang, M. (2010). pH-Sensitive siRNA nanovector for targeted gene silencing and cytotoxic effect in cancer cells. *Molecular Pharmaceutics*, 7(6): 1930–1939.

Moreno-Sánchez, R., Saavedra, E., Gallardo-Pérez, J.C., Rumjanek, F.D. and Rodríguez-Enríquez, S. (2016). Understanding the cancer cell phenotype beyond the limitations of current omics analyses', *The FEBS Journal*, 283(1): 54–73.

Moros, M., Idiago-López, J., Asín, L., Moreno-Antolín, E., Beola, L., Grazú, V., Fratila, R.M., Gutiérrez, L. and de la Fuente, J.M. (2019). Triggering antitumoural drug release and gene expression by magnetic hyperthermia. *Advanced Drug Delivery Reviews*, 138: 326–343.

Moros, M., Lewinska, A., Merola, F., Ferraro, P., Wnuk, M., Tino, A. and Tortiglione, C. (2020). Gold Nanorods and Nanoprisms Mediate Different Photothermal Cell Death Mechanisms In Vitro and In Vivo. *ACS applied materials & interfaces*, 12(12): 13718–13730.

Mu, Q., Lin, G., Patton, V.K., Wang, K., Press, O.W. and Zhang, M. (2016). Gemcitabine and Chlorotoxin Conjugated Iron Oxide Nanoparticles for Glioblastoma Therapy. *Journal of materials chemistry. B, Materials for biology and medicine*, 4(1): 32–36.

Nasseri, B., Yilmaz, M., Turk, M., Kocum, I.C. and Piskin, E. (2016). Antenna-type radiofrequency generator in nanoparticle-mediated hyperthermia. *RSC Advances*, 6(54): 48427–48434.

Norouzi, H., Khoshgard, K. and Akbarzadeh, F. (2018). In vitro outlook of gold nanoparticles in photo-thermal therapy: a literature review. *Lasers in Medical Science*, 33(4): 917–926.

Noujaim, D., van Golen, C.M., van Golen, K.L., Grauman, A. and Feldman, E.L. (2002). N-Myc and Bcl-2 coexpression induces MMP-2 secretion and activation in human neuroblastoma cells. *Oncogene*, 21(29): 4549–4557.

Oei, A.L., Kok, H.P., Oei, S.B., Horsman, M.R., Stalpers, L.J.A., Franken, N.A.P. and Crezee, J. (2020). Molecular and biological rationale of hyperthermia as radio- and chemosensitizer. *Advanced Drug Delivery Reviews*, 163–164: 84–97.

Ohta, S., Kikuchi, E., Ishijima, A., Azuma, T., Sakuma, I. and Ito, T. (2020). Investigating the optimum size of nanoparticles for their delivery into the brain assisted by focused ultrasound-induced blood–brain barrier opening. *Scientific Reports*, 10(1): 18220.

Ojeda, P.G., Wang, C.K. and Craik, D.J. (2016). Chlorotoxin: Structure, activity, and potential uses in cancer therapy. *Biopolymers*, 106(1): 25–36.

Olsen, M.L., Schade, S., Lyons, S.A., Amaral, M.D. and Sontheimer, H. (2003). Expression of Voltage-Gated Chloride Channels in Human Glioma Cells. *The Journal of Neuroscience*, 23(13): 5572–5582.

Opris, I., Lebedev, M.A., Pulgar, V.M., Vidu, R., Enachescu, M. and Casanova, M.F. (2020). Editorial: Nanotechnologies in Neuroscience and Neuroengineering. *Frontiers in Neuroscience*, 14: 33.

Othman, H., Wieninger, S.A., ElAyeb, M., Nilges, M. and Srairi-Abid, N. (2017). In Silico prediction of the molecular basis of ClTx and AaCTx interaction with matrix metalloproteinase-2 (MMP-2) to inhibit glioma cell invasion. *Journal of Biomolecular Structure and Dynamics*, 35(13): 2815–2829.

Pandey, A., Singh, K., Subramanian, S., Korde, A., Singh, R. and Sawant, K. (2020). Heterogeneous surface architectured pH responsive Metal-Drug Nano-conjugates for mitochondria targeted therapy of Glioblastomas: A multimodal intranasal approach. *Chemical Engineering Journal*, 394: 124419.

Pardridge, W.M. (2012). Drug transport across the blood–brain barrier. *Journal of Cerebral Blood Flow & Metabolism*, 32(11): 1959–1972.

Patil, C.G., Walker, D.G., Miller, D.M., Butte, P., Morrison, B., Kittle, D.S., Hansen, S.J., Nufer, K.L., Byrnes-Blake, K.A., Yamada, M., Lin, L.L., Pham, K., Perry, J., Parrish-Novak, J., Ishak, L., Prow, T., Black, K. and Mamelak, A.N. (2019). Phase 1 Safety, Pharmacokinetics, and Fluorescence Imaging Study of Tozuleristide (BLZ-100) in Adults With Newly Diagnosed or Recurrent Gliomas. *Neurosurgery*, 85(4): E641–E649.

Patil, R., Galstyan, A., Sun, T., Shatalova, E.S., Butte, P., Mamelak, A.N., Carico, C., Kittle, D.S., Grodzinski, Z.B., Chiechi, A., Ding, H., Black, K.L., Ljubimova, J.Y. and Holler, E. (2019). Polymalic acid chlorotoxin nanoconjugate for near-infrared fluorescence guided resection of glioblastoma multiforme. *Biomaterials*, 206: 146–159.

Pennington, M.W., Czerwinski, A. and Norton, R.S. (2018). Peptide therapeutics from venom: Current status and potential. *Bioorganic & Medicinal Chemistry*, 26(10): 2738–2758.

Pinel, S., Thomas, N., Boura, C. and Barberi-Heyob, M. (2019). Approaches to physical stimulation of metallic nanoparticles for glioblastoma treatment. *Advanced Drug Delivery Reviews*, 138: 344–357.

Porcel, E., Liehn, S., Remita, H., Usami, N., Kobayashi, K., Furusawa, Y., Le Sech, C. and Lacombe, S. (2010). Platinum nanoparticles: a promising material for future cancer therapy?'. *Nanotechnology*, 21(8): 85103.

Prabhakar, U., Maeda, H., Jain, R.K., Sevick-Muraca, E.M., Zamboni, W., Farokhzad, O.C., Barry, S.T., Gabizon, A., Grodzinski, P. and Blakey, D.C. (2013). Challenges and Key Considerations of the Enhanced Permeability and Retention Effect for Nanomedicine Drug Delivery in Oncology. *Cancer Research*, 73(8): 2412–2417.

Pudela, C., Balyasny, S. and Applebaum, M.A. (2020). Nervous system: Embryonal tumors: Neuroblastoma. *Atlas of genetics and cytogenetics in oncology and haematology*, 24(7): 284–290.

Pullen, N.A., Pickford, A.R., Perry, M.M., Jaworski, D.M., Loveson, K.F., Arthur, D.J., Holliday, J.R., Meter, T.E.V., Peckham, R., Younas, W., Briggs, S.E., MacDonald, S., Butterfield, T., Constantinou, M. and Fillmore, H.L. (2018). Current insights into matrix metalloproteinases and glioma progression: transcending the degradation boundary. *Metalloproteinases In Medicine*, 5: 13–30.

Qiao, W., Zhao, L., Wu, S., Liu, C., Guo, L., Xing, Y. and Zhao, J. (2017). SPECT imaging and radionuclide therapy of glioma using 131I labeled Buthus martensii Karsch chlorotoxin. *Journal of Neuro-Oncology*, 133(2): 287–295.

Qin, C., He, B., Dai, W., Zhang, H., Wang, X., Wang, J., Zhang, X., Wang, G. Yin, L. and Zhang, Q. (2014a). Inhibition of metastatic tumor growth and metastasis via targeting metastatic breast cancer by chlorotoxin-modified liposomes. *Molecular Pharmaceutics*, 11(10): 3233–3241.

Qin, C., He, B., Dai, W., Lin, Z., Zhang, H., Wang, X., Wang, J., Zhang, X., Wang, G., Yin, L. and Zhang, Q. (2014b). The impact of a chlorotoxin-modified liposome system on receptor MMP-2 and the receptor-associated protein ClC-3. *Biomaterials*, 35(22): 5908–5920.

Quintero-Fabián, S., Arreola, R., Becerril-Villanueva, E., Torres-Romero, J.C., Arana-Argáez, V., Lara-Riegos, J., Ramírez-Camacho, M.A. and Alvarez-Sánchez, M.E. (2019). Role of Matrix Metalloproteinases in Angiogenesis and Cancer. *Frontiers in Oncology*, 9: 1370.

Rabab'h, O., Al-Ramadan, A., Shah, J., Lopez-Negrete, H. and Gharaibeh, A. (2021). Twenty Years After Glioblastoma Multiforme Diagnosis: A Case of Long-Term Survival. *Cureus*, 13(6): e16061.

Raeeszadeh-Sarmazdeh, M., Do, L.D. and Hritz, B.G. (2020). Metalloproteinases and Their Inhibitors: Potential for the Development of New Therapeutics. *Cells*, 9(5): 1313.

Rajan, A. and Sahu, N.K. (2020). Review on magnetic nanoparticle-mediated hyperthermia for cancer therapy. *Journal of Nanoparticle Research*, 22(11): 319.

Ransom, C.B., O'Neal, J.T. and Sontheimer, H. (2001). Volume-Activated Chloride Currents Contribute to the Resting Conductance and Invasive Migration of Human Glioma Cells. *Journal of Neuroscience*, 21(19): 7674–7683.

Raoof, M., Corr, S.J., Kaluarachchi, W.D., Massey, K.L., Briggs, K., Zhu, C., Cheney, M.A., Wilson, L.J. and Curley, S.A. (2012). Stability of antibody-conjugated gold nanoparticles in the endolysosomal nanoenvironment: implications for noninvasive radiofrequency-based cancer therapy. *Nanomedicine: Nanotechnology, Biology and Medicine*, 8(7): 1096–1105.

Raoof, M. and Curley, S.A. (2011). Non-invasive radiofrequency-induced targeted hyperthermia for the treatment of hepatocellular carcinoma. *International Journal of Hepatology*, 2011: 676957.

Rapoport, N., Nam, K.-H., Gupta, R., Gao, Z., Mohan, P., Payne, A., Todd, N., Liu, X., Kim, T., Shea, J., Scaife, C., Parker, D.L., Jeong, E.-K. and Kennedy, A.M. (2011). Ultrasound-mediated tumor imaging and nanotherapy using drug loaded, block copolymer stabilized perfluorocarbon nanoemulsions. *Journal of Controlled Release*, 153(1): 4–15.

Reshma, V.G. and Mohanan, P.V. (2019). Quantum dots: Applications and safety consequences. *Journal of Luminescence*, 205: 287–298.

Ribatti, D., Surico, G., Vacca, A., De Leonardis, F., Lastilla, G., Montaldo, P.G., Rigillo, N. and Ponzoni, M. (2001). Angiogenesis extent and expression of matrix metalloproteinase-2 and -9 correlate with progression in human neuroblastoma. *Life Sciences*, 68(10): 1161–1168.

Rifatbegovic, F., Frech, C., Abbasi, M.R., Taschner-Mandl, S., Weiss, T., Schmidt, W.M., Schmidt, I., Ladenstein, R., Ambros, I.M. and Ambros, P.F. (2018). Neuroblastoma cells undergo transcriptomic alterations upon dissemination into the bone marrow and subsequent tumor progression. *International Journal of Cancer*, 142(2): 297–307.

Rjeibi, I., Mabrouk, K., Mosrati, H., Berenguer, C., Mejdoub, H., Villard, C., Laffitte, D., Bertin, D., Ouafik, L., Luis, J., Elayeb, M. and Srairi-Abid, N. (2011). Purification, synthesis and characterization of AaCtx, the first chlorotoxin-like peptide from Androctonus australis scorpion venom. *Peptides*, 32(4): 656–663.

Roche, J., Drabkin, H. and Brambilla, E. (2013). *Neuropilin and Its Ligands in Normal Lung and Cancer*, *Madame Curie Bioscience Database [Internet]*. Landes Bioscience. Available at: https://www.ncbi.nlm.nih.gov/books/NBK6324/ (Accessed: 14 December 2021).

Rohrer, T., Trachsel, D., Engelcke, G. and Hammer, J. (2002). Congenital central hypoventilation syndrome associated with Hirschsprung's disease and neuroblastoma: case of multiple neurocristopathies. *Pediatric Pulmonology*, 33(1): 71–76.

Roma-Rodrigues, C., Rivas-García, L., Baptista, P.V. and Fernandes, A.R. (2020). Gene Therapy in Cancer Treatment: Why Go Nano?. *Pharmaceutics*, 12(3): 233.

Roomi, M.W., Ivanov, V., Kalinovsky, T., Niedzwiecki, A. and Rath, M. (2007). Inhibition of glioma cell line A-172 MMP activity and cell invasion in vitro by a nutrient mixture. *Medical Oncology (Northwood, London, England)*, 24(2): 231–238.

Roomi, M.W., Kalinovsky, T., Rath, M. and Niedzwiecki, A. (2017). Modulation of MMP-2 and MMP-9 secretion by cytokines, inducers and inhibitors in human glioblastoma T-98G cells. *Oncology Reports*, 37(3): 1907–1913.

Röschmann, P. (1987). Radiofrequency penetration and absorption in the human body: limitations to high-field whole-body nuclear magnetic resonance imaging. *Medical Physics*, 14(6): 922–931.

Rosso, J.P. and Rochat, H. (1985). Characterization of ten proteins from the venom of the Moroccan scorpion Androctonus mauretanicus mauretanicus, six of which are toxic to the mouse. *Toxicon: Official Journal of the International Society on Toxinology*, 23(1):113–125.

Rothenberger, N.J., Somasundaram, A. and Stabile, L.P. (2018). The Role of the Estrogen Pathway in the Tumor Microenvironment. *International Journal of Molecular Sciences*, 19(2): 611.

Roy, S., Bag, A.K., Singh, R.K., Talmadge, J.E., Batra, S.K. and Datta, K. (2017). Multifaceted Role of Neuropilins in the Immune System: Potential Targets for Immunotherapy. *Frontiers in Immunology*, 8: 1228.

Saeedi, M., Eslamifar, M., Khezri, K. and Dizaj, S.M. (2019). Applications of nanotechnology in drug delivery to the central nervous system. *Biomedicine & Pharmacotherapy*, 111: 666–675.

Saha Roy, S. and Vadlamudi, R.K. (2012). Role of estrogen receptor signaling in breast cancer metastasis. *International Journal of Breast Cancer*, 2012: 654698.

Salado-Leza, D., Traore, A., Porcel, E., Dragoe, D., Muñoz, A., Remita, H., García, G. and Lacombe, S. (2019). Radio-Enhancing Properties of Bimetallic Au:Pt Nanoparticles: Experimental and Theoretical Evidence. *International Journal of Molecular Sciences*, 20(22): E5648.

San, B.H., Moh, S.H. and Kim, K.K. (2013). Investigation of the heating properties of platinum nanoparticles under a radiofrequency current. *International Journal of Hyperthermia: The Official Journal of European Society for Hyperthermic Oncology, North American Hyperthermia Group*, 29(2): 99–105.

Sarin, H., Kanevsky, A.S., Wu, H., Brimacombe, K.R., Fung, S.H., Sousa, A.A., Auh, S., Wilson, C.M., Sharma, K., Aronova, M.A., Leapman, R.D., Griffiths, G.L. and Hall, M.D. (2008). Effective transvascular delivery of nanoparticles across the blood-brain tumor barrier into malignant glioma cells. *Journal of Translational Medicine*, 6: 80.

Sangaiya, P. and Jayaprakash, R. (2018). A Review on Iron Oxide Nanoparticles and Their Biomedical Applications. *Journal of Superconductivity and Novel Magnetism*, 31(11): 3397–3413.

Sasikumar, P.G. and Ramachandra, M. (2018). Small-Molecule Immune Checkpoint Inhibitors Targeting PD-1/PD-L1 and Other Emerging Checkpoint Pathways. *BioDrugs: Clinical Immunotherapeutics, Biopharmaceuticals and Gene Therapy*, 32(5): 481–497.

Sbeih, A.H., Salami, K., Morabito, F. and Saleh, H. (2020). Epidemiological and Clinical Data in Low and Intermediate Risk Neuroblastoma: A Single Institution Experience and Survival Outcomes in Jerusalem. *Asian Pacific Journal of Cancer Care*, 5(3): 139–144.

Schacht, J., Talaska, A.E. and Rybak, L.P. (2012). Cisplatin and Aminoglycoside Antibiotics: Hearing Loss and Its Prevention. *Anatomical record (Hoboken, N.J. : 2007)*, 295(11): 1837–1850.

Seckinger, A., Meissner, T., Moreaux, J., Depeweg, D., Hillengass, J., Hose, K., Rème, T., Rösen-Wolff, A., Jauch, A., Schnettler, R., Ewerbeck, V., Goldschmidt, H., Klein, B. and Hose, D. (2012). Clinical and prognostic role of annexin A2 in multiple myeloma. *Blood*, 120(5): 1087–1094.

Sengul, A.B. and Asmatulu, E. (2020). Toxicity of metal and metal oxide nanoparticles: a review. *Environmental Chemistry Letters*, 18(5): 1659–1683.

Sevastre, A., Costachi, A., Tataranu, L. G., Brandusa, C., Artene, S. A., Stovicek, O., Alexandru, O., Danoiu, S., Sfredel, V. and Dricu, A. (2021). Glioblastoma Pharmacotherapy: A Multifaceted Perspective of Conventional and Emerging Treatments (Review). *Experimental and Therapeutic Medicine*, 22 (6): 1–18.

Sharifi, I., Shokrollahi, H. and Amiri, S. (2012). Ferrite-based magnetic nanofluids used in hyperthermia applications. *Journal of Magnetism and Magnetic Materials*, 324(6): 903–915.

Sharma, G., Braga, C.B., Chen, K.-E., Jia, X., Ramanujam, V., Collins, B.M., Rittner, R. and Mobli, M. (2021). Structural basis for the binding of the cancer targeting scorpion toxin, ClTx, to the vascular endothelia growth factor receptor neuropilin-1. *Current Research in Structural Biology*, 3: 179–186.

Shohet, J. and Foster, J. (2017). Neuroblastoma. *BMJ*, 357.

Siddhartha, R. and Garg, M. (2021). Molecular and clinical insights of matrix metalloproteinases into cancer spread and potential therapeutic interventions. *Toxicology and Applied Pharmacology*, 426: 115593.

Singh, N., Miner, A., Hennis, L. and Mittal, S. (2021). Mechanisms of temozolomide resistance in glioblastoma - a comprehensive review. *Cancer drug resistance (Alhambra, Calif.)*, 4: 17–43.

Sirsi, S.R. and Borden, M.A. (2012). Advances in Ultrasound Mediated Gene Therapy Using Microbubble Contrast Agents. *Theranostics*, 2(12): 1208–1222.

Sk, U.H. and Kojima, C. (2015). Dendrimers for theranostic applications. *Biomolecular Concepts*, 6(3): 205–217.

Skandalakis, G.P., Rivera, D.R., Rizea, C.D., Bouras, A., Raj, J.G.J., Bozec, D. and Hadjipanayis, C.G. (2020). Hyperthermia treatment advances for brain tumors. *International journal of hyperthermia : the official journal of European Society for Hyperthermic Oncology, North American Hyperthermia Group*, 37(2): 3–19.

Smith, V. and Foster, J. (2018). High-Risk Neuroblastoma Treatment Review. *Children*, 5(9): 114.

Sokolova, V., Mekky, G., van der Meer, S.B., Seeds, M.C., Atala, A.J. and Epple, M. (2020). Transport of ultrasmall gold nanoparticles (2 nm) across the blood–brain barrier in a six-cell brain spheroid model. *Scientific Reports*, 10(1): 18033.

Song, Y., Qu, Z., Li, J., Shi, L., Zhao, W., Wang, H., Sun, T., Jia, T. and Sun, Y. (2021). Fabrication of the biomimetic DOX/Au@Pt nanoparticles hybrid nanostructures for the combinational chemo/photothermal cancer therapy. *Journal of Alloys and Compounds*, 881: 160592.

Song, Y., Shi, Q., Zhu, C., Luo, Y., Lu, Q., Li, H., Ye, R., Du, D. and Lin, Y. (2017). Mitochondrial Reactive Oxygen Species Burst for Cancer Therapy Triggered by Near-Infrared Light. *Nanoscale*, 2017.

Soroceanu, L., Gillespie, Y., Khazaeli, M.B. and Sontheimer, H. (1998). Use of chlorotoxin for targeting of primary brain tumors. *Cancer Research*, 58(21): 4871–4879.

Soroceanu, L., Manning, T.J. and Sontheimer, H. (1999). Modulation of glioma cell migration and invasion using Cl(-) and K(+) ion channel blockers. *The Journal of Neuroscience: The Official Journal of the Society for Neuroscience*, 19(14): 5942–5954.

Southgate, H.E.D., Chen, L., Curtin, N.J. and Tweddle, D.A. (2020). Targeting the DNA Damage Response for the Treatment of High Risk Neuroblastoma. *Frontiers in Oncology*, 10: 371.

Speckhart, B., Antony, R. and Fernandez, K.S. (2017). Long-term side effects of high-risk neuroblastoma survivors in a referral center in central Illinois. *Journal of Clinical Oncology*, 35(5_suppl): 129–129.

Srinivasan, E.S., Sankey, E.W., Grabowski, M.M., Chongsathidkiet, P. and Fecci, P.E. (2020). The intersection between immunotherapy and laser interstitial thermal therapy: a multipronged future of neuro-oncology. *International Journal of Hyperthermia*, 37(2): 27–34.

Staderini, M., Megia-Fernandez, A., Dhaliwal, K. and Bradley, M. (2018). Peptides for optical medical imaging and steps towards therapy. *Bioorganic & Medicinal Chemistry*, 26(10): 2816–2826.

Staquicini, D.I., Rangel, R., Guzman-Rojas, L., Staquicini, F.I., Dobroff, A.S., Tarleton, C.A., Ozbun, M.A., Kolonin, M.G., Gelovani, J.G., Marchiò, S., Sidman, R.L., Hajjar, K.A., Arap, W. and Pasqualini, R. (2017). Intracellular targeting of annexin A2 inhibits tumor cell adhesion, migration, and in vivo grafting. *Scientific Reports*, 7(1): 4243.

Stigliano, R.V., Shubitidze, F., Petryk, J.D., Shoshiashvili, L., Petryk, A.A. and Hoopes, P.J. (2016). Mitigation of eddy current heating during magnetic nanoparticle hyperthermia therapy. *International journal of hyperthermia : the official journal of European Society for Hyperthermic Oncology, North American Hyperthermia Group*, 32(7): 735–748.

Strother, D.R., London, W.B., Schmidt, M.L., Brodeur, G.M., Shimada, H., Thorner, P., Collins, M.H., Tagge, E., Adkins, S., Reynolds, C.P., Murray, K., Lavey, R.S., Matthay, K.K., Castleberry, R., Maris, J.M. and Cohn, S.L. (2012). Outcome After Surgery Alone or With Restricted Use of Chemotherapy for Patients With Low-Risk Neuroblastoma: Results of Children's Oncology Group Study P9641. *Journal of Clinical Oncology*, 30(15): 1842–1848.

Stroud, M.R., Hansen, S.J. and Olson, J.M. (2011). In Vivo Bio-imaging Using Chlorotoxin-based Conjugates. *Current Pharmaceutical Design*, 17(38): 4362–4371.

Stupp, R., Taillibert, S., Kanner, A., Read, W., Steinberg, D.M., Lhermitte, B., Toms, S., Idbaih, A., Ahluwalia, M.S., Fink, K., Di Meco, F., Lieberman, F., Zhu, J.-J., Stragliotto, G., Tran, D.D., Brem, S., Hottinger, A.F., Kirson, E.D., Lavy-Shahaf, G., Weinberg, U., Kim, C.-Y., Paek, S.-H., Nicholas, G., Bruna, J., Hirte, H., Weller, M., Palti, Y., Hegi, M.E. and Ram, Z. (2017). Effect of Tumor-Treating Fields Plus Maintenance Temozolomide vs Maintenance Temozolomide Alone on Survival in Patients With Glioblastoma: A Randomized Clinical Trial. *JAMA*, 318(23): 2306–2316.

Su, C., Ren, X., Nie, F., Li, T., Lv, W., Li, H. and Zhang, Y. (2021). Current advances in ultrasound-combined nanobubbles for cancer-targeted therapy: a review of the current status and future perspectives. *RSC Advances*, 11(21): 12915–12928.

Su, S. and M. Kang, P. (2020). Recent Advances in Nanocarrier-Assisted Therapeutics Delivery Systems. *Pharmaceutics*, 12(9): 837.

Sugiura, Y., Shimada, H., Seeger, R.C., Laug, W.E. and DeClerck, Y.A. (1998). Matrix metalloproteinases-2 and -9 are expressed in human neuroblastoma: contribution of stromal cells to their production and correlation with metastasis. *Cancer Research*, 58(10): 2209–2216.

Suk, J.S., Xu, Q., Kim, N., Hanes, J. and Ensign, L.M. (2016). PEGylation as a strategy for improving nanoparticle-based drug and gene delivery. *Advanced drug delivery reviews*, 99(Pt A): 28–51.

Sun, C., Du, K., Fang, C., Bhattarai, N., Veiseh, O., Kivit, F., Stephen, Z., Lee, D., Ellenbogen, R.G., Ratner, B. and Zhang, M. (2010). PEG-Mediated Synthesis of Highly Dispersive Multifunctional Superparamagnetic Nanoparticles: Their Physicochemical Properties and Function In Vivo. *ACS nano*, 4(4): 2402–2410.

Sun, C., Fang, C., Stephen, Z., Veiseh, O., Hansen, S., Lee, D., Ellenbogen, R.G., Olson, J. and Zhang, M. (2008a). Tumor-targeted drug delivery and MRI contrast enhancement by chlorotoxin-conjugated iron oxide nanoparticles. *Nanomedicine (London, England)*, 3(4): 495–505.

Sun, C., Veiseh, O., Gunn, J., Fang, C., Hansen, S., Lee, D., Sze, R., Ellenbogen, R.G., Olson, J. and Zhang, M. (2008b). In vivo MRI detection of gliomas by chlorotoxin-conjugated superparamagnetic nanoprobes. *Small (Weinheim an Der Bergstrasse, Germany)*, 4(3): 372–379.

Sun, N., Zhao, L., Qiao, W., Xing, Y. and Zhao, J. (2017). BmK CT and 125I-BmK CT suppress the invasion of glioma cells in vitro via matrix metalloproteinase-2. *Molecular Medicine Reports*, 15(5): 2703–2708.

Sun, N., Zhao, L., Zhu, J., Li, Y., Song, N., Xing, Y., Qiao, W., Huang, H. and Zhao, J. (2019). 131I-labeled polyethylenimine-entrapped gold nanoparticles for targeted tumor SPECT/CT imaging and radionuclide therapy. *International Journal of Nanomedicine*, 14: 4367–4381.

Sung, H., Ferlay, J., Siegel, R.L., Laversanne, M., Soerjomataram, I., Jemal, A. and Bray, F. (2021). Global Cancer Statistics 2020: GLOBOCAN Estimates of Incidence and Mortality Worldwide for 36 Cancers in 185 Countries. *CA: A Cancer Journal for Clinicians*, 71(3): 209–249.

Swift, C.C., Eklund, M.J., Kraveka, J.M. and Alazraki, A.L. Updates in Diagnosis, Management, and Treatment of Neuroblastoma. *RadioGraphics*, 38(2): 566–580.

Tahtamouni, L., Ahram, M., Koblinski, J. and Rolfo, C. (2019). Molecular Regulation of Cancer Cell Migration, Invasion, and Metastasis. *Analytical Cellular Pathology*, 2019: e1356508.

Tamborini, M., Locatelli, E., Rasile, M., Monaco, I., Rodighiero, S., Corradini, I., Franchini, M.C., Passoni, L. and Matteoli, M. (2016). A Combined Approach Employing Chlorotoxin-Nanovectors and Low Dose Radiation To Reach Infiltrating Tumor Niches in Glioblastoma. *ACS nano*, 10(2): 2509–2520.

Tan, A.C., Ashley, D.M., López, G.Y., Malinzak, M., Friedman, H.S. and Khasraw, M. (2020). Management of glioblastoma: State of the art and future directions. *CA: A Cancer Journal for Clinicians*, 70(4): 299–312.

Tang, J., Jiang, X., Wang, L., Zhang, H., Hu, Z., Liu, Y., Wu, X. and Chen, C. (2014). Au@Pt nanostructures: a novel photothermal conversion agent for cancer therapy. *Nanoscale*, 6(7): 3670–3678.

Tarantini, A., Wegner, K.D., Dussert, F., Sarret, G., Beal, D., Mattera, L., Lincheneau, C., Proux, O., Truffier-Boutry, D., Moriscot, C., Gallet, B., Jouneau, P.-H., Reiss, P. and Carrière, M. (2019). Physicochemical Alterations and Toxicity of InP Alloyed Quantum Dots Aged in Environmental Conditions: A Safer by Design Evaluation. *NanoImpact*, 14: 100168

Tardáguila-García, A., García-Morales, E., García-Alamino, J.M., Álvaro-Afonso, F.J., Molines-Barroso, R.J. and Lázaro-Martínez, J.L. (2019). Metalloproteinases in chronic and acute wounds: A systematic review and meta-analysis. *Wound Repair and Regeneration*, 27(4): 415–420.

Tatenhorst, L., Rescher, U., Gerke, V. and Paulus, W. (2006). Knockdown of annexin 2 decreases migration of human glioma cells in vitro. *Neuropathology and Applied Neurobiology*, 32(3): 271–277.

Thompson, C.H., Olivetti, P.R., Fuller, M.D., Freeman, C.S., McMaster, D., French, R.J., Pohl, J., Kubanek, J. and McCarty, N.A. (2009). Isolation and characterization of a high affinity peptide inhibitor of ClC-2 chloride channels. *The Journal of Biological Chemistry*, 284(38): 26051–26062.

Thon, N., Tonn, J.-C. and Kreth, F.-W. (2019). The surgical perspective in precision treatment of diffuse gliomas. *OncoTargets and Therapy*, 12: 1497–1508.

Thorek, D.L.J., Chen, A.K., Czupryna, J. and Tsourkas, A. (2006). Superparamagnetic iron oxide nanoparticle probes for molecular imaging. *Annals of Biomedical Engineering*, 34(1): 23–38.

Thuerauf, N. and Fromm, M.F. (2006). The role of the transporter P-glycoprotein for disposition and effects of centrally acting drugs and for the pathogenesis of CNS diseases. *European Archives of Psychiatry and Clinical Neuroscience*, 256(5): 281–286.

Trahair, T.N., Vowels, M.R., Johnston, K., Cohn, R.J., Russell, S.J., Neville, K.A., Carroll, S. and Marshall, G.M. (2007). Long-term outcomes in children with high-risk neuroblastoma treated with autologous stem cell transplantation. *Bone Marrow Transplantation*, 40(8): 741–746.

Turner, K.L., Honasoge, A., Robert, S.M., McFerrin, M.M., Sontheimer, H. and Turner, K.L. (2014). A pro-invasive role for the Ca2+-activated K+ channel KCa3.1 in malignant glioma. *Glia*, 62(6): 971–981.

Turner, K.L. and Sontheimer, H. (2014). Cl- and K+ channels and their role in primary brain tumour biology. *Philosophical Transactions of the Royal Society of London. Series B, Biological Sciences*, 369(1638): 20130095.

Ullrich, N., Bordey, A., Gillespie, G.Y. and Sontheimer, H. (1998). Expression of voltage-activated chloride currents in acute slices of human gliomas. *Neuroscience*, 83(4): 1161–1173.

Ullrich, N., Gillespie, G.Y. and Sontheimer, H. (1996). Human astrocytoma cells express a unique chloride current. *Neuroreport*, 7(5): 1020–1024.

Ullrich, N. and Sontheimer, H. (1996). Biophysical and pharmacological characterization of chloride currents in human astrocytoma cells. *The American Journal of Physiology*, 270(5 Pt 1): C1511-1521.

Ullrich, N. and Sontheimer, H. (1997). Cell cycle-dependent expression of a glioma-specific chloride current: proposed link to cytoskeletal changes. *The American Journal of Physiology*, 273(4): C1290-1297.

Valls, M.D., Soldado, M., Arasa, J., Perez-Aso, M., Williams, A.J., Cronstein, B.N., Noguera, M.A., Terencio, M.C. and Montesinos, M.C. (2021). Annexin A2-Mediated Plasminogen Activation in Endothelial Cells Contributes to the Proangiogenic Effect of Adenosine A2A Receptors. *Frontiers in Pharmacology*, 12: 709.

Veiseh, M., Gabikian, P., Bahrami, S.-B., Veiseh, O., Zhang, M., Hackman, R.C., Ravanpay, A.C., Stroud, M.R., Kusuma, Y., Hansen, S.J., Kwok, D., Munoz, N.M., Sze, R.W., Grady, W.M., Greenberg, N.M., Ellenbogen, R.G and Olson, J.M. (2007). Tumor Paint: A Chlorotoxin:Cy5.5 Bioconjugate for Intraoperative Visualization of Cancer Foci. *Cancer Research*, 67(14): 6882–6888.

Veiseh, O., Gunn, J.W., Kievit, F.M., Sun, C., Fang, C., Lee, J.S.H. and Zhang, M. (2009a). Inhibition of tumor-cell invasion with chlorotoxin-bound superparamagnetic nanoparticles. *Small (Weinheim an Der Bergstrasse, Germany)*, 5(2): 256–264.

Veiseh, O., Kievit, F.M., Fang, C., Mu, N., Jana, S., Leung, M.C., Mok, H., Ellenbogen, R.G., Park, J.O. and Zhang, M. (2010). Chlorotoxin bound magnetic nanovector tailored for cancer cell targeting, imaging, and siRNA delivery. *Biomaterials*, 31(31): 8032–8042.

Veiseh, O., Kievit, F.M., Gunn, J.W., Ratner, B.D. and Zhang, M. (2009b). A ligand-mediated nanovector for targeted gene delivery and transfection in cancer cells. *Biomaterials*, 30(4): 649–657.

Veiseh, O., Sun, C., Fang, C., Bhattarai, N., Gunn, J., Kievit, F., Du, K., Pullar, B., Lee, D., Ellenbogen, R.G., Olson, J. and Zhang, M.(2009c). Specific Targeting of Brain Tumors with an Optical/Magnetic Resonance Imaging Nanoprobe across the Blood-Brain Barrier. *Cancer Research*, 69(15): 6200–6207.

Veiseh, O., Sun, C., Gunn, J., Kohler, N., Gabikian, P., Lee, D., Bhattarai, N., Ellenbogen, R., Sze, R., Hallahan, A., Olson, J. and Zhang, M. (2005). Optical and MRI Multifunctional Nanoprobe for Targeting Gliomas. *Nano Letters*, 5(6): 1003–1008.

Veschi, V., Verona, F. and Thiele, C.J. (2019). Cancer Stem Cells and Neuroblastoma: Characteristics and Therapeutic Targeting Options. *Frontiers in Endocrinology*, 10: 782.

Walker, C., Mojares, E. and del Río Hernández, A. (2018). Role of Extracellular Matrix in Development and Cancer Progression. *International Journal of Molecular Sciences*, 19(10): 3028.

Wan, J., Meng, X., Liu, E. and Chen, K. (2010). Incorporation of magnetite nanoparticle clusters in fluorescent silica nanoparticles for high-performance brain tumor delineation. *Nanotechnology*, 21(23): 235104.

Wang, B., Xie, J., He, H.-Y., Huang, E.-W., Cao, Q.-H., Luo, L., Liao, Y.-S. and Guo, Y. (2017). Suppression of CLC-3 chloride channel reduces the aggressiveness of glioma through inhibiting nuclear factor-κB pathway. *Oncotarget*, 8(38): 63788–63798.

Wang, J., Deng, L., Zhuang, H., Liu, J., Liu, D., Li, X., Jin, S., Zhu, L., Wang, H. and Lin, B. (2019). Interaction of HE4 and ANXA2 exists in various malignant cells—HE4–ANXA2–MMP2 protein complex promotes cell migration. *Cancer Cell International*, 19(1): 161.

Wang, J., Yao, W. and Li, K. (2020). Applications and prospects of targeted therapy for neuroblastoma. *World Journal of Pediatric Surgery*, 3(2): e000164.

Wang, K., Kievit, F.M., Chiarelli, P.A., Stephen, Z.R., Lin, G., Silber, J.R., Ellenbogen, R.G. and Zhang, M. (2021). siRNA Nanoparticle Suppresses Drug-Resistant Gene and Prolongs Survival in an Orthotopic Glioblastoma Xenograft Mouse Model. *Advanced Functional Materials*, 31(6): 2007166.

Wang, X. and Guo, Z. (2015). Chlorotoxin-conjugated onconase as a potential anti-glioma drug. *Oncology Letters*, 9(3): 1337–1342.

Wang, X.-M., Luo, X. and Guo, Z.-Y. (2013). Recombinant expression and downstream processing of the disulfide-rich tumor-targeting peptide chlorotoxin. *Experimental and Therapeutic Medicine*, 6(4): 1049–1053.

Wang, X., Prager, B.C., Wu, Q., Kim, L.J.Y., Gimple, R.C., Shi, Y., Yang, K., Morton, A.R., Zhou, W., Zhu, Z., Obara, E.A.A., Miller, T.E., Song, A., Lai, S., Hubert, C.G., Jin, X., Huang, Z., Fang, X., Dixit, D., Tao, W., Zhai, K., Chen, C., Dong, Z., Zhang, G., Dombrowski, S.M., Hamerlik, P., Mack, S.C., Bao, S. and Rich, J.N. (2018). Reciprocal Signaling between Glioblastoma Stem Cells and Differentiated Tumor Cells Promotes Malignant Progression. *Cell Stem Cell*, 22(4): 514-528.e5.

Wang, Y., Chen, K., Cai, Yihong, Cai, Yuanxia, Yuan, X., Wang, L., Wu, Z. and Wu, Y. (2017). Annexin A2 could enhance multidrug resistance by regulating NF-κB signaling pathway in pediatric neuroblastoma. *Journal of Experimental & Clinical Cancer Research*, 36(1): 111.

Wang, Y., Li, K., Han, S., Tian, Y., Hu, P., Xu, X., He, Y., Pan, W., Gao, Y., Zhang, Z., Zhang, J. and Wei, L. (2019). Chlorotoxin targets ERα/VASP signaling pathway to combat breast cancer. *Cancer Medicine*, 8(4): 1679–1693.

Wei, C., Wang, X., Zheng, M. and Cheng, H. (2012). Calcium gradients underlying cell migration. *Current Opinion in Cell Biology*, 24(2): 254–261.

Welch, D.R. and Hurst, D.R. (2019). Defining the Hallmarks of Metastasis. *Cancer Research*, 79(12): 3011–3027.

Winer, A., Adams, S. and Mignatti, P. (2018). Matrix Metalloproteinase Inhibitors in Cancer Therapy: Turning Past Failures Into Future Successes. *Molecular Cancer Therapeutics*, 17(6): 1147–1155.

Worm, D.J., Els-Heindl, S. and Beck-Sickinger, A.G. (2020). Targeting of peptide-binding receptors on cancer cells with peptide-drug conjugates. *Peptide Science*, 112(3): e24171.

Wu, C., Hansen, S.J., Hou, Q., Yu, J., Zeigler, M., Jin, Y., Burnham, D.R., McNeill, J.D., Olson, J.M. and Chiu, D.T. (2011). Design of highly emissive polymer dot bioconjugates for in vivo tumor targeting. *Angewandte Chemie (International Ed. in English)*, 50(15): 3430–3434.

Wu, J. (2021). The Enhanced Permeability and Retention (EPR) Effect: The Significance of the Concept and Methods to Enhance Its Application. *Journal of Personalized Medicine*, 11(8): 771.

Wu, J. and Li, R.-K. (2017). Ultrasound-targeted microbubble destruction in gene therapy: A new tool to cure human diseases. *Genes & Diseases*, 4(2): 64–74.

Wu, Z., Huang, Z., Yin, G., Cai, B., Wang, L. and Gao, F. (2017). RGD/CTX-conjugated multifunctional Eu–Gd2O3 NRs for targeting detection and inhibition of early tumor. *Journal of Materials Chemistry B*, 5(25): 4863–4875.

Xiang, Y., Liang, L., Wang, X., Wang, J., Zhang, X. and Zhang, Q. (2011). Chloride channel-mediated brain glioma targeting of chlorotoxin-modified doxorubicine-loaded liposomes. *Journal of Controlled Release: Official Journal of the Controlled Release Society*, 152(3): 402–410.

Xiang, Y., Wu, Q., Liang, L., Wang, X., Wang, J., Zhang, X., Pu, X. and Zhang, Q. (2012). Chlorotoxin-modified stealth liposomes encapsulating levodopa for the targeting delivery against Parkinson's disease in the MPTP-induced mice model. *Journal of Drug Targeting*, 20(1): 67–75.

Xu, T., Fan, Z., Li, W., Dietel, B., Wu, Y., Beckmann, M.W., Wrosch, J.K., Buchfelder, M., Eyupoglu, I.Y., Cao, Z. and Savaskan, N.E. (2016). Identification of two novel Chlorotoxin derivatives CA4 and CTX-23 with chemotherapeutic and anti-angiogenic potential. *Scientific Reports*, 6(1): 19799.

Yamada, M., Miller, D.M., Lowe, M., Rowe, C., Wood, D., Soyer, H.P., Byrnes-Blake, K., Parrish-Novak, J., Ishak, L., Olson, J.M., Brandt, G., Griffin, P., Spelman, L. and Prow, T.W. (2021). A first-in-human study of BLZ-100 (tozuleristide) demonstrates tolerability and safety in skin cancer patients. *Contemporary Clinical Trials Communications*, 23: 100830.

Yang, Q., Peng, J., Xiao, Y., Li, W., Tan, L., Xu, X. and Qian, Z. (2018). Porous Au@Pt Nanoparticles: Therapeutic Platform for Tumor Chemo-Photothermal Co-Therapy and Alleviating Doxorubicin-Induced Oxidative Damage. *ACS Applied Materials & Interfaces*, 10(1): 150–164.

Yetisgin, A.A., Cetinel, S., Zuvin, M., Kosar, A. and Kutlu, O. (2020) Therapeutic Nanoparticles and Their Targeted Delivery Applications. *Molecules (Basel, Switzerland)*, 25(9): E2193.

Yi, G.-Z., Huang, G., Guo, M., Zhang, X., Wang, H., Deng, S., Li, Y., Xiang, W., Chen, Z., Pan, J., Li, Z., Yu, L., Lei, B., Liu, Y. and Qi, S. (2019). Acquired temozolomide resistance in MGMT-deficient glioblastoma cells is associated with regulation of DNA repair by DHC2. *Brain: A Journal of Neurology*, 142(8): 2352–2366.

Yildirim, A., Blum, N.T. and Goodwin, A.P. (2019). Colloids, nanoparticles, and materials for imaging, delivery, ablation, and theranostics by focused ultrasound (FUS). *Theranostics*, 9(9): 2572–2594.

Yoo, B., Ifediba, M.A., Ghosh, S., Medarova, Z. and Moore, A. (2014). Combination treatment with theranostic nanoparticles for glioblastoma sensitization to TMZ. *Molecular Imaging and Biology*, 16(5): 680–689.

Yu, C.-F., Chen, F.-H., Lu, M.-H., Hong, J.-H. and Chiang, C.-S. (2017). Dual roles of tumour cells-derived matrix metalloproteinase 2 on brain tumour growth and invasion. *British Journal of Cancer*, 117(12): 1828–1836.

Yu, X.-F., Sun, Z., Li, M., Xiang, Y., Wang, Q.-Q., Tang, F., Wu, Y., Cao, Z. and Li, W. (2010). Neurotoxin-conjugated upconversion nanoprobes for direct visualization of tumors under near-infrared irradiation. *Biomaterials*, 31(33): 8724–8731.

Yue, P., He, L., Qiu, S., Li, Y., Liao, Y., Li, X., Xie, D. and Peng, Y. (2014). OX26/CTX-conjugated PEGylated liposome as a dual-targeting gene delivery system for brain glioma. *Molecular Cancer*, 13: 191.

Zhang, Q., Ye, Z., Yang, Q., He, X., Wang, H. and Zhao, Z. (2012). Upregulated expression of Annexin II is a prognostic marker for patients with gastric cancer. *World Journal of Surgical Oncology*, 10(1): 103.

Zhang, W., Huang, Z., Pu, X., Chen, X., Yin, G., Wang, L., Zhang, F. and Gao, F. (2020). Fabrication of doxorubicin and chlorotoxin-linked Eu-Gd2O3 nanorods with dual-model imaging and targeted therapy of brain tumor. *Chinese Chemical Letters*, 31(1): 285–291.

Zhao, L., Li, Y., Zhu, J., Sun, N., Song, N., Xing, Y., Huang, H. and Zhao, J. (2019). Chlorotoxin peptide-functionalized polyethylenimine-entrapped gold nanoparticles for glioma SPECT/CT imaging and radionuclide therapy. *Journal of Nanobiotechnology*, 17(1): 30.

Zhao, L., Shi, X. and Zhao, J. (2015a). Chlorotoxin-conjugated nanoparticles for targeted imaging and therapy of glioma. *Current Topics in Medicinal Chemistry*, 15(13): 1196–1208.

Zhao, L., Zhu, J., Cheng, Y., Xiong, Z., Tang, Y., Guo, L., Shi, X. and Zhao, J. (2015b). Chlorotoxin-Conjugated Multifunctional Dendrimers Labeled with Radionuclide 131I for Single Photon Emission Computed Tomography Imaging and Radiotherapy of Gliomas. *ACS applied materials & interfaces*, 7(35): 19798–19808.

Zhao, L., Zhu, J., Gong, J., Song, N., Wu, S., Qiao, W., Yang, J., Zhu, M. and Zhao, J. (2020a). Polyethylenimine-based theranostic nanoplatform for glioma-targeting single-photon emission computed tomography imaging and anticancer drug delivery. *Journal of Nanobiotechnology*, 18(1): 143.

Zhao, L., Zhu, J., Wang, T., Liu, C., Song, N., Wu, S., Qiao, W., Yang, J., Zhu, M. and Zhao, J. (2020b). A novel Buthus martensii Karsch chlorotoxin derivative for glioma SPECT imaging. *New Journal of Chemistry*, 44(35): 14947–14952.

Zhao, M., van Straten, D., Broekman, M.L.D., Préat, V. and Schiffelers, R.M. (2020). Nanocarrier-based drug combination therapy for glioblastoma. *Theranostics*, 10(3): 1355–1372.

Zhao, Q., Liu, Y., Zhang, Y., Meng, L., Wei, J., Wang, B., Wang, H., Xin, Y., Dong, L. and Jiang, X. (2020). Role and toxicity of radiation therapy in neuroblastoma patients: A literature review. *Critical Reviews in Oncology/Hematology*, 149: 102924.

Zhao, R., Xiang, J., Wang, B., Chen, L. and Tan, S. (2019). Increased expression of MMP-2 and MMP-9 indicates poor prognosis in glioma recurrence. *Biomedicine & Pharmacotherapy*, 118: 109369.

Zhao, R., Xiang, J., Wang, B., Chen, L. and Tan, S. (2022). Recent Advances in the Development of Noble Metal NPs for Cancer Therapy. *Bioinorganic Chemistry and Applications*, 2022: e2444516.

Zhu, S., Lee, J.-S., Guo, F., Shin, J., Perez-Atayde, A.R., Kutok, J.L., Rodig, S.J., Neuberg, D.S., Helman, D., Feng, H., Stewart, R.A., Wang, W., George, R.E., Kanki, J.P. and Look, A.T (2012). Activated ALK Collaborates with MYCN in Neuroblastoma Pathogenesis. *Cancer Cell*, 21(3): 362–373.

CHAPTER THREE:

The synthesis and characterization of chlorotoxin functionalised metallic nanoparticles

Taahirah Boltman[1], Mervin Meyer[2] * Okobi Ekpo[1]

[1] Department of Medical Biosciences, University of the Western Cape, Cape Town, Robert Sobukwe Road, Bellville 7535, South Africa; 2917424@myuwc.ac.za (T.B.)

[2] DSI/Mintek Nanotechnology Innovation Centre, Biolabels Node, Department of Biotechnology, University of the Western Cape, Cape Town, Robert Sobukwe Road, Bellville 7535, South Africa

*Correspondence: memeyer@uwc.ac.za (M.M.); Tel.: +27-21-5952032 (M.M.)

Abstract

The upregulation of matrix metalloproteinase-2 (MMP-2) is an active contributor to the progression of many cancers to the metastatic stage. Chlorotoxin (CTX) is a targeting peptide of intense focus, due to its ability to specifically bind to MMP-2 and block chloride channels, resulting in the inhibition of cancer cell migration and invasion. Given the advancement of nanotechnology in biomedical fields, surface functionalization of nanoparticles (NPs) with CTX can produce promising diagnostic and therapeutic agents for the treatment of cancer. Bimetallic gold platinum NPs (AuPtNPs) has generated much excitement for anti-cancer applications as it demonstrates more pronounced photothermal therapy (PTT) effects than its monometallic gold NPs (AuNPs) and platinum NPs (PtNPs) counterparts. In this study, we demonstrated the synthesis of two novel CTX functionalised NPs via streptavidin-biotin interaction to produce CTX functionalized monometallic gold NPs (CTX-AuNPs) and bimetallic gold platinum NPs (CTX-AuPtNPs). The physicochemical properties of the NPs were characterized by Ultraviolet-Visible Spectroscopy (UV-Vis), Dynamic Light Scattering (DLS) analysis, Fourier Transform Infra-Red Spectroscopy (FTIR), Transmission Electron Microscopy (TEM), Energy Dispersive X-ray Spectra (EDX) analysis and Selected Area Electron Diffraction (SAED) pattern analysis. CTX-AuNPs and CTX-AuPtNPs with a hydrodynamic size of approximately 16 nm and 21 nm, respectively were synthesised successfully. TEM revealed a core size of approximately 5 nm and EDX analysis confirmed the presence of Au and Pt in bimetallic

AuPtNPs. The NPs were highly stable in biological media over a 48-hour period. Darkfield microscopy showed that these NPs are taken up by U87 human malignant glioblastoma and SH-SY5Y human neuroblastoma cancer cells. Therefore, these NPs have the potential of being investigated for future *in vitro* studies and applications of non-invasive NP-mediated radiofrequency (RF) targeted hyperthermia.

1. Introduction

Peptides isolated from scorpion venom have opened an exciting avenue for the development of novel target specific tools for the diagnosis and treatment of cancer (Pennington, Czerwinski and Norton, 2018). The mechanisms through which scorpion venom peptides target cancer cells are diverse, so too are their mechanisms of cytotoxicity and anti-tumour activity which include inhibition of ion channels and other molecular targets involved in cell migration and invasion (Dueñas-Cuellar *et al.*, 2020). Chlorotoxin (CTX) is a 36-amino acid peptide, derived from *Leiurus quinquestriatus* (scorpion) venom and has been shown to be a tumour-targeting ligand owing to its strong affinity for a range of tumours, including glioblastoma multiforme (GB), neuroblastoma (NB), medulloblastoma, prostate cancer, ovarian cancer, lung cancer, sarcoma and intestinal cancer (Lyons, O'Neal and Sontheimer, 2002; Kesavan *et al.*, 2010; Dardevet *et al.*, 2015; Cohen-Inbar and Zaaroor, 2016; Tarokh, Naderi-Manesh and Nazari, 2017; Wang *et al.*, 2019).

Although the precise mechanism of CTX binding is not yet fully elucidated, a few potential target candidates have been identified as the primary cell surface targets (Chapter 2). Matrix metalloproteinases (MMPs), and specific chloride channels was identified as possible targets, mostly through investigations in GB cells (Deshane, Garner and Sontheimer, 2003; McFerrin and Sontheimer, 2006; Lui *et al.*, 2010). Matrix metalloproteinases (MMPs) are calcium-dependent zinc containing endopeptidases, which are responsible for the tissue remodelling and degradation of the extracellular matrix (ECM) during cancer invasion of normal tissue (Quintero-Fabián *et al.*, 2019). The upregulation of MMP2 and MMP-9, has been implicated as active contributors to the progression of malignant GB and NB by increasing cancer-cell growth, migration, invasion, and angiogenesis (Ara *et al.*, 1998; Forsyth *et al.*, 1999). Chloride channel 3 (ClC-3) is specifically upregulated in

93

human GB and is involved in cell cytoskeleton rearrangements and cell shape and movements during cell migration (Wang *et al.*, 2017). MMP-2 and ClC-3 are upregulated in human glioblastoma (GB) cells but not in normal glial cells and neurons (Deshane, Garner and Sontheimer, 2003). MMP-2 and ClC-3 form a protein complex located in the same membrane domain which is targeted by CTX and consequently leads to the inhibition of cancer cell migration and invasion in gliomas (Deshane, Garner and Sontheimer, 2003; Lui *et al.*, 2010; Xiang *et al.*, 2011).

The surface protein annexin A2, a calcium-binding cytoskeletal protein localized at the extracellular surface of numerous tumour cell types are typically involved in cell migration (Zhang *et al.*, 2013), invasion (Wang *et al.*, 2015) adhesion (Tong *et al.*, 2018), and was also identified as a receptor for CTX in human cancer cell lines (Kesavan *et al.*, 2010; Wang, Luo and Guo, 2013). The most recently identified likely target of CTX are estrogen receptor alpha (ERα) (Wang *et al*., 2019) and Neuropilin-1 (NRP1) (McGonigle *et al.*, 2019; Sharma *et al.*, 2021). CTX has also been shown in both animal models and humans to permeate intact blood brain barriers (BBBs), targeting GB cells and displayed no cytotoxic effects on normal glial cells and neurons (Khanyile *et al.*, 2019). Taken together this makes CTX an attractive alternative targeting agent in the development of targeted therapeutic strategies for cancers associated with the above-mentioned molecular targets.

GB is the most aggressive and consistently debilitating primary brain tumours diagnosed in adults, with a dismal median survival time of 12−15 months and a 5-year survival rate of less than 10 % (Tan *et al.*, 2020). Current treatments for these tumours are plagued with systemic toxicity due to the untargeted approach of these treatments (Fang *et al.*, 2015). Based on the unique pathological and physiological characteristics of the BBB, most chemotherapeutic drugs cannot enter the brain (Achar, Myers and Ghosh, 2021) and brain endothelial cells express multi-drug transporters such as P-glycoprotein (P-gp) which play a part in reducing the levels of drug delivered to the tumour (Kulczar *et al.*, 2017). These factors necessitate the development of novel therapeutic strategies that encompass high specificity and has the potential to cross the BBB. The unique biophysical properties of nanomaterials have enabled the development of nanoparticle-based platforms for the diagnosis and treatment of cancers.

While nanotechnology has been used to develop solutions for the diagnosis and treatment of several diseases, great successes has been achieved in the fight against cancer. Nanoparticles (NPs) ranging from 5-200 nm have been reported to cross the BBB, however NPs less than 15 nm in diameter may

cross the intact BBB more readily (Sokolova *et al.*, 2020; Ohta *et al.*, 2020). Additionally, smaller NPs are highly favoured for active targeting strategies due to their larger surface area which allows for increased surface loading of targeting and/or therapeutic agents, while also promoting entry through small membrane passageways and increased drug bioavailability (Yetisgin *et al.*, 2020). Polyethylene glycol (PEG) is a Food and Drug Administration (FDA) approved synthetic polymer commonly conjugated onto the surface of NPs, in a process called "PEGylation'' (Suk *et al.*, 2016). PEG coatings on NPs improve the biophysical and chemical properties of NPs which contributes to NPs avoiding phagocytosis and prolonging systemic circulation times *in vivo* (Hoang Thi *et al.*, 2020). Moreover, they act as a bridge to conjugate targeting molecules for active targeting (Shi *et al.*, 2021). Active targeting of NP drug delivery systems in cancer allows the anti-cancer activity to be directed to cancer cells specifically, through targeted delivery facilitated by specific recognition binding sites that are either overexpressed on the surface of cancer cells or expressed at low levels in normal cells (Yoo *et al.*, 2019). Targeted delivery using NPs reduce toxicity towards normal cells and enhance anti-cancer activity in diseased cells, thus addressing the lack of specificity with current cancer treatments, while also protecting drugs from degradation and increasing the circulation time of drugs (E. S. Ali *et al.*, 2021). Active targeting strategies has been achieved by conjugating NPs with different targeting molecules such as antibodies, peptides and aptamers (Yu, Park, and Jon 2012). Although monoclonal antibodies (mAbs) have been widely used as targeting molecules for the targeted delivery of NP/drug complexes, they are also associated with several limitations, which includes their large size, immunogenicity and the difficulty in conjugating mAbs to NPs (Wang *et al.*, 2008). Peptides, when compared to antibodies are more attractive targeting molecules due to their smaller size, lower immunogenicity, lower production cost, similar binding affinities to mAbs, easier synthesis and modification (Wang *et al.*, 2008). Compared to small molecule ligands, peptides have higher diversity, specificity, and targeting capability (Vlieghe *et al.*, 2010; Sasikumar and Ramachandra, 2018). Due to these factors, peptides such as CTX are more widely investigated as targeting agents for NP-based drug delivery development.

To address the challenges posed by GB, the cancer targeting and BBB penetrating properties of CTX has been combined to develop more effective multifunctional cancer targeting nano-systems. In recent years, a variety of different types of CTX-conjugated NPs with imaging and therapeutic functionalities have been developed and studied in GB tumours (Ojeda, Wang and Craik, 2016; Cohen, Burks and Frank, 2018; Zhao *et al.*, 2019) (Chapter 2). Currently, CTX-conjugated

95

fluorescent imaging agents are on trial and are yielding promising results for safer surgical resection of tumours (Fidel *et al.*, 2015; Baik *et al.*, 2016; Patil *et al.*, 2019; Yamada *et al.*, 2021). CTX-conjugated NPs reported in literature include iron oxides, liposomes, dendrimers, quantum dots, and rare-earth up-conversion NPs (Cohen, Burks and Frank, 2018; Khanyile *et al.*, 2019; Yeini *et al.*, 2021) (Chapter 2). While research groups also reported on the synthesis of CTX-conjugated gold (Au) and CTX-conjugated silver NPs (AgNPs) for applications in cancer diagnosis and treatment (Locatelli *et al.*, 2014; Tamborini *et al.*, 2016; Zhao *et al.*, 2019). However, no reports exist for the synthesis of CTX-bimetallic NPs constructed of noble metals.

AuNPs have been used for a diverse range of applications including imaging (Mahan and Doiron, 2018), photothermal therapy (PTT) (Yang *et al.*, 2019), drug delivery (Siddique and Chow, 2020), catalysis (Zhao *et al.*, 2015), biosensing (Zhang *et al.*, 2020) and in the development of vaccines (Mateu Ferrando, Lay and Polito, 2021). AuNPs are well suited for such applications due to their unique optical properties (Huang and El-Sayed, 2010), ease of functionalization (Häkkinen, 2012), facile synthesis, and tuneable shape and size (Piella, Bastús and Puntes, 2016). Bimetallic NPs (BNPs) are constructed of more than one type of metal atoms and have recently attracted great attention in the biomedical field due to improved features which is due to the synergistic effects originating from the combined properties of the different metal atoms (Medina-Cruz *et al.*, 2020). BNPs found application in catalysis, electronics, optical devices, and treatment of infections (Loza, Heggen and Epple, 2020; S. Ali *et al.*, 2021). In recent years BNPs has generated much interest as anti-tumour agents due to their suitability for drug delivery and enhanced properties for photothermal therapy (PTT) (Loza, Heggen and Epple, 2020; S. Ali *et al.*, 2021). PTT is a minimally invasive procedure based on the conversion of light energy, usually in the near-infrared (NIR) region, into heat energy to thermally ablate cells (Ray *et al.*, 2012).

NP-mediated PTT is an efficient method of inducing localized hyperthermia in diseased cells only. Hyperthermia treatments involve intracellular heat stress in the temperature range of 40-46 ⁰C (Rajan and Sahu, 2020). It causes mitochondrial swelling, protein denaturation, alteration in signal transduction, cellular structure rupturing and induction of apoptosis or necrosis (Rajan and Sahu, 2020). The disadvantages of conventional hyperthermia therapy include that it is an invasive procedure, results in incomplete tumour destruction, have low penetration of heat in the tumour (lesions > 4-5cm in diameter), excessive heating of surrounding healthy tissue as the treatment is non-specific, thermal under-dosage in the target region and dissipation of heat by blood flow (Chang *et*

al., 2018). Metallic NPs (MNPs) such as AuNPs and different types of alloy/bimetallic platinum NPs have a strong local surface plasmon resonance (SPR) effect (Graham, Macneill and Levi-polyachenko, 2013; Amendola *et al.*, 2017; Kunwar *et al*., 2019). Therefore, upon exposure to light, these MNPs can strongly absorb photon energy which is then converted into photothermal energy for PTT induced cytotoxicity (Norouzi, Khoshgard and Akbarzadeh, 2018).

AuNPs have been used in both *in vivo* and *in vitro* studies to demonstrate PTT induced thermal cytotoxicity through exposure to near-infrared (NIR) light (650–950 nm) (Moros *et al.*, 2020). Recent studies reported that bimetallic gold platinum NPs (AuPtNPs) of different sizes and shapes used for PTT exhibit better photothermal effects than its monometallic counterparts AuNP and platinum nanoparticles (PtNPs) (Tang *et al.*, 2014; Yang *et al.*, 2018; Depciuch *et al.*, 2019; Fathima and Mujeeb, 2021; Song *et al.*, 2021). Bimetallic AuPtNPs also demonstrated higher radiation enhancing properties in comparison to monometallic AuNPs (Salado-Leza *et al.*, 2019). A major drawback of NIR-induced PTT is that it is restricted to use for subcutaneous/superficial malignant tumours because of the minimal tissue penetration (~ 3 cm depth) of NIR light and may therefore not be useful for deep seated brain tumours (Henderson and Morries, 2015). Here, other applications such as radiofrequency (RF) ablation is recommended as RF waves has been shown to penetrate tissues located much deeper , e.g., at 220 MHz, RF penetration is 7 cm and at 85 MHz, it increases to 17 cm, allowing for the treatment of deep-seated tumours more effectively (Erdreich and Klauenberg, 2001; Day, Morton and West, 2009; Raoof and Curley, 2011). Radio waves are low-frequency electromagnetic waves that have low tissue-specific absorption rate (SAR) and therefore have great whole-body tissue penetration and is considered safe for humans (Raoof and Curley, 2011). While the heating properties of NPs using RF waves have been investigated for AuNP and PtNPs and demonstrate promise for enhancing non-invasive RF anti-cancer thermal therapy, there are limited reports on the targeted use of bimetallic AuPtNPs for this application (San, Moh and Kim, 2013; Corr and Curley, 2017). This warrants further investigation of AuPtNPs as potential heating agents for RF-based thermal therapies for deeply located tumours such as GB.

Herein we report a facile three-step preparation method to produce highly stable CTX functionalized AuNPs and AuPtNPs via streptavidin-biotin interaction. This approach is simple as the risk of disrupting the peptide functionality is minimized. The risk of introducing toxic reagents during the coupling reaction and extensive purification methods, are also avoided. To the best of our knowledge, this method of CTX functionalization onto NPs was not reported previously. In the present study we

demonstrate the development of biologically stable CTX-AuNPs and CTX-AuPtNPs showing specificity and uptake towards Human GB and NB cancer cell lines. The synthesized NPs were characterized using physical and optical measurement techniques including, ultraviolet-visible spectroscopy (UV-Vis), dynamic light scattering (DLS) analysis, transmission electron microscopy (TEM), energy-dispersive X-ray spectroscopy (EDX) analysis and fourier-transform infrared spectroscopy (FTIR). These NPs can be investigated in the future for targeted non-invasive RF-induced hyperthermia of GB.

2. Results and discussion

CTX has emerged as a promising therapeutic targeting peptide for a broad list of tumours, with preferential binding to glioma tumours via overexpressed MMP-2 cell surface protein and specific chloride channels, resulting in the inhibition of cancer cell migration and invasion (Deshane, Garner and Sontheimer, 2003; Lui *et al.*, 2010; Xiang *et al.*, 2011). This property and the possibility of conjugating CTX to NPs have enabled its diverse use in various biomedical applications for cancer such as in tumour imaging, drug delivery and radiotherapy (Ojeda, Wang and Craik, 2016; Cohen, Burks and Frank, 2018; Zhao *et al.*, 2019). BNPs AuPtNPs show promise in anti-cancer applications for NP-mediated hyperthermia treatments using different photothermal applications with some reporting on more pronounced effects when compared to their monometallic NP counterparts, due to synergistic effects of combined metal atoms (Liu *et al.*, 2017; Yang *et al.*, 2018; Depciuch *et al.*, 2019; Salado-Leza *et al.*, 2019; Fathima and Mujeeb, 2021; Song *et al.*, 2021). Therefore, the current study explored the development of bimetallic AuPtNP and monometallic AuNP that are less than 5 nm in diameter and is functionalized with CTX for future applications using RF-induced hyperthermia treatment for cancer. The size is not only advantageous for targeting brain tumours, but smaller NPs are capable of more efficient heating than larger NPs (> 50 nm) as previously described (Moran *et al.*, 2009).

2.1. Synthesis and Ultraviolet-visible (UV-Vis) Spectroscopy analysis of NPs

CTX functionalized AuNPs and AuPtNPs were synthesized using a facile 3-step preparation method as illustrated in Figure 11 (3. Materials and Methods, pg. 116). Citrate AuNPs and citrate AuPtNPs were synthesized by chemical reduction using sodium borohydride ($NaBH_4$) as previously described, with some alterations (Etame *et al.*, 2011; Qu *et al.*, 2011). The first indication of successful synthesis

is the characteristic colour changes from a pale-yellow solution to a bright red colour for citrate AuNPs and a dark brown colour for the formation of citrate AuPtNPs as shown in Figure 2 (A) and (B). The colour changes after the reduction process by $NaBH_4$ are attributed to the excitations of surface plasmon vibrations associated with the NPs present within the solutions (Huang and El-Sayed, 2010). The surface plasmon resonance (SPR) of metallic NPs induces a strong absorption of incident light and can thus be measured using a UV–vis absorption spectroscopy, which is a useful tool to characterize NPs size and surface characteristics (Huang and El-Sayed, 2010). Successful AuNPs production is accompanied by a distinct absorption maxima (λ max) in the range of 500-600 nm (Balasooriya *et al.*, 2017). The λ max of citrate AuNPs appeared at 508 nm which is in accordance with λ max of exceedingly small AuNPs (< 10nm), as previously reported (Jiang *et al.*, 2014; Piella, Bastús and Puntes, 2016; Oliveira *et al.*, 2020). For surface functionalization with polyethylene glycol (PEG), ligand exchange is a technique commonly used to generate covalently attached coatings on NP surfaces via the displacement of citrate ions (Guerrini, Alvarez-Puebla and Pazos-Perez, 2018). Following surface functionalization with a mixture of PEG-biotin and PEG-OH (1:10 ratio) and bioconjugation of CTX, there was a distinct red shift in the λ max from 508 nm to 518 nm and 521 nm, respectively, suggesting an increase in the size of the NPs and successful surface functionalization (Sosibo *et al.*, 2015; Daniels *et al.*, 2017). Figure 1 (B) shows the absence of a λ max in the absorption spectra of citrate bimetallic AuPtNPs, PEG-AuPtNPS and CTX-AuPtNPs, confirming successful AuPtNP synthesis. The structures of BNPs produced, are dependent on the synthesis method and atomic ratios used, this can be categorized into four structural types: alloy, intermetallic, subclusters, and core-shells (Srinoi *et al.*, 2018). The UV-Vis spectra of the bimetallic AuPtNPs reported in this study, is in accordance with the UV-Vis spectra reported in literature for bimetallic AuPtNPs with more of an alloy structure and PtNPs which do not display a characteristic λ max but rather a typical scattering pattern (Pal, 2015; Sørensen *et al.*, 2016; Olajire and Adesina, 2017; Zhu *et al.*, 2017; Formaggio *et al.*, 2019). Previous reports have also confirmed the absence of the characteristic AuNPs λ max in the UV-Vis spectrum of AuPtNPs as indicative of the core-shell structure where the shell is composed by platinum and the core by gold (Westsson and Koper, 2014; Zhao *et al.*, 2014; Usón *et al.*, 2015).
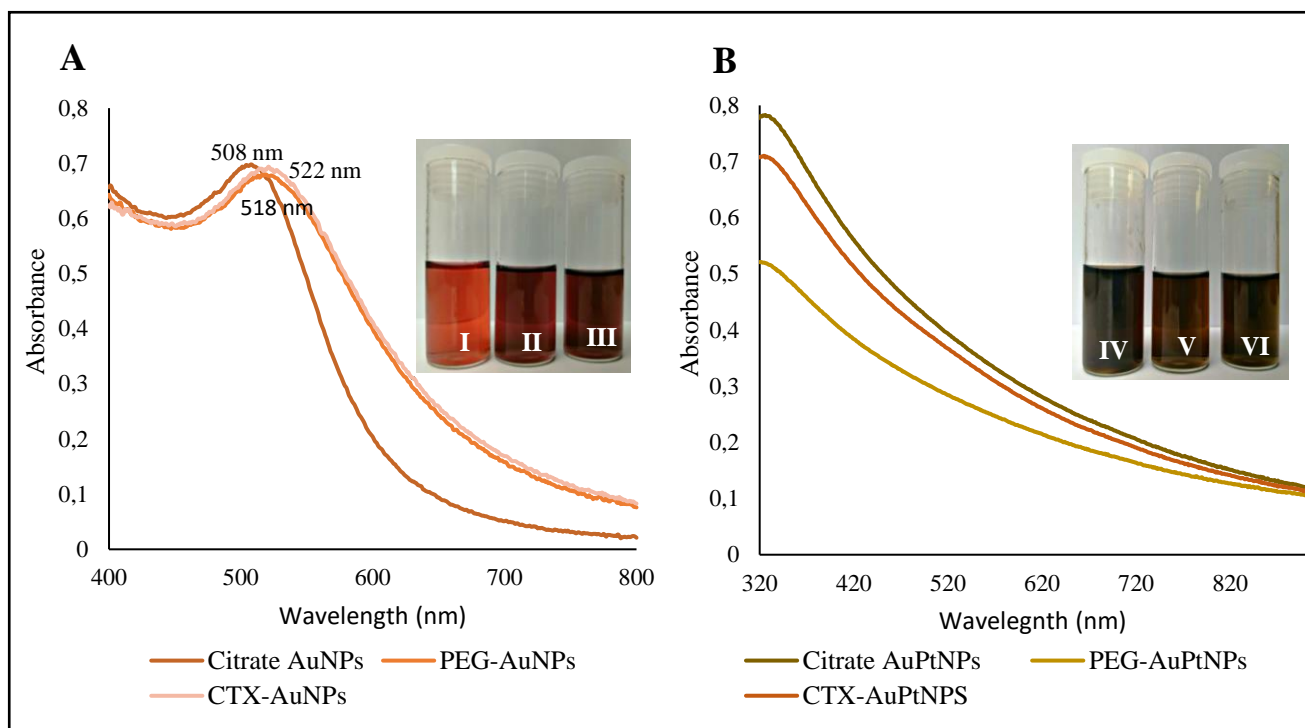
Figure 1: UV-Visible absorption spectrum of NPs. UV-Vis absorption spectrum of all AuNPs (A); with the colour changes and the λ max of Citrate AuNPs (I) at 508 nm, PEG-AuNPs (II) at 518 nm and CTX-AuNPs (III) at 522 nm. UV-Vis absorption spectrum of all AuPtNPs (B) and colour changes of Citrate AuPtNPs (IV), PEG-AuPtNPS (V) and CTX-AuPtNPs (VI).

2.2. Dynamic Light Scattering (DLS) analysis of NPs

The size distribution, uniformity and surface charge are important physicochemical properties to consider in the development of NPs for biomedical applications. Photon correlation spectroscopy, based on dynamic light scattering (DLS) technology is used to determine the average size distribution by intensity (Z-average) also called the hydrodynamic size, polydispersity index (PDI) and average zeta potential (ζ-potential) of NPs in solution. The Z-average is the mean hydrodynamic size of the NPs in suspension, the polydispersity index (PDI) provides information about uniformity of NPs, where PDI values < 0.05 indicate highly monodisperse distribution of NPs, PDI ranges of 0.05 – 0.7 indicate monodispersed samples, while PDI values > 0.7 indicate polydisperse distribution of NPs where NPs may be aggregated (Nidhin *et al.*, 2008; Danaei *et al.*, 2018). The ζ-potential is the surface charge present on NPs and is used to predict the stability of NPs. ζ-potential values between -30 mV

100

and +30 mV are normally considered stable for biological applications as they will repel each other and tend to not aggregate in solution (Hunter, Midmore and Zhang, 2001; Kaszuba *et al.*, 2010).

Figure 2 shows the size distribution by intensity (Fig. 2 A) and ζ-potential distribution (Fig. 2 B) for citrate AuNPs (Z-average: 6.316 nm: PDI: 0.410; ζ-potential: -30.7 mV); PEG-AuNPs (Z-average: 14.20 nm; PDI: 0.334; ζ-potential: -17.3 mV) and CTX-AuNPs (Z-average: 16.46; PDI: 0.328; ζ-potential: -10.5 mV) as measured by DLS. These results were reproducible as reported in Table 1, where the average size distribution by intensity of citrate AuNPs, PEG-AuNPs and CTX-AuNPs increased from 6.79 ± 2.21 nm to 14.31 ± 1.61 nm to 16.71 ± 2.48 nm, respectively. There was a distinct increase in hydrodynamic size of the NPs which was in line with the UV-Vis absorption spectrum data and further confirmed successful surface functionalization. The increase in hydrodynamic size of NPs after surface functionalization is supported in literature with similar findings from other studies (Manson *et al.*, 2011; Dziawer *et al.*, 2017). Citrate AuNPs, PEG-AuNPs and CTX-AuNPs demonstrated a highly monodispersed distribution of NPs with PDI values below 0.5 (AuNPs: 0.38 ± 0.07; PEG-AuNPs: 0.39 ± 0.04; CTX-AuNPs: 0.39 ± 0.07). The ζ-potential values for citrate AuNPs (Table 1) was reported at -30.00 ± 1.72 mV and indicated that the AuNPs are highly stable as previously reported (Barros *et al.*, 2019). Following functionalization with PEG, the ζ-potential of PEG-AuNPs decreased significantly to -16.92 ± 0.76 mV and decreased further after CTX conjugation to -11.04 ± 2.12 mV, respectively. This decrease in ζ-potential is verification that the surface of the NPs was altered, which suggests successful functionalisation with PEG and CTX. This results is in agreement with previous reports which showed a similar decrease in ζ-potential following surface functionalization (Etame *et al.*, 2011; Zhang *et al.*, 2011; Zhao *et al.*, 2019). In Figure 3, the size distribution by intensity (Fig. 3 A) and ζ-potential distribution (Fig. 3 B) of citrate AuPtNPs (Z-average: 5.736 nm: PDI: 0.382; ζ-potential: -31.1 mV); PEG-AuPtNPs (Z-average: 14.74 nm; PDI: 0.270; ζ-potential: -20.5 mV) and CTX-AuPtNPs (Z-average: 21.01; PDI: 0.446; ζ-potential: -14.00 mV) as measured by DLS is illustrated. A summary of repeated experiments is reported in Table 2 and shows the reproducibility of results. The average size distribution by intensity of citrate AuPtNPs, PEG-AuPtNPs and CTX-AuPtNPs increased from 7.71 ± 1.14 nm to 14.34 ± 0.74 nm to 21.13 ± 1.62 nm, respectively. The noticeable increase in hydrodynamic size of AuPtNPs after PEG and CTX is introduced, also suggests successful surface modification (Liang *et al.*, 2017; Salado-Leza *et al.*, 2019). The reported PDIs for all AuPtNPs are < 0.5 (citrate AuPtNPs: 0.36 ± 0.03; PEG-AuPtNPs: 0.27 ± 0.09; CTX-AuPtNPs: 0.46 ± 0.03), indicating a monodisperse distribution of

the NPs. The ζ-potential of citrate AuPtNPs are highly stable at -31.60 ± 2.05 mV, while after surface functionalization with PEG (-20.08 ± 1.64 mV) and CTX conjugation (-14.53 ± 2.74 mV) increased slightly. The negative ζ-potential average values shifted towards a neutral charge, further confirming successful surface modification as previously reported with other studies (Zhao *et al.*, 2019; Oladipo *et al.*, 2020).
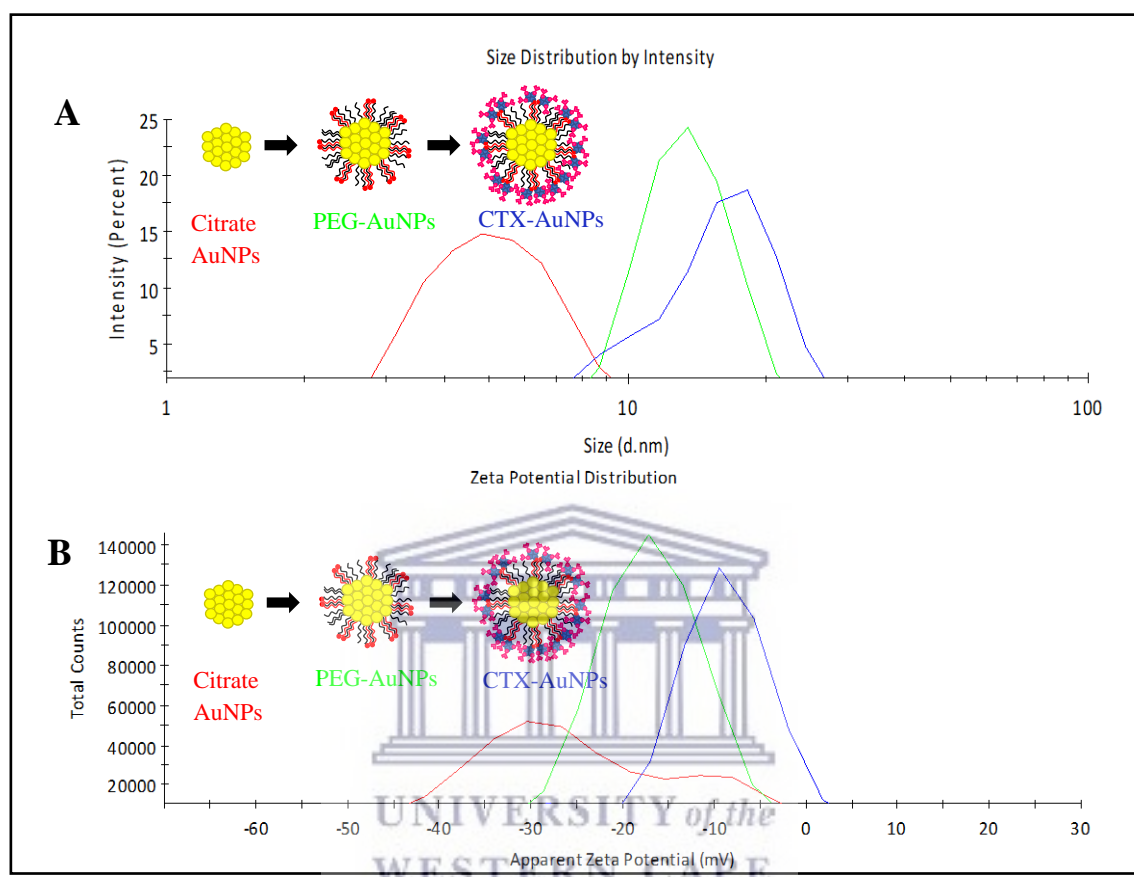
Figure 2. Average size distribution by intensity (A) and zeta potential distribution (B) of different AuNPs: Citrate AuNPs (red), PEG-AuNPs (green) and CTX-AuNPs (blue).

Table 1. Summary of the physical properties as measured by DLS of different AuNPs

Nanoparticle	Z-Average (nm)	PDI	ζ-Potential (mV)	λ max
Citrate AuNPs	6.79 ± 2.21	0.38 ± 0.07	-30.00 ± 1.72	508.3 ± 0.52
PEG-AuNPs	14.31 ± 1.61	0.39 ± 0.04	-16.92 ± 0.76	518.5 ± 0.55
CTX-AuNPs	16.71 ± 2.48	0.39 ± 0.07	-11.04 ± 2.12	521.0 ± 0.63

*Data expressed as mean ± standard deviation (SD) from six independent experiments. PDI: polydispersity index and λ max: absorption maxima.

https://etd.uwc.ac.za/
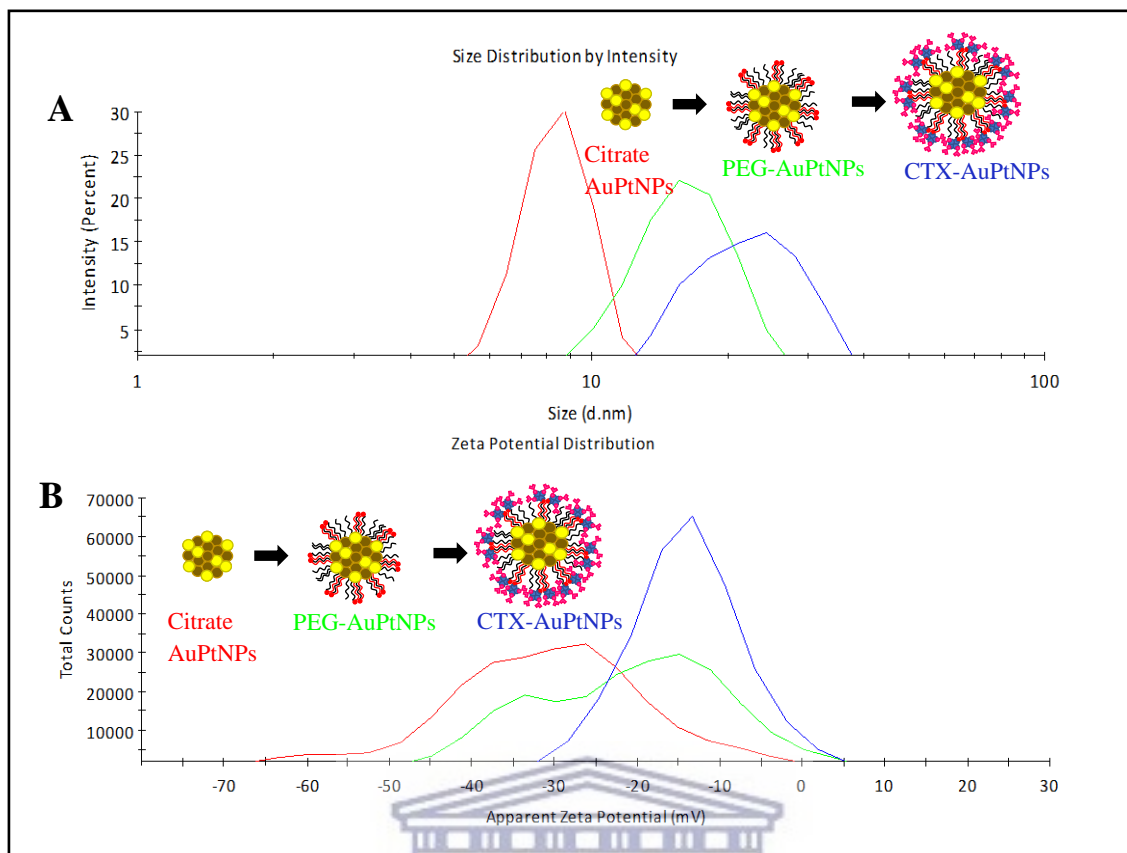
Figure 3. Average size distribution by intensity (A) and zeta potential distribution (B) of different AuPtNPs: Citrate AuPtNPs (red), PEG-AuPtNPs (green) and CTX-AuPtNPs (blue).

Table 2. Summary of the physical properties as measured by DLS of different AuPtNPs

Nanoparticle	Z-Average (nm)	PDI	ζ-Potential (mV)
Citrate AuPtNPs	7.71 ± 1.14	0.36 ± 0.03	-31.60 ± 2.05
PEG-AuPtNPs	14.34 ± 0.74	0.27 ± 0.09	-20.08 ± 1.64
CTX-AuPtNPs	21.13 ± 1.62	0.46 ± 0.03	-14.53 ± 2.74

*Data expressed as mean ± SD from six independent experiments. PDI: polydispersity index

103

2.3. Transmission Electron Microscopy (TEM), Selected Area Electron Diffraction (SAED) Pattern and Energy Dispersive X-Ray (EDX) analysis

TEM studies confirmed an average core diameter of approximately 5 nm for both AuNPs and AuPtNPs, which remained constant after surface functionalization with PEG and with CTX (Fig. 4.IV, V, VI and Fig. 5. IV, V, VI). The use of the strong reducing agent $NaBH_4$ in the presence of sodium citrate as a stabilizing agent produced NPs < 10 nm (Fig. 4 and 5), as reported previously (Etame *et al.*, 2011;Qu *et al.*, 2011). The morphology of citrate AuNPs (4.90 ± 0.71 nm), PEG-AuNPs (4.58 ± 0.73 nm) and CTX-AuNPs (4.69 ± 0.67 nm) was spherical in shape, uniform in structure and monodispersed with almost equidistant arrangement after surface functionalization (Fig. 4. I, II and III). The presence of PEG and CTX on AuNP surfaces stabilized the NPs solution through electrostatic interactions which prevented aggregation of NPs and this is supported by the low PDI values reported in DLS analysis (Politi *et al.*, 2015). EDX results confirmed the presence of Au in all AuNPs and both Au and Pt presence in all AuPtNPs (Fig. 4, Fig. 5 and provided in Supplementary information, Fig. 12 and Fig.13, pg. 137-139). In Figure 4. X and Figure 5. X, black arrows indicate the presence of Au in CTX-AuNPs and Au and Pt in CTX-AuPtNPs, respectively. The presence of strong peaks for carbon, copper and zinc is attributed to the TEM grids used (Fig.4, Fig. 5 and provided in Supplementary information, Fig. 12 and 13, pg. 137-139). Citrate AuPtNPs (4.99 ± 0.93 nm) were predominantly spherically shaped NPs with a few hexagonal, cylindrical, and triangular shaped NPs also present (Fig. 5. I). This mixture of geometrical shapes for AuPtNPs alloys has been reported previously and is related to the Au/Pt atom ratios (Pal, 2015; Olajire and Adesina, 2017; Formaggio *et al.*, 2019; Salado-Leza *et al.*, 2019). Following surface functionalization of AuPtNPs with PEG and CTX, the NPs maintained their shape and size however, it is evident that there is a more equidistant arrangement of NPs (Fig. 5. II and III) indicating improved stability after surface functionalization with no aggregation as was observed in a similar study where PEG was used to produce more stable AuPtNPs (Salado-Leza *et al.*, 2019). In this study, the reported core sizes of ~ 5 nm for all NPs is attractive for NP-mediated hyperthermia applications, crossing the BBB and cell nucleus (Etame *et al.*, 2011; Barua and Mitragotri, 2014). The selected area electron diffraction (SAED) pattern for NPs confirmed their crystalline nature (Fig.4. VII, VIII IX and Fig. 5. VII, VIII IX). In Figure 4. VII, the rings for the citrate AuNPs were indexed and was found to correspond to the (111), (200), (220), (311) and (222) reflections of face-centered cubic (fcc) of gold, as previously reported (Elbagory *et al.*, 2016). After indexing the rings for PEG-AuNPs and CTX-AuNPs, they

were found to correspond to the (111) and (200) reflections of fcc gold (Fig. 4. VIII and IX, respectively). The SAED patterns of citrate AuPtNPs and CTX-AuPtNPs (Fig 5. VII and IX, respectively) presents several concentric circles indexed at (111), (200), (220), (311) and (222) and the rings for PEG-AuPtNPs (Fig 5. VIII) correspond to (111) and (200) reflections, which could all be ascribed to planes associated with that of small AuPt alloy nano-structures as reported in literature (Wang *et al.*, 2011; Weng *et al.*, 2016; Chen *et al.*, 2021).
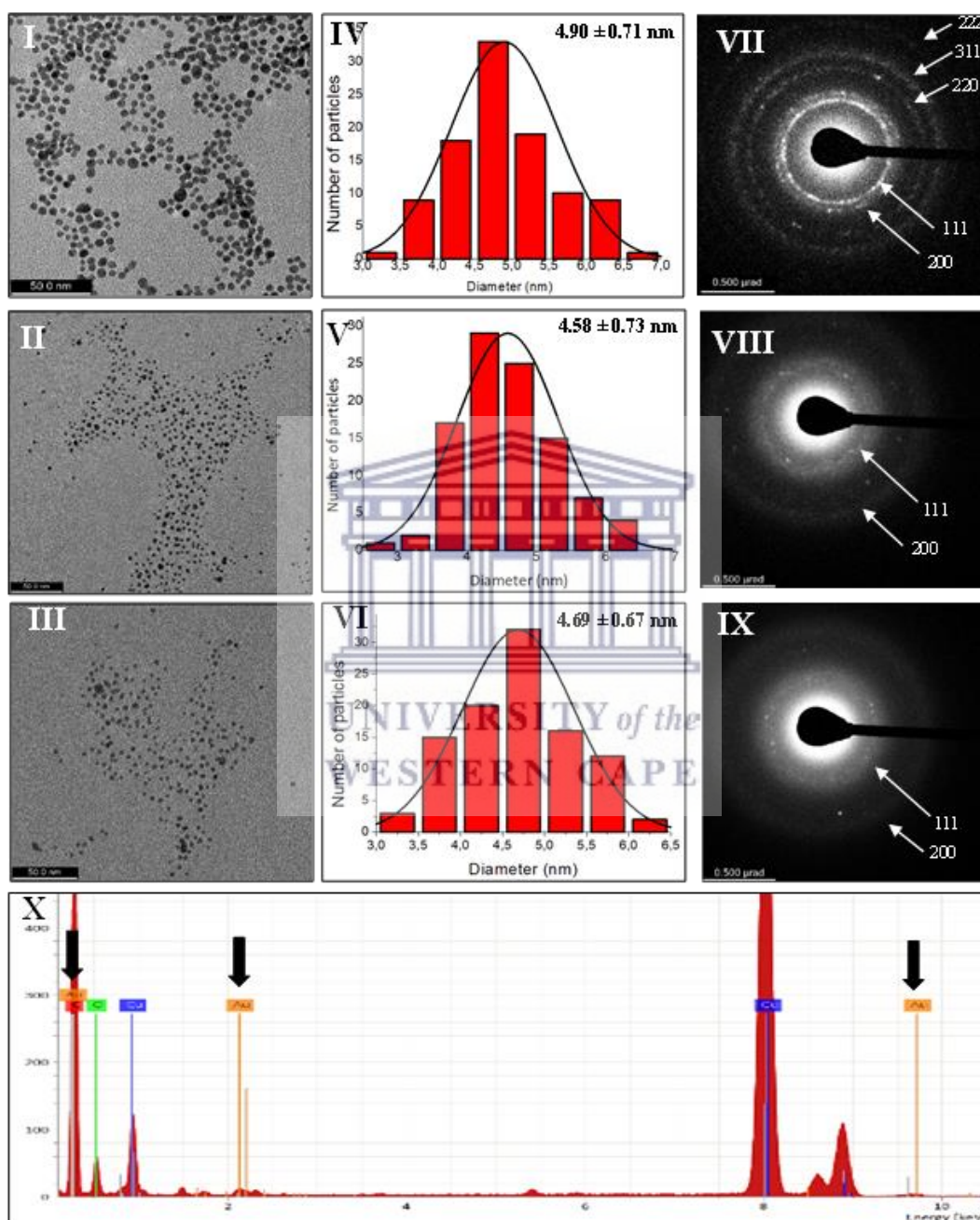
Figure 4. Transmission Electron Microscopy (TEM), Selected Area Electron Diffraction (SAED) Pattern and Energy Dispersive X-Ray (EDX) analysis of different AuNPs. TEM

micrographs at 50 nm magnification of citrate AuNPs (I), PEG-AuNPs (II) and CTX-AuNPs (III). Core size distribution histogram (size in nm is presented as mean ± SD) of citrate AuNPs (IV), PEG-AuNPs (V) and CTX-AuNPs (VI). SAED pattern of citrate AuNPs (VII), PEG-AuNPs (VIII) and CTX-AuNPs (IX) and EDX of CTX-AuNPs, where black arrows show Au peaks (X)
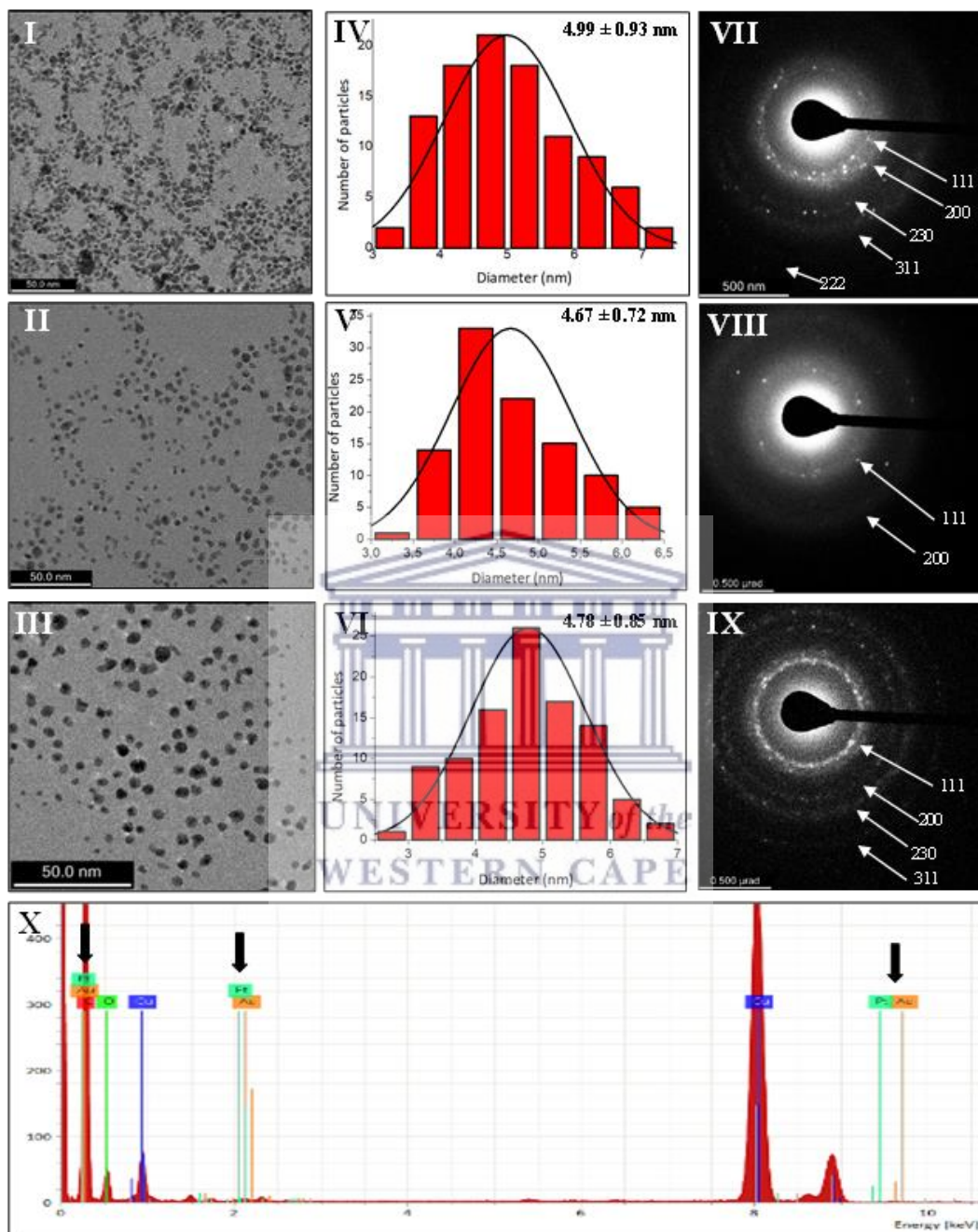
Figure 5. Transmission Electron Microscopy (TEM), Selected Area Electron Diffraction (SAED) Pattern and Energy Dispersive X-Ray (EDX) analysis of different AuPtNPs. TEM micrographs at 50 nm magnification of citrate AuPtNPs (I), PEG-AuPtNPs (II) and CTX-AuPtNPs

106

(III). Core size distribution histogram (size in nm is presented as mean ± SD) of citrate AuPtNPs (IV), PEG-AuPtNPs (V) and CTX-AuPtNPs (VI). SAED pattern of citrate AuPtNPs (VII), PEG-AuPtNPs (VIII) and CTX-AuPtNPs (IX) and EDX of CTX-AuPtNPs, where black arrows show Au and Pt peaks (X).

2.4.   Fourier-transform Infrared (FTIR) Spectroscopy analysis of NPs

FTIR spectra provide structural and conformational information of NPs capped with surface molecules of interest. Figure 6 shows FTIR spectra of citrate AuNPs (I) and citrate AuPtNPs (II). The evidence of the surface functionalisation of NPs by citrate ions can be observed by the characteristic peaks at 1399/1398 and 1582/1586 cm⁻¹ which correspond to the symmetric and anti-symmetric stretching of COO^-. This data confirmed the interaction between citrate ions and NPs. The citrate molecule have three COO- groups (Wulandari *et al.*, 2008) and were responsible for anchoring on Au/AuPt surface. These results correspond with previous reports of citrate capped NPs (Wulandari *et al.*, 2008; Sanches *et al.*, 2011; Mohan *et al.*, 2013; Sakellari, Hondow and Gardiner, 2020).
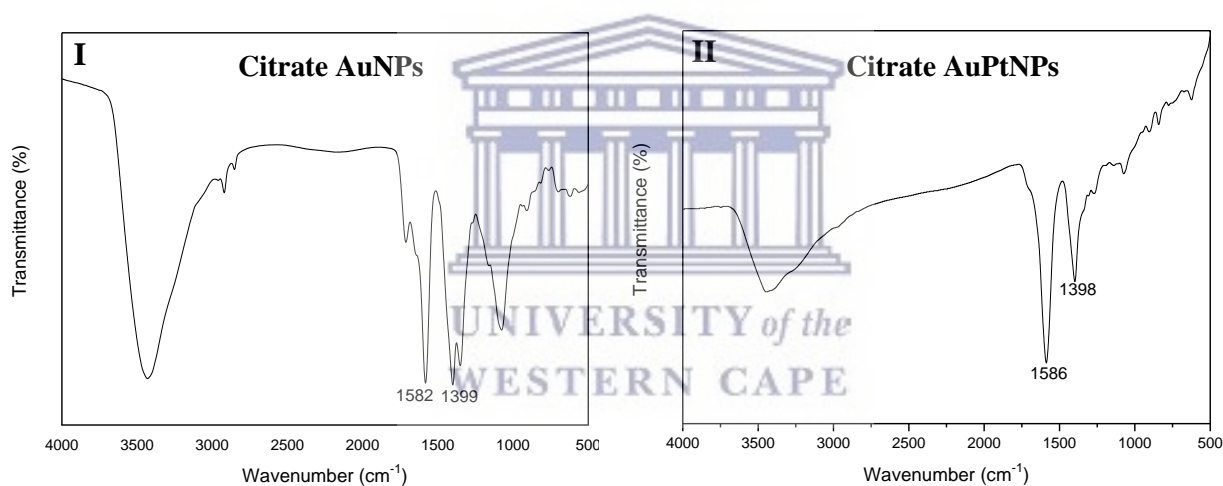
Figure 6. FTIR spectra of Citrate AuNPs (I) and Citrate AuPtNPs (II)

The FTIR spectra of PEG-AuNPs (I) and PEG-AuPtNPs (II) are shown in Figure 7. Prominent differences were visible in the spectra for the PEG capped NPs spectrum compared to that for the citrate capped AuNP (Figure 6). The presence of PEG molecules on the spectra of the AuNP and AuPtNPs was possibly attributed to the increase in the relative intensity of the peaks associated with CO stretching (1686 cm⁻¹ for PEG-AuNPs and 1689 cm⁻¹ for PEG-AuPtNPs) and bending

107

(1349/1350 cm^{-1}) (C–H bending, –CH_2 and –CH_3), and the presence of additional peaks associated with N–H wagging (600–900 cm^{-1}). Narrowing of the CH_2 stretching at 2857 cm^{-1} may be as a result of glycol moieties expressed as previously described (Manson *et al.*, 2011; Kumar, Meenan and Dixon, 2012). The FTIR spectrum of PEG-NPs was in agreement with similar PEG-NPs reported in literature (Manson *et al.*, 2011; Kumar, Meenan and Dixon, 2012; Harrison *et al.*, 2016).
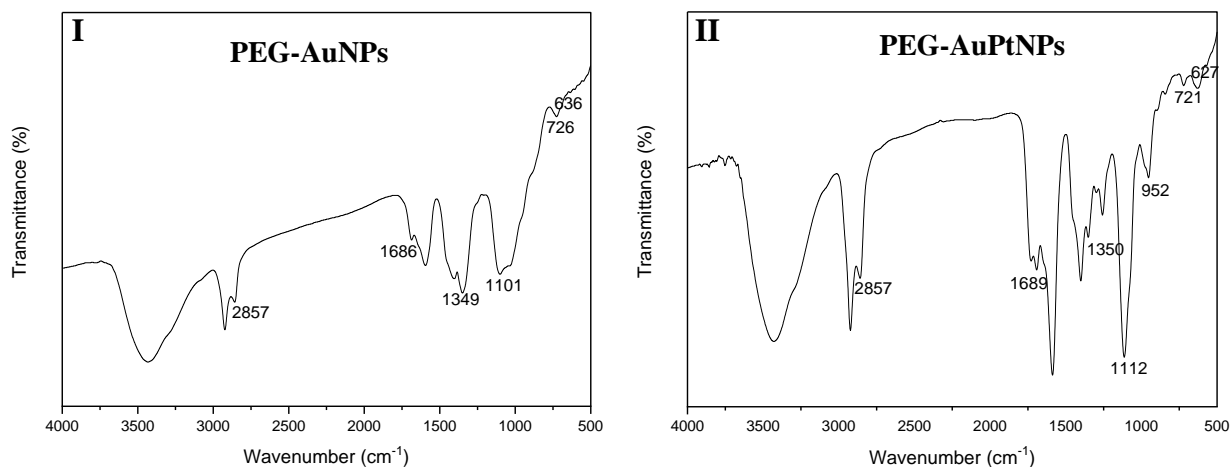
Figure 7. FTIR spectra of PEG-AuNPs (I) and PEG-AuPtNPs (II)

Figure 8 shows FTIR spectra of CTX-AuNPs (I) and CTX-AuPtNPs (II). The presence of CTX on the NPs was observed by the presence of amine found at peaks 1648/1646 cm^{-1} and carboxylate peaks at 1588/1587 cm^{-1} and 1349/1353 cm^{-1}. CTX attachment was further verified by the methyl symmetric/asymmetric stretch located at 2923/2921 and 2853/2852 cm^{-1} of the alanine residues of CTX. This appearance suggested the successful conjugation of CTX onto NPs. These results are similar to previously reported FTIR peaks for CTX and CTX-NPs in literature (Sun *et al.*, 2008a; Fang *et al.*, 2010; Gu *et al.*, 2014; Wang *et al.*, 2014; Chen *et al.*, 2015).

108
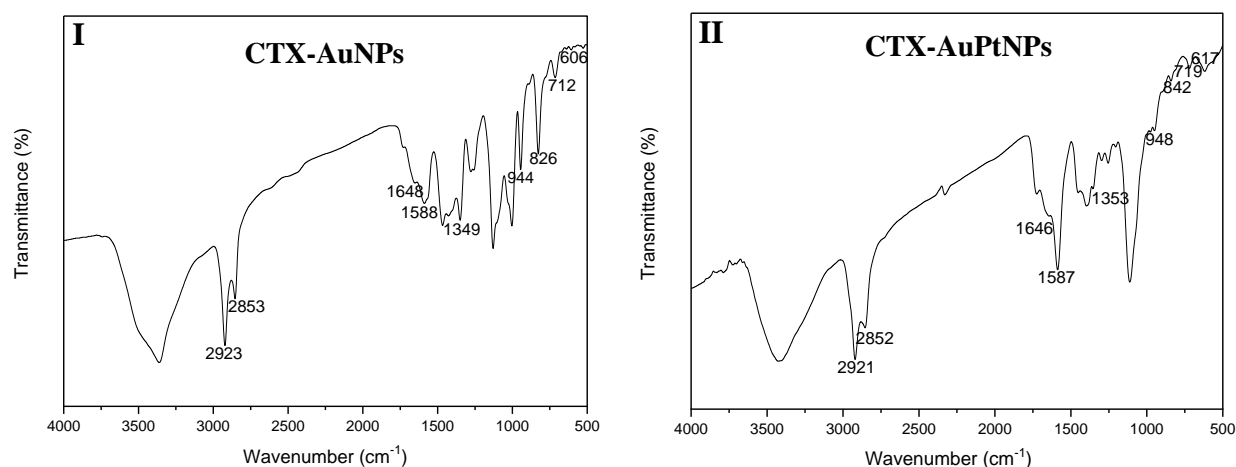
Figure 8. FTIR spectra of CTX-AuNPs (I) and CTX-AuPtNPs (II)

2.5.   Stability of NPs in supplemented biological medium

Biological medium is a buffered solution which is comprised of proteins such as serum albumin or globulins, and several biomolecules including amino acids, and ionic salts. These constituents may affect the hydrodynamic behaviour of NPs causing the NPs to become unstable through molecule/protein adsorption or loss of surface functionality, resulting in NP aggregation (Moore *et al.*, 2015). These processes can further influence the *in vitro* behaviour and significantly alter NP mobility. Therefore, it is important to investigate the stability of NPs in biological media before proceeding with *in vitro* or *in vivo* studies and to determine if NPs can retain their stability in biological environments. In this study, the stability of synthesised NPs was assessed in Dulbecco's Modified Eagle Medium (DMEM) (supplemented with 10 % foetal bovine serum), a widely used basal medium for supporting the growth of many different mammalian cells. The stability of the NPs was assessed by investigating changes in hydrodynamic size, PDI and ζ-potential after a 48-hour period at 37 ⁰C. (Table 3). Tables 1 and 2 (Section 2.2., pg 102-103) showed that the Z-average values for citrate AuNPs and citrate AuPtNPs after synthesis were 6.79 ± 2.21 nm and 7.71 ± 1.14 nm, respectively. The Z-average values for citrate AuNPs and citrate AuPtNPs increased to 21.55 ± 3.28 nm and 26.00 ± 2.78 nm, respectively after 48 hours in DMEM at 37 ⁰C. This suggested that the hydrodynamic size of both citrate AuNPs and citrate AuPtNPs increased significantly. This was accompanied by a slight decrease in the ζ-potential; however, reported values were still close to -30 mV, therefore they were stable in DMEM (AuNPs: -24.87 ± 1.19 mV and AuPtNPs: -23.50 ± 2.78 mV). The increase in hydrodynamic size of citrate NPs could be attributed to adsorption of plasma

109

proteins from foetal bovine serum (FBS) onto the surface of NPs, ion concentration, pH, loss of surface functionality all resulting in the formation of aggregates when placed into cell culture media as previously explained (Moore *et al.*, 2015; Saw *et al.*, 2018). Serum proteins present in DMEM could form a protein "corona" around the NPs and shield the surface charge, contributing to the aggregation and ultimately increase in the hydrodynamic size of NPs and less negative surface charges as reported previously in similar studies (Gebauer *et al.*, 2012; Saw *et al.*, 2018). Electrostatically stabilized NPs have generally shown poor stability in culture media (Moore *et al.*, 2015). Generally, steric stabilization is a more successful approach to increase the stability of NPs in suspension and is accomplished via synthetic polymer surface coating such as PEG. PEG is a well investigated and a frequently used polymer since it has been shown to decrease protein adsorption, and contribute to overall biological stability of NPs *in vivo* (Gref *et al.*, 2000). PEG-NPs have improved colloidal stability in biological medium (Manson *et al.*, 2011; Stebounova, Guio and Grassian, 2011; Hirsch *et al.*, 2013). In this study steric stabilization with PEG-OH and PEG-biotin improved NP colloidal stability and possibly also prevented NP aggregation. PEG-AuNPs was the most stable NPs in DMEM as the hydrodynamic size increased by only 1 nm when compared to the size of PEG-AuNPs after synthesis (Table 1 in section 2.2 and Table 3). This compared well with a study which evaluated AuNPs in different biological medium, where PEG-AuNPs maintained stability in Roswell Park Memorial Institute Medium (RPMI) and DMEM for up to 3 days (Barreto *et al.*, 2015). PEG-AuPtNPs in DMEM also increased in hydrodynamic size and in ζ-potential (23.12 ± 1.58 nm; -12.90 ± 0.53 mV) (Table 3) when compared to PEG-AuPtNPs post synthesis (14.34 ± 0.74 nm; -20.08 ± 1.64 mV) (Table 2 in section 2.2). The hydrodynamic sizes of CTX functionalized NPs had little appreciable changes after being incubated in DMEM supplemented with 10 % FBS for a period of 48 hours, confirming the favourable colloidal stability of these peptide functionalized NPs, as supported in literature for other CTX functionalized NPs in culture media (Stephen *et al.*, 2014; Mu *et al.*, 2015; Agarwal *et al.*, 2019). The current study suggests that the synthesized NPs are favourable for biomedical applications because it has been reported that NPs with low surface charges are more likely to evade phagocytosis by macrophages and to be internalized by non-phagocytic cells than NPs with high negative charges (Saw *et al.*, 2018). It was also reported that low negative surface charges may enhance the cell selectivity of NPs and prevent non-specific binding to non-target cells before arriving at the target tumour site (Yamamoto *et al.*, 2001). There was a slight increase in the PDI values after placing the NPs in DMEM when compared to PDI values post synthesis (Table 1 and Table 2 in section 2.2) however, it remained below 0.5 for all NPs after introduction to DMEM,

indicating a maintained degree of monodisperse solutions of NPs with less likelihood of aggregation, as previously described (Fröhlich *et al.*, 2013; Vinardell *et al.*, 2017).

Table 3. Stability of Nanoparticles in DMEM (with 10 % FBS) after 48-hours incubation at 37 ⁰C

Nanoparticle	Z-average	PDI	ζ-potential (mV)
Citrate AuNPs	21.55 ± 3.28	0.44 ± 0.05	-24.87 ± 1.19
PEG-AuNPs	15.14 ± 0.85	0.38 ± 0.13	-16.07 ± 0.46
CTX-AuNPs	23.29 ± 1.79	0.46 ± 0.01	-12.10 ± 1.81
Citrate AuPtNPs	26.00 ± 2.78	0.44 ± 0.04	-23.50 ± 2.78
PEGAuPtNPs	23.12 ± 1.58	0.48 ± 0.07	-12.90 ± 0.53
CTX-AuPtNPs	26.77 ± 9.53	0.49 ± 0.03	-12.80 ± 0.82

*Data expressed as mean ± SD from three independent experiments. PDI: polydispersity index

2.6. CTX binding efficiency to U87 and SH-SY5Y cells

CTX was shown to cross the BBB and selectively bind to gliomas and other tumours of the neuroectodermal origin through overexpression of MMP-2 without any effect on normal glial cells or neurons (Deshane, Garner and Sontheimer, 2003; Veiseh *et al.*, 2007; Cohen-Inbar and Zaaroor, 2016). The binding efficiency of CTX to U87 human glioblastoma cell line and SH-SY5Y human neuroblastoma cell line was determined by flow cytometry using a simple competitive binding assay and FITC-tagged CTX (FITC-CTX). The concentration of 0.13 mM CTX and 0.03 mM FITC-CTX used in these experiments was optimized (data not shown). Figure 5. A and B shows that FITC-CTX binds to both cell lines with 98.57 ± 0.28 % and 86.46 ± 1.32 % of U87 and SY-SY5Y cells, respectively staining positive with FITC-CTX. A competitive binding assay using untagged CTX showed that the percentage FITC positive cells reduced from 98.57 ± 0.28 % to 50.02 ± 1.10 % for U87 and from 86.46 ± 1.32 % to 72.22 ± 2.21 % for SY-SY5Y cells. This demonstration of competitive binding between CTX and FITC-CTX demonstrated the specific binding of CTX to these cells. A higher percentage of U87 cells bound to FITC-CTX than SY-SY5Y cells, which seemed to suggest that U87 cells contain more binding targets for CTX than SY-SY5Y cells. It is possible that expression levels of the known targets, such as MMP2, ClC-3 and Annexin A2, are higher in U87 cells compared to SY-SY5Y cells. Soroceanu *et al.* (1998) showed CTX binding to various glioma cell lines including D54-MG, SK-1-MG, U87-MG, U105-MG, U251-MG and U373-MG. Lyons and

111

colleagues (Lyons, O'Neal and Sontheimer, 2002) further confirmed CTX binding to 74/79 human brain tumours as well as human neuroblastoma cell lines including SK-N-MC and SH-SY5Y. This study also confirmed that these cell lines can be used to assess the targeted uptake of CTX functionalised NPs.
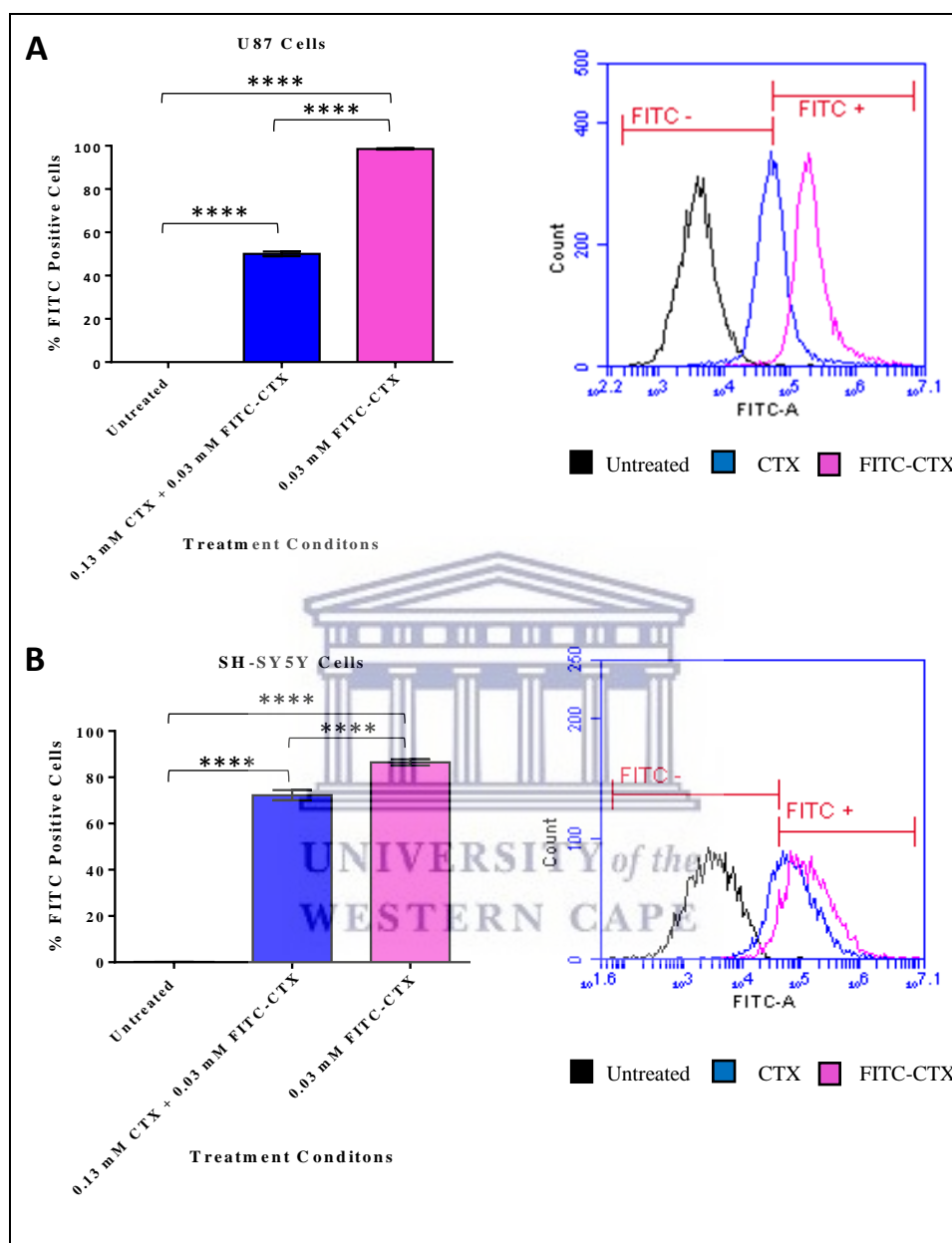
Figure 9. Binding of FITC tagged CTX to U87 cells (A) and SHY-SY5Y cells (B). Cells were treated with either 0.03 mM FITC-CTX or co-treated with 0.03 mM FITC-CTX and 0.13 mM CTX for 1 hour at 37 °C. Fluorescence of the cells were analysed by flow cytometry. Experiments were

112

performed in triplicates. Bar graphs represent the mean ± standard error of the mean (SEM) of three independent experiments and significance of difference is indicated with **** ($P \leq 0.0001$).

2.7. Uptake of NPs in U87 and SH-SY5Y cells

Darkfield microscopy was used to observe the uptake of metallic NPs with a treatment of 225 µg/ml for 24 hours. The cell nuclei were stained with DAPI (Figure 6). By using dark-field and fluorescence microscopy, the presence of metallic NPs such as AuNPs produces a bright yellow colour due to the more intense scattering of light (Huo *et al.*, 2014), while cellular structures such as nuclei can also be observed. The images showed that most of the NPs were localized in the cytoplasm or surrounding the nucleus but does not seem to have entered the nucleus, however bright spots are observed with AuNPs and CTX-AuNPs inside the nucleus in U87 cells. NPs showed uptake in U87 and SH-SY5Y cells with bright yellow spots present around the nucleus. These results match a previous study for metallic NPs, where smaller NPs < 10 nm (2 and 6 nm) accumulated around the nucleus and could enter the nucleus, whereas larger NPs (10 and 16 nm) tend to be found in the cytoplasm (Sukhanova *et al.*, 2018).

Untreated U87

Untreated SH-SY5Y

Citrate AuPtNPs U87

Citrate AuPtNPs SH-SY5Y

113

PEG-AuPtNPs U87

PEG-AuPtNPs SH-SY5Y

CTX-AuPtNPs U87

CTX-AuPtNPs SH-SY5Y

Citrate AuNPs U87

Citrate AuNPs SH-SY5Y

PEG-AuNPs U87

PEG-AuNPs SH-SY5Y

114
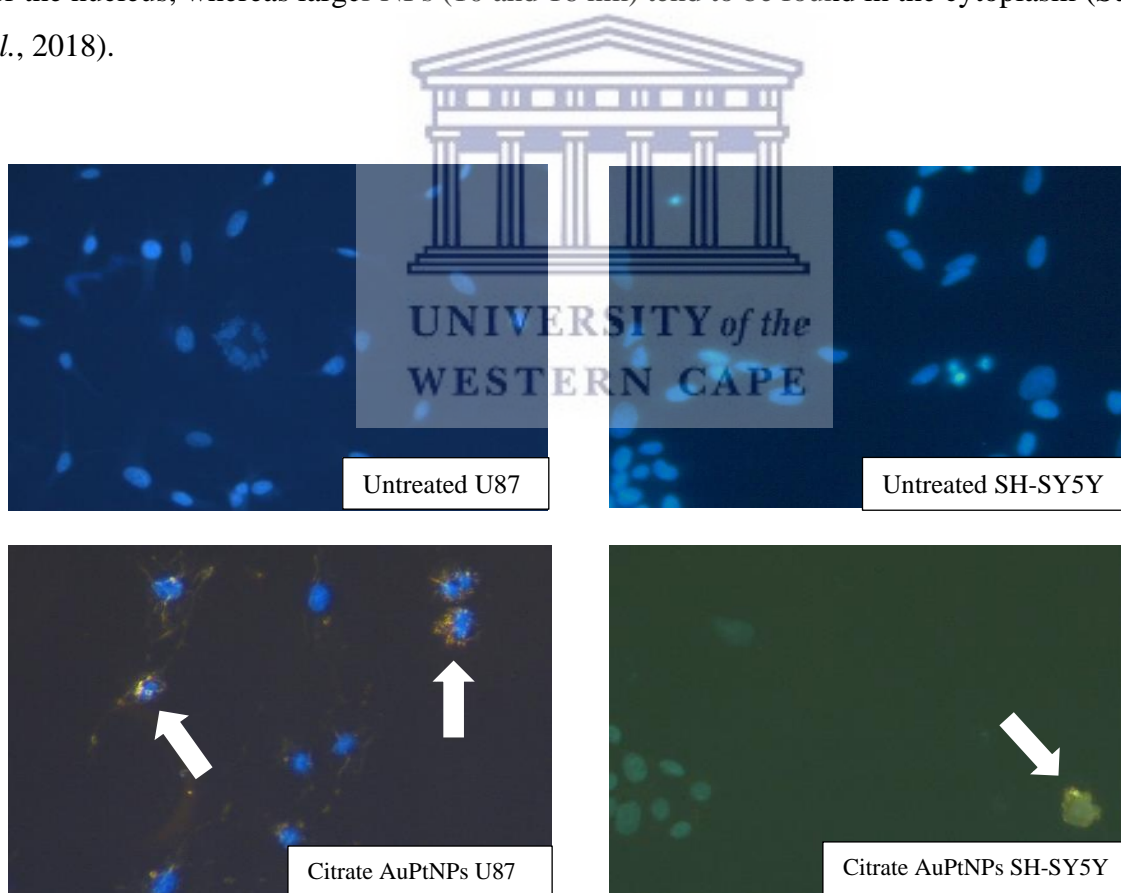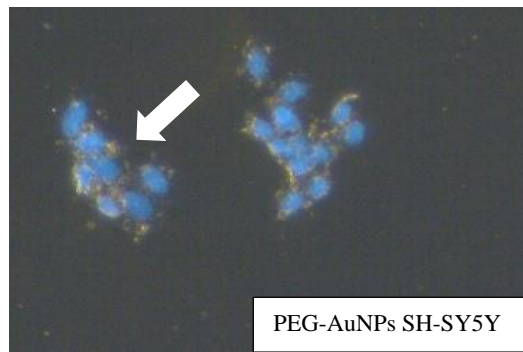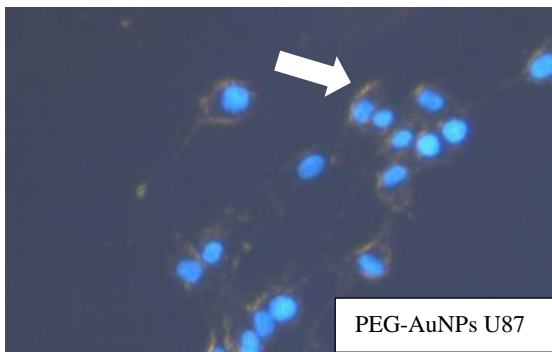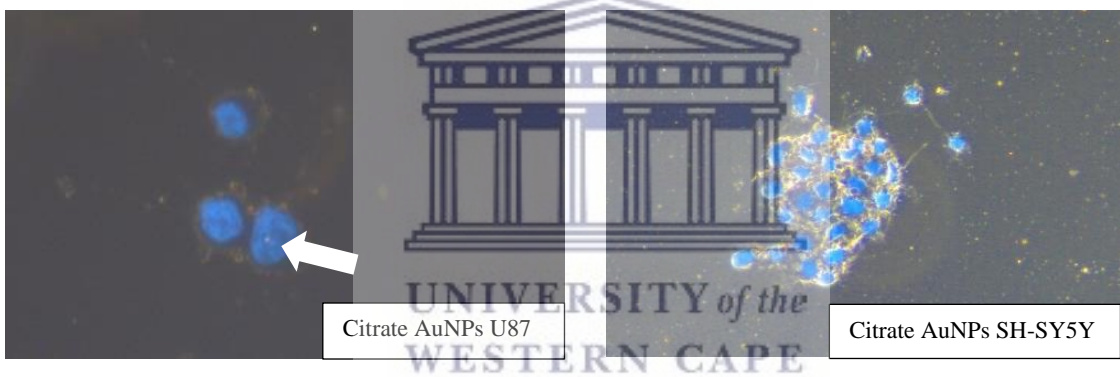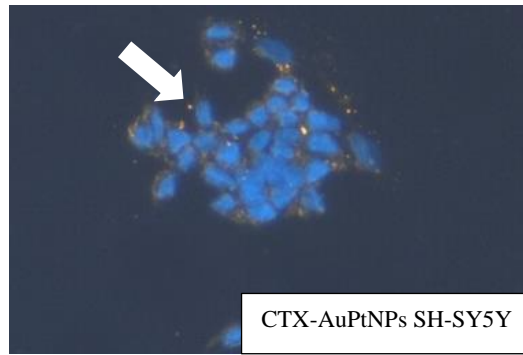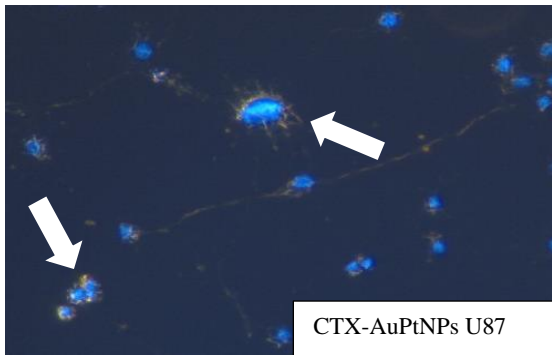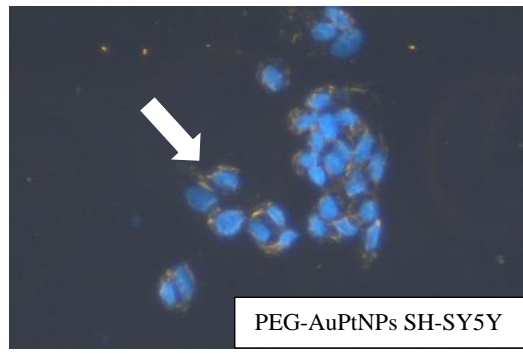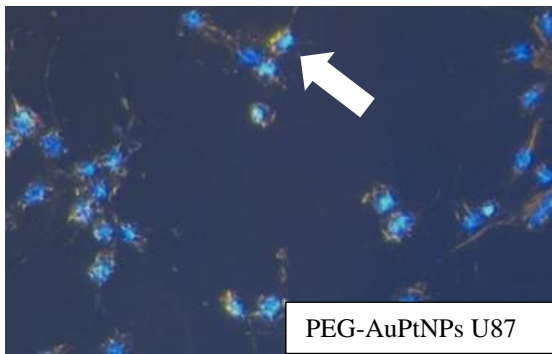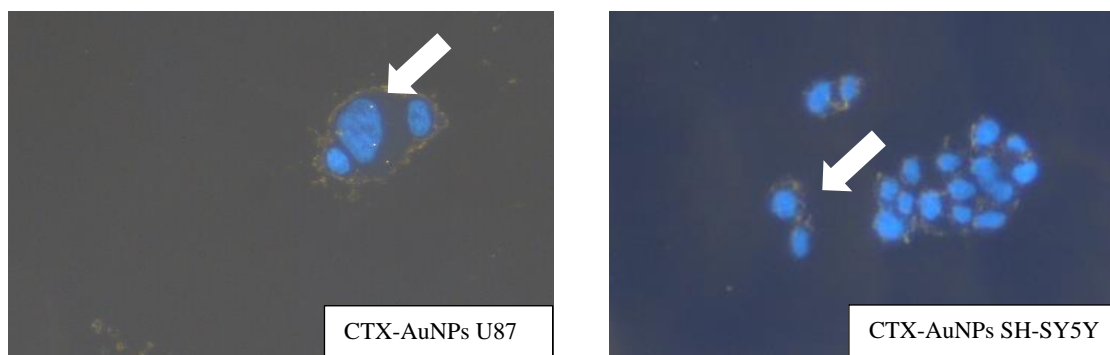
Figure 10. Darkfield fluorescence microscopy of U87 cells (A) and SH-SY5Y (B) cells. Image was acquired at 20X and 40X magnification, cell nuclei are shown in blue (DAPI) and NPs are shown as the bright yellow colour around the nuclei. (A) NPs are readily visualized in cells, mostly located within the cytoplasm but some show NPs within the nuclei (white arrows).

3. Materials and methods

CTX may hold great promise for the development of novel highly specific diagnostic and therapeutic nano-based platforms for cancer. The focus of the current study was to design and optimize well-controlled, stable CTX-functionalized NPs as delivery systems. In this study, we present a 3-step preparation method for the synthesis of CTX-AuNPs and CTX-AuPtNPs as seen in Figure 11: A) Step1: Citrate capped AuNPS and AuPtNPs are prepared, B) Step 2: PEGylation occurs with PEG-OH and PEG-biotin (1% PEG-biotin and 99% PEG-OH), allowing for the final step, C) Step 3: biotinylated CTX is conjugated onto the surface of NPs via streptavidin. In this study, PEG-OH was used because of its solubility and biological compatibility, while the PEG-biotin allowed the immobilization of streptavidin—a linker between PEG-biotin on the surface of NPs and biotinylated CTX. This method was efficient for attaching CTX, as the peptide functionality was maintained, and the use of toxic reagents often used during the coupling reactions in previous studies for attaching CTX to NPs as well as the further rigorous purification methods was avoided (Sun *et al.*, 2008b; Kievit *et al.*, 2010; Locatelli *et al.*, 2014; Mu *et al.*, 2015; Tamborini *et al.*, 2016; Agarwal *et al.*, 2019; Zhao *et al.*, 2019, 2020). To the best of our knowledge this route of CTX functionalization has not been reported before, therefore we were encouraged to explore this method. The resultant CTX-functionalized NPs are attractive in the areas of active NP targeting research for different types of tumours expressing molecular targets of interest, with the potential for further investigation into NP-mediated RF targeted hyperthermia.
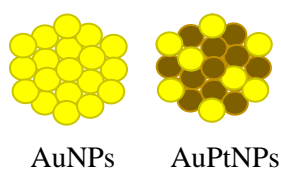
115
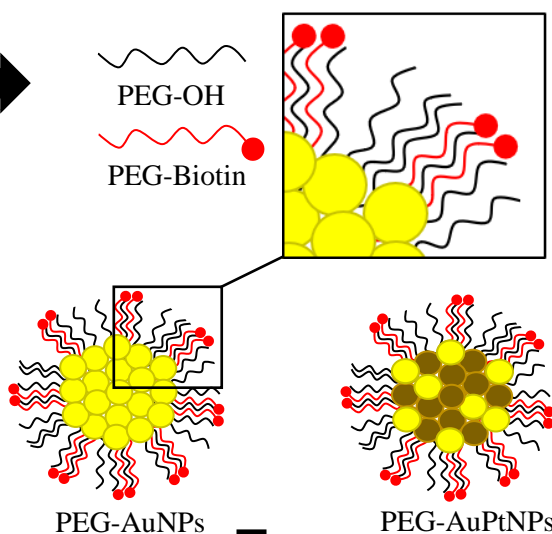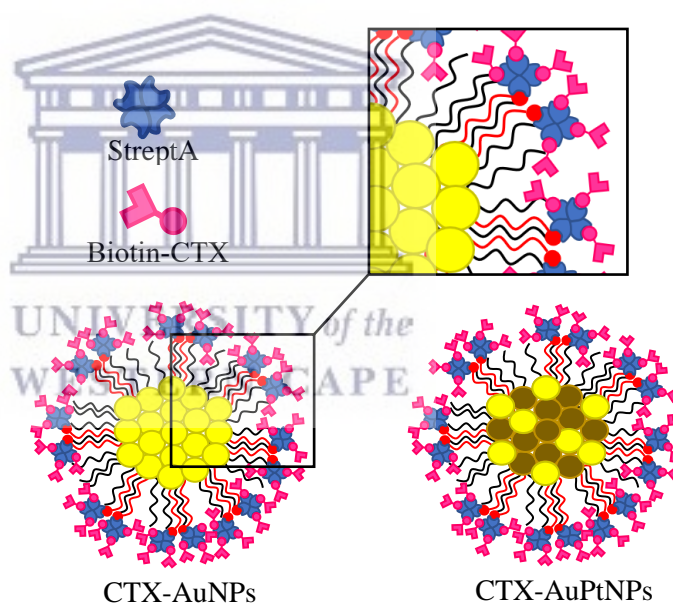
Figure 11. Schematic representation of the three-step synthesis of NPs: A) Citrate capped nanoparticles, B) Polyethylene glycol (PEG) functionalized nanoparticles and C) Chlorotoxin (CTX) functionalized nanoparticles.

3.1. Chemicals and reagents

Gold (III) chloride trihydrate (≥99.9% trace metals basis), chloroplatinic acid hydrate (≥99.9% trace metals basis), sodium citrate, sodium borohydride (ReagentPlus®, 99%), streptavidin (strepA) and Fluoroshield™ with DAPI were acquired from Sigma-Aldrich (Sigma-Aldrich,

St. Louis, Missouri, United States of America). The PEG molecules, 2-{2-[2-(2-{2-[2-(1-mercaptoundec-11-yloxy)- ethoxy]-ethoxy}-ethoxy)-ethoxy]-ethoxy}-ethanol (PEG-OH, $C_{23}H_{48}O_7S$, 468.69 g/mol) and N-(2-{2-[2-(2-{2-[2-(1-mercaptoundec-11-yloxy)-ethoxy]-ethoxy}-ethoxy)-ethoxy]-ethoxy}-ethyl) biotinamide (PEG-biotin, $C_{33}H_{63}N_3O_8S2$, 694.00 g/mol) were purchased from Prochimia Surfaces (Sopot, Poland). Biotin-chlorotoxin and FITC-chlorotoxin: NH2-Met - Cys - Met - Pro - Cys - Phe - Thr - Thr - Asp - His - Gln - Met - Ala - Arg - Lys - Cys - Asp - Asp - Cys - Cys - Gly - Gly - Lys - Gly - Arg - Gly - Lys - Cys - Tyr - Gly - Pro - Gln - Cys - Leu - Cys - Arg-Lys（biotin) and FITC...NH2-Met - Cys - Met - Pro - Cys - Phe - Thr - Thr -Asp - His - Gln - Met - Ala - Arg - Lys - Cys - Asp - Asp -Cys - Cys - Gly - Gly - Lys - Gly - Arg - Gly - Lys - Cys - Tyr -Gly - Pro - Gln - Cys - Leu - Cys - Arg-lys was manufactured and purchased from GL Biochem (Shanghai) Ltd. (Shanghai, China). Dulbecco's Modified Eagle's Medium (DMEM), Foetal Bovine Serum (FBS), Phosphate Buffered Saline solution (PBS) and Penicillin-Streptomycin solution was obtained from Gibco, Life Technologies Corporation (Paisley, United Kingdom). Penicillin and 100 µg/ml streptomycin and 0.25 % trypsin EDTA were acquired from Lonza Group Ltd. (Verviers, Belgium). Non-sterile 96 well polystyrene microplates and sterile cell culture grade 6 well plates were purchased from Bio-Smart Scientific (Cape Town, South Africa). All other chemicals used in this study were of analytical grade and purchased from Kimix Chemicals and Lab Supplies cc (Cape Town, South Africa).

3.2. Preparation of NPs

3.2.1. Synthesis of citrate capped AuNPs and AuPtNPs

All glassware used in NP synthesis was first rinsed with aqua regia (nitric acid and hydrochloric acid; 1: 3) and then with ultrapure Millipore water (18.2 Ω at 25 °C). Millipore water (18.2 Ω at 25 °C) was used for all the experiments. Citrate capped NPs were prepared using previously reported

117

methodologies with few modifications (Etame *et al.*, 2011; Qu *et al.*, 2011). For the preparation of citrate AuNPs, 1.25 ml of 0.01 M Gold (III) chloride trihydrate was added to 47.5 ml ultrapure Millipore water (18.2 Ω at 25 °C) in a 100 ml glass Erlenmeyer flask and this mixture was stirred on a low speed (100 rpm) for 2 minutes at 22-25 °C on an AGIMATIC-N magnetic stirrer (J.P. SELECTA, s.a.; Barcelona, Spain). To this mixture, 1.25 ml of 0.01 M sodium citrate was added, and the mixture was stirred for 4 minutes, after which 1.5 ml freshly prepared ice-cold 0.1 M sodium borohydride ($NaBH_4$) was added, and the mixture was vigorously stirred (500 rpm) for 1 minute. The reaction mixture was left undisturbed in the dark at 22-25 °C for 24 hours.

For the preparation of citrate AuPtNPs, 1 ml of 1 mM Gold (III) chloride trihydrate and 1 ml of 1 mM chloroplatinic acid hydrate was added to 18 ml ultrapure Millipore water (18.2 Ω at 25°C) in a 100 ml glass Erlenmeyer flask and stirred on a low speed (100 rpm) for 2 minutes at 22-25°C. To this solution, 850 µl 100 mM sodium citrate was added, and the reaction mixture was stirred on a low speed for 3 minutes, after which 600 µl freshly prepared ice-cold 100 mM $NaBH_4$ was added in a dropwise manner while the reaction mixture was stirred vigorously for a further 1 minute. The reaction was left undisturbed in the dark at 22-25 °C for 24 hours to decompose residual $NaBH_4$. Both citrate NP solutions were filtered using a 0.22 µm Millipore filter and placed in the dark at 4°C until further use.

3.2.2. Synthesis of PEG-AuNPs and PEG-AuPtNPs

PEG capped NPs were prepared using a previously reported methodology with some alterations (Sosibo *et al.*, 2015). For the preparation of PEG-AuNPs, 10.5 µl of PEG-OH (18.8 mg/ml) and 0.2 µl PEG-biotin (8.4mg/ml) were added simultaneously to 10 ml as synthesized citrate capped AuNPs and stirred for 7 hours at 22-25 °C. The 10 ml PEG-AuNPs, reaction mixtures were centrifuged at 14000 rpm for 2 hours at 4 °C using an Eppendorf AG centrifuge 5417R with a standard rotor F-45-30-11 (Eppendorf AG, Hamburg, Germany). After centrifugation, the supernatant was discarded, and the collected 10 ml pellets was resuspended in 5 ml of Millipore water (18.2 Ω at 25 °C).

For the preparation of PEG-AuPtNPs, as synthesized citrate AuPtNPs was first centrifuged at 14000 rpm for 60 mins at 4 °C and the pellets containing the NPs were resuspended in 1ml Millipore water. A solution of 2 µl of PEG-OH (18.8 mg/ml) and 0.5 µl PEG-biotin (8.4 mg/ml) were added simultaneously to 10 ml of centrifuged citrate AuPtNPs and stirred for 7 hours at 22-25 °C. The 10

118

ml PEG-AuPtNPs reaction mixtures were centrifuged at 14000 rpm for 90 minutes at 4 °C and 1 ml pellet was resuspended in 700 µl of Millipore water (18.2 Ω at 25 °C). The purified PEG-NPs were stored in the dark at 4 °C until further use.

3.2.3. Synthesis of CTX-AuNPs and CTX-AuPtNPs

Following the synthesis and purification of PEG-biotin-functionalized NPs (PEG-AuNPs and PEG-AuPtNPs), streptavidin was introduced via the biotin-avidin interaction. For the synthesis of CTX-AuNPs, the purified PEG-AuNPs (4 ml) was mixed with 0.4 µl streptavidin (1 mg/ml) and for the synthesis of CTX-AuPtNPs, the purified PEG-AuPtNPs (4 ml) was mixed with 0.6 µl of streptavidin (1 mg/ml). The mixtures were stirred for 3 hours in the dark at 4 °C. Following this, 4 µl of biotinylated CTX (1 mg/ml) was added to the streptavidin functionalized NP mixtures, which was stirred for a further 5 hours in the dark at 4 °C. The resultant CTX-AuNPs and CTX-AuPtNPs were centrifuged at 14000 rpm for 2 hours and 2 collected pellets were resuspend in 1 ml Millipore water. The purified CTX-AuNPs and CTX-AuPtNPs were stored in the dark at 4 °C until further use.

3.3. Cell culture and maintenance

The U87 human malignant glioblastoma cells were kindly donated by Professor Sharon Prince, Department of Human Biology, University of Cape Town, South Africa. The SH-SY5Y human neuroblastoma cells were a generous donation from the Blackburn Laboratory, University of Cape Town, South Africa. Both U87 and SH-SY5Y cells were cultured in Dulbecco Modified Eagles Medium (DMEM) supplemented with 10 % foetal bovine serum (FBS, Gibco, Life Technologies Corporation, Paisley, UK) and 1% 100 U/ml penicillin and 100 µg/ml streptomycin (Lonza Group Ltd. Verviers, Belgium). Cells were grown in a humidified incubator at 37 °C with 5 % CO_2. The cell growth media were changed every 2-3 days and sub-culturing of cells were performed when cells reached 80 % confluency. The cells were washed with phosphate buffered saline (PBS) (Gibco, Life Technologies Corporation, Paisley, UK) and removed from the culture plates using a solution of 0.25 % trypsin EDTA (Lonza Group Ltd., Verviers, Belgium).

3.4. Assessment of CTX binding to U87 and SH-SY5Y cells

To determine whether CTX was able to bind specifically to U87 and SH-SY5Y cells, the cells were exposed to FITC-tagged CTX (FITC-CTX) and analysed by flow cytometry as previously described with modifications (Thovhogi *et al.*, 2015). Briefly, U87 cells and SH-SY5Y cells (1.75×10^5 cell per well) were cultured in a humidified incubator at 37 °C with 5 % CO_2 in 6 well cell culture plates for 24 hours. To assess the binding of FITC-CTX to the cells, the culture medium was replaced with 500 ul DMEM containing 0.03 mM FITC-CTX. The cells were incubated for a further 1 hour. To assess the specific binding of CTX to the cells, a competitive binding experiment was performed using untagged CTX. The cells were treated as described above except that the DMEM contained 0.03 mM FITC-CTX and 0.13 mM CTX. These concentrations of CTX and FITC-CTX were determined by optimisation (data not shown). Following treatment, floating cells in each respective treatment well were transferred to 15 ml centrifuge tubes and the adherent cells were gently trypsinized using 0.25 % EDTA trypsin (Lonza Group Ltd., Verviers, Belgium) and DMEM was used to deactivate the trypsin and cells were added to the respective tubes containing floating cells. The cells were centrifuged at 3,500 rpm for 5 minutes using a DLAB DM0412 centrifuge equipped with a A12-10P, A6-50P rotor type (DLAB Scientific Inc., California, United States of America) and the supernatant was removed to obtain a cell pellet. The cell pellet was resuspended in 300 µl DMEM and transferred on ice and analysed by measuring fluorescence intensity on flow cytometry using BD Accuri™ C6 Flow Cytometer instrument (BD Biosciences, Erembodegem, Belgium) using detector FL-1 and BD Accuri C6 Plus Software to analyse results. A minimum of 10,000 cells per sample were acquired. All experiments were performed in triplicate wells and repeated thrice.

3.5. Cellular uptake of NPs

U87 and SH-SY5Y cells were seeded in 6 well cell culture dishes at a density of 1.5×10^5 cells per well onto sterile glass cover slips (thickness: 1.5 H round, Diameter: 12 mm) and allowed to attach for 24 hours prior to exposure to the NPs. Thereafter, DMEM was removed, and either replaced with 1.5 ml fresh DMEM (for untreated cells) or 225 µg/ml 1.5 ml of citrate AuNPs, citrate AuPtNPs, PEG-AuNPs, PEG-AuPtNPs, CTX-AuNPs or CTX-AuPtNPs prepared in supplemented DMEM. The stock solutions of NPs were prepared by the collection of pellets in 1 ml Eppendorf tubes after centrifugation (pellets were air dried at 25 °C and weighed) to prepare concentrations of 1 mg/ml in

Millipore water as previously described (Dube *et al.*, 2020; Majoumouo *et al.*, 2020). The cells were placed back into the incubator for 24 hours. Thereafter, the cells were washed gently twice with PBS, fixed with 1-2 ml 10 % formaldehyde (prepared in PBS) for 10-15 minutes. Slides were gently washed once with PBS and mounted onto the microscope slide using Fluoroshield™ with DAPI (Sigma-Aldrich, St. Louis, Missouri, United States of America). The slides were viewed using a Leica DM500 microscope (Leica Microsystems, Germany) at 20X and 40X magnification. A digital camera and Lecia software were used to capture and store images. Experiments were performed in triplicates.

3.6. Instrumentation for NP characterization

3.6.1. Ultraviolet-visible (UV-Vis) spectrophotometer analysis

UV-Vis absorption spectra of all the AuNPs were acquired using POLARstar Omega microplate reader (BMG Labtech, Offenburg, Germany), 300 µl sample was added in a Greiner flat bottom non-sterile 96 well plate and the wavelengths of 280 - 600 nm at a resolution of 1 nm were read. The UV-Vis absorption spectra of AuPtNPs were characterized on a Varian Cary 50 spectrophotometer (Varian Cary 50, New Jersey, USA) in a 1 cm optical path quartz cuvette over wavelengths of 200 - 1000 nm at a resolution of 1 nm. The absorbance maxima (λ max) of six independent experiments for AuNPs are presented with dynamic light scattering data.

3.6.2. Dynamic Light Scattering (DLS) analysis

The hydrodynamic size (Z-Average size), polydispersity index (PDI) and zeta potential (ζ-potential) measurements of all NPs in solution were measured using a Nano-ZS90 Zetasizer instrument (Malvern Instruments Ltd., Malvern, UK). For hydrodynamic size and PDI analysis, a sample of 1 ml NP solution was transferred to a 12 mm disposable plastic cuvette and analysed at 25 °C at an angle of 173 °C to the laser beam. The intensity-weighted mean value was measured and the average of three measurements was taken. For, ζ-potential a disposable folded capillary cell was rinsed with distilled water using a 1 ml syringe prior to analyses as recommended by the manufacturer and 700 µl of NP solution was added to the cell and measured. The samples were analysed with a voltage of 4 mV at 25 °C at an angle of 173 °C to the laser beam and the average of three measurements were taken. Six independent experiments were analysed for NP characterization studies and 3 independent experiments were analysed for stability studies using DLS.

121

3.6.3. Transmission Electron Microscopy (TEM), Selected Area Electron Diffraction (SAED) pattern and Energy Dispersive X-Ray (EDX) analysis

To determine the core sizes of NPs, samples were prepared by drop-coating 1µl of each sample solution onto a carbon coated copper grid. This was then dried under a Xenon lamp. Transmission electron micrographs and selected area electron diffraction characterization were conducted using a 200kV FEI Tecnai F20 field-emission TEM, equipped with a LaB6 filament and operating at 200KeV (FEI Company, Oregon, USA). All images were captured using a Direct Electron DE-16 camera. Energy dispersive X-ray (EDX) spectra were collected using the Bruker Quanta 200 XFlash 6 EDX spectrometer that is installed with TEM and is used for the elemental analysis or chemical characterization of samples.

3.6.4. Fourier-transform Infrared (FTIR) spectroscopy

The FTIR spectra were obtained from JASCO 460 plus spectrophotometer (Perkin Elmer, Massachusetts, MA, USA) with potassium bromide (KBr) at a frequency ranging from 4000 to 400 cm^{-}1 in a KBr matrix as previously described (Dube *et al.*, 2020; Majoumouo *et al.*, 2020). NPs were centrifuged at 14000 rpm for 2 hours at 4 °C and the pellets were air dried at 25 °C. The dried pellets were individually mixed with KBr powder and pressed into a pellet for measurement. Pressed pure KBr was used for background correction. The baseline corrections were performed for all spectra.

4. Statistical analysis

Data for DLS characterization of NPs are expressed as mean ± standard deviation (SD) from 3 or 6 independent experiments and were assessed using GraphPad Prism 6 software (GraphPad Software, San Diego, California, United States of America). Core sizes acquired from TEM micrographs, was calculated using Image J (100 NPs were analysed per image) and Origin 8 software was used to construct histograms. Origin 8 was also used to construct FTIR graphs. Data generated for the CTX binding efficiency study are expressed as mean ± standard error of mean (SEM) of three independent experiments and analysed using the GraphPad Prism 6 software. Significance of difference was determined using one-way analysis of variance (ANOVA) with level of significance denoted with asterisks: **** $P \leq 0.0001$.

5. Conclusions

In this study monometallic AuNP (CTX-AuNPs) and bimetallic AuPtNPs (CTX-AuPtNPs) that can potentially be targeted to cancer cells and used for targeted RF thermal ablation of cancer cells were designed and successfully synthesised in a facile 3 step method. Cancer targeting can be achieved through the binding of CTX to cell surface proteins such as MMP-2, ClC-3, annexin A2, ERα and NRP1, which are all overexpressed in some cancers. This study confirmed using flow cytometry the specific binding of CTX to U87 human glioblastoma and SH-SY5Y human neuroblastoma cells and therefore also demonstrated the suitability of this cancer targeting peptide for use as a targeting moiety for the NPs developed in this study.

UV-Vis absorbance spectra demonstrated an increase in the λ max of citrate AuNPs (508nm), PEG-AuNPs (518) and CTX-AuNPs (521), while the absence of a λ max for AuPtNPs confirmed the formation of bimetallic NPs. These results were in good agreement with the increase in hydrodynamic size and surface changes reported from the DLS characterization. Both citrate capped AuNPs and AuPtNPs had a hydrodynamic size of approximately 7 nm and increased slightly after PEG and CTX surface functionalization, with a reported size of approximately 16 nm and 21 nm for CTX-AuNPs and CTX-AuPtNPs respectively. The shift in ζ-potential from a starting value of approximately -30 mV to more neutral charges recorded with PEG and CTX functionalization confirmed surface modification of NPs. FTIR also confirmed the presence of citrate, PEG and CTX on NPs. TEM measurements showed roughly spherical and monodispersed NPs with a core size of approximately 5 nm for all NPs. EDX further confirmed the presence of Au in all AuNPs and both Au and Pt in all AuPtNPs. NPs displayed stability in DMEM supplemented with 10 % FBS over 48-hour incubation period.

The results generated in this study indicated that the developed nanosystems have the potential for application in RF cancer ablation and therefore needs to be investigated further for *in vitro* and *in vivo* applications.

6. Future perspectives

Our study provided the synthesis and characterization of two new CTX-based NPs, and the results represents a promising step towards the development of novel targeting NPs for RF-induced

123

hyperthermia treatment of NB and GB tumours. It is important in the development of multifunctional nano-systems to extensively investigate the biocompatibility and potential anti-cancer effects of NPs *in vitro* before proceeding with further investigations of dual applications such as NP-mediated hyperthermia treatments and *in vivo* investigations. Therefore, further studies will investigate the cytotoxicity and anti-cancer properties of CTX-NPs and biocompatibility of NPs in selected cell lines.

7. References

Achar, A., Myers, R. and Ghosh, C. (2021). Drug Delivery Challenges in Brain Disorders across the Blood-Brain Barrier: Novel Methods and Future Considerations for Improved Therapy. *Biomedicines*, 9(12): 1834.

Agarwal, S., Mohamed, M.S., Mizuki, T., Maekawa, T. and Kumar, D.S. (2019). Chlorotoxin modified morusin–PLGA nanoparticles for targeted glioblastoma therapy. *Journal of Materials Chemistry B*, 7(39): 5896–5919.

Ali, E.S., Sharker, S.M., Islam, M.T., Khan, I.N., Shaw, S., Rahman, M.A., Uddin, S.J., Shill, M.C., Rehman, S., Das, N., Ahmad, S., Shilpi, J.A., Tripathi, S., Mishra, S.K. and Mubarak, M.S. (2021). Targeting cancer cells with nanotherapeutics and nanodiagnostics: Current status and future perspectives. *Seminars in cancer biology*, 69: 52–68.

Ali, S., Sharma, A.S., Ahmad, W., Zareef, M., Hassan, M.M., Viswadevarayalu, A., Jiao, T., Li, H. and Chen, Q. (2021). Noble Metals Based Bimetallic and Trimetallic Nanoparticles: Controlled Synthesis, Antimicrobial and Anticancer Applications. *Critical Reviews in Analytical Chemistry*, 51(5): 454–481.

Amendola, V., Pilot, R., Frasconi, M., Maragò, O.M. and Iatì, M.A. (2017). Surface plasmon resonance in gold nanoparticles: a review. *Journal of Physics. Condensed Matter: An Institute of Physics Journal*, 29(20): 203002.

Ara, T., Fukuzawa, M., Kusafuka, T., Komoto, Y., Oue, T., Inoue, M. and Okada, A. (1998). Immunohistochemical expression of MMP-2, MMP-9, and TIMP-2 in neuroblastoma: association with tumor progression and clinical outcome. *Journal of Pediatric Surgery*, 33(8): 1272–1278.

Baik, F.M., Hansen, S., Knoblaugh, S.E., Sahetya, D., Mitchell, R.M., Xu, C., Olson, J.M., Parrish-Novak, J. and Méndez, E. (2016). Fluorescence Identification of Head and Neck Squamous Cell Carcinoma and High-Risk Oral Dysplasia With BLZ-100, a Chlorotoxin-Indocyanine Green Conjugate. *JAMA otolaryngology-- head & neck surgery*, 142(4): 330–338.

Balasooriya, E.R., Jayasinghe, C.D., Jayawardena, U.A., Ruwanthika, R.W.D., Mendis de Silva, R. and Udagama, P.V. (2017). Honey Mediated Green Synthesis of Nanoparticles: New Era of Safe Nanotechnology. *Journal of Nanomaterials*, 2017: 1-10.

Barreto, G., Morales, G., Cañizo, A. and Eyler, N. (2015). Microwave Assisted Synthesis of ZnO Tridimensional Nanostructures. *Procedia Materials Science*, 8: 535–540.

Barros, H.R. de, Santos, M.C., Barbosa, L.R.S., Piovan, L. and Riegel-Vidotti, I.C. (2019). Physicochemical Study of the Interaction between Gold Nanoparticles and Lipase from *Candida* sp. (CALB): Insights into the Nano-Bio Interface. *Journal of the Brazilian Chemical Society*, 30: 2231–2242.

Barua, S. and Mitragotri, S. (2014). Challenges associated with Penetration of Nanoparticles across Cell and Tissue Barriers: A Review of Current Status and Future Prospects. *Nano today*, 9(2): 223–243.

Chang, D., Lim, M., Goos, J.A.C.M., Qiao, R., Ng, Y.Y., Mansfeld, F.M., Jackson, M., Davis, T.P. and Kavallaris, M. (2018). Biologically Targeted Magnetic Hyperthermia: Potential and Limitations. *Frontiers in Pharmacology*, 9: 831.

Chen, K., Zhao, H., Wang, Z. and Lan, M. (2021). A novel signal amplification label based on AuPt alloy nanoparticles supported by high-active carbon for the electrochemical detection of circulating tumor DNA. *Analytica Chimica Acta*, 1169: 338628.

Chen, S., Ahmadiantehrani, M., Publicover, N.G., Hunter, K.W. and Zhu, X. (2015). Thermal decomposition-based synthesis of Ag-In-S/ZnS quantum dots and their chlorotoxin-modified micelles for brain tumor cell targeting. *RSC Advances*, 5(74): 60612–60620.

Cohen, G., Burks, S.R. and Frank, J.A. (2018). Chlorotoxin-A Multimodal Imaging Platform for Targeting Glioma Tumors. *Toxins*, 10(12): E496.

Cohen-Inbar, O. and Zaaroor, M. (2016). Glioblastoma multiforme targeted therapy: The Chlorotoxin story. *Journal of Clinical Neuroscience: Official Journal of the Neurosurgical Society of Australasia*, 33: 52–58.

Corr, S.J. and Curley, S.A. (2017). Chapter 1 - Gold nanoparticles for noninvasive radiofrequency cancer hyperthermia', in Mathur, A.B. (ed.) *Nanotechnology in Cancer*. William Andrew Publishing (Micro and Nano Technologies), 1–18.

Danaei, M., Dehghankhold, M., Ataei, S., Hasanzadeh Davarani, F., Javanmard, R., Dokhani, A., Khorasani, S. and Mozafari, M.R. (2018). Impact of Particle Size and Polydispersity Index on the Clinical Applications of Lipidic Nanocarrier Systems. *Pharmaceutics*, 10(2): E57.

Daniels, J.L., Crawford, T.M., Andreev, O.A. and Reshetnyak, Y.K. (2017). Synthesis and characterization of pHLIP® coated gold nanoparticles. *Biochemistry and Biophysics Reports*, 10: 62–69.

Dardevet, L., Rani, D., Abd El Aziz, T., Bazin, I., Sabatier, J.-M., Fadl, M., Brambilla, E. and De Waard, M. (2015). Chlorotoxin: A Helpful Natural Scorpion Peptide to Diagnose Glioma and Fight Tumor Invasion. *Toxins*, 7(4): 1079–1101.

Day, E.S., Morton, J.G. and West, J.L. (2009). Nanoparticles for thermal cancer therapy. *Journal of Biomechanical Engineering*, 131(7): 074001.

Depciuch, J., Stec, M., Klebowski, B., Baran, J. and Parlinska-Wojtan, M. (2019). Platinum–gold nanoraspberries as effective photosensitizer in anticancer photothermal therapy. *Journal of Nanobiotechnology*, 17(1): 107.

Deshane, J., Garner, C.C. and Sontheimer, H. (2003). Chlorotoxin Inhibits Glioma Cell Invasion via Matrix Metalloproteinase-2. *Journal of Biological Chemistry*, 278(6): 4135–4144.

Dube, P., Meyer, S., Madiehe, A. and Meyer, M. (2020). Antibacterial activity of biogenic silver and gold nanoparticles synthesized from Salvia africana-lutea and Sutherlandia frutescens. *Nanotechnology*, 31(50): 505607.

Dueñas-Cuellar, R.A., Santana, C.J.C., Magalhães, A.C.M., Pires, O.R., Fontes, W. and Castro, M.S. (2020). Scorpion Toxins and Ion Channels: Potential Applications in Cancer Therapy, *Toxins*, 12(5): 326.

Dziawer, L., Koźmiński, P., Męczyńska-Wielgosz, S., Pruszyński, M., Łyczko, M., Wąs, B., Celichowski, G., Grobelny, J., Jastrzębski, J. and Bilewicz, A. (2017). Gold nanoparticle bioconjugates labelled with 211At for targeted alpha therapy. *RSC Advances*, 7(65): 41024–41032.

Elbagory, A.M., Cupido, C.N., Meyer, M. and Hussein, A.A. (2016). Large Scale Screening of Southern African Plant Extracts for the Green Synthesis of Gold Nanoparticles Using Microtitre-Plate Method. *Molecules (Basel, Switzerland)*, 21(11): E1498.

Erdreich, L.S. and Klauenberg, B.J. (2001). Radio frequency radiation exposure standards: considerations for harmonization. *Health Physics*, 80(5): 430–439.

Etame, A.B., Smith, C.A., Chan, W.C.W. and Rutka, J.T. (2011). Design and Potential Application of PEGylated Gold Nanoparticles with Size-Dependent Permeation through Brain Microvasculature. *Nanomedicine: Nanotechnology, Biology and Medicine*, 7(6): 992–1000.

Fang, C., Veiseh, O., Kievit, F., Bhattarai, N., Wang, F., Stephen, Z., Li, C., Lee, D., Ellenbogen, R.G. and Zhang, M. (2010). Functionalization of iron oxide magnetic nanoparticles with targeting ligands: their physicochemical properties and in vivo behavior', *Nanomedicine (London, England)*, 5(9): 1357–1369.

Fang, C., Wang, K., Stephen, Z.R., Mu, Q., Kievit, F.M., Chiu, D.T., Press, O.W. and Zhang, M. (2015). Temozolomide nanoparticles for targeted glioblastoma therapy. *ACS applied materials & interfaces*, 7(12): 6674–6682.

Fathima, R. and Mujeeb, A. (2021). Enhanced nonlinear and thermo optical properties of laser synthesized surfactant-free Au-Pt bimetallic nanoparticles. *Journal of Molecular Liquids*, 343: 117711.

Fidel, J., Kennedy, K.C., Dernell, W.S., Hansen, S., Wiss, V., Stroud, M.R., Molho, J.I., Knoblaugh, S.E., Meganck, J., Olson, J.M., Rice, B. and Parrish-Novak, J. (2015). Preclinical validation of the utility of BLZ-100 in providing fluorescence contrast for imaging canine spontaneous solid tumors. *Cancer research*, 75(20): 4283–4291.

Formaggio, D.M.D., de Oliveira Neto, X.A., Rodrigues, L.D.A., de Andrade, V.M., Nunes, B.C., Lopes-Ferreira, M., Ferreira, F.G., Wachesk, C.C., Camargo, E.R., Conceição, K. and Tada, D.B. (2019). In vivo toxicity and antimicrobial activity of AuPt bimetallic nanoparticles. *Journal of Nanoparticle Research*, 21(11): 244.

Forsyth, P.A., Wong, H., Laing, T.D., Rewcastle, N.B., Morris, D.G., Muzik, H., Leco, K.J., Johnston, R.N., Brasher, P.M., Sutherland, G. and Edwards, D.R. (1999). Gelatinase-A (MMP-2), gelatinase-B (MMP-9) and membrane type matrix metalloproteinase-1 (MT1-MMP) are involved in different aspects of the pathophysiology of malignant gliomas. *British Journal of Cancer*, 79(11–12): 1828–1835.

Fröhlich, E., Bonstingl, G., Höfler, A., Meindl, C., Leitinger, G., Pieber, T.R. and Roblegg, E. Comparison of two in vitro systems to assess cellular effects of nanoparticles-containing aerosols. *Toxicology in Vitro*, 27–360(1): 409–417.

Gebauer, J.S., Malissek, M., Simon, S., Knauer, S.K., Maskos, M., Stauber, R.H., Peukert, W. and Treuel, L. (2012). Impact of the Nanoparticle–Protein Corona on Colloidal Stability and Protein Structure. *Langmuir*, 28(25): 9673–9679.

Graham, E.G., Macneill, C.M. and Levi-polyachenko, N.H. (2013). Review of metal, carbon and polymer nanoparticles for infrared photothermal therapy. *Nano LIFE*, 3(3): 2013.

Gref, R., Lück, M., Quellec, P., Marchand, M., Dellacherie, E., Harnisch, S., Blunk, T. and Müller, R.H. (2000)."Stealth" corona-core nanoparticles surface modified by polyethylene glycol (PEG): influences of the corona (PEG chain length and surface density) and of the core composition on phagocytic uptake and plasma protein adsorption. *Colloids and Surfaces. B, Biointerfaces*, 18(3–4): 301–313.

Gu, W., Song, G., Li, S., Shao, C., Yan, C. and Ye, L. (2014). Chlorotoxin-conjugated, PEGylated Gd2O3 nanoparticles as a glioma-specific magnetic resonance imaging contrast agent. *RSC Advances*, 4(91): 50254–50260.

Guerrini, L., Alvarez-Puebla, R.A. and Pazos-Perez, N. (2018). Surface Modifications of Nanoparticles for Stability in Biological Fluids. *Materials (Basel, Switzerland)*, 11(7): E1154.

Häkkinen, H. (2012). The gold–sulfur interface at the nanoscale. *Nature Chemistry*, 4(6): 443–455.

Harrison, E., Nicol, J.R., Macias-Montero, M., Burke, G.A., Coulter, J.A., Meenan, B.J. and Dixon, D. (2016). A comparison of gold nanoparticle surface co-functionalization approaches using Polyethylene Glycol (PEG) and the effect on stability, non-specific protein adsorption and internalization. *Materials Science & Engineering. C, Materials for Biological Applications*, 62: 710–718.

Henderson, T.A. and Morries, L.D. (2015). Near-infrared photonic energy penetration: can infrared phototherapy effectively reach the human brain?. *Neuropsychiatric Disease and Treatment*, 11: 2191–2208.

Hirsch, V., Kinnear, C., Moniatte, M., Rothen-Rutishauser, B., Clift, M.J.D. and Fink, A. (2013) Surface charge of polymer coated SPIONs influences the serum protein adsorption, colloidal stability and subsequent cell interaction in vitro. *Nanoscale*, 5(9): 3723–3732.

Hoang Thi, T.T., Pilkington, E.H., Nguyen, D.H., Lee, J.S., Park, K.D. and Truong, N.P. (2020). The Importance of Poly(ethylene glycol) Alternatives for Overcoming PEG Immunogenicity in Drug Delivery and Bioconjugation. *Polymers*, 12(2): E298.

Huang, X. and El-Sayed, M.A. (2010). Gold nanoparticles: Optical properties and implementations in cancer diagnosis and photothermal therapy. *Journal of Advanced Research*, 1(1): 13–28.

Hunter, R.J., Midmore, B.R. and Zhang, H. (2001). Zeta Potential of Highly Charged Thin Double-Layer Systems. *Journal of Colloid and Interface Science*, 237(1): 147–149.

Huo, S., Jin, S., Ma, X., Xue, X., Yang, K., Kumar, A., Wang, P.C., Zhang, J., Hu, Z. and Liang, X.-J. (2014). Ultrasmall Gold Nanoparticles as Carriers for Nucleus-Based Gene Therapy Due to Size-Dependent Nuclear Entry. *ACS Nano*, 8(6): 5852–5862.

Jiang, N., Yang, X.-Y., Ying, G.-L., Shen, L., Liu, J., Geng, W., Dai, L.-J., Liu, S.-Y., Cao, J., Tian, G., Sun, T.-L., Li, S.-P. and Su, B.-L. (2014). "Self-repairing" nanoshell for cell protection. *Chemical Science*, 6(1): 486–491.

Kaszuba, M., Corbett, J., Watson, F.M. and Jones, A. (2010). High-concentration zeta potential measurements using light-scattering techniques. *Philosophical Transactions. Series A, Mathematical, Physical, and Engineering Sciences*, 368(1927): 4439–4451.

Kesavan, K., Ratliff, J., Johnson, E.W., Dahlberg, W., Asara, J.M., Misra, P., Frangioni, J.V. and Jacoby, D.B. (2010). Annexin A2 is a molecular target for TM601, a peptide with tumor-targeting and anti-angiogenic effects. *The Journal of Biological Chemistry*, 285(7): 4366–4374.

Khanyile, S., Masamba, P., Oyinloye, B.E., Mbatha, L.S., and Kappo, A.P. (2019). Current Biochemical Applications and Future Prospects of Chlorotoxin in Cancer Diagnostics and Therapeutics. *Advanced Pharmaceutical Bulletin*, 9(4): 510–520.

Kievit, F.M., Veiseh, O., Fang, C., Bhattarai, N., Lee, D., Ellenbogen, R.G. and Zhang, M. (2010). Chlorotoxin Labeled Magnetic Nanovectors for Targeted Gene Delivery to Glioma. *ACS Nano*, 4(8): 4587–4594.

Kulczar, C., Lubin, K.E., Lefebvre, S., Miller, D.W. and Knipp, G.T. (2017). Development of a direct contact astrocyte-human cerebral microvessel endothelial cells blood-brain barrier coculture model. *The Journal of Pharmacy and Pharmacology*, 69(12): 1684–1696.

Kumar, D., Meenan, B.J. and Dixon, D. (2012). Glutathione-mediated release of Bodipy® from PEG cofunctionalized gold nanoparticles. *International Journal of Nanomedicine*, 7: 4007–4022.

Kunwar, S., Pandey, P., Pandit, S., Sui, M. and Lee, J. (2019). Improved Morphological and Localized Surface Plasmon Resonance (LSPR) Properties of Fully Alloyed Bimetallic AgPt and Monometallic Pt NPs Via the One-Step Solid-State Dewetting (SSD) of the Ag/Pt Bilayers. *Nanoscale Research Letter*, 14 (1): 332.

Liang, H., Wu, Y., Ou, X.-Y., Li, J.-Y. and Li, J. (2017). Au@Pt nanoparticles as catalase mimics to attenuate tumor hypoxia and enhance immune cell-mediated cytotoxicity. *Nanotechnology*, 28(46): 465702.

Liu, X., Zhang, X., Zhu, M., Lin, G., Liu, J., Zhou, Z., Tian, X. and Pan, Y. (2017). PEGylated Au@Pt Nanodendrites as Novel Theranostic Agents for Computed Tomography Imaging and Photothermal/Radiation Synergistic Therapy. *ACS Applied Materials & Interfaces*, 9(1): 279–285.

Locatelli, E., Naddaka, M., Uboldi, C., Loudos, G., Fragogeorgi, E., Molinari, V., Pucci, A., Tsotakos, T., Psimadas, D., Ponti, J. and Franchini, M.C. (2014). Targeted delivery of silver nanoparticles and alisertib: in vitro and in vivo synergistic effect against glioblastoma. *Nanomedicine (London, England)*, 9(6): 839–849.

Loza, K., Heggen, M. and Epple, M. (2020). Synthesis, Structure, Properties, and Applications of Bimetallic Nanoparticles of Noble Metals. *Advanced Functional Materials*, 30(21): 1909260.

Lui, V.C.H., Lung, S.S.S., Pu, J.K.S., Hung, K.N. and Leung, G.K.K. (2010). Invasion of human glioma cells is regulated by multiple chloride channels including ClC-3. *Anticancer Research*, 30(11): 4515–4524.

Lyons, S.A., O'Neal, J. and Sontheimer, H. (2002). Chlorotoxin, a scorpion-derived peptide, specifically binds to gliomas and tumors of neuroectodermal origin. *Glia*, 39(2): 162–173.

Mahan, M.M. and Doiron, A.L. (2018). Gold Nanoparticles as X-Ray, CT, and Multimodal Imaging Contrast Agents: Formulation, Targeting, and Methodology. *Journal of Nanomaterials*, 2018: e5837276.

Majoumouo, M.S., Sharma, J.R., Sibuyi, N.R.S., Tincho, M.B., Boyom, F.F. and Meyer, M. (2020). Synthesis of Biogenic Gold Nanoparticles from Terminalia mantaly Extracts and the Evaluation of Their In Vitro Cytotoxic Effects in Cancer Cells. *Molecules*, 25(19): 4469.

Manson, J., Kumar, D., Meenan, B.J. and Dixon, D. (2011). Polyethylene glycol functionalized gold nanoparticles: the influence of capping density on stability in various media. *Gold Bulletin*, 44(2): 99–105.

Mateu Ferrando, R., Lay, L. and Polito, L. (2021). Gold nanoparticle-based platforms for vaccine development. *Drug Discovery Today: Technologies* [Preprint].

McFerrin, M.B. and Sontheimer, H. (2006). A role for ion channels in glioma cell invasion. *Neuron Glia Biology*, 2(1): 39–49.

McGonigle, S., Majumder, U., Kolber-Simonds, D., Wu, J., Hart, A., Noland, T., TenDyke, K., Custar, D., Li, D., Du, H., Postema, M.H.D., Lai, W.G., Twine, N.C., Woodall-Jappe, M. and Nomoto, K. (2019). Neuropilin-1 drives tumor-specific uptake of chlorotoxin. *Cell communication and signaling: CCS*, 17(1): 67.

Medina-Cruz, D., Saleh, B., Vernet-Crua, A., Nieto-Argüello, A., Lomelí-Marroquín, D., Vélez-Escamilla, L.Y., Cholula-Díaz, J.L., García-Martín, J.M. and Webster, T. (2020). Bimetallic Nanoparticles for Biomedical Applications: A Review in Li, B., Moriarty, T., Webster, T., Xing, M.

(eds). *Racing for the Surface: Antimicrobial and Interface Tissue Engineering*. Cham: Springer International Publishing: 397–434.

Mohan, J.C., Praveen, G., Chennazhi, K.P., Jayakumar, R. and Nair, S.V. (2013). Functionalised gold nanoparticles for selective induction of in vitro apoptosis among human cancer cell lines. *Journal of Experimental Nanoscience*, 8(1): 32–45.

Moore, T.L., Rodriguez-Lorenzo, L., Hirsch, V., Balog, S., Urban, D., Jud, C., Rothen-Rutishauser, B., Lattuada, M. and Petri-Fink, A. (2015). Nanoparticle colloidal stability in cell culture media and impact on cellular interactions. *Chemical Society Reviews*, 44(17): 6287–6305.

Moran, C.H., Wainerdi, S.M., Cherukuri, T.K., Kittrell, C., Wiley, B.J., Nicholas, N.W., Curley, S.A., Kanzius, J.S. and Cherukuri, P. (2009). Size-dependent joule heating of gold nanoparticles using capacitively coupled radiofrequency fields. *Nano Research*, 2(5): 400–405.

Moros, M., Lewinska, A., Merola, F., Ferraro, P., Wnuk, M., Tino, A. and Tortiglione, C. (2020). Gold Nanorods and Nanoprisms Mediate Different Photothermal Cell Death Mechanisms In Vitro and In Vivo. *ACS applied materials & interfaces*, 12(12): 13718–13730.

Mu, Q., Lin, G., Patton, V.K., Wang, K., Press, O.W. and Zhang, M. (2015). Gemcitabine and chlorotoxin conjugated iron oxide nanoparticles for glioblastoma therapy. *Journal of Materials Chemistry B*, 4(1): 32–36.

Nidhin, M., Indumathy, R., Sreeram, K.J. and Nair, B.U. (2008). Synthesis of iron oxide nanoparticles of narrow size distribution on polysaccharide templates. *Bulletin of Materials Science*, 31(1): 93–96.

Norouzi, H., Khoshgard, K. and Akbarzadeh, F. (2018). In vitro outlook of gold nanoparticles in photo-thermal therapy: a literature review. *Lasers in Medical Science*, 33(4): 917–926.

Ohta, S., Kikuchi, E., Ishijima, A., Azuma, T., Sakuma, I. and Ito, T. (2020). Investigating the optimum size of nanoparticles for their delivery into the brain assisted by focused ultrasound-induced blood–brain barrier opening. *Scientific Reports*, 10(1): 18220.

Ojeda, P.G., Wang, C.K. and Craik, D.J. (2016). Chlorotoxin: Structure, activity, and potential uses in cancer therapy. *Biopolymers*, 106(1): 25–36.

Oladipo, A.O., Iku, S.I.I., Ntwasa, M., Nkambule, T.T.I., Mamba, B.B. and Msagati, T.A.M. (2020). Doxorubicin conjugated hydrophilic AuPt bimetallic nanoparticles fabricated from Phragmites australis: Characterization and cytotoxic activity against human cancer cells. *Journal of Drug Delivery Science and Technology*, 57: 101749.

Olajire, A.A. and Adesina, O.O. (2017). Green Approach to Synthesis of Pt and Bimetallic Au@Pt Nanoparticles Using Carica Papaya Leaf Extract and Their Characterization. *Journal of Nanostructures*, 7(4): 338–344.

Oliveira, J.P., Prado, A.R., Keijok, W.J., Ribeiro, M.R.N., Pontes, M.J., Nogueira, B.V., and Guimarães, M.C.C. (2020). A helpful method for controlled synthesis of monodisperse gold nanoparticles through response surface modeling. *Arabian Journal of Chemistry*, 13(1): 216–226.

Pal, A. (2015). Gold–platinum alloy nanoparticles through water-in-oil microemulsion. *Journal of Nanostructure in Chemistry*, 5(1): 65–69.

Patil, C.G., Walker, D.G., Miller, D.M., Butte, P., Morrison, B., Kittle, D.S., Hansen, S.J., Nufer, K.L., Byrnes-Blake, K.A., Yamada, M., Lin, L.L., Pham, K., Perry, J., Parrish-Novak, J., Ishak, L., Prow, T., Black, K. and Mamelak, A.N. (2019). Phase 1 Safety, Pharmacokinetics, and Fluorescence Imaging Study of Tozuleristide (BLZ-100) in Adults With Newly Diagnosed or Recurrent Gliomas. *Neurosurgery*, 85(4): E641–E649.

Pennington, M.W., Czerwinski, A. and Norton, R.S. (2018). Peptide therapeutics from venom: Current status and potential. *Bioorganic & Medicinal Chemistry*, 26(10): 2738–2758.

Piella, J., Bastús, N.G. and Puntes, V. (2016). Size-Controlled Synthesis of Sub-10-nanometer Citrate-Stabilized Gold Nanoparticles and Related Optical Properties. *Chemistry of Materials*, 28(4): 1066–1075.

Politi, J., Spadavecchia, J., Fiorentino, G., Antonucci, I., Casale, S. and De Stefano, L. (2015). Interaction of Thermus thermophilus ArsC enzyme and gold nanoparticles naked-eye assays speciation between As(III) and As(V). *Nanotechnology*, 26(43): 435703.

Qu, J., Liu, H., Wei, Y., Wu, X., Yue, R., Chen, Y. and Yang, J. (2011). Coalescence of Ag2S and Au nanocrystals at room temperature. *Journal of Materials Chemistry*, 21(32): 11750–11753.

Quintero-Fabián, S., Arreola, R., Becerril-Villanueva, E., Torres-Romero, J.C., Arana-Argáez, V., Lara-Riegos, J., Ramírez-Camacho, M.A., Alvarez-Sánchez, M.E. (2019). Role of Matrix Metalloproteinases in Angiogenesis and Cancer. *Frontiers in Oncology*, 9: 1370.

Rajan, A. and Sahu, N.K. (2020). Review on magnetic nanoparticle-mediated hyperthermia for cancer therapy. *Journal of Nanoparticle Research*, 22(11): 319.

Raoof, M. and Curley, S.A. (2011). Non-invasive radiofrequency-induced targeted hyperthermia for the treatment of hepatocellular carcinoma. *International Journal of Hepatology*, 2011: 676957.

Ray, P.C., Khan, S.A., Singh, A.K., Senapati, D. and Fan, Z. (2012). Nanomaterials for targeted detection and photothermal killing of bacteria. *Chemical Society Reviews*, 41(8): 3193–3209.

Sakellari, G.I., Hondow, N. and Gardiner, P.H.E. (2020). Factors Influencing the Surface Functionalization of Citrate Stabilized Gold Nanoparticles with Cysteamine, 3-Mercaptopropionic Acid or l-Selenocystine for Sensor Applications. *Chemosensors*, 8(3): 80.

Salado-Leza, D., Traore, A., Porcel, E., Dragoe, D., Muñoz, A., Remita, H., García, G. and Lacombe, S. (2019). Radio-Enhancing Properties of Bimetallic Au:Pt Nanoparticles: Experimental and Theoretical Evidence. *International Journal of Molecular Sciences*, 20(22): 5648

San, B.H., Moh, S.H. and Kim, K.K. (2013). Investigation of the heating properties of platinum nanoparticles under a radiofrequency current. *International Journal of Hyperthermia: The Official Journal of European Society for Hyperthermic Oncology, North American Hyperthermia Group*, 29(2): 99–105.

Sanches, E.A., Soares, J.C., Iost, R.M., Marangoni, V.S., Trovati, G., Batista, T., Mafud, A.C., Zucolotto, V. and Mascarenhas, Y.P. (2011). Structural Characterization of Emeraldine-Salt Polyaniline/Gold Nanoparticles Complexes. *Journal of Nanomaterials*, 2011: e697071.

Sasikumar, P.G. and Ramachandra, M. (2018). Small-Molecule Immune Checkpoint Inhibitors Targeting PD-1/PD-L1 and Other Emerging Checkpoint Pathways. *BioDrugs: Clinical Immunotherapeutics, Biopharmaceuticals and Gene Therapy*, 32(5): 481–497.

Saw, W.S., Ujihara, M., Chong, W.Y., Voon, S.H., Imae, T., Kiew, L.V., Lee, H.B., Sim, K.S. and Chung, L.Y. (2018). Size-dependent effect of cystine/citric acid-capped confeito-like gold nanoparticles on cellular uptake and photothermal cancer therapy. *Colloids and Surfaces B: Biointerfaces*, 161: 365–374.

Sharma, G., Braga, C.B., Chen, K.-E., Jia, X., Ramanujam, V., Collins, B.M., Rittner, R. and Mobli, M. (2021). Structural basis for the binding of the cancer targeting scorpion toxin, ClTx, to the vascular endothelia growth factor receptor neuropilin-1. *Current Research in Structural Biology*, 3: 179–186.

Shi, L., Zhang, J., Zhao, M., Tang, S., Cheng, X., Zhang, W., Li, W., Liu, X., Peng, H. and Wang, Q. (2021). Effects of polyethylene glycol on the surface of nanoparticles for targeted drug delivery. *Nanoscale*, 13(24): 10748–10764.

Siddique, S. and Chow, J.C.L. (2020). Gold Nanoparticles for Drug Delivery and Cancer Therapy. *Applied Sciences*, 10(11): 3824.

Sokolova, V., Mekky, G., van der Meer, S.B., Seeds, M.C., Atala, A.J. and Epple, M. (2020). Transport of ultrasmall gold nanoparticles (2 nm) across the blood–brain barrier in a six-cell brain spheroid model. *Scientific Reports*, 10(1): 18033.

Song, Y., Qu, Z., Li, J., Shi, L., Zhao, W., Wang, H., Sun, T., Jia, T. and Sun, Y. (2021). Fabrication of the biomimetic DOX/Au@Pt nanoparticles hybrid nanostructures for the combinational chemo/photothermal cancer therapy. *Journal of Alloys and Compounds*, 881: 160592.

Sørensen, S.N., Engelbrekt, C., Lützhøft, H.-C.H., Jiménez-Lamana, J., Noori, J.S., Alatraktchi, F.A., Delgado, C.G., Slaveykova, V.I. and Baun, A. (2016). A Multimethod Approach for Investigating Algal Toxicity of Platinum Nanoparticles. *Environmental Science & Technology*, 50(19): 10635–10643.

Soroceanu, L., Gillespie, Y., Khazaeli, M.B. and Sontheimer, H. (1998). Use of chlorotoxin for targeting of primary brain tumors. *Cancer Research*, 58(21): 4871–4879.

Sosibo, N.M., Keter, F.K., Skepu, A., Tshikhudo, R.T. and Revaprasadu, N. (2015). Facile Attachment of TAT Peptide on Gold Monolayer Protected Clusters: Synthesis and Characterization. *Nanomaterials (Basel, Switzerland)*, 5(3): 1211–1222.

Srinoi, P., Chen, Y.-T., Vittur, V., Marquez, M.D. and Lee, T.R. (2018). Bimetallic Nanoparticles: Enhanced Magnetic and Optical Properties for Emerging Biological Applications. *Applied Sciences*, 8(7): 1106.

Stebounova, L.V., Guio, E. and Grassian, V.H. (2011). Silver nanoparticles in simulated biological media: a study of aggregation, sedimentation, and dissolution. *Journal of Nanoparticle Research*, 13(1): 233–244.

Stephen, Z.R., Kievit, F.M., Veiseh, O., Chiarelli, P.A., Fang, C., Wang, K., Hatzinger, S.J., Ellenbogen, R.G., Silber, J.R. and Zhang, M. (2014). Redox-responsive magnetic nanoparticle for targeted convection-enhanced delivery of O6-benzylguanine to brain tumors. *ACS nano*, 8(10): 10383–10395.

Suk, J.S., Xu, Q., Kim, N., Hanes, J., Ensign, L.M. and Suk, J.S. (2016). PEGylation as a strategy for improving nanoparticle-based drug and gene delivery. *Advanced drug delivery reviews*, 99(Pt A): 28–51.

Sukhanova, A., Bozrova, S., Sokolov, P., Berestovoy, M., Karaulov, A. and Nabiev, I. (2018). Dependence of Nanoparticle Toxicity on Their Physical and Chemical Properties. *Nanoscale Research Letters*, 13(1): 44.

Sun, C., Fang, C., Stephen, Z., Veiseh, O., Hansen, S., Lee, D., Ellenbogen, R.G., Olson, J. and Zhang, M. (2008a). Tumor-targeted drug delivery and MRI contrast enhancement by chlorotoxin-conjugated iron oxide nanoparticles. *Nanomedicine (London, England)*, 3(4): 495–505.

Sun, C., Fang, C., Stephen, Z., Veiseh, O., Hansen, S., Lee, D., Ellenbogen, R.G., Olson, J. and Zhang, M. (2008b). In vivo MRI detection of gliomas by chlorotoxin-conjugated superparamagnetic nanoprobes. *Small (Weinheim an Der Bergstrasse, Germany)*, 4(3): 372–379.

Tamborini, M., Locatelli, E., Rasile, M., Monaco, I., Rodighiero, S., Corradini, I., Franchini, M.C., Passoni, L., and Matteoli, M. (2016). A Combined Approach Employing Chlorotoxin-Nanovectors and Low Dose Radiation To Reach Infiltrating Tumor Niches in Glioblastoma. *ACS nano*, 10(2): 2509–2520.

Tan, A.C., Ashley, D.M., López, G.Y., Malinzak, M., Friedman, H.S., Khasraw, M. and Tan, A.C. (2020). Management of glioblastoma: State of the art and future directions. *CA: a cancer journal for clinicians*, 70(4): 299–312.

Tang, J., Jiang, X., Wang, L., Zhang, H., Hu, Z., Liu, Y., Wu, X., and Chen, C. (2014). Au@Pt nanostructures: a novel photothermal conversion agent for cancer therapy. *Nanoscale*, 6(7): 3670–3678.

Tarokh, Z., Naderi-Manesh, H. and Nazari, M. (2017). Towards prostate cancer gene therapy: Development of a chlorotoxin-targeted nanovector for toxic (melittin) gene delivery. *European Journal of Pharmaceutical Sciences: Official Journal of the European Federation for Pharmaceutical Sciences*, 99: 209–218.

Thovhogi, N., Sibuyi, N., Meyer, M., Onani, M. and Madiehe, A. (2015). Targeted delivery using peptide-functionalised gold nanoparticles to white adipose tissues of obese rats. *Journal of Nanoparticle Research*, 17(2): 112.

Tong, W.Y., Alnakhli, M., Bhardwaj, R., Apostolou, S., Sinha, S., Fraser, C., Kuchel, T. and Kuss, B., Voelcker, N.H. (2018). Delivery of siRNA in vitro and in vivo using PEI-capped porous silicon

nanoparticles to silence MRP1 and inhibit proliferation in glioblastoma. *Journal of Nanobiotechnology*, 16(1): 38.

Usón, L., Sebastian, V., Mayoral, A., Hueso, J.L., Eguizabal, A., Arruebo, M. and Santamaria, J. (2015). Spontaneous formation of Au-Pt alloyed nanoparticles using pure nano-counterparts as starters: a ligand and size dependent process. *Nanoscale*, 7(22): 10152–10161.

Veiseh, M., Gabikian, P., Bahrami, S.-B., Veiseh, O., Zhang, M., Hackman, R.C., Ravanpay, A.C., Stroud, M.R., Kusuma, Y., Hansen, S.J., Kwok, D., Munoz, N.M., Sze, R.W., Grady, W.M., Greenberg, N.M., Ellenbogen, R.G. and Olson, J.M. (2007). Tumor Paint: A Chlorotoxin:Cy5.5 Bioconjugate for Intraoperative Visualization of Cancer Foci. *Cancer Research*, 67(14): 6882–6888.

Vinardell, M.P., Llanas, H., Marics, L. and Mitjans, M. (2017). In Vitro Comparative Skin Irritation Induced by Nano and Non-Nano Zinc Oxide. *Nanomaterials (Basel, Switzerland)*, 7(3): E56.

Vlieghe, P., Lisowski, V., Martinez, J. and Khrestchatisky, M. (2010). Synthetic therapeutic peptides: science and market', *Drug Discovery Today*, 15(1–2): 40–56.

Wang, A.Z., Gu, F., Zhang, L., Chan, J.M., Radovic-Moreno, A., Shaikh, M.R. and Farokhzad, O.C. (2008). Biofunctionalized targeted nanoparticles for therapeutic applications. *Expert Opinion on Biological Therapy*, 8(8): 1063–1070.

Wang, B., Xie, J., He, H.-Y., Huang, E.-W., Cao, Q.-H., Luo, L., Liao, Y.-S. and Guo, Y. (2017). Suppression of CLC-3 chloride channel reduces the aggressiveness of glioma through inhibiting nuclear factor-κB pathway. *Oncotarget*, 8(38): 63788–63798.

Wang, C.-L., Hsao, B.-J., Lai, S.-F., Chen, W.-C., Chen, H.-H., Chen, Y.-Y., Chien, C.-C., Cai, X., Kempson, I.M., Hwu, Y. and Margaritondo, G. (2011). One-pot synthesis of AuPt alloyed nanoparticles by intense x-ray irradiation. *Nanotechnology*, 22(6): 065605.

Wang, H., Gu, W., Xiao, N., Ye, L. and Xu, Q. (2014). Chlorotoxin-conjugated graphene oxide for targeted delivery of an anticancer drug. *International Journal of Nanomedicine*, 9: 1433–1442.

Wang, K., Kievit, F.M., Jeon, M., Silber, J.R., Ellenbogen, R.G. and Zhang, M. (2015). Nanoparticle-Mediated Target Delivery of TRAIL as Gene Therapy for Glioblastoma. *Advanced Healthcare Materials*, 4(17): 2719–2726.

Wang, X.-M., Luo, X. and Guo, Z.-Y. (2013). Recombinant expression and downstream processing of the disulfide-rich tumor-targeting peptide chlorotoxin. *Experimental and Therapeutic Medicine*, 6(4)1049–1053.

Wang, Y., Li, K., Han, S., Tian, Y., Hu, P., Xu, X., He, Y., Pan, W., Gao, Y., Zhang, Z. and Zhang, J., Wei, L. (2019). Chlorotoxin targets ERα/VASP signaling pathway to combat breast cancer. *Cancer Medicine*, 8(4): 1679–1693.

Weng, X., Liu, Y., Wang, K.-K., Feng, J.-J., Yuan, J., Wang, A.-J. and Xu, Q.-Q. (2016). Single-step aqueous synthesis of AuPt alloy nanodendrites with superior electrocatalytic activity for oxygen reduction and hydrogen evolution reaction. *International Journal of Hydrogen Energy*, 40(41): 18193–18202.

Westsson, E. and Koper, G.J.M. (2014). How to Determine the Core-Shell Nature in Bimetallic Catalyst Particles?. *Catalysts*, 4(4): 375–396.

Wulandari, P., Li, X., Tamada, K. and Hara, M. (2008). Conformational study of citrates adsorbed on gold nanoparticles using fourier transform infrared spectroscopy. *Journal of Nonlinear Optical Physics & Materials*, 17(02): 185–192.

Xiang, Y., Liang, L., Wang, X., Wang, J., Zhang, X. and Zhang, Q. (2011). Chloride channel-mediated brain glioma targeting of chlorotoxin-modified doxorubicine-loaded liposomes. *Journal of Controlled Release: Official Journal of the Controlled Release Society*, 152(3): 402–410.

Yamada, M., Miller, D.M., Lowe, M., Rowe, C., Wood, D., Soyer, H.P., Byrnes-Blake, K., Parrish-Novak, J., Ishak, L., Olson, J.M., Brandt, G., Griffin, P., Spelman, L. and Prow, T.W. (2021). A first-in-human study of BLZ-100 (tozuleristide) demonstrates tolerability and safety in skin cancer patients. *Contemporary Clinical Trials Communications*, 23: 100830.

Yamamoto, Y., Nagasaki, Y., Kato, Y., Sugiyama, Y. and Kataoka, K. (2001). Long-circulating poly(ethylene glycol)–poly(d,l-lactide) block copolymer micelles with modulated surface charge. *Journal of Controlled Release*, 77(1): 27–38.

Yang, Q., Peng, J., Xiao, Y., Li, W., Tan, L., Xu, X. and Qian, Z. (2018). Porous Au@Pt Nanoparticles: Therapeutic Platform for Tumor Chemo-Photothermal Co-Therapy and Alleviating Doxorubicin-Induced Oxidative Damage. *ACS Applied Materials & Interfaces*, 10(1): 150–164.

Yang, W., Liang, H., Ma, S., Wang, D. and Huang, J. (2019). Gold nanoparticle based photothermal therapy: Development and application for effective cancer treatment. *Sustainable Materials and Technologies*, 22: e00109.

Yeini, E., Ofek, P., Albeck, N., Rodriguez Ajamil, D., Neufeld, L., Eldar-Boock, A., Kleiner, R., Vaskovich, D., Koshrovski-Michael, S., Dangoor, S.I., Krivitsky, A., Burgos Luna, C., Shenbach-Koltin, G., Goldenfeld, M., Hadad, O., Tiram, G. and Satchi-Fainaro, R. (2021). Targeting Glioblastoma: Advances in Drug Delivery and Novel Therapeutic Approaches. *Advanced Therapeutics*, 4(1): 2000124.

Yetisgin, A.A., Cetinel, S., Zuvin, M., Kosar, A. and Kutlu, O. (2020). Therapeutic Nanoparticles and Their Targeted Delivery Applications. *Molecules (Basel, Switzerland)*, 25(9): E2193.

Yoo, J., Park, C., Yi, G., Lee, D. and Koo, H. (2019). Active Targeting Strategies Using Biological Ligands for Nanoparticle Drug Delivery Systems. *Cancers*, 11(5): 640.

Yu, M.K., Park, J. and Jon, S. (2012). Targeting Strategies for Multifunctional Nanoparticles in Cancer Imaging and Therapy. *Theranostics*, 2(1): 3–44.

Zhang, L., Mazouzi, Y., Salmain, M., Liedberg, B. and Boujday, S. (2020). Antibody-Gold Nanoparticle Bioconjugates for Biosensors: Synthesis, Characterization and Selected Applications. *Biosensors & Bioelectronics*, 165: 112370.

Zhang, W., Zhao, P., Xu, X.-L., Cai, L., Song, Z.-S., Cao, D.-Y., Tao, K.-S., Zhou, W.-P., Chen, Z.-N. and Dou, K.-F. (2013). Annexin A2 Promotes the Migration and Invasion of Human

Hepatocellular Carcinoma Cells In Vitro by Regulating the Shedding of CD147-Harboring Microvesicles from Tumor Cells. *PLOS ONE*, 8(8): e67268.

Zhang, X.-D., Wu, D., Shen, X., Liu, P.-X., Yang, N., Zhao, B., Zhang, H., Sun, Y.-M., Zhang, L.-A. and Fan, F.-Y. (2011). Size-dependent in vivo toxicity of PEG-coated gold nanoparticles. *International Journal of Nanomedicine*, 6: 2071–2081.

Zhao, L., Li, Y., Zhu, J., Sun, N., Song, N., Xing, Y., Huang, H. and Zhao, J. (2019). Chlorotoxin peptide-functionalized polyethylenimine-entrapped gold nanoparticles for glioma SPECT/CT imaging and radionuclide therapy. *Journal of Nanobiotechnology*, 17(1): 30.

Zhao, M., van Straten, D., Broekman, M.L.D., Préat, V., Schiffelers, R.M. and Zhao, M. (2020). Nanocarrier-based drug combination therapy for glioblastoma. *Theranostics*, 10(3): 1355–1372.

Zhao, P., Feng, X., Huang, D., Yang, G. and Astruc, D. (2015). Basic concepts and recent advances in nitrophenol reduction by gold- and other transition metal nanoparticles. *Coordination Chemistry Reviews*, 287: 114–136.

Zhao, Y., Ye, C., Liu, W., Chen, R. and Jiang, X. (2014). Tuning the Composition of AuPt Bimetallic Nanoparticles for Antibacterial Application. *Angewandte Chemie International Edition*, 53(31): 8127–8131.

Zhu, W., Wu, Z., Foo, G.S., Gao, X., Zhou, M., Liu, B., Veith, G.M., Wu, P., Browning, K.L., Lee, H.N., Li, H., Dai, S. and Zhu, H. (2017). Taming interfacial electronic properties of platinum nanoparticles on vacancy-abundant boron nitride nanosheets for enhanced catalysis. *Nature Communications*, 8(1): 15291.

UNIVERSITY *of the*

WESTERN CAPE

The synthesis and characterization of chlorotoxin functionalised metallic nanoparticles

Taahirah Boltman[1], Mervin Meyer[2]* Okobi Ekpo[1]

[1] Department of Medical Biosciences, University of the Western Cape, Cape Town, Robert Sobukwe Road, Bellville 7535, South Africa; 2917424@myuwc.ac.za (T.B.)

[2] DSI/Mintek Nanotechnology Innovation Centre, Biolabels Node, Department of Biotechnology, University of the Western Cape, Cape Town, Robert Sobukwe Road, Bellville 7535, South Africa

*Correspondence: memeyer@uwc.ac.za (M.M.); Tel.: +27-21-5952032 (M.M.)
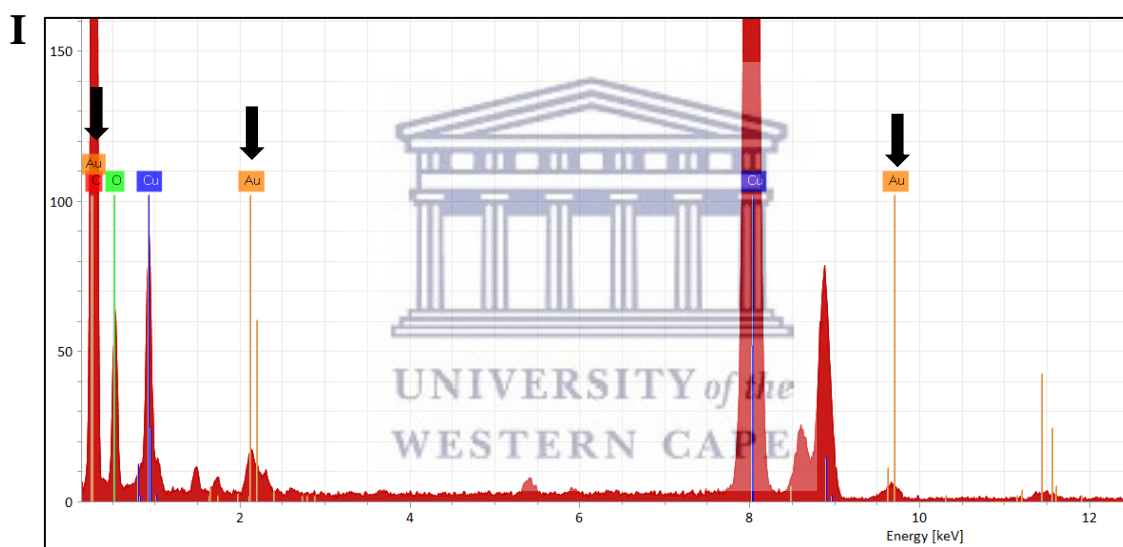
Element	At. No.	Netto	Mass [%]	Mass Norm. [%]	Atom [%]	abs. error [%] (1 sigma)	rel. error [%] (1 sigma)
Carbon	6	39954	88,30991	88,43672	93,5421	10,6232	12,02945
Oxygen	8	3671	6,992061	7,002103	5,560046	1,185785	16,95901
Copper	29	88728	4,257685	4,263799	0,852437	0,13231	3,107568
Zinc	30	4244	0,201874	0,202164	0,039278	0,030997	15,35452
Gold	79	951	0,095073	0,09521	0,006141	0,02895	30,45068
		Sum	99,8566	100	100		
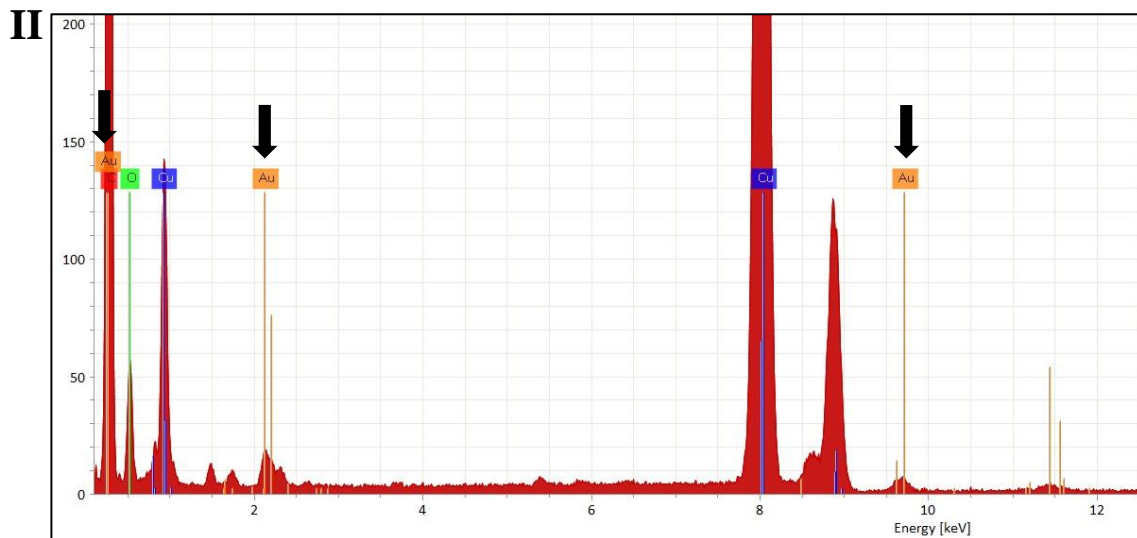
Element	At. No.	Netto	Mass [%]	Mass Norm. [%]	Atom [%]	abs. error [%] (1 sigma)	rel. error [%] (1 sigma)
Carbon	6	45372	87,89185	88,02963	94,34898	10,46468	11,90632
Oxygen	8	3223	5,3784	5,386831	4,334282	0,941798	17,51074
Copper	29	149127	6,449801	6,459912	1,308657	0,186833	2,896718
Gold	79	1203	0,123437	0,12363	0,00808	0,029758	24,10746
		Sum	99,84349	100	100		

	Element	At. No.	Netto	Mass [%]	Mass Norm. [%]	Atom [%]	abs. error [%] (1 sigma)	rel. error [%] (1 sigma)
III	Carbon	6	35935	84,93439	85,45442	92,71767	10,31063	12,13953
	Oxygen	8	3450	7,025449	7,068463	5,757428	1,205948	17,16543
	Copper	29	129507	7,370864	7,415994	1,520857	0,210129	2,850799
	Gold	79	406	0,060753	0,061125	0,004044	0,02846	46,84593
			Sum	99,39145	100	100		

Figure 12. Energy Dispersive X-Ray (EDX) of AuNPs (I), PEG-AuNPs (II) and CTX-AuNPs (III).

Black arrows indicate Au peaks
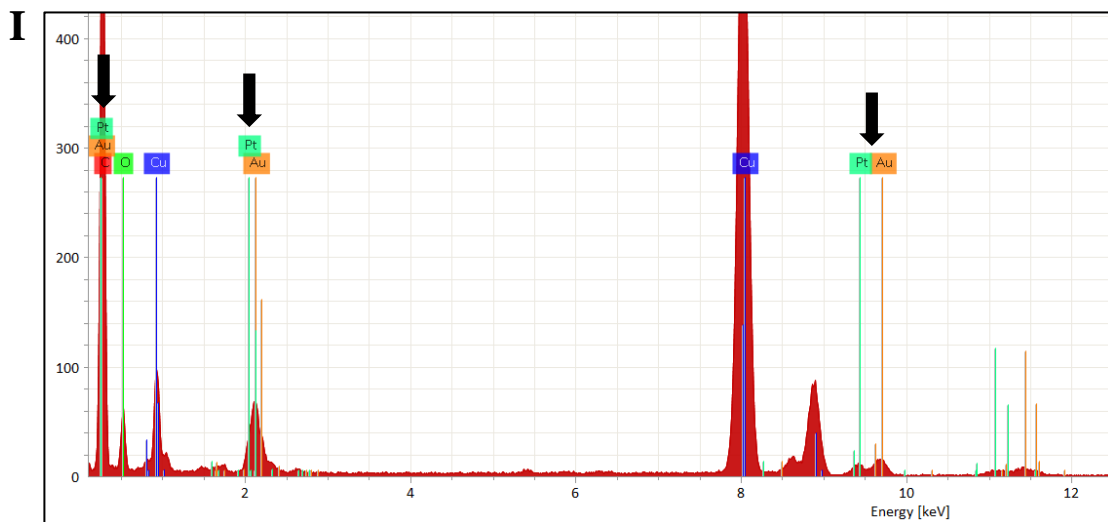
Element	At. No.	Netto	Mass [%]	Mass Norm. [%]	Atom [%]	abs. error [%] (1 sigma)	rel. error [%] (1 sigma)
Carbon	6	36069	87,33178	87,43	93,46131	10,59753	12,13479
Oxygen	8	3253	6,786189	6,793822	5,452065	1,179543	17,38153
Copper	29	97650	5,181491	5,187319	1,048106	0,155462	3,000341
Platinum	78	1784	0,207964	0,208197	0,013703	0,032192	15,4795
Gold	79	3297	0,380233	0,380661	0,024814	0,036397	9,572342
		Sum	99,88765	100	100		

II
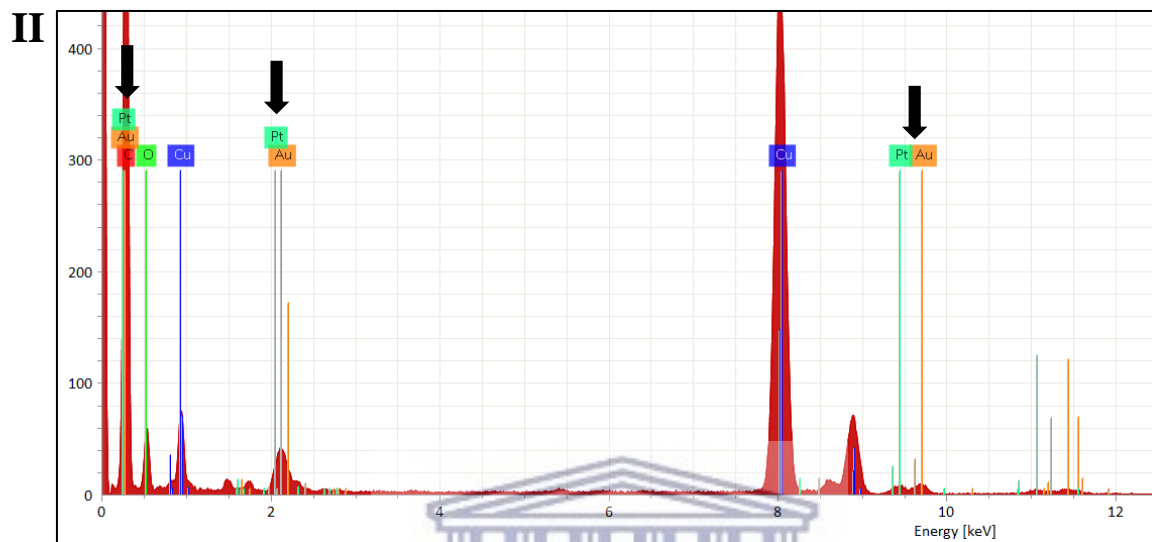
Element	At. No.	Netto	Mass [%]	Mass Norm. [%]	Atom [%]	abs. error [%] (1 sigma)	rel. error [%] (1 sigma)
Carbon	6	45761	90,08915	90,20557	94,69129	10,71846	11,89762
Oxygen	8	3408	5,781199	5,78867	4,561744	0,999237	17,28425
Copper	29	82123	3,6445	3,64921	0,724047	0,116937	3,208593
Platinum	78	1852	0,160684	0,160892	0,010399	0,030503	18,98323
Gold	79	2267	0,195405	0,195657	0,012524	0,031342	16,03968
		Sum	99,87094	100	100		

III

Element	At. No.	Netto	Mass [%]	Mass Norm. [%]	Atom [%]	abs. error [%] (1 sigma)	rel. error [%] (1 sigma)
Carbon	6	37901	89,0617	89,18081	94,13702	10,76106	12,0827
Oxygen	8	3090	6,255717	6,264084	4,963889	1,100738	17,59572
Copper	29	89123	4,477044	4,483032	0,894441	0,137834	3,078676
Platinum	78	125	0,020796	0,020824	0,001353	0,001979	9,515371
Gold	79	310	0,051178	0,051246	0,003299	0,02826	55,22021
		Sum	99,86643	100	100		

Figure 13. Energy Dispersive X-Ray (EDX) of AuPtNPs (I), PEG-AuPtNPs (II) and CTX-AuPtNPs (III). Black arrows indicate Au and Pt peaks.

139

CHAPTER FOUR:

The toxicity and anti-cancer properties of chlorotoxin peptide-functionalized gold and gold platinum nanoparticles in neuroblastoma and glioblastoma cells

Taahirah Boltman[1], Okobi Ekpo[1] and Mervin Meyer[2]*

[1] Department of Medical Biosciences, University of the Western Cape, Cape Town, Robert Sobukwe Road, Bellville 7535, South Africa; 2917424@myuwc.ac.za (T.B.)

[2] DSI/Mintek Nanotechnology Innovation Centre, Biolabels Node, Department of Biotechnology, University of the Western Cape, Cape Town, Robert Sobukwe Road, Bellville 7535, South Africa

*Correspondence: memeyer@uwc.ac.za (M.M.); Tel.: +27-21-5952032 (M.M.)

Abstract:

The treatment of two prominent nervous system (NS) tumours, glioblastoma multiforme (GB) and neuroblastoma (NB), remains a challenge. Current treatment modalities are largely ineffective due to systemic toxicity, drug resistance and poor targeted delivery efficiency. Additionally, most chemotherapeutic agents are unable to penetrate the blood brain barrier (BBB). Therefore, the development of novel therapeutic strategies that encompass high specificity and demonstrate the capacity to bypass the BBB are required. Chlorotoxin (CTX) is recognized as a highly selective targeting peptide for gliomas and tumours of neuroectodermal origin. CTX functionalized nanoparticles (NPs) have been proposed as an innovative tool in addressing the challenges associated with diagnosis and treatment of NS tumours with a variety of different types continuously being developed and actively researched. Bimetallic NPs offer improved anti-cancer properties based on the synergistic effects of combined metal atoms. There is a limitation on the development of CTX bimetallic NPs for investigating targeted NP-mediated radiofrequency (RF) field-based hyperthermia treatment in NS tumours. In our previous study we successfully developed two biologically stable CTX metallic NPs, namely, CTX functionalized gold NPs (CTX-AuNPs) and CTX functionalized bimetallic gold platinum NPs (CTX-AuPtNPs) which demonstrated uptake in cancerous U87 human GB and SH-SY5Y human NB cell lines. In this study we investigated the inherent toxicity of these

NPs in U87 and SH-SY5Y cell lines as well as the non-cancerous Human KMST-6 cell line, by assessing their effects on the cell viability, apoptosis, oxidative stress and mitochondrial activity. Cell survival and cell migration was also investigated. CTX-AuPtNPs produced the most significant anti-cancer activity in U87 cell lines possibly through receptor mediated endocytosis via CTX enabled uptake. Findings obtained from this study clearly demonstrated targeting and synergistic effects of combined noble metals in CTX-AuPtNPs for anti-cancer applications with the potential to be investigated for RF field-induced targeted hyperthermia.

Keywords: bimetallic gold platinum nanoparticles (AuPtNPs), cell cytotoxicity, chlorotoxin (CTX), glioblastoma multiforme (GB), nanoparticles (NPs) and neuroblastoma (NB).

1. Introduction

Nervous system (NS) tumours, in particular high-risk neuroblastoma (NB) and glioblastoma multiforme (GB), constitute some of the highly aggressive cancers diagnosed in both children and adults. GB is the deadliest primary brain tumours diagnosed in adults with a poor median survival time of 12-15 months and a 5-year survival rate of less than 7 % (Wu *et al.*, 2021). NB are the most commonly diagnosed solid extra-cranial brain tumours in children and remains one of the major challenges in paediatric oncology with a 5-year survival rate for patients presenting with high-risk NB tumours below 50 % (Smith and Foster, 2018). The current treatment options for advanced stage GB and NB are largely unsatisfactory and there has been no significant improvement in effective therapeutic strategies for these two cancers in recent years, as both remain incurable. Extensive surgery is not curable and standard chemotherapeutic drugs and radiation treatments are plagued with systemic toxicity, drug resistance and poor targeted delivery efficiency (Smith and Foster, 2018; Burster *et al.*, 2021). Additionally, the special pathological and physiological characteristics of the blood-brain barrier (BBB) diminishes the therapeutic value of most chemotherapeutic drugs for brain tumours (Ferraris *et al.*, 2020). Despite the medical advances in the management of NS tumours, the treatment of these tumours remains a challenge.

Treatment failure of these tumours are attributed to properties involved in cell migration and invasion (Welch and Hurst, 2019). Chloride ion channel 3 (ClC-3) is specifically upregulated in human GB and is involved in cell cytoskeleton rearrangements, and cell shape movements during cell migration (Griffin *et al.*, 2020). Tumour progression is associated with the overexpression of matrix

metalloproteinases (MMPs) (Cathcart, Pulkoski-Gross and Cao, 2015). Matrix metalloproteinases (MMPs) are a family of zinc-dependent endopeptidases and are involved in tissue-remodelling processes, including wound healing, embryo implantation, tumour invasion, metastasis, and angiogenesis (Visse and Nagase 2003; Quintero-Fabián *et al.*, 2019). There is significant evidence which implicates MMP-2 as active contributors in the progression of advanced stage GB and NB through the progression of cancer cell proliferation, migration, invasion, and angiogenesis (Forsyth *et al.*, 1999; Ribatti *et al.*, 2001; Zhou *et al.*, 2019; Hall *et al.*, 2020). Annexin A2 is a calcium-binding cytoskeletal protein localized at the extracellular surface of GB and NB cells that is also involved in tumour progression through cell migration and invasion (Wang *et al.*, 2017; Chen *et al.*, 2019; Li *et al.*, 2021). Annexin A2 has been implicated in enhancing multi-drug resistance in NB (Wang *et al.*, 2017). Therefore, taking into consideration the functions of these proteins, which are not over-expressed in non-cancerous cells, they may provide an alternative method for the development of targeted treatments for malignant NS tumours.

Nanoparticles (NPs) in a size range of 1-100 nm functionalized with targeting molecules such as peptides remains an area of active research producing promising novel targeted diagnostic and therapeutic nano-systems (Liu *et al.*, 2021). To address the challenges associated with the treatment of GB and NB, in our previous study (Chapter 3), we reported for the first time on the synthesis and characterization of biologically stable chlorotoxin (CTX) gold NPs (CTX-AuNPs) and bimetallic CTX gold platinum NPs (AuPtNPs) and demonstrated *in vitro* cell uptake in U87 human GB and SH-SY5Y human NB cell lines and high binding affinity of free CTX to these cell lines. The CTX-NPs had an average core size of approximately 5 nm and a hydrodynamic size of approximately 16 nm for CTX-AuNPs and 21 nm for CTX-AuPtNPs, potentially allowing efficient targeting and access across the BBB. CTX is a promising small scorpion venom derived peptide of interest that selectively binds to overexpressed molecular targets including ClC-3, MMP-2 and Annexin A2 present on cancerous cells without any effect on normal cells (Lyons, O'Neal and Sontheimer, 2002; Deshane, Garner and Sontheimer, 2003; Kesavan *et al.*, 2010). This in turn leads to the inhibition of cancer cell migration and invasion (Kasai *et al.*, 2012; Dardevet *et al.*, 2015; Cohen, Burks and Frank, 2018). CTX demonstrates high specificity and avidity for GB and NB and can cross the BBB (Soroceanu *et al.*, 1998; Lyons, O'Neal and Sontheimer, 2002; Cohen, Burks and Frank, 2018). Annexin A2 expression in BBB vascular endothelial cells has been suggested as a potential mechanism through which CTX crosses the BBB (Kesavan *et al.*, 2010). While NPs of 15 > 50 nm diameter size readily

crosses the intact BBB, large and advanced brain tumours with extensive angiogenesis and disrupted BBB allow NPs of size ranges of 5-200 nm to cross (Ohta *et al.*, 2020; Sokolova *et al.*, 2020).

Monometallic NPs (MNPs) such as AuNPs and platinum NPs (PtNPs) have been widely studied and have found applications for cancer in various areas such as imaging (Zhao *et al.*, 2017; Luo *et al.*, 2021), target specific drug delivery (Siddique and Chow, 2020; Mukherjee *et al.*, 2020) and photothermal therapy (PTT) using near infra-red (NIR) light (650–950 nm) (Manikandan, Hasan and Wu, 2013; Moros *et al.*, 2020). PTT is a minimally invasive hyperthermia technique to induce intracellular heat stress in the temperature range of 41-47 ºC resulting in cell death (Rajan and Sahu, 2020). Recently bimetallic AuPtNPs exhibited more pronounced PTT effects using NIR as a result of the synergistic effects of the combined metal atoms (Tang *et al.*, 2014; Liu *et al.*, 2017; Song *et al.*, 2017a; Yang *et al.*, 2018; Depciuch *et al.*, 2019; Fathima and Mujeeb, 2021; Song *et al.*, 2021). However, NIR PTT is best suited for subcutaneous malignant tumours because of the limited tissue penetration (~ 3 cm depth) by NIR light, and this may not be advantageous for deep-seated brain tumours such as GB (Henderson and Morries, 2015). Hence, other applications such as external radiofrequency (RF) ablation are more promising as radio wave energy has been shown to penetrate more deeply-located tumours (~ 7-17 cm depth) than NIR light and are considered safe for use in whole-body tissue penetration (Raoof *et al.*, 2012; Nasseri *et al.*, 2016). While AuNP and PtNPs show promise for non-invasive RF field-induced hyperthermia for anti-cancer therapy, there are no reports on the use of this application with AuPtNPs for NS tumours (Raoof and Curley, 2011; Corr *et al.*, 2013; San, Moh and Kim, 2013; Rejinold, Jayakumar and Kim, 2015; Yousaf *et al.*, 2021). NP-mediated hyperthermia therapies are also known to sensitize cells to other forms of standard therapy, including radiation and chemotherapy (Moros *et al.*, 2019, 2020; Oei *et al.*, 2020). Therefore, our developed CTX-NPs have potential as multifunctional nano-systems for targeting of GB and NB tumours and thermal ablation using non-invasive RF field-induced targeted hyperthermia.

It is crucial in the development of multifunctional nano-systems to extensively investigate the potential anti-cancer properties and biocompatibility *in vitro* before proceeding with further investigations of dual applications and *in vivo* experiments. Size, shape, concentrations, time, synthesis method, surface functionalization and cell type are factors implicated in cytotoxicity of metallic NPs (MNPs) (Sani, Cao and Cui, 2021). MNPs such as AuNPs and PtNPs have been widely studied in GB and NB cancer cell lines with various toxicity effects being reported. Few studies report no significant toxicity observed in U87 human GB cell line with treatment of 7-60 nm AuNPs (Mishra

143

et al., 2016; Coluccia *et al.*, 2018), while a recent study by Aboyewa *et al.* (2021) reported on AuNPs > 60 nm significantly affecting U87 cell viability at concentrations of 31-1000 µg/ml. The surface modification of NPs with polyethylene glycol (PEGylation) is a common strategy used to increase the biocompatibility of metallic NPs *in vitro* and *in vivo*, in addition to being exploited for active targeting (Shi *et al.*, 2021). PEG-AuNPs in a size of < 100 nm had no cytotoxic effects at concentrations of 25-200 µg/ml on U87 cells (Bhamidipati and Fabris, 2017), however increasing the concentrations to 10 mg/ml of PEG-AuNPs induced cell death in U87 cells (Correard *et al.*, 2014). At NP concentrations of 100 pM and 200 pM, the cell viability of SH-SY5Y Human NB cell line remained > 95 % following incubation with 18 nm AuNPs surface coated with citrate (Moore *et al.*, 2015). In a recent study by Zhang *et al.* (2020), 25 µg/ml of 4.5 nm PEG-AuNP induced cell apoptosis through upregulating reactive oxygen stress (ROS) production and disordering the mitochondrial membrane potential in SH-SY5Y cells. Platinum NPs (PtNPs) induce cytotoxicity in similar way to platinum-based chemotherapeutic drugs such as cisplatin (Jeyaraj *et al.*, 2019) and in a recent study by Gurunathan *et al.* (2020), SH-SY5Y cells pre-treated with PtNPs caused the cells be more sensitive to the cytotoxic effect of cisplatin (Pawar *et al.*, 2021). PtNPs was also reported to be more effective in inducing apoptosis in U87 cells when compared to cisplatin treatment (Kutwin *et al.*, 2017).

Although monometallic NPs show promise as a therapeutic option for various cancers, there remains a discrepancy between preclinical results and clinical outcomes. Given that human tumours are intrinsically heterogeneous, bimetallic NPs may be more effective for cancers due to synergistic effects which may also be exploited for hyperthermia treatments (McNamara and Tofail, 2015; Srinoi *et al.*, 2018). AuPtNPs in a size range of > 30 nm demonstrated no significant toxicity towards different cancer cell lines at low concentrations (Tang *et al.*, 2014; Oladipo *et al.*, 2020). No acute cytotoxicity to either Human umbilical vein endothelial cells (HUVEC) or 4T1 breast cancer cell line at 75 µg/ml was observed (Liu *et al.*, 2017) with PEGylated AuPtNPs in a size range of approximately 30 nm. Boomi *et al.* (2019) reported a significant decrease in cell viability in HepG liver cancer cells with treatment of < 10 nm AuPtNPs at 75-225 µg/ml, whereas Chaturvedi *et al.*, (2021) demonstrated that 16 nm AuPtNPs significantly reduced the cell viability of HCT 116 human colon cancer cells at 100 and 200 µg/ml to 25 % and 10 %, respectively, with cell death as a result of apoptosis. AuPtNPs for cancer applications is relatively recent and to the best of our knowledge, no reports in published literature exist on the toxicity of AuPtNPs, PEG-AuPtNPs and CTX-AuPtNPs in U87 and SH-SY5Y cancer cell lines at concentrations as high as 300 µg/ml. Therefore, it is important to investigate the

toxicity and anti-cancer properties of AuPtNPs in these cell lines, especially given that AuPtNPs have immense potential in anti-cancer applications for RF induced hyperthermia treatment.

In the current study we assessed the inherent (i.e., without the use of RF induced hyperthermia) anti-cancer effects of previously reported CTX-NPs (Chapter 3) in various human cancer cell lines. An *in vitro* assessment of the toxicity and anti-cancer activity of CTX-NPs was performed by investigating the effects on cell proliferation, changes in cell morphology, apoptosis, oxidative stress, mitochondrial activity, cell survival and anti-migratory properties in U87, SH-SY5Y and the non-cancerous KMST-6 human fibroblast cell lines. The most significant anti-cancer activity was obtained in U87 cells using CTX-AuPtNPs, while the cytocompatibility observed in KMST-6 cells highlights the safety of CTX-NPs and selectivity for cancerous cell lines.

2. Results and discussion

This study aimed to investigate the inherent toxicity of CTX conjugated monometallic (Au) and bimetallic (AuPt) NPs in cancer cell lines (U87 and SH-SY5Y) that are known to express receptors for CTX. It was previously shown that free CTX and CTX conjugated AuNPs and AuPtNPs can be targeted to U87 and SH-SY5Y cells (Chapter 3). It has been proposed that CTX binds to several molecular targets which include chloride channels (Soroceanu *et al.*, 1998), MMP-2 (Deshane, Garner and Sontheimer, 2003) annexin A2 (Kesavan *et al.*, 2010), estrogen receptor alpha (ERα) (Wang *et al.*, 2019) and neuropilin-1 (NRP-1) (McGonigle *et al.*, 2019, Sharma *et al*., 2021). Additionally, CTX has been shown to penetrate the BBB (Dardevet *et al.*, 2015; Cohen-Inbar and Zaaroor, 2016; Cohen, Burks and Frank, 2018). The abundantly expressed MMP-2 and ClC-3, are the main receptors involved in GB targeting (Qin *et al.*, 2014). ClC-3 and MMP-2 form a protein complex which is targeted by the CTX-peptide and it is proposed that this action inhibits glioma cell invasion by endocytosis of the MMP-2/ClC-3 protein complex (Deshane, Garner and Sontheimer, 2003; McFerrin and Sontheimer, 2006; Lui *et al.*, 2010). It has also been reported in literature that U87 and SH-SY5Y cell lines express receptors for CTX targeting and that the uptake of CTX conjugated NP is facilitated through this receptor-dependent cellular internalization (Soroceanu *et al.*, 1998; Lyons, O'Neal and Sontheimer, 2002; Qin *et al.*, 2014).

2.1.   NPs induced cytotoxicity in U87 and SH-SY5Y cell lines

In this study the toxicity of 6 NPs was investigated of which 3 are based on monometallic AuNPs (citrate AuNPs, PEG-AuNPs and CTX-AuNPs) and 3 based on bimetallic AuPtNPs (citrate AuPtNPs, PEG-AuPtNPs and CTX-AuPtNPs). The synthesis of these NPs was described previously (Chapter 3). The strategy for synthesis involved the construction of citrate AuNPs and citrate AuPtNPs which was then sequentially modified, first by PEGylation to produce PEG-AuNPs and PEG-AuPtNPs, and then the conjugation of the CTX peptide to produce CTX-AuNPs and CTX-AuPtNPs, respectively. As illustrated previously, CTX-AuNPs and CTX-AuPtNPs have great potential for application in the treatment of GB through non-invasive RF field-induced targeted hyperthermia and can be targeted to cells that express the receptors for CTX. However, in this study the inherent toxicity of the NPs was investigated without the use of RF activation.

The cytotoxicity of the 6 NPs was evaluated in two cancer cell lines (U87 and SH-SY5) and in a non-cancerous cell line (KMST-6) using the WST-1 cell viability assay to determine the half maximal inhibitory concentration (IC_{50}) (Table 1, pg. 149). Various cancer cell lines are known to overexpress MMP-2, one of the main molecular targets of CTX, whereas fibroblasts typically express MMPs at lower levels (Ravanti *et al.*, 1999) and a previous study reported that CTX does not bind to 40 human non-tumour tissues including non-cancerous brain tissues and 6 human skin fibroblast cell lines (Lyons, O'Neal and Sontheimer, 2002). Therefore, we selected KMST-6 Human skin fibroblasts as a non-cancerous cell line in this study. The cells were treated for 48 hours at a range of concentrations from 75-300 µg/ml after which the cell viability was determined and IC_{50} values extrapolated (Table 1). In general, the cell viability of all 3 cell lines were affected by the NPs. However, the responses of the various cell lines varied significantly, with the viability of the non-cancerous KMST-6 cells appearing to be less affected by the NPs, since the IC_{50} values for the NPs were generally higher for this cell line compared to the U87 and SH-SY5 cell lines. The U87 cell line appeared to be more sensitive to the effects of the NPs, since the IC_{50} values for the NPs were generally lower for this cell line compared to the other cell lines. Based on the IC_{50} values, the bimetallic citrate AuPtNPs were more toxic than the monometallic citrate AuNPs (Table 1). Toxicity induced by citrate NPs may result from the acidic nature of citrate as previously explained (Vijayakumar and Ganesan, 2012). Once the citrate NPs were modified by PEGylation and CTX conjugation this apparent correlation between toxicity and metallic complexity did not completely hold. AuNPs were more cytotoxic in U87 than

146

SH-SY5Y cells, this is in line with a finding reported by Park *et al.* (2017) in which the viability of SH-SY5Y cells was not affected by the treatment with citrate capped AuNPs with concentrations up to 100 µg/ml. However, NPs < 4 nm induced apoptosis in SH-SY5Y cells (Pan *et al.*, 2009; Imperatore *et al.*, 2015). In this study, the cytotoxicity observed after treatment with approximately 5 nm AuNPs is in line with previous reports of AuNP-induced cytotoxicity in a size range under 10 nm (Pan *et al.*, 2009; Schaeublin *et al.*, 2011; Vijayakumar and Ganesan, 2012; Coradeghini *et al.*, 2013; Shang, Nienhaus and Nienhaus, 2014; Dong *et al.*, 2015; Imperatore *et al.*, 2015; Bhamidipati and Fabris, 2017; Park *et al.*, 2017). The higher cytotoxic effects of AuPtNPs as compared to AuNPs may potentially be due to synergistic effects of the 2 metals (Au and Pt) or because of Pt. It was shown that platinum NPs (PtNPs) induce cytotoxicity in a similar way to platinum-based chemotherapeutic drugs with smaller PtNPs reported as apoptotic inducers in various cancer cell lines (Shiny, Mukherjee and Chandrasekaran, 2016; Bendale, Bendale and Paul, 2017; Kutwin *et al.*, 2017; Almeer *et al.*, 2018; Loan, Do and Yoo, 2018; Şahin *et al.*, 2018; Gurunathan *et al.*, 2020). According to Kutwin *et al.* (2017), PtNPs significantly affected cell proliferation rate and the morphology of U87 cells, and therefore, cells suffer from membrane disruption, reduced density and decreased migration while these NPs also induced apoptosis in neuro-2a brain neuroblastoma. In a recent study by Gurunathan *et al.* (2020), SH-SY5Y cells pre-treated with PtNPs sensitized cells to treatment with cisplatin. Numerous studies demonstrated the cytotoxicity and anticancer effects of AuPtNPs in different cancer cell lines, however, in this study we report for the first time the effects in U87, SH-SY5Y and KMST-6 cell lines at concentrations as high as 300 µg/ml treatment for 48 hours. Tang *et al.* (2014) indicated that AuPtNPs caused negligible toxicity to the human breast cancer cells, MDAMB-231, at 10 mg/ml for 24 hours treatment. Chaturvedi *et al.* (2021) showed the cell viability of human colon cancer cell line HCT 116 cells was reduced to 50 % when treated with a concentration of 12.5 µg/ml AuPtNPs, while at 100 and 200 µg/ml, it is significantly reduced to 25 % and 10 %, respectively. In a study by Boomi *et al.* (2019), cell viability was significantly reduced in HepG2 human liver cancer cells with treatment of AuPtNPs at 75-225 µg/ml. Shin *et al.* (2018) showed AuPtNPs significantly inhibited cell proliferation of bladder cancer EJ cells in a dose-dependent manner by inducing G1 phase cell cycle arrest (Shin *et al.*, 2018). In this study, AuNPs and AuPtNPs was generally not toxic to KMST-6 cells at low concentrations and is in line with previous studies demonstrating little toxicity towards normal cells and in other fibroblast cells (Correard *et al.*, 2014; Uchiyama *et al.*, 2014; Jo *et al.*, 2015; Mishra *et al.*, 2016; Park *et al.*, 2017; Adewale *et al.*, 2019; Formaggio *et al.*, 2019; Majoumouo *et al.*, 2020).

147

Citrate AuPtNPs and PEG-AuPtNPs, respectively and generally demonstrated the highest and lowest toxicity (Table 1). It is known that the modification of the NP surface by the attachment of polyethylene glycol (or PEGylation) can increase the biocompatibility of nanomaterials due to its amphiphilic nature and high solubility (Zhang *et al.*, 2020). It is therefore not surprising that the PEGylated NPs demonstrated lower toxicity. These findings are also in agreement with a previous studies where it has been shown that negatively charged particles present a lower cell interaction (Hoang Thi *et al.*, 2020) and that PEGylated NPs only weakly interact with cells resulting in long circulation times *in vivo* (Bouzas *et al.*, 2014). The low cytotoxicity of PEGylated NPs in various cells reported in this study, is consistent with previous studies that reported on the low cytotoxicity and good biocompatibility of similar PEG-AuNPs and PEG-AuPtNPs in various cell lines (Lau *et al.*, 2012; Bhamidipati and Fabris, 2017; Liang *et al.*, 2017; Liu *et al.*, 2017; Massard *et al.*, 2017; Zhang *et al.*, 2020).

The lowest IC_{50} concentration (166 µg/ml) is reported in U87 cells with the treatment of bimetallic CTX-AuPtNPs, suggesting CTX-AuPtNPs are more cytotoxic than the other NPs and U87 cells are more sensitive to the effects of these NPs. CTX-AuPtNPs seem to be not selectively affected on cytotoxicity of SH-SY5Y cells compared to control cells. This may be attributed to selective cytotoxicity of AuPtNPs in different cell lines as observed in this study where treatment of AuPtNPs in SH-SY5Y and KMST-6 cell lines show similar IC_{50} values, whereas U87 cells seem to be more sensitive to the treatment of citrate AuPtNPs. The results with CTX-NPs demonstrated selective toxicity towards U87 and SH-SY5 cells which are both known to express MMP-2 and Annexin A2 receptors at high levels, with U87 cell line showing a higher expression level for CTX molecular targets than other cell lines (Lyons, O'Neal and Sontheimer, 2002; Kesavan *et al.*, 2010; Park *et al.*, 2006; Lee *et al.*, 2012; Marchiq *et al.*, 2015; Xu *et al.*, 2016). The KMST-6 cells do not express these molecular targets as highly as cancerous cells and therefore highlights the safety profile of CTX-NPs, and is in line with previous studies with CTX in similar fibroblast cell lines (Lyons, O'Neal and Sontheimer, 2002; Dastpeyman *et al.*, 2019). The monometallic CTX-AuNPs also demonstrated similar selective toxicity, but to a lesser extent than the bimetallic CTX-AuPtNPs. It was previously demonstrated that CTX conjugated NPs are specifically targeted to cells that over express ClC-3 and MMP-2 receptors such as U87 cells and that these cells show increased uptake of CTX conjugated NPs when compared to untargeted NPs (Chapter 3).

As demonstrated in other studies, the varied responses observed for metallic NPs appeared to be dependent on a number of factors (Schaeublin *et al.*, 2011; Vijayakumar and Ganesan, 2012; Shang, Nienhaus and Nienhaus, 2014; Coradeghini *et al.*, 2013; Dong *et al.*, 2015; Bhamidipati and Fabris, 2017). In this study these factors included the specific cell line in question, the expression levels of CTX receptors, the physicochemical properties of the NPs which include whether the NPs are mono- or bimetallic and the functionalisation of the NPs which will have an impact on properties such as surface charge. It is possible that the differential response observed for CTX-AuPtNPs and CTX-AuNPs in these 3 cell lines is due to the differential expression of CTX receptors on the surface of these cells. In this scenario increased concentrations of CTX-AuPtNPs and CTX-AuNPs accumulate within cells, such as U87 cells that express higher levels of the CTX targeting receptors.

Table 1. Half maximal inhibitory concentration (IC_{50}) of different NPs on selected cell lines

Nanoparticles	Cell Lines and IC_{50} values (µg/ml) ± SD		
	U87	**SH-SY5Y**	**KMST-6**
Citrate AuNPs	207.00 ± 1.86	> 300	281.80 ± 1.82
Citrate AuPtNPs	184.70 ± 1.90	201.90 ± 1.89	205.60 ± 1.95
PEG-AuNPs	202.40 ± 1.76	> 300	239.60 ± 1.81
PEG-AuPtNPs	> 300	> 300	> 300
CTX-AuNPs	255.60 ± 1.76	273.40 ± 1.12	> 300
CTX-AuPtNPs	166.00 ± 2.00	> 300	> 300

*Note: The half maximal inhibitory concentration (IC_{50}) was obtained using GraphPad Prism 6 (GraphPad software, San Diego, California, United States of America). Data is presented from three independent experiments.

2.2. NPs induced morphological changes in U87 and SH-SY5Y cell lines

Treatments with 75-300 µg/ml of various NPs was accompanied by distinct morphological changes as demonstrated in Figure 1. The astrocyte-like shape of U87 cells (untreated) and neuroblast-like shape of SH-SY-5Y cells (untreated) changed to a spherical shape after exposure to the different NPs (morphological changes for 225 µg/ml treatment is shown only in Figure 1) for 48 hours, this is indicative of cellular stress and cell death caused by NPs as previously reported (Patra *et al.*, 2007;

149

Yang, Lohse and Murphy, 2014; Ma *et al.*, 2017). It is also clear that the density of cells is lower when compared to the untreated control samples, which is indicative of increased cell death in the NP treated samples. While the percentage of cells that changed their morphology was not quantified, it agrees with the cell viability data which suggested that treatment with the NPs at this and higher concentrations result in the death of the cells. Based on the morphology of the cells and the density of the cells, it appears that treatments with CTX-AuPtNP was more toxic in both U87 and SH-SY-5Y cells.

A

Untreated U87   Citrate AuNPs   Citrate AuPtNPs

PEG-AUNPs   PEG-AuPtNPs

CTX-AuNPs   CTX-AuPtNPs

B
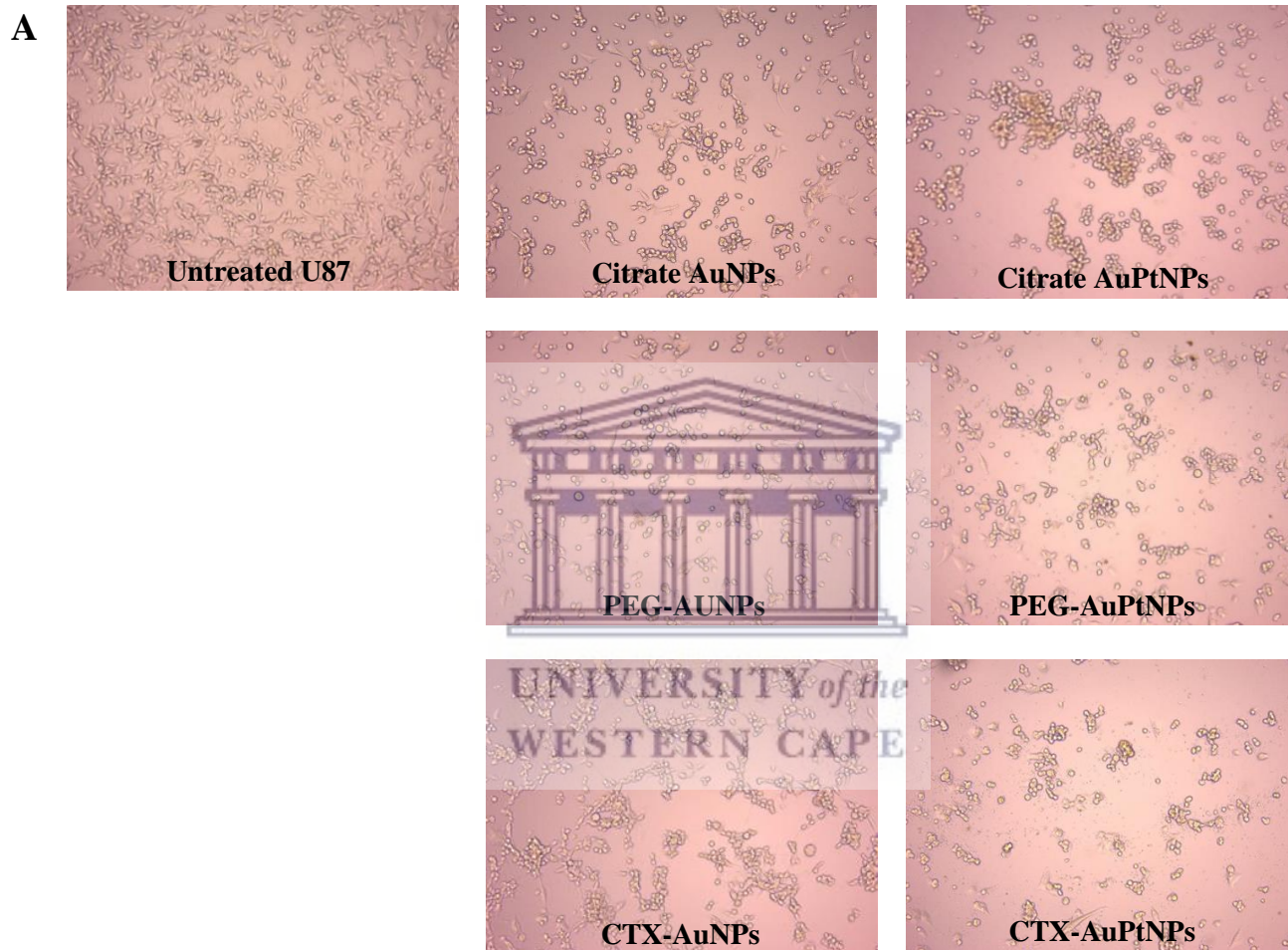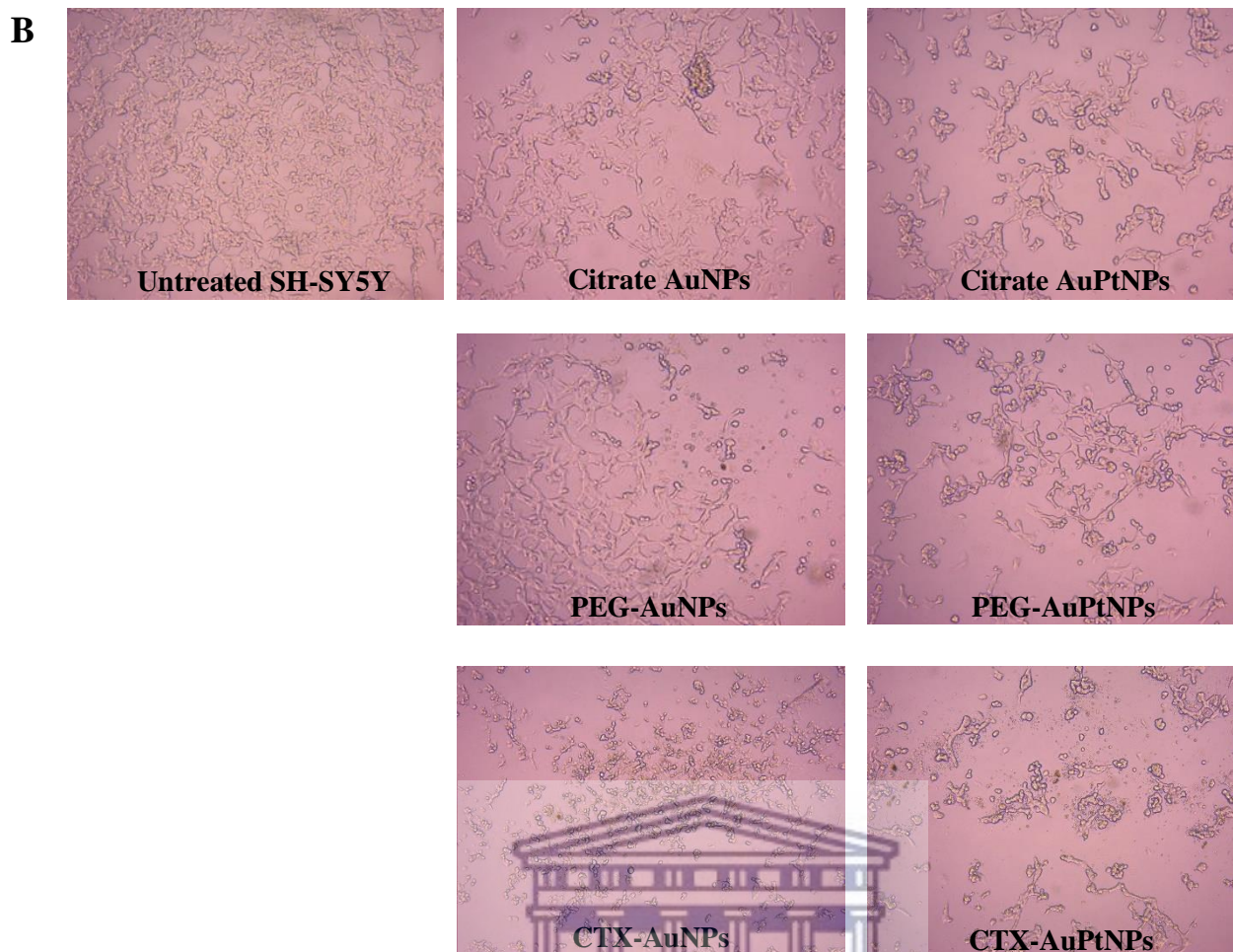
Figure 1. The morphological changes induced by nanoparticle treatment in U87 and SH-SY5Y cells. The effects of AuNPs; AuPtNPs; PEG-AuNPs; PEG-AuPtNPs; CTX-AuNPs and CTX-AuPtNPs on cell morphology as compared to untreated cells. U87 cells (A) and SH-SY5Y (B) cells were treated for 48 hours with 225 µg/ml of the different NPs. Images were acquired using a light microscope at 100X magnification.

2.3. CTX-AuPtNPs induced apoptosis in U87 cell line

One of the characteristics of aggressive GB and cancer in general is decreased sensitivity to apoptosis (Valdés-Rives *et al.*, 2017). Apoptosis is an essential mechanism by which the homeostatic balance between cell proliferation and cell death is maintained (Zhang *et al.*, 2018). During apoptosis, cells activate molecular pathways that results in cell death when they become damaged, and cellular mechanisms failed to repair this damage. This process can be achieved through the activation of one of two major molecular pathways, the extrinsic or the intrinsic pathway (Fulda and Debatin, 2006). Both pathways lead to the proteolytic activation caspases (Fulda and Debatin, 2006). These proteases

151

induce cell changes that include chromatin condensation, DNA fragmentation, membrane blebbing, and cell shrinkage (Zhang *et al.*, 2018). Caspase-independent cell death (CICD) occurs when a signal that normally induces apoptosis fails to activate caspases (Tait and Green, 2008). CICD often share common characteristics with apoptotic cell death, which includes upstream signalling pathways that are important for both forms of death such as mitochondrial outer membrane permeabilization (Tait and Green, 2008). Resistance to apoptosis is one of the main characteristics cancer cells acquire through genetic mutations and is considered to be an important target for therapeutic intervention (Pfeffer and Singh, 2018). The onset of the execution phase of apoptosis has been linked to the translocation of phosphatidylserine from the interior to the exterior surface of the cell membrane. Several bioassays, which include the Cell-APOPercentage™ assay (Biocolor Ltd.) has been developed to detect and quantify the translocation of phosphatidylserine during apoptosis. Based on the cell viability results, CTX-AuPtNPs are more cytotoxic than the other NPs and U87 cells are more sensitive to the effects of these NPs (Table 1). Consequently, this cell line was selected to further study cell death induced by CTX-AuPtNPs. To assess and quantify the induction of apoptosis in U87 cells treated for 48 hours with CTX-AuPtNPs at a concentration equivalent to the IC_{50} value (166 µg/ml). Figure 2 shows that this concentration of CTX-AuPtNPs induced apoptosis in U87 cells after 48 hours treatment. Tamoxifen was used as a positive control. Tamoxifen is a non-steroidal antiestrogen drug used extensively to treat ER^+ breast cancer and is known to induce apoptosis in various cancer cell lines including malignant glioma cells (Moodbidri and Shirsat, 2005; Li *et al.*, 2011, 2017; Rouhimoghadam *et al.*, 2018). CTX was previously reported as not potent enough to result in tumour cell apoptosis, therefore it is often investigated as a targeting molecule for GB (Kesavan *et al.*, 2010). In this study, the synergistic cytotoxic effects of Au and Pt in the bimetallic CTX-AuPtNPs resulted in increased cell death which was caused by the induction of apoptosis. This is supported by recent studies which investigated the toxicity of similar bimetallic NPs including AuPtNPs in human colon cancer, cervical cancer, lung cancer and breast cancer cell lines, and showed similar enhanced anti-cancer activity when compared to their mono-metallic NP counterparts (Ghosh *et al.*, 2015; Princely *et al.*, 2020; Chaturvedi *et al.*, 2021). A previous study showed that PtNPs inhibited cell growth and induced apoptosis in cervical cancer cells (Alshatwi, Athinarayanan and Vaiyapuri Subbarayan, 2015). PtNPs may induce apoptosis in a similar manner to platinum-based chemotherapeutic drugs such as cisplatin, carboplatin, and oxaliplatin (Kutwin *et al.*, 2017; Gurunathan *et al.*, 2020). In this study, we report for the first time on the induction of apoptosis by

small AuPtNPs (~ 5 nm) in U87 cells. Additionally, the presence of CTX on the NP surface also provided the CTX-AuPtNPs selective toxicity towards cells that express the receptors for CTX.
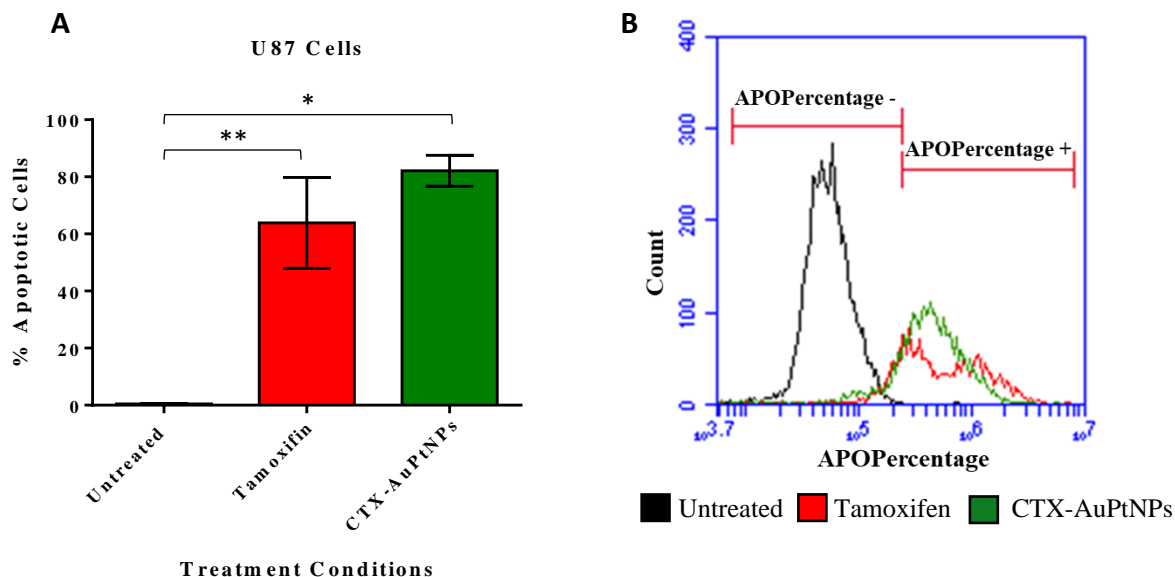
Figure 2. Apoptosis induced by CTX-AuPtNPs in U87 cells. The effects of CTX-AuPtNPs on the induction of apoptosis was investigated using the APOPercentage™ assay. U87 cells were treated for 48 hours with 166 µg/ml CTX-AuPtNPs (equivalent to IC_{50} value). Cells treated with 50 µM tamoxifen served as a positive control. Cells staining positive for apoptosis was quantified by flow cytometry. The experiment was repeated thrice. The bar graph in A shows a summary of three independent experiments and B shows representative overlayed histograms for each of the treatments and the untreated. Bars represent the mean ± SEM of triplicate experiments. Significance of difference is indicated with * ($P \leq 0.05$) and ** ($P \leq 0.01$).

2.4. CTX-AuPtNPs induced oxidative stress in U87 cell line

Reactive oxygen species (ROS) is essential for the regulation of physiological cellular functions through redox signalling and modulation of cellular redox balance (Milkovic *et al.*, 2019). Excessive production of ROS can be detrimental to cells and can lead to oxidative stress (Pizzino *et al.*, 2017). Oxidative stress is implicated in a wide variety of natural and pathological processes, including apoptosis (Sinha *et al.*, 2013). ROS destabilizes mitochondria and attack various cellular components including DNA, leading to the generation of oxidized and modified cellular components, and the eventual induction of p53 modulated apoptosis (Milkovic *et al.*, 2019). Increased ROS production is one of the mechanisms of some forms of conventional treatments and the inhibition of cancer cell

https://etd.uwc.ac.za/

proliferation (Kumari *et al.*, 2018). ROS generation, is one of the most frequently reported NP-associated toxicities (Manke, Wang and Rojanasakul, 2013; Horie and Tabei, 2021; Sani, Cao and Cui, 2021). Cellular internalization of NPs has been shown to activate immune cells including macrophages and neutrophils, contributing to ROS (Abdal Dayem *et al.*, 2017). Oxidative stress induced by NPs is reported to be dependent on various factors such as particle surface, size, composition, and presence of metals, while cellular responses such as mitochondrial respiration, NP cell interaction, and immune cell activation are responsible for ROS-mediated damage (Manke, Wang and Rojanasakul, 2013). NPs with smaller particle size are reported to induce higher ROS owing to their unique characteristics such as high surface to volume ratio and high surface charge (Manke, Wang and Rojanasakul, 2013; Kumari *et al.*, 2018). Since oxidative stress is a key determinant of NP-induced injury, it is necessary to characterize the ROS response resulting from NPs. Therefore, in this study, the production of ROS within U87 cells was measured using the CM-H$_2$DCFDA fluorogenic probe which permeates freely into cells and when its acetate groups are cleaved by intracellular esterases or oxidized by the presence of ROS to a highly fluorescent compound 2,7-dichlorofluorescin (DCF), which can be detected and quantified by flow cytometry or fluorescence microscopy.

In this study, we used the CM-H$_2$DCFDA fluorogenic probe/ ROS-sensitive dye to investigate the formation of intracellular ROS in U87 cells treated with CTX-AuPtNPs at the IC$_{50}$ value (166 µg/ml). Hydrogen peroxide (H$_2$O$_2$) was used as a positive control as it is a known model oxidant that induces oxidative stress in cells including glioma cells (Datta *et al.*, 2002; Berte *et al.*, 2016; Park, 2018). In Figure 3, treatment with CTX-AuPtNPs and H$_2$O$_2$ showed a significant increase in the production of ROS when compared to untreated cells. This suggested that upon NP treatment, ROS production may result from the generation of ROS inside the nucleus. These results match a similar study where Agarwal *et al.* (2019) observed ROS activity in U87 cells after treatment with CTX-conjugated morusin loaded PLGA NPs. Various other metal NPs report on the increased production of ROS in U87 cells following NP treatment (Ostrovsky *et al.*, 2009; Richard *et al.*, 2016; Kusaczuk *et al.*, 2018). ROS production in cells may be attributed to the synergistic effects of bimetallic AuPtNPs and the size of core NPs (~ 5 nm) as previously reported with similar NPs being able to quench ROS by cells (Manke, Wang and Rojanasakul, 2013; Kutwin *et al.*, 2017). Previous studies reported on the ROS scavenging activity of larger AuPtNPs which alleviated the doxorubicin induced oxidative stress damage in cells (Yang *et al.*, 2018), however this is the first report demonstrating the overproduction

154

of ROS in U87 cell line as a result of small AuPtNPs treatment. ROS generation in the untreated U87 cells could be due to the high mitotic index of the cells as described previously (Agarwal *et al.*, 2019). The experiment was conducted once and revealed highly comparable results, however more experiments are required. It is evident that these results raised the possibility that the ROS activity is due to cellular internalization of CTX-AuPtNPs, especially when considered with the accompanying bioassays mentioned in this paper.
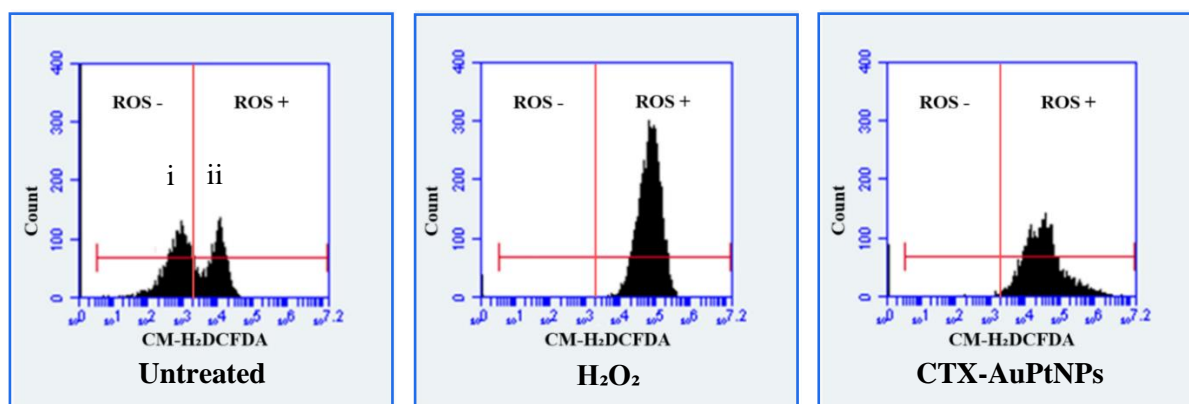
Figure 3. Oxidative stress induced by CTX-AuPtNPs in U87 cells. The effects of CTX-AuPtNPs on the production of intracellular ROS was investigated using the ROS-sensitive dye CM-H$_2$DCFDA. U87 cells were treated for 48 hours with 166 µg/ml CTX-AuPtNPs (equivalent to IC$_{50}$ value). Cells treated with 3 % H$_2$O$_2$ served as a positive control. Cells staining positive for ROS production were quantified by flow cytometry. The experiment was performed once in triplicates. Representative histograms show each of the treatments and the untreated. Vertical lines indicate that the population of cells after 10^3 were stained positive for intracellular ROS production. The Untreated histogram displays two distinguishable cell populations (i and ii), the population i shows negative fluorescence, while population ii shows positive fluorescence and therefore considered positive for ROS production.

2.5. CTX-AuPtNPs decreased mitochondrial membrane potential (Δψ) in U87 cell line

In this study, apoptosis has been implicated as a major mechanism of cell death possibly caused by NP-induced oxidative stress. Among the different apoptotic pathways, the intrinsic mitochondrial apoptotic pathway plays a major role in metal NP-induced cell death since mitochondria are one of the major target cell organelles for NP-induced oxidative stress (Abdal Dayem *et al.*, 2017). High levels of ROS in the mitochondria can result in damage to membrane phospholipids inducing

155

mitochondrial membrane depolarization (Manke, Wang and Rojanasakul, 2013). It has been reported previously that once NPs enter into the mitochondria, they stimulate ROS through impaired electron transport chain, structural damage, activation of nicotinamide adenine dinucleotide phosphate (NADPH)-like enzyme system, and depolarization of the mitochondrial membrane (Zorov, Juhaszova and Sollott, 2014). Tetramethyl rhodamine, ethyl ester (TMRE) is used to detect and quantify changes in mitochondrial membrane potential ($\Delta\psi$) in live cells by flow cytometry and fluorescence microscopy. TMRE is a positively charged, red orange, fluorescent dye that accumulates in active mitochondria due to their negative charge. Depolarized or inactive mitochondria have decreased mitochondrial membrane potential and fail to sequester TMRE (Rono and Oliver, 2020). In Figure 4, a significant decrease in the mitochondrial membrane potential can be observed after treatment with CTX-AuPtNP and the positive control carbonylcyanide-3-chlorophenylhydrazone (CCCP). CCCP is a protonophore and one of the commonly used mitochondrial uncoupling agents that increases the proton permeability across the mitochondrial inner membranes, thus dissipating the transmembrane potential and depolarizing the mitochondria (Zhang *et al.*, 2016; Allaway *et al.*, 2018). Untreated cells and cells after treatment with CTX-AuPtNPs showed the % cells with depolarised mitochondria are 4.41 ± 0.82 % and 61.17 ± 8.62 %, respectively (Fig.4 A).

This study shows that the possible mechanism of increased toxicity of the CTX-AuPtNP in U87 cells is associated with increased oxidative stress, mitochondrial depolarisation, and the eventual induction of apoptosis (Figure 5, pg. 158). These results support observations from previous studies, whereby an increase in mitochondrial depolarization was observed after treatment with various AuNPs based on sizes (Song *et al.*, 2017a; Gallud *et al.*, 2019). A previous report showed that PtNPs had a high affinity to mitochondria and demonstrated that the lethal DNA damage of U87 cells induced apoptosis (Kutwin *et al.*, 2017). A previous study reported on mitochondrial-targeted multifunctional mesoporous AuPtNPs (> 20 nm) for dual-mode photodynamic and PTT of human breast cancer MCF-7 cells (Song *et al.*, 2017b), however, to the best of our knowledge this is the first report assessing the effects of small AuPtNPs (~ 5nm) on mitochondrial membrane potential in U87 cells.
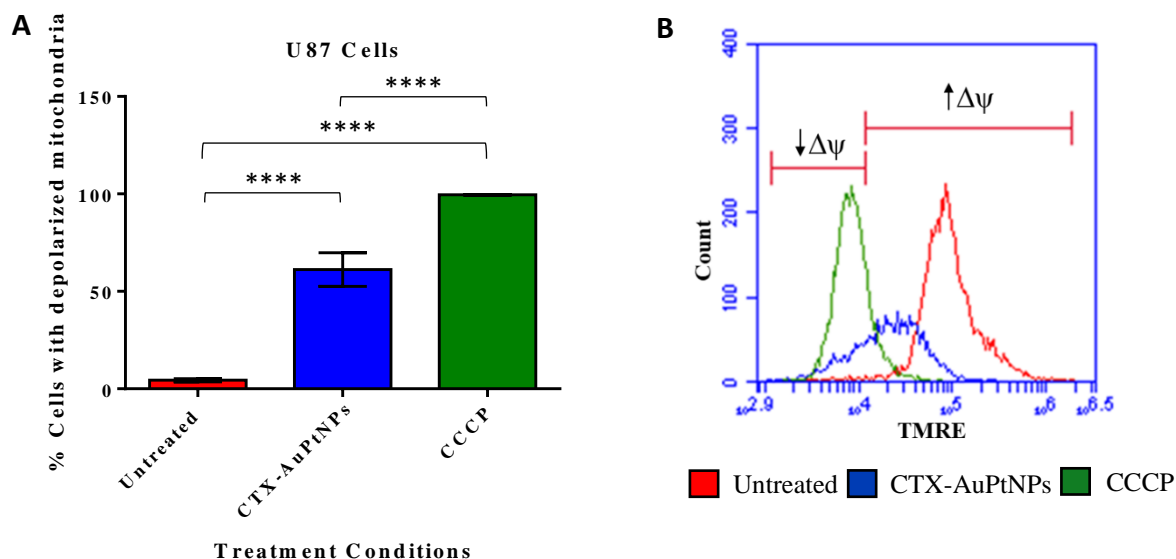
Figure 4. Effects of CTX-AuPtNP-treatment on mitochondrial function of U87 cells. U87 cells were treated for 48 hours with 166 µg/ml CTX-AuPtNPs (equivalent to IC_{50} value) and the mitochondrial membrane potential of the cells was assessed using the Tetramethylrhodamine, ethyl ester (TMRE) dye. Cells treated with 500 µM CCCP served as a positive control. Cell fluorescence was detected and quantified by flow cytometry. The experiment was repeated thrice. The bar graph in A shows a summary of three independent experiments and B shows representative histograms for each of the treatments and the untreated. Bars represent the mean ± SEM of triplicate experiments and significance of difference is indicated with **** ($P \leq 0.0001$).
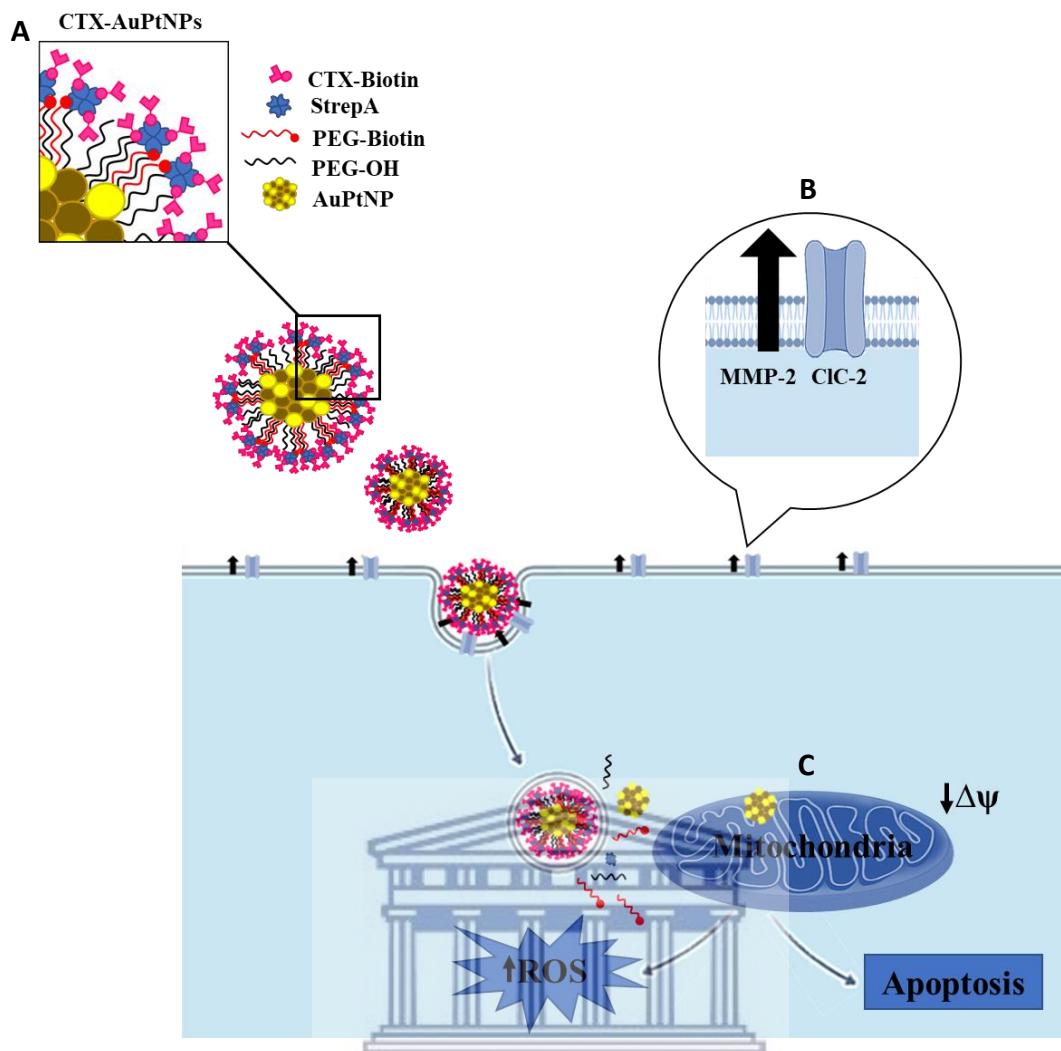
Figure 5. Schematic illustration of the possible mechanism of cell death induced by CTX-AuPtNPs in U87 cells. CTX-AuPtNPs consists of AuPtNP core, surface functionalized with PEG-OH and PEG-biotin and CTX is attached via streptavidin (A). CTX-AuPtNPs produced the anti-cancer activity in U87 cell lines possibly through receptor mediated endocytosis recognizing overexpressed MMP-2 and ClC-3 located on the same membrane domain (B) and induced apoptosis through possible elevation of ROS and decreased mitochondrial membrane potential (C) (image created with BioRender.com). Further investigations are required to fully understand the increase in ROS and specific pathways involved in apoptosis, as well as the binding of CTX-AuPtNPs to MMP-2 and ClC-3.

2.6. CTX-NPs inhibited colony formation and cell survival in U87 cell line

Clonogenicity can be described as a hallmark of malignant cell types and it is often evaluated using a clonogenic assay which measures the efficacy of novel compounds and anti-cancer products (Fiebig, Maier and Burger, 2004). It is often used to determine the reproductive capacity of cells to form colonies when cells are seeded in low densities after being exposed to an anti-cancer agent. A colony is considered as an aggregate of 50 cells (Franken *et al.*, 2006). To determine the effect of NPs on clonogenicity and cell survival, a clonogenic assay was performed for a 20-day period. Figure 6 A and B shows the inhibition in colony formation in U87 cells when treated with IC_{50} concentrations of citrate NPs and CTX-NPs (Table 1). The % colony area reported for U87 cells treated with IC_{50} concentrations of citrate AuNP (207 µg/ml) and citrate AuPtNPs (184 µg/ml) showed a significant decrease when compared to untreated cells (control) at 80.02 ± 4.41 % and 60.14 ± 5.60 % for citrate AuNPs and AuPtNPs respectively. When colony formation was quantified for CTX-AuNPs and CTX-AuPtNPs a significant decrease in the number of colonies was observed when compared to untreated cells and cells treated with citrate AuNPs and citrate AuPtNPs. The % colony area of U87 cells following treatment with IC_{50} concentrations of CTX-AuNPs (255 µg/ml) and CTX-AuPtNPs (166 µg/ml) was 11.07 ± 4.13 % and 3.19 ± 1.32 %, respectively. The near complete inhibition in colony formation with CTX-NPs could have been as a result of CTX blocking the receptors involved in cell migration on the surface of cells, this is further supported by the colony formation when compared to treatment with CTX-void NPs. Therefore, it is evident that the colony formation as well as cell survival is dependent on the NP type as CTX significantly prevented clonogenic survival. Our findings are consistent with our cell viability results. The results reported in this study are similar to previous reports for CTX and *Buthus martensii Karsch* chlorotoxin-like peptide (BmK CT) clonogenic assays inhibiting colony formation in cancer cells (Stephen *et al.*, 2014; Kievit *et al.*, 2017; Wu *et al.*, 2018; Wang *et al.*, 2021).

A

U87 Cells

% Colony Area Relative to Untreated

Nanoparticle Treatment

B Untreated   Citrate AuNPs   Citrate AuPtNPs   CTX-AuNPs   CTX-AuPtNPs
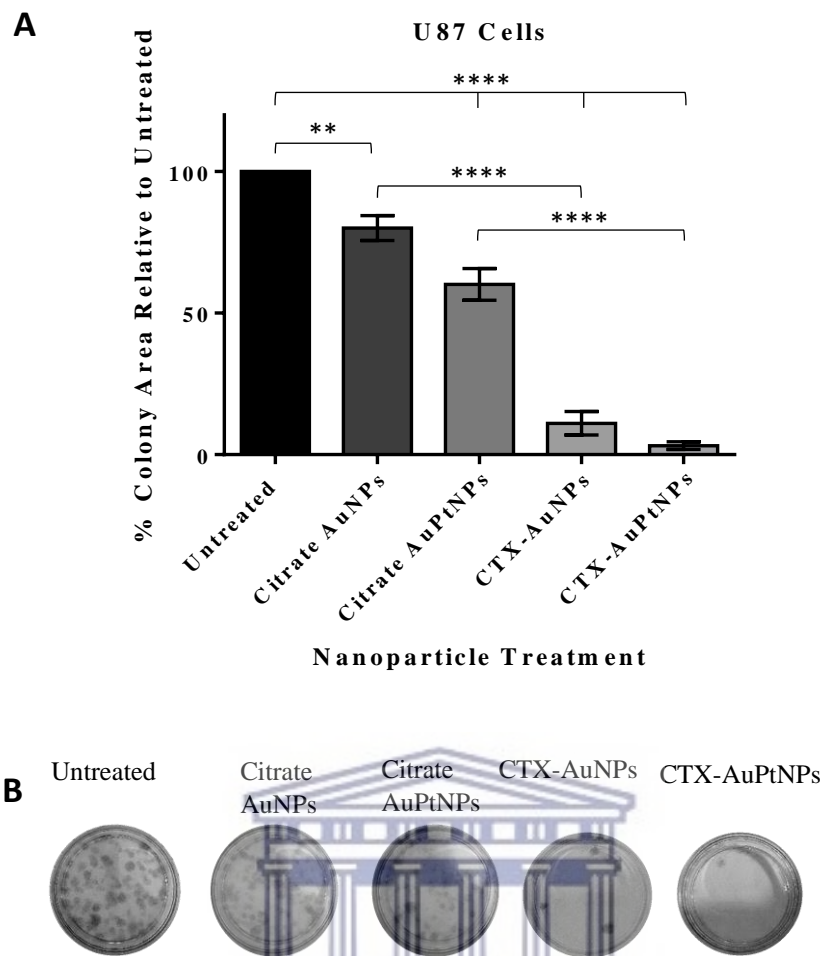
Figure 6. Inhibition of colony formation in U87 cells after treatment with citrate NPs and CTX-NPs. U87 cells were treated with citrate AuNPs, citrate AuPtNPs, CTX-AuNPs and CTX-AuPtNPs at concentrations equivalent to IC_{50} values and monitored for a period of 20 days to assess colony formation. The bar graph in A represents the % colony area relative to untreated cells (control). The experiment was repeated thrice. Bars represent the mean ± SEM of three independent experiments and B shows colony formation in representative culture plates. Significance of difference is indicated with **($P \le 0.01$) and ****($P \le 0.0001$).

2.7. CTX-NPs potential inhibitory effects on U87 cell migration

In addition to cell viability, cell migration is also an important factor for tumour enlargement. The identified molecular targets for CTX are all involved in malignant cell migration and invasion, including ClC-3 (Lui *et al.*, 2010), Annexin A2 (Kesavan *et al.*, 2010), and MMP-2 (Deshane, Garner and Sontheimer, 2003; Qin *et al.*, 2014). High levels of MMP-2 play a vital role in the virulent

160

progression of various cancers by contributing to angiogenesis, metastasis, and invasion (Quintero-Fabián *et al.*, 2019). ClC-3 is important in cellular movements during cell migration in glioma cells (Habela, Olsen and Sontheimer, 2008). CTX is known to inhibit tumour cell migration and invasion through mechanisms that may involve multiple pathways (Kasai *et al.*, 2012; Ojeda, Wang and Craik, 2016; El-Ghlban *et al.*, 2014; Dastpeyman *et al.*, 2019). In glioma cells MMP-2 and ClC-3 form a protein complex located in the same membrane domain which is targeted by CTX and could potentially inhibit cell invasion by induction of the endocytosis of the MMP-2/ClC-3 protein complex (Deshane, Garner and Sontheimer, 2003; Qin *et al.*, 2014).

In our previous study (Chapter 3) we demonstrated that CTX binds to U87 cells. Therefore, a wound healing assay using U87, was performed to investigate the anti-migratory properties of the CTX-NPs. This was evaluated by means of an *in vitro* wound healing assay using a scratch-wound model. Figure 7 indicates that CTX-NPs significantly inhibited the closure of the wounds in U87 cells. After 48 hours, the % wound closure was found to be 100 % for the untreated U87 cells, while CTX-AuNPs and CTX-AuPtNPs inhibited wound closure by 44.23 ± 1.81 % and 22.24.74 ± 0.35 %, respectively (Fig.6 A and B).

Based on these results, CTX-NPs inhibited U87 cell migration, with CTX-AuPtNPs displaying a slightly more efficient inhibitory effect than CTX-AuNPs in both cell lines. The results are consistent with previous studies demonstrating the inhibitory properties of CTX and CTX-like peptides on cell migration and invasion in glioma cell lines (Deshane, Garner and Sontheimer, 2003; McFerrin and Sontheimer, 2006; Kesavan *et al.*, 2010; Rjeibi *et al.*, 2011; Qin *et al.*, 2014; Wu *et al.*, 2018; Dastpeyman *et al.*, 2019). The results reported in this study agree with the clonogenic assay results and the possibility that CTX-NPs inhibits U87 cell migration through the MMP-2/ClC-3 protein complex or A2 interaction or both. Therefore, more experiments to investigate the expression levels of proteins that are related to cell migration in this cell line are required to confirm the precise mechanism of inhibition of CTX-NPs. In addition, the assessment of CTX-void NPs (citrate AuNPs, citrate AuPtNPs, PEG-AuNPs and PEG-AuPtNPs) also need to be investiagted for wound healing to conclusively report on the inhitory effects observed for CTX-NPs in this study.
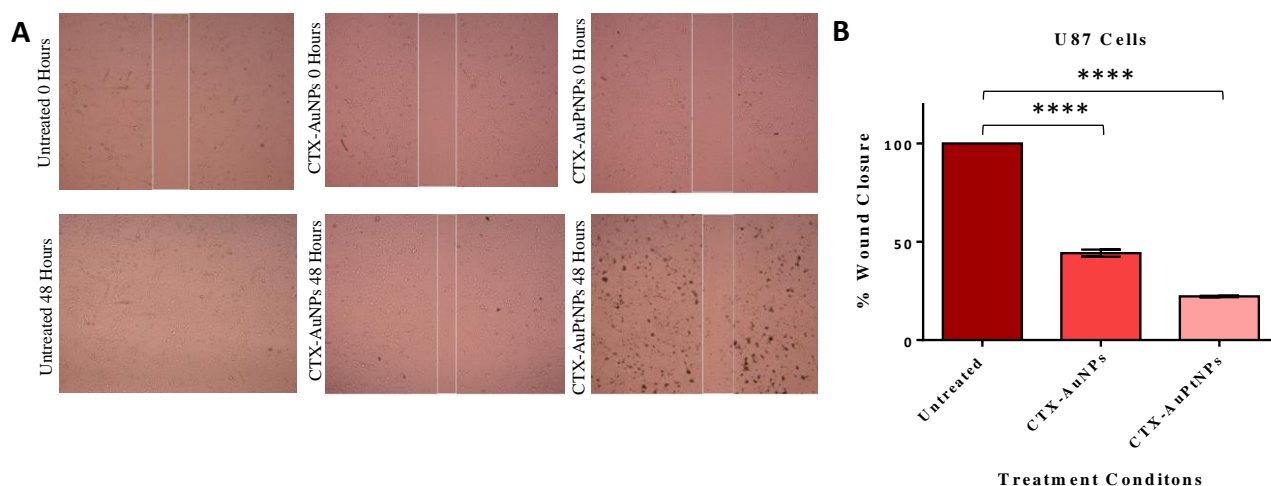
Figure 7. Inhibition of cell migration in U87 cells after treatment with CTX-NPs. Cell migratory effects in U87 cells at 0 and 48-hour treatments with concentrations equivalent to IC_{50} values of CTX-AuNPs and CTX-AuPtNPs was investigated using a wound healing assay. After 24 hours of allowing the cells to reach a confluent monolayer, the cells were wounded with a scratch and incubated in the absence or presence of CTX-NPs for 48 hours. Images were acquired using the light microscope using a 4x/0.10 objective. Figure 7 A show images in representative culture plates for each of the treatments and the untreated for U87 cells. The bar graph in B represent the % wound closure in U87 cells after 48 hours treatment with CTX-AuNPs and CTX-AuPtNPs. Data is represented as mean ± SEM and significance of difference is indicated with **** ($P \leq 0.0001$).

3. Materials and Methods

3.1. Biological assays, chemicals, and reagents

The cell proliferation reagent WST-1 was acquired from Sigma (Roche, United Kingdom). The APOPercentage Assay was acquired from Biocolor Ltd. (Carrickfergus, Ireland); the Tetramethylrhodamine, ethyl ester (TMRE) and 5- (and 6) -chloromethyl-20,70-dichlorofluorescein diacetate acetyl ester (CM-H2DCFDA) from the Reactive Oxygen Species (ROS) Detection Reagents Kit was acquired from Molecular Probes (Invitrogen, Oregon, United States of America). Dulbecco's Modified Eagle's Medium (DMEM), Foetal Bovine Serum (FBS), Phosphate Buffered Saline solution (PBS) and Penicillin-Streptomycin solution was obtained from Gibco, Life Technologies Corporation (Paisley, United Kingdom). Penicillin and 100 µg/ml streptomycin and 0.25 % trypsin EDTA were acquired from Lonza Group Ltd. (Verviers, Belgium). Dimethyl sulfoxide (DMSO),

crystal violet, tamoxifen and carbonylcyanide-3-chlorophenylhydrazone (CCCP) were obtained from Sigma-Aldrich (St. Louis, Missouri, United States of America). Hydrogen peroxide (H_2O_2) (30 % m/v) was acquired from AnalaR NORMAPUR® (England, United Kingdom), methanol and glacial acetic acid solution was obtained from Kimix Chemical & Laboratory Suppliers cc (Cape Town, South Africa). All plasticware including sterile cell culture grade 96-well plates and 6-well plates was acquired from Bio-Smart Scientific (Cape Town, South Africa).

3.2.   Nanoparticle synthesis and characterization

The preparation, purification and characterization of NPs was performed at the University of the Western Cape as previously described (Chapter 3). The preparation of stock concentrations of NPs to prepare working concentrations was also previously described (Chapter 3).

3.3.   Cell culture and maintenance

The U87 human malignant glioblastoma cells and SH-SY5Y human neuroblastoma cells was a generous donation from Professor Sharon Prince, Department of Human Biology and Blackburn Laboratory, respectively from the University of Cape Town, South Africa. The KMST-6 human non-cancer skin fibroblast cells was kindly donated by Professor Denver Hendricks, Department of Clinical and Laboratory Medicine, University of Cape Town, South Africa. U87, SH-SY5Y and KMST-6 cells were cultured in Dulbecco Modified Eagles Medium (DMEM) supplemented with 10 % foetal bovine serum (FBS) and 1 % 100 U/ml penicillin and 100 µg/ml streptomycin. Cells were grown in a humidified incubator at 37 °C with 5 % CO_2. The cell growth media (DMEM) was replaced every 2-3 days. Sub-culturing of cells occurred when cells reached 80 % confluency. The cells were washed with PBS and removed from the culture plates using a solution of 0.25 % trypsin EDTA.

3.4.   Cytotoxicity assay and determination of IC$_{50}$ values

The cell viability test was performed using the WST-1 assay (Cell Proliferation Reagent, Roche, United Kingdom), as per the manufacturer's instructions and as described previously (Thovhogi *et al.*, 2015; Galow and Gimsa, 2017; Sibuyi *et al.*, 2017). To determine the effects of the NPs on the viability of U87, SH-SY5Y and KMST-6 cells. Briefly, SH-SY5Y cells (5×10^3 cells/well); U87 cells

163

and KMST-6 cells (6 x 10³ cells/ well) were seeded in 96-well cell culture plates and left 24 hours for attachment in an incubator with a humidified atmosphere of 5 % CO_2 at 37 ⁰C. Thereafter, cells were treated with 100 µl of DMEM or 100 µl of increasing concentrations (75 µg/ml, 150 µg/ml, 225 µg/ml and 300 µg/ml) of citrate AuNPs, citrate AuPtNPs, PEG-AuNPs, PEG-AuPtNPs, CTX-AuNPs or CTX-AuPtNPs. The NPs were prepared in supplemented DMEM; untreated wells (negative control) were replaced with 100 µl fresh DMEM without NPs and 3 % DMSO (Sigma-Aldrich, St Louis, Missouri, USA) was used as a positive control (data not shown) and the plates were placed in the incubator for 48 hours. Thereafter, all wells were replaced with 100 µl DMEM and 10 µl of WST-1 was added to each well and further incubated for 4 hours. For NP interference test, an interference control was also performed as previously described, where cells treated with increasing concentrations of all NPs were left without the WST-1 dye (Thovhogi *et al.*, 2015; van der Zande *et al.*, 2016; Sibuyi *et al.*, 2017; Majoumouo *et al.*, 2020). The absorbance was measured using a BMG Labtech Omega® POLARStar multimodal plate reader (BMG, LABTECH, Germany) at 450 nm (620 nm was used as a reference wavelength and subtracted). Cell viability was calculated and expressed as a percentage of untreated cells using the optical density (OD) obtained, where % viability = OD treated - OD blank/ OD untreated - OD blank X 100 as previously reported (Thovhogi *et al.*, 2015; van der Zande *et al.*, 2016; Sibuyi *et al.*, 2017). The concentration of the NPs that will decrease 50 % of cell viability, the half maximal inhibitory concentration (IC_{50}), was generated using GraphPad Prism 6 (GraphPad software, San Diego, California, United States of America) as previously reported (Bézivin *et al.*, 2003; Al-Qubaisi *et al.*, 2011; Aboyewa *et al.*, 2021; Wusu *et al.*, 2021). All experiments were performed in triplicate wells and repeated thrice.

3.5.   Assessing changes in cell morphology

U87 cells (6 x 10³ cells/well) and SH-SY5Y cells (5 x 10³ cells/ well) were seeded in 96-well cell culture plates and left 24 hours for attachment in an incubator with a humidified atmosphere of 5 % CO_2 at 37 ⁰C. Thereafter, cells were treated with increasing concentrations (75 µg/ml, 150 µg/ml, 225 µg/ml and 300 µg/ml) of citrate AuNPs, citrate AuPtNPs, PEG-AuNPs, PEG-AuPtNPs, CTX-AuNPs or CTX-AuPtNPs. The NPs were prepared in supplemented DMEM; untreated wells were replaced with 100 µl fresh DMEM and the plates were placed in the incubator for 48 hours. Following 48 hours of treatment, changes in cell morphology for the various treatment conditions were observed using the Carl Zeiss Primo Vert Model 370 Inverted Microscope with (Carl Zeiss Microscopy GmbH,

164

Gottingen, Germany) 10X objective lens. Images were captured using the Zeiss software version 2.3. Experiments were performed once in triplicate wells.

3.6. The Cell-APOPercentage™ apoptosis assay

The Cell-APOPercentage™ apoptosis assay (Biocolor Ltd., Carrickfergus, Ireland) was used to quantify apoptosis in cell cultures treated with NPs, following protocols described previously with a few modifications (Meyer *et al.*, 2008; Sibuyi *et al.*, 2017). U87 cells were seeded at a density of 1.75 $\times 10^5$ cells per well in 6-well plates and placed in an incubator with a humidified atmosphere of 5 % CO_2 at 37 ⁰C for 24 hours to form a cell monolayer. After 24 hours, culture medium was gently aspirated and treated with either 2 ml of supplemented DMEM for untreated or IC_{50} concentration (166 µg/ml) of CTX-AuPtNPs for 48 hours. Tamoxifen (Sigma-Aldrich, St. Louis, Missouri, United States of America) (50 µM) was used as a positive control for 24 hours treatment. Following treatment, floating cells in each respective treatment were transferred to 15 ml centrifuge tubes and the adherent cells were gently trypsinized using 0.25 % EDTA trypsin (Lonza Group Ltd., Verviers, Belgium) and DMEM was used to deactivate the trypsin and cells were added to the respective tubes containing floating cells. The cells were centrifuged at 3,500 rpm for 5 minutes using a DLAB DM0412 centrifuge with a A12-10P, A6-50P rotor type (DLAB Scientific Inc., California, United States of America) and the supernatant was discarded to obtain a cell pellet. Cell pellets were resuspended in 200 µl diluted Cell-APOPercentage™ dye and allowed to incubate for 30 min in a humidified incubator at 37 °C with 5 % CO_2. The Cell-APOPercentage™ dye was diluted in DMEM 1:160 (v/v) as a final concentration to resuspend pellets. After incubation, the cells were washed with 4 ml of PBS (Gibco, Life Technologies Corporation, Paisley, United Kingdom), centrifuged at 3,500 rpm for 5 minutes and the supernatant was discarded to obtain a cell pellet. The pellet was resuspended in 200 µl DMEM and transferred on ice and analysed by measuring fluorescence intensity on flow cytometry using BD Accuri™ C6 Flow Cytometer instrument (BD Biosciences, Erembodegem, Belgium) using detector FL-2 and BD Accuri C6 Plus Software to analyse results. A minimum of 10,000 cells per sample were acquired. All experiments were performed in triplicate wells and repeated thrice.

3.7. Assessing oxidative stress using the Reactive Oxygen Species (ROS) Detection Reagents Kit

The production of intracellular ROS was evaluated using the fluorogenic molecular probe 5-(and 6)-chloromethyl-20,70-dichlorofluorescein diacetate acetyl ester (CM-H$_2$DCFDA) (Molecular probes, Invitrogen, Oregon, United States of America) and analysed by flow cytometry as previously described with modifications (Badmus *et al.*, 2020). U87 cells were seeded at a density of 1.75×10^5 cells per well in 6-well plates and incubated in an incubator with a humidified atmosphere of 5 % CO$_2$ at 37 ⁰C for 24 hours to form a cell monolayer. Following 24 hours, culture medium was gently aspirated and treated with either 2 ml of supplemented DMEM for the untreated or IC$_{50}$ concentration (166 µg/ml) of CTX-AuPtNPs for 48 hours. Cells treated for 1 hour with hydrogen peroxide (AnalaR NORMAPUR®, England, United Kingdom) (3 %) was used as a positive control. After treatment, floating cells in each respective treatment were transferred to 15 ml centrifuge tubes and the adherent cells were gently trypsinized using 0.25 % EDTA trypsin. The cells were centrifuged using a DLAB DM0412 centrifuge with a A12-10P, A6-50P rotor type at 3,500 rpm for 5 min and the supernatant was discarded to obtain a cell pellet. Cell pellets were resuspended in complete 200 µl PBS containing CM-H$_2$DCFDA prepared to a final concentration of 7.5 µM. Samples were incubated for 30 minutes in a humidified incubator at 37 °C with 5 % CO$_2$. Cells were washed with 4 ml of PBS, and the samples were centrifuged at 3,500 rpm for 5 minutes. The supernatant was discarded, and the cell pellets were collected. The cell pellets were resuspended in 200 µl PBS and transferred on ice and analysed by measuring fluorescence intensity on flow cytometry using BD Accuri™ C6 Flow Cytometer instrument (BD Biosciences, Erembodegem, Belgium) using detector FL-2 and BD Accuri C6 Plus Software to analyse results. A minimum of 10,000 cells per sample were acquired. Experiments were performed once in triplicate wells.

3.8. Assessing mitochondrial membrane potential (Δψ) using TMRE assay

For detection of changes in the mitochondrial membrane potential TMRE assay (Molecular Probes, Invitrogen, Oregon, United States of America) was used as previously reported with modifications (Reuther *et al.*, 2014; Alimoradi *et al.*, 2018). U87 cells were seeded at a density of 1.75×10^5 cells per well in 6-well plates and incubated in an incubator with a humidified atmosphere of 5 % CO$_2$ at 37 ⁰C for 24 hours to form a cell monolayer. After 24 hours, culture medium was gently aspirated and

166

treated with either 2 ml of supplemented DMEM for untreated or IC_{50} concentration (166 µg/ml) of CTX-AuPtNPs for 48 hours. Carbonyl cyanide m-chlorophenyl hydrazone (CCCP) (Sigma-Aldrich, St. Louis, Missouri, United States of America) (500 µM) was used as a positive control for 1 hour treatment. Following treatment, floating cells in each respective treatment well were transferred to 15 ml centrifuge tubes and the adherent cells were gently trypsinized using 0.25 % EDTA trypsin and added to the respective tubes containing floating cells. The cells were centrifuged at 3,500 rpm using a DLAB DM0412 centrifuge with a A12-10P, A6-50P rotor type for 5 minutes and the supernatant was discarded to obtain a cell pellet. Cell pellets were resuspended in 200 µl of DMEM containing tetramethyl rhodamine, ethyl ester (TMRE) dye prepared to a final concentration of 100 nM and allowed to incubate for 30 minutes in a humidified incubator at 37 °C with 5 % CO_2. After the incubation, the cells were washed with 4 ml of PBS, centrifuged at 3,500 rpm for 5 minutes and the supernatant was removed to obtain a cell pellet. The collected cell pellet was resuspended in 200 µl DMEM and transferred on ice and analysed by measuring fluorescence intensity on flow cytometry using BD Accuri™ C6 Flow Cytometer instrument (BD Biosciences, Erembodegem, Belgium) using detector FL-2 and BD Accuri C6 Plus Software to analyse results. A minimum of 10,000 cells per sample were acquired. All experiments were performed in triplicate wells and repeated thrice.

3.9. Assessing cell survival using clonogenic assay

Clonogenic assay was conducted to investigate the effect of NPs on cell proliferation and survival as previously described (Omoruyi, Enogieru and Ekpo, 2019). Briefly, U87 cells were seeded at a density of 1.75×10^5 cells per dish in 60 mm cell culture dishes and left for 24 hours for attachment in a humidified incubator at 37 °C with 5 % CO_2. Thereafter, growth medium in untreated (control) dishes were replaced with fresh DMEM, while the experimental plates were treated for 48 hours with citrate AuNPs, citrate AuPtNPs, CTX-AuNPs or CTX-AuPtNPs using concentrations equivalent to IC_{50} concentrations (Table 1). Following the treatment, cells were collected by trypsinization, counted and re-plated in 35 mm cell culture dishes at a density of 5×10^2 cells per dish. The cells were then incubated in a humidified incubator at 37 °C with 5 % CO_2 for 20 days with routine media changes to allow for colony formation. After 20 days had passed, colonies were washed twice with PBS, fixed with methanol and glacial acetic acid solution (3:1) (Kimix Chemical & Laboratory Suppliers cc, Cape Town, South Africa) for 15 minutes, washed twice with PBS again and stained with 0.5 % crystal violet stain (Sigma-Aldrich, St. Louis, Missouri, United States of America) for another 15

minutes. The dishes were washed with PBS and immersed in double distilled water for further washing, then left to air dry. Images of the dishes were acquired and areas covered by colonies were calculated using Image J software and expressed as a percentage of untreated control which was set to a hundred percent as previously reported (Omoruyi, Enogieru and Ekpo, 2019). All experiments were performed in triplicate wells and repeated thrice.

3.10. *In vitro* wound healing assay

In order to assess the inhibition of cell migration after treatment with CTX-NPs, a wound healing assay was performed as previously described (Wu *et al.*, 2018; Wang *et al.*, 2019). Briefly, U87 cells (1.5×10^5 cells per well) were grown onto 24-well plates for 24 hours in a humidified incubator at 37 °C with 5 % CO_2. A scratch was performed within the cell monolayer using a sterile 200 µl pipette. The cells were gently washed once with PBS to remove non-adherent cells and then treated with either 1 ml of DMEM or 1 ml of the CTX-NPs using concentrations equivalent to IC_{50} concentrations (Table 1) prepared in DMEM and placed back into the incubator for 48 hours. Images were captured using a Carl Zeiss Primo Vert Model 370 Inverted Microscope (Carl Zeiss Microscopy GmbH, Gottingen, Germany) at 0 hours and 48 hours using a 4x/0.10 objective. Cell migration was assessed by measuring the size of the gaps with image J as previously reported (Wu *et al.*, 2018) and bar graphs was constructed using GraphPad Prism 6. The experiment was performed once in triplicates wells.

4) Statistical analysis

Data generated from this study are expressed as mean ± standard error of mean (SEM) of three independent experiments and analysed using the GraphPad Prism 6 (GraphPad Software, San Diego, California, United States of America). Significance of difference was determined using one-way analysis of variance (ANOVA) with the level of significance denoted with an asterisk(s): * ($P \leq 0.05$); ** ($P \leq 0.01$); ***($P \leq 0.001$) and **** ($P \leq 0.0001$) and no * denotes no significance of differences ($P > 0.05$).

5) Conclusion

It can be concluded that all 6 NP systems (AuNPs, AuPtNPs, PEG-AuNPs, PEG-AuPtNPs, CTX-AuNPs and CTX-AuPtNPs) that was investigated in this study have inherent toxicity towards the 3

cell lines (U87, SH-SY5Y and KMST-6) that were selected for this study. The NPs demonstrated differential toxicity, with U87 cells being more susceptible to the effects of the NPs. The bimetallic NP, CTX-AuPtNPs demonstrated higher cytotoxicity than the other NPs in cancer cell lines, including CTX-AuNPs. This cytotoxicity can be associated with the induction of oxidative stress, increased mitochondrial depolarization and the induction of apoptosis. CTX-AuPtNPs also demonstrated increased and possibly selective toxicity towards the cancerous cell lines (U87 and SH-SY5Y), with minimal effect on the non-cancerous KMST-6 cell line. This apparent cytocompatibility observed with the non-cancerous cell line KMST-6 highlights the safety profile of CTX-AuPtNPs. It is known that U87 and SH-SY5Y cells express cell surface receptors for CTX and that CTX-AuPtNPs can be targeted to these cells. The high inherent toxicity of CTX-AuPtNPs at low concentrations, bodes well for the future RF-induced hyperthermia applications of these CTX conjugated NPs for the treatment of brain tumours. Findings obtained from this study demonstrated targeting and synergistic effects of combined noble metals in CTX-AuPtNPs for anti-cancer applications with the potential to be investigated for non-invasive RF field-induced targeted hyperthermia and may provide new hope for the management of NS tumours.

6) Future perspective

The potential of targeted CTX-NPs for brain cancer treatment is immense, and a variety of systems have been developed and studied, with a few entering pre-clinical trials. However, target specific bimetallic NPs constructed of noble metals with a synergistic effect including the potential for hyperthermia treatment for brain tumours are not as common and relatively recent in neuroscience research. Thus, more studies are required to explain the synergistic effect of CTX-AuPtNPs *in vivo* and their potential use for RF-induced hyperthermia. Therefore, future studies will explore the non-invasive RF-induced targeted hyperthermia using CTX-AuPtNPs for glioblastoma *in vitro* and *in vivo*. In this study, KMST-6 was used as a non-cancerous cell line that does not overexpress the surface proteins targeted by CTX, however the evaluation of CTX-AuPtNPs in a non-cancerous cell line of the central nervous system such as Normal Human Astrocytes (NHA) will be conducted. Further experiments will be performed to fully understand the increase in oxidative stress and the mechanisms that may be involved in apoptotic cell death with treatment of CTX-AuPtNPs. Additionally, CTX targets a broad list of solid tumours and tumour cell lines of neuroectodermal

origin, therefore this work has the potential to be expanded for both CTX-AuNPs and CTX-AuPtNPs anti-cancer investigations in other cancers.

7) References

Abdal Dayem, A., Hossain, M.K., Lee, S.B., Kim, K., Saha, S.K., Yang, G.-M., Choi, H.Y. and Cho, S.-G. (2017). The Role of Reactive Oxygen Species (ROS) in the Biological Activities of Metallic Nanoparticles. *International Journal of Molecular Sciencemousins*, 18(1): 120.

Aboyewa, J.A., Sibuyi, N.R.S., Meyer, M. and Oguntibeju, O.O. (2021). Gold Nanoparticles Synthesized Using Extracts of Cyclopia intermedia, Commonly Known as Honeybush, Amplify the Cytotoxic Effects of Doxorubicin*Nanomaterials (Basel, Switzerland)*, 11(1): E132.

Adewale, O.B., Davids, H., Cairncross, L. and Roux, S. (2019). Toxicological Behavior of Gold Nanoparticles on Various Models: Influence of Physicochemical Properties and Other Factors. *International Journal of Toxicology*, 38(5): 357–384.

Agarwal, S., Mohamed, M.S., Mizuki, T., Maekawa, T. and Kumar, D.S. (2019). Chlorotoxin modified morusin–PLGA nanoparticles for targeted glioblastoma therapy. *Journal of Materials Chemistry B*, 7(39): 5896–5919.

Alimoradi, H., Greish, K., Barzegar-Fallah, A., Alshaibani, L and Pittalà, V. (2018). Nitric oxide-releasing nanoparticles improve doxorubicin anticancer activity. *International Journal of Nanomedicine*, 13: 7771–7787.

Allaway, R.J., Wood, M.D., Downey, S.L., Bouley, S.J., Traphagen, N.A., Wells, J.D., Batra, J., Melancon, S.N., Ringelberg, C., Seibel, W., Ratner, N. and Sanchez, Y. (2018). Exploiting mitochondrial and metabolic homeostasis as a vulnerability in NF1 deficient cells. *Oncotarget*, 9(22): 15860–15875.

Almeer, R.S., Ali, D., Alarifi, S., Alkahtani, S. and Almansour, M. (2018). Green Platinum Nanoparticles Interaction With HEK293 Cells: Cellular Toxicity, Apoptosis, and Genetic Damage. *Dose-Response*, 16(4): 1559325818807382.

Al-Qubaisi, M., Rozita, R., Yeap, S.-K., Omar, A.-R., Ali, A.-M. and Alitheen, N.B. (2011). Selective Cytotoxicity of Goniothalamin against Hepatoblastoma HepG2 Cells. *Molecules*, 16(4): 2944–2959.

Alshatwi, A.A., Athinarayanan, J. and Vaiyapuri Subbarayan, P. (2015). Green synthesis of platinum nanoparticles that induce cell death and G2/M-phase cell cycle arrest in human cervical cancer cells. *Journal of Materials Science. Materials in Medicine*, 26(1): 5330.

Badmus, J.A., Ekpo, O.E., Sharma, J.R., Sibuyi, N.R.S., Meyer, M., Hussein, A.A. and Hiss, D.C. (2020). An Insight into the Mechanism of Holamine- and Funtumine-Induced Cell Death in Cancer Cells. *Molecules (Basel, Switzerland)*, 25(23): E5716.

Bendale, Y., Bendale, V. and Paul, S. (2017). Evaluation of cytotoxic activity of platinum nanoparticles against normal and cancer cells and its anticancer potential through induction of apoptosis. *Integrative Medicine Research*, 6(2): 141–148.

Berte, N., Lokan, S., Eich, M., Kim, E. and Kaina, B. (2016). Artesunate enhances the therapeutic response of glioma cells to temozolomide by inhibition of homologous recombination and senescence. *Oncotarget*, 7(41): 67235–67250.

Bézivin, C., Tomasi, S., Lohézic-Le Dévéhat, F. and Boustie, J. (2003). Cytotoxic activity of some lichen extracts on murine and human cancer cell lines. *Phytomedicine: International Journal of Phytotherapy and Phytopharmacology*, 10(6–7): 499–503.

Bhamidipati, M. and Fabris, L. (2017). Multiparametric Assessment of Gold Nanoparticle Cytotoxicity in Cancerous and Healthy Cells: The Role of Size, Shape, and Surface Chemistry. *Bioconjugate Chemistry*, 28(2): 449–460.

Boomi, P., Poorani, G.P., Palanisamy, S., Selvam, S., Ramanathan, G., Ravikumar, S., Barabadi, H., Prabu, H.G., Jeyakanthan, J. and Saravanan, M. (2019). Evaluation of Antibacterial and Anticancer Potential of Polyaniline-Bimetal Nanocomposites Synthesized from Chemical Reduction Method. *Journal of Cluster Science*, 30(3): 715–726.

Bouzas, V., Haller, T., Hobi, N., Felder, E., Pastoriza-Santos, I. and Pérez-Gil, J. (2014). Nontoxic impact of PEG-coated gold nanospheres on functional pulmonary surfactant-secreting alveolar type II cells. *Nanotoxicology*, 8(8): 813–823.

Burster, T., Traut, R., Yermekkyzy, Z., Mayer, K., Westhoff, M.-A., Bischof, J. and Knippschild, U. (2021). Critical View of Novel Treatment Strategies for Glioblastoma: Failure and Success of Resistance Mechanisms by Glioblastoma Cells. *Frontiers in Cell and Developmental Biology*, 9: 2290.

Cathcart, J., Pulkoski-Gross, A. and Cao, J. (2015). Targeting matrix metalloproteinases in cancer: Bringing new life to old ideas. *Genes & Diseases*, 2(1): 26–34.

Chaturvedi, V.K., Yadav, N., Rai, N.K., Bohara, R.A., Rai, S.N., Aleya, L. and Singh, M.P. (2021). Two birds with one stone: oyster mushroom mediated bimetallic Au-Pt nanoparticles for agro-waste management and anticancer activity. *Environmental Science and Pollution Research International*, 28(11): 13761–13775.

Chen, L., Lin, L., Xian, N. and Zheng, Z. (2019). Annexin A2 regulates glioma cell proliferation through the STAT3-cyclin D1 pathway. *Oncology Reports*, 42(1): 399–413.

Cohen, G., Burks, S.R. and Frank, J.A. (2018). Chlorotoxin-A Multimodal Imaging Platform for Targeting Glioma Tumors. *Toxins*, 10(12): E496

Cohen-Inbar, O. and Zaaroor, M. (2016). Glioblastoma multiforme targeted therapy: The Chlorotoxin story. *Journal of Clinical Neuroscience: Official Journal of the Neurosurgical Society of Australasia*, 33: 52–58.

Coluccia, D., Figueiredo, C.A., Wu, M.Y., Riemenschneider, A.N., Diaz, R., Luck, A., Smith, C., Das, S., Ackerley, C., O'Reilly, M., Hynynen, K. and Rutka, J.T. (2018). Enhancing glioblastoma treatment using cisplatin-gold-nanoparticle conjugates and targeted delivery with magnetic resonance-guided focused ultrasound. *Nanomedicine: Nanotechnology, Biology, and Medicine*, 14(4): 1137–1148.

Coradeghini, R., Gioria, S., García, C.P., Nativo, P., Franchini, F., Gilliland, D., Ponti, J. and Rossi, F. (2013). Size-dependent toxicity and cell interaction mechanisms of gold nanoparticles on mouse fibroblasts. *Toxicology Letters*, 217(3): 205–216.

Corr, S.J., Cisneros, B.T., Green, L., Raoof, M. and Curley, S.A. (2013). Protocols for Assessing Radiofrequency Interactions with Gold Nanoparticles and Biological Systems for Non-invasive Hyperthermia Cancer Therapy. *JoVE (Journal of Visualized Experiments)*, (78): e50480.

Correard, F., Maximova, K., Estève, M.-A., Villard, C., Roy, M., Al-Kattan, A., Sentis, M., Gingras, M., Kabashin, A.V. and Braguer, D. (2014). Gold nanoparticles prepared by laser ablation in aqueous biocompatible solutions: assessment of safety and biological identity for nanomedicine applications. *International Journal of Nanomedicine*, 9: 5415–5430.

Dardevet, L., Rani, D., Abd El Aziz, T., Bazin, I., Sabatier, J.-M., Fadl, M., Brambilla, E. and De Waard, M. (2015). Chlorotoxin: A Helpful Natural Scorpion Peptide to Diagnose Glioma and Fight Tumor Invasion. *Toxins*, 7(4): 1079–1101.

Dastpeyman, M., Giacomin, P., Wilson, D., Nolan, M.J., Bansal, P.S. and Daly, N.L. (2019). A C-Terminal Fragment of Chlorotoxin Retains Bioactivity and Inhibits Cell Migration. *Frontiers in Pharmacology*, 10: 250.

Datta, K., Babbar, P., Srivastava, T., Sinha, S. and Chattopadhyay, P. (2002). p53 dependent apoptosis in glioma cell lines in response to hydrogen peroxide induced oxidative stress. *The International Journal of Biochemistry & Cell Biology*, 34(2): 148–157.

Depciuch, J., Stec, M., Klebowski, B., Baran, J. and Parlinska-Wojtan, M. (2019). Platinum–gold nanoraspberries as effective photosensitizer in anticancer photothermal therapy. *Journal of Nanobiotechnology*, 17(1): 107.

Deshane, J., Garner, C.C. and Sontheimer, H. (2003). Chlorotoxin Inhibits Glioma Cell Invasion via Matrix Metalloproteinase-2. *Journal of Biological Chemistry*, 278(6): 4135–4144.

Dong, L., Li, M., Zhang, S., Li, J., Shen, G., Tu, Y., Zhu, J. and Tao, J. (2015). Cytotoxicity of BSA-Stabilized Gold Nanoclusters: In Vitro and In Vivo Study. *Small (Weinheim an Der Bergstrasse, Germany)*, 11(21): 2571–2581.

El-Ghlban, S., Kasai, T., Shigehiro, T., Yin, H.X., Sekhar, S., Ida, M., Sanchez, A., Mizutani, A., Kudoh, T., Murakami, H. and Seno, M. (2014). Chlorotoxin-Fc Fusion Inhibits Release of MMP-2 from Pancreatic Cancer Cells. *BioMed Research International*, 2014: e152659.

Fathima, R. and Mujeeb, A. (2021). Enhanced nonlinear and thermo optical properties of laser synthesized surfactant-free Au-Pt bimetallic nanoparticles. *Journal of Molecular Liquids*, 343: 117711.

Ferraris, C., Cavalli, R., Panciani, P.P. and Battaglia, L. (2020). Overcoming the Blood-Brain Barrier: Successes and Challenges in Developing Nanoparticle-Mediated Drug Delivery Systems for the Treatment of Brain Tumours. *International Journal of Nanomedicine*, 15: 2999–3022.

Fiebig, H.H., Maier, A. and Burger, A.M. (2004). Clonogenic assay with established human tumour xenografts: correlation of in vitro to in vivo activity as a basis for anticancer drug discovery. *European Journal of Cancer (Oxford, England: 1990)*, 40(6): 802–820.

Formaggio, D.M.D., de Oliveira Neto, X.A., Rodrigues, L.D.A., de Andrade, V.M., Nunes, B.C., Lopes-Ferreira, M., Ferreira, F.G., Wachesk, C.C., Camargo, E.R., Conceição, K. and Tada, D.B. (2019). In vivo toxicity and antimicrobial activity of AuPt bimetallic nanoparticles. *Journal of Nanoparticle Research*, 21(11): 244.

Forsyth, P.A., Wong, H., Laing, T.D., Rewcastle, N.B., Morris, D.G., Muzik, H., Leco, K.J., Johnston, R.N., Brasher, P.M., Sutherland, G. and Edwards, D.R. (1999). Gelatinase-A (MMP-2), gelatinase-B (MMP-9) and membrane type matrix metalloproteinase-1 (MT1-MMP) are involved in different aspects of the pathophysiology of malignant gliomas. *British Journal of Cancer*, 79(11–12): 1828–1835.

Franken, N.A.P., Rodermond, H.M., Stap, J., Haveman, J. and van Bree, C. (2006). Clonogenic assay of cells in vitro. *Nature Protocols*, 1(5): 2315–2319.

Fulda, S. and Debatin, K.-M. (2006). Extrinsic versus intrinsic apoptosis pathways in anticancer chemotherapy. *Oncogene*, 25(34): 4798–4811.

Gallud, A., Klöditz, K., Ytterberg, J., Östberg, N., Katayama, S., Skoog, T., Gogvadze, V., Chen, Y.-Z., Xue, D., Moya, S., Ruiz, J., Astruc, D., Zubarev, R., Kere, J. and Fadeel, B. (2019). Cationic gold nanoparticles elicit mitochondrial dysfunction: a multi-omics study. *Scientific Reports*, 9(1): 4366.

Galow, A.-M. and Gimsa, J. (2017). WST-assay data reveal a pH dependence of the mitochondrial succinate reductase in osteoblast-like cells. *Data in Brief*, 12: 442–446.

Ghosh, S., Nitnavare, R., Dewle, A., Tomar, G.B., Chippalkatti, R., More, P., Kitture, R., Kale, S., Bellare, J. and Chopade, B.A. (2015). Novel platinum-palladium bimetallic nanoparticles synthesized by Dioscorea bulbifera: anticancer and antioxidant activities. *International Journal of Nanomedicine*, 10: 7477–7490.

Griffin, M., Khan, R., Basu, S. and Smith, S. (2020). Ion Channels as Therapeutic Targets in High Grade Gliomas. *Cancers*, 12(10): 3068.

Gurunathan, S., Jeyaraj, M., Kang, M.-H. and Kim, J.-H. (2020). Anticancer Properties of Platinum Nanoparticles and Retinoic Acid: Combination Therapy for the Treatment of Human Neuroblastoma Cancer. *International Journal of Molecular Sciences*, 21(18): E6792.

Habela, C.W., Olsen, M.L. and Sontheimer, H. (2008). ClC3 is a critical regulator of the cell cycle in normal and malignant glial cells. *The Journal of Neuroscience: The Official Journal of the Society for Neuroscience*, 28(37): 9205–9217.

Hall, M.K., Whitman, A.A., Weidner, D.A. and Schwalbe, R.A. (2020). Knockdown of N-Acetylglucosaminyltransferase-II Reduces Matrix Metalloproteinase 2 Activity and Suppresses Tumorigenicity in Neuroblastoma Cell Line. *Biology*, 9(4): 71.

Henderson, T.A. and Morries, L.D. (2015). Near-infrared photonic energy penetration: can infrared phototherapy effectively reach the human brain?. *Neuropsychiatric Disease and Treatment*, 11: 2191–2208.

Hoang Thi, T.T., Pilkington, E.H., Nguyen, D.H., Lee, J.S., Park, K.D. and Truong, N.P. (2020). The Importance of Poly(ethylene glycol) Alternatives for Overcoming PEG Immunogenicity in Drug Delivery and Bioconjugation. *Polymers*, 12(2): E298.

Horie, M. and Tabei, Y. (2021). Role of oxidative stress in nanoparticles toxicity. *Free Radical Research*, 55(4): 331–342.

Imperatore, R., Carotenuto, G., Di Grazia, M.A., Ferrandino, I., Palomba, L., Mariotti, R., Vitale, E., De Nicola, S., Longo, A. and Cristino, L. (2015). Imidazole-stabilized gold nanoparticles induce neuronal apoptosis: an in vitro and in vivo study. *Journal of Biomedical Materials Research. Part A*, 103(4): 1436–1446.

Jeyaraj, M., Gurunathan, S., Qasim, M., Kang, M.-H. and Kim, J.-H. (2019). A Comprehensive Review on the Synthesis, Characterization, and Biomedical Application of Platinum Nanoparticles. *Nanomaterials*, 9(12): 1719.

Jo, M.-R., Bae, S.-H., Go, M.-R., Kim, H.-J., Hwang, Y.-G. and Choi, S.-J. (2015). Toxicity and Biokinetics of Colloidal Gold Nanoparticles. *Nanomaterials*, 5(2): 835–850.

Kasai, T., Nakamura, K., Vaidyanath, A., Chen, L., Sekhar, S., El-Ghlban, S., Okada, M., Mizutani, A., Kudoh, T., Murakami, H. and Seno, M. (2012). Chlorotoxin Fused to IgG-Fc Inhibits Glioblastoma Cell Motility via Receptor-Mediated Endocytosis. *Journal of Drug Delivery*, 2012: 975763.

Kesavan, K., Ratliff, J., Johnson, E.W., Dahlberg, W., Asara, J.M., Misra, P., Frangioni, J.V. and Jacoby, D.B. (2010). Annexin A2 is a molecular target for TM601, a peptide with tumor-targeting and anti-angiogenic effects. *The Journal of Biological Chemistry*, 285(7): 4366–4374.

Kievit, F.M., Wang, K., Ozawa, T., Tarudji, A.W., Silber, J.R., Holland, E.C., Ellenbogen, R.G. and Zhang, M. (2017). Nanoparticle-mediated knockdown of DNA repair sensitizes cells to radiotherapy and extends survival in a genetic mouse model of glioblastoma. *Nanomedicine: Nanotechnology, Biology and Medicine*, 13(7): 2131–2139.

Kumari, S., Badana, A.K., G, M.M., G, S. and Malla, R. (2018). Reactive Oxygen Species: A Key Constituent in Cancer Survival. *Biomarker Insights*, 13: 1177271918755391.

Kusaczuk, M., Krętowski, R., Naumowicz, M., Stypułkowska, A. and Cechowska-Pasko, M. (2018). Silica nanoparticle-induced oxidative stress and mitochondrial damage is followed by activation of intrinsic apoptosis pathway in glioblastoma cells. *International Journal of Nanomedicine*, 13: 2279–2294.

Kutwin, M., Sawosz, E., Jaworski, S., Hinzmann, M., Wierzbicki, M., Hotowy, A., Grodzik, M., Winnicka, A. and Chwalibog, A. (2017). Investigation of platinum nanoparticle properties against U87 glioblastoma multiforme. *Archives of medical science: AMS*, 13(6): 1322–1334.

Lau, I.P., Chen, H., Wang, J., Ong, H.C., Leung, K.C.-F., Ho, H.P. and Kong, S.K. (2012). In vitro effect of CTAB- and PEG-coated gold nanorods on the induction of eryptosis/erythroptosis in human erythrocytes. *Nanotoxicology*, 6: 847–856.

Lee, H.J., Park, M.K., Bae, H.C., Yoon, H.J., Kim, S.Y. and Lee, C.H. (2012). Transglutaminase-2 Is Involved in All-Trans Retinoic Acid-Induced Invasion and Matrix Metalloproteinases Expression of SH-SY5Y Neuroblastoma Cells via NF-κB Pathway. *Biomolecules & Therapeutics*, 20(3): 286–292.

Li, C., Zhou, C., Wang, S., Feng, Y., Lin, W., Lin, S., Wang, Y., Huang, H., Liu, P., Mu, Y.-G. and Shen, X. (2011). Sensitization of Glioma Cells to Tamoxifen-Induced Apoptosis by Pl3-Kinase Inhibitor through the GSK-3β/β-Catenin Signaling Pathway. *PLoS ONE*, 6(10): e27053.

Li, W., Shi, X., Xu, Y., Wan, J., Wei, S. and Zhu, R. (2017). Tamoxifen promotes apoptosis and inhibits invasion in estrogen-positive breast cancer MCF-7 cells. *Molecular Medicine Reports*, 16(1): 478–484.

Li, X., Nie, S., Lv, Z., Ma, L., Song, Y., Hu, Z., Hu, X., Liu, Z., Zhou, G., Dai, Z., Song, T., Liu, J. and Wang, S. (2021). Overexpression of Annexin A2 promotes proliferation by forming a Glypican 1/c-Myc positive feedback loop: prognostic significance in human glioma. *Cell Death & Disease*, 12(3): 1–13.

Liang, H., Wu, Y., Ou, X.-Y., Li, J.-Y. and Li, J. (2017). Au@Pt nanoparticles as catalase mimics to attenuate tumor hypoxia and enhance immune cell-mediated cytotoxicity. *Nanotechnology*, 28(46): 465702.

Liu, M., Fang, X., Yang, Y. and Wang, C. (2021). Peptide-Enabled Targeted Delivery Systems for Therapeutic Applications. *Frontiers in Bioengineering and Biotechnology*, 9: 577.

Liu, X., Zhang, X., Zhu, M., Lin, G., Liu, J., Zhou, Z., Tian, X. and Pan, Y. (2017). PEGylated Au@Pt Nanodendrites as Novel Theranostic Agents for Computed Tomography Imaging and Photothermal/Radiation Synergistic Therapy. *ACS Applied Materials & Interfaces*, 9(1): 279–285.

Loan, T.T., Do, L.T. and Yoo, H. (2018). Platinum Nanoparticles Induce Apoptosis on Raw 264.7 Macrophage Cells. *Journal of Nanoscience and Nanotechnology*, 18(2): 861–864.

Lui, V.C.H., Lung, S.S.S., Pu, J.K.S., Hung, K.N. and Leung, G.K.K. (2010). Invasion of human glioma cells is regulated by multiple chloride channels including ClC-3. *Anticancer Research*, 30(11): 4515–4524.

Luo, D., Wang, X., Burda, C. and Basilion, J.P. (2021). Recent Development of Gold Nanoparticles as Contrast Agents for Cancer Diagnosis. *Cancers*, 13(8): 1825.

Lyons, S.A., O'Neal, J. and Sontheimer, H. (2002). Chlorotoxin, a scorpion-derived peptide, specifically binds to gliomas and tumors of neuroectodermal origin. *Glia*, 39(2): 162–173.

Ma, X., Hartmann, R., Jimenez de Aberasturi, D., Yang, F., Soenen, S.J.H., Manshian, B.B., Franz, J., Valdeperez, D., Pelaz, B., Feliu, N., Hampp, N., Riethmüller, C., Vieker, H., Frese, N., Gölzhäuser,

A., Simonich, M., Tanguay, R.L., Liang, X.-J. and Parak, W.J. (2017). Colloidal Gold Nanoparticles Induce Changes in Cellular and Subcellular Morphology. *ACS nano*, 11(8): 7807–7820.

Majoumouo, M.S., Sharma, J.R., Sibuyi, N.R.S., Tincho, M.B., Boyom, F.F. and Meyer, M. (2020). Synthesis of Biogenic Gold Nanoparticles from Terminalia mantaly Extracts and the Evaluation of Their In Vitro Cytotoxic Effects in Cancer Cells. *Molecules*, 25(19): 4469.

Manikandan, M., Hasan, N. and Wu, H.-F. (2013). Platinum nanoparticles for the photothermal treatment of Neuro 2A cancer cells. *Biomaterials*, 34(23): 5833–5842.

Manke, A., Wang, L. and Rojanasakul, Y. (2013). Mechanisms of nanoparticle-induced oxidative stress and toxicity. *BioMed Research International*, 2013: 942916.

Marchiq, I., Albrengues, J., Granja, S., Gaggioli, C., Pouysségur, J. and Simon, M.-P. (2015). Knock out of the BASIGIN/CD147 chaperone of lactate/H+ symporters disproves its pro-tumour action via extracellular matrix metalloproteases (MMPs) induction. *Oncotarget*, 6(28): 24636–24648.

Massard, C., Dubois, C., Raspal, V., Daumar, P., Sibaud, Y., Mounetou, E., Bamdad, M. and Awitor, O.K. (2017). Cytotoxicity Study of Gold Nanoparticles on the Basal-Like Triple-Negative HCC-1937 Breast Cancer Cell Line. *Journal of Biomaterials and Nanobiotechnology*, 9(1): 13–25.

McFerrin, M.B. and Sontheimer, H. (2006). A role for ion channels in glioma cell invasion. *Neuron Glia Biology*, 2(1): 39–49.

McGonigle, S., Majumder, U., Kolber-Simonds, D., Wu, J., Hart, A., Noland, T., TenDyke, K., Custar, D., Li, D., Du, H., Postema, M.H.D., Lai, W.G., Twine, N.C., Woodall-Jappe, M. and Nomoto, K. (2019). Neuropilin-1 drives tumor-specific uptake of chlorotoxin. *Cell communication and signaling: CCS*, 17(1): 67.

McNamara, K. and Tofail, S.A.M. (2015). Nanosystems: the use of nanoalloys, metallic, bimetallic, and magnetic nanoparticles in biomedical applications. *Physical Chemistry Chemical Physics*, 17(42): 27981–27995.

Meyer, M., Essack, M., Kanyanda, S. and Rees, J. (2008). A low-cost flow cytometric assay for the detection and quantification of apoptosis using an anionic halogenated fluorescein dye. *BioTechniques*, 45(3): 317–320.

Milkovic, L., Cipak Gasparovic, A., Cindric, M., Mouthuy, P.-A. and Zarkovic, N. (2019). Short Overview of ROS as Cell Function Regulators and Their Implications in Therapy Concepts. *Cells*, 8(8): E793.

Mishra, P., Ray, S., Sinha, S., Das, B., Khan, Md.I., Behera, S.K., Yun, S.-I., Tripathy, S.K. and Mishra, A. (2016). Facile bio-synthesis of gold nanoparticles by using extract of Hibiscus sabdariffa and evaluation of its cytotoxicity against U87 glioblastoma cells under hyperglycemic condition. *Biochemical Engineering Journal*, 105: 264–272.

Moodbidri, M.S. and Shirsat, N.V. (2005). Activated JNK brings about accelerated apoptosis of Bcl-2-overexpressing C6 glioma cells on treatment with tamoxifen. *Journal of Neurochemistry*, 92(1): 1–9.

Moore, T.L., Rodriguez-Lorenzo, L., Hirsch, V., Balog, S., Urban, D., Jud, C., Rothen-Rutishauser, B., Lattuada, M. and Petri-Fink, A. (2015). Nanoparticle colloidal stability in cell culture media and impact on cellular interactions. *Chemical Society Reviews*, 44(17): 6287–6305.

Moros, M., Idiago-López, J., Asín, L., Moreno-Antolín, E., Beola, L., Grazú, V., Fratila, R.M., Gutiérrez, L. and de la Fuente, J.M. (2019). Triggering antitumoural drug release and gene expression by magnetic hyperthermia. *Advanced Drug Delivery Reviews*, 138: 326–343.

Moros, M., Lewinska, A., Merola, F., Ferraro, P., Wnuk, M., Tino, A. and Tortiglione, C. (2020). Gold Nanorods and Nanoprisms Mediate Different Photothermal Cell Death Mechanisms In Vitro and In Vivo. *ACS applied materials & interfaces*, 12(12): 13718–13730.

Mukherjee, S., Kotcherlakota, R., Haque, S., Bhattacharya, D., Kumar, J.M., Chakravarty, S. and Patra, C.R. (2020). Improved delivery of doxorubicin using rationally designed PEGylated platinum nanoparticles for the treatment of melanoma. *Materials Science and Engineering: C*, 108: 110375.

Nasseri, B., Yilmaz, M., Turk, M., Kocum, I.C. and Piskin, E., (2016). Antenna-type radiofrequency generator in nanoparticle-mediated hyperthermia. *RSC Advances*, 6(54): 48427–48434.

Oei, A.L., Kok, H.P., Oei, S.B., Horsman, M.R., Stalpers, L.J.A., Franken, N.A.P. and Crezee, J. (2020). Molecular and biological rationale of hyperthermia as radio- and chemosensitizer. *Advanced Drug Delivery Reviews*, 163–164: 84–97.

Ohta, S., Kikuchi, E., Ishijima, A., Azuma, T., Sakuma, I. and Ito, T. (2020). Investigating the optimum size of nanoparticles for their delivery into the brain assisted by focused ultrasound-induced blood–brain barrier opening. *Scientific Reports*, 10(1): 18220.

Ojeda, P.G., Wang, C.K. and Craik, D.J. (2016). Chlorotoxin: Structure, activity, and potential uses in cancer therapy. *Biopolymers*, 106(1): 25–36.

Oladipo, A.O., Iku, S.I.I., Ntwasa, M., Nkambule, T.T.I., Mamba, B.B. and Msagati, T.A.M. (2020). Doxorubicin conjugated hydrophilic AuPt bimetallic nanoparticles fabricated from Phragmites australis: Characterization and cytotoxic activity against human cancer cells. *Journal of Drug Delivery Science and Technology*, 57: 101749.

Omoruyi, S., Enogieru, A. and Ekpo, O. (2019). Preliminary Cytotoxic Activity of Sutherlandia frutescens and Carpobrotus edulis on Malignant glioblastoma Cells. *Tropical Journal of Natural Product Research,* 3(4): 175-179.

Ostrovsky, S., Kazimirsky, G., Gedanken, A. and Brodie, C. (2009). Selective cytotoxic effect of ZnO nanoparticles on glioma cells. *Nano Research*, 2(11): 882–890.

Pan, Y., Leifert, A., Ruau, D., Neuss, S., Bornemann, J., Schmid, G., Brandau, W., Simon, U. and Jahnen-Dechent, W. (2009). Gold nanoparticles of diameter 1.4 nm trigger necrosis by oxidative stress and mitochondrial damage. *Small (Weinheim an Der Bergstrasse, Germany)*, 5(18): 2067–2076.

Park, C.-M., Park, M.-J., Kwak, H.-J., Lee, H.-C., Kim, M.-S., Lee, S.-H., Park, I.-C., Rhee, C.H. and Hong, S.-I. (2006). Ionizing Radiation Enhances Matrix Metalloproteinase-2 Secretion and Invasion

of Glioma Cells through Src/Epidermal Growth Factor Receptor–Mediated p38/Akt and Phosphatidylinositol 3-Kinase/Akt Signaling Pathways. *Cancer Research*, 66(17): 8511–8519.

Park, S.Y., Chae, S.Y., Park, J.O., Lee, K.J. and Park, G. (2017). Kalopanacis Cortex extract-capped gold nanoparticles activate NRF2 signaling and ameliorate damage in human neuronal SH-SY5Y cells exposed to oxygen–glucose deprivation and reoxygenation. *International Journal of Nanomedicine*, 12: 4563–4578.

Park, W.H. (2018). Hydrogen peroxide inhibits the growth of lung cancer cells via the induction of cell death and G1-phase arrest. *Oncology Reports*, 40(3): 1787–1794.

Patra, H.K., Banerjee, S., Chaudhuri, U., Lahiri, P. and Dasgupta, A.K. (2007). Cell selective response to gold nanoparticles. *Nanomedicine: Nanotechnology, Biology, and Medicine*, 3(2): 111–119.

Pawar, A.A., Sahoo, J., Verma, A., Lodh, A. and Lakkakula, J. (2021). Usage of Platinum Nanoparticles for Anticancer Therapy over Last Decade: A Review. *Particle & Particle Systems Characterization*, 38(10): 2100115.

Pfeffer, C.M. and Singh, A.T.K. (2018). Apoptosis: A Target for Anticancer Therapy. *International Journal of Molecular Sciences*, 19(2): E448.

Pizzino, G., Irrera, N., Cucinotta, M., Pallio, G., Mannino, F., Arcoraci, V., Squadrito, F., Altavilla, D. and Bitto, A. (2017). Oxidative Stress: Harms and Benefits for Human Health. *Oxidative Medicine and Cellular Longevity*, 2017: 8416763.

Princely, S.X., Puja, P., Vinita, M.N., Devan, U., Velangani, A.J., Sunita, S., Yuvakkumar, R., Velmurugan, P., Ravi, A.V., Govarthanan, M. and Kumar, P. (2020). Anti-proliferative and anti-migratory effects of flower-like bimetallic (Au@Pt) nanoparticles. *Materials Letters*, 267: 127491.

Qin, C., He, B., Dai, W., Lin, Z., Zhang, H., Wang, X., Wang, J., Zhang, X., Wang, G., Yin, L. and Zhang, Q. (2014). The impact of a chlorotoxin-modified liposome system on receptor MMP-2 and the receptor-associated protein ClC-3. *Biomaterials*, 35(22): 5908–5920.

Quintero-Fabián, S., Arreola, R., Becerril-Villanueva, E., Torres-Romero, J.C., Arana-Argáez, V., Lara-Riegos, J., Ramírez-Camacho, M.A. and Alvarez-Sánchez, M.E. (2019). Role of Matrix Metalloproteinases in Angiogenesis and Cancer. *Frontiers in Oncology*, 9: 1370.

Rajan, A. and Sahu, N.K. (2020). Review on magnetic nanoparticle-mediated hyperthermia for cancer therapy. *Journal of Nanoparticle Research*, 22(11): 319.

Raoof, M., Corr, S.J., Kaluarachchi, W.D., Massey, K.L., Briggs, K., Zhu, C., Cheney, M.A., Wilson, L.J. and Curley, S.A. (2012). Stability of antibody-conjugated gold nanoparticles in the endolysosomal nanoenvironment: implications for noninvasive radiofrequency-based cancer therapy. *Nanomedicine: Nanotechnology, Biology and Medicine*, 8(7): 1096–1105.

Raoof, M. and Curley, S.A. (2011). Non-invasive radiofrequency-induced targeted hyperthermia for the treatment of hepatocellular carcinoma. *International Journal of Hepatology*, 2011: 676957.

Ravanti, L., Heino, J., López-Otín, C. and Kähäri, V.M. (1999). Induction of collagenase-3 (MMP-13) expression in human skin fibroblasts by three-dimensional collagen is mediated by p38 mitogen-activated protein kinase. *The Journal of Biological Chemistry*, 274(4): 2446–2455.

Rejinold, N.S., Jayakumar, R. and Kim, Y.-C. (2015). Radio frequency responsive nano-biomaterials for cancer therapy. *Journal of Controlled Release*, 204: 85–97.

Reuther, C., Ganjam, G.K., Dolga, A.M. and Culmsee, C. (2014). The serine protease inhibitor TLCK attenuates intrinsic death pathways in neurons upstream of mitochondrial demise. *Apoptosis*, 19(11): 1545–1558.

Ribatti, D., Surico, G., Vacca, A., De Leonardis, F., Lastilla, G., Montaldo, P.G., Rigillo, N. and Ponzoni, M. (2001). Angiogenesis extent and expression of matrix metalloproteinase-2 and -9 correlate with progression in human neuroblastoma. *Life Sciences*, 68(10): 1161–1168.

Richard, S., Saric, A., Boucher, M., Slomianny, C., Geffroy, F., Mériaux, S., Lalatonne, Y., Petit, P.X. and Motte, L. (2016). Antioxidative Theranostic Iron Oxide Nanoparticles toward Brain Tumors Imaging and ROS Production. *ACS Chemical Biology*, 11(10): 2812–2819.

Rjeibi, I., Mabrouk, K., Mosrati, H., Berenguer, C., Mejdoub, H., Villard, C., Laffitte, D., Bertin, D., Ouafik, L., Luis, J., Elayeb, M. and Srairi-Abid, N. (2011). Purification, synthesis and characterization of AaCtx, the first chlorotoxin-like peptide from Androctonus australis scorpion venom. *Peptides*, 32(4): 656–663.

Rono, C. and Oliver, T.R. (2020). Near infrared light exposure is associated with increased mitochondrial membrane potential in retinal pigmented epithelial cells. *Photochemical & Photobiological Sciences: Official Journal of the European Photochemistry Association and the European Society for Photobiology*, 19(10): 1455–1459.

Rouhimoghadam, M., Safarian, S., Carroll, J.S., Sheibani, N. and Bidkhori, G. (2018). Tamoxifen-Induced Apoptosis of MCF-7 Cells via GPR30/PI3K/MAPKs Interactions: Verification by ODE Modeling and RNA Sequencing. *Frontiers in Physiology*, 9: 907.

Şahin, B., Aygün, A., Gündüz, H., Şahin, K., Demir, E., Akocak, S. and Şen, F. (2018). Cytotoxic effects of platinum nanoparticles obtained from pomegranate extract by the green synthesis method on the MCF-7 cell line. *Colloids and Surfaces B: Biointerfaces*, 163: 119–124.

San, B.H., Moh, S.H. and Kim, K.K. (2013). Investigation of the heating properties of platinum nanoparticles under a radiofrequency current. *International Journal of Hyperthermia: The Official Journal of European Society for Hyperthermic Oncology, North American Hyperthermia Group*, 29(2): 99–105.

Sani, A., Cao, C. and Cui, D. (2021). Toxicity of gold nanoparticles (AuNPs): A review. *Biochemistry and Biophysics Reports*, 26: 100991.

Schaeublin, N.M., Braydich-Stolle, L.K., Schrand, A.M., Miller, J.M., Hutchison, J., Schlager, J.J. and Hussain, S.M. (2011). Surface charge of gold nanoparticles mediates mechanism of toxicity. *Nanoscale*, 3(2): 410–420.

179

Shang, L., Nienhaus, K. and Nienhaus, G.U. (2014). Engineered nanoparticles interacting with cells: size matters. *Journal of Nanobiotechnology*, 12(1): 5.

Sharma, G., Braga, C.B., Chen, K.-E., Jia, X., Ramanujam, V., Collins, B.M., Rittner, R. and Mobli, M. (2021). Structural basis for the binding of the cancer targeting scorpion toxin, ClTx, to the vascular endothelia growth factor receptor neuropilin-1. *Current Research in Structural Biology*, 3: 179–186.

Shi, L., Zhang, J., Zhao, M., Tang, S., Cheng, X., Zhang, W., Li, W., Liu, X., Peng, H. and Wang, Q. (2021). Effects of polyethylene glycol on the surface of nanoparticles for targeted drug delivery. *Nanoscale*, 13(24): 10748–10764.

Shin, S.-S., Noh, D.-H., Hwang, B., Lee, J.-W., Park, S.L., Park, S.-S., Moon, B., Kim, W.-J. and Moon, S.-K. (2018). Inhibitory effect of Au@Pt-NSs on proliferation, migration, and invasion of EJ bladder carcinoma cells: involvement of cell cycle regulators, signaling pathways, and transcription factor-mediated MMP-9 expression. *International Journal of Nanomedicine*, 13: 3295–3310.

Shiny, P.J., Mukherjee, A. and Chandrasekaran, N. (2016). DNA damage and mitochondria-mediated apoptosis of A549 lung carcinoma cells induced by biosynthesised silver and platinum nanoparticles. *RSC Advances*, 6(33): 27775–27787.

Sibuyi, N.R.S, Thovhogi, N., Gabuza, K.B., Meyer, M.D., Drah, M., Onani, M.O., Skepu, A., Madiehe, A.M. and Meyer, M. (2017). Peptide-functionalized nanoparticles for the selective induction of apoptosis in target cells. *Nanomedicine (London, England)*, 12(14): 1631–1645.

Siddique, S. and Chow, J.C.L. (2020). Gold Nanoparticles for Drug Delivery and Cancer Therapy. *Applied Sciences*, 10(11): 3824.

Sinha, K., Das, J., Pal, P.B. and Sil, P.C. (2013). Oxidative stress: the mitochondria-dependent and mitochondria-independent pathways of apoptosis. *Archives of Toxicology*, 87(7): 1157–1180.

Smith, V. and Foster, J. (2018). High-Risk Neuroblastoma Treatment Review. *Children*, 5(9): 114.

Sokolova, V., Mekky, G., van der Meer, S.B., Seeds, M.C., Atala, A.J. and Epple, M. (2020). Transport of ultrasmall gold nanoparticles (2 nm) across the blood–brain barrier in a six-cell brain spheroid model. *Scientific Reports*, 10(1): 18033.

Song, Y., Shi, Q., Zhu, C., Luo, Y., Lu, Q., Li, H., Ye, R., Du, D. and Lin, Y. (2017a). Mitochondrial Reactive Oxygen Species Burst for Cancer Therapy Triggered by Near-Infrared Light. *Nanoscale*, 2017.

Song, Y., Shi, Q., Zhu, C., Luo, Y., Lu, Q., Li, H., Ye, R., Du, D. and Lin, Y. (2017b). Mitochondrial-targeted multifunctional mesoporous Au@Pt nanoparticles for dual-mode photodynamic and photothermal therapy of cancers. *Nanoscale*, 9(41): 15813–15824.

Song, Y., Qu, Z., Li, J., Shi, L., Zhao, W., Wang, H., Sun, T., Jia, T. and Sun, Y. (2021). Fabrication of the biomimetic DOX/Au@Pt nanoparticles hybrid nanostructures for the combinational chemo/photothermal cancer therapy. *Journal of Alloys and Compounds*, 881: 160592.

180

Soroceanu, L., Gillespie, Y., Khazaeli, M.B. and Sontheimer, H. (1998). Use of chlorotoxin for targeting of primary brain tumors. *Cancer Research*, 58(21): 4871–4879.

Srinoi, P., Chen, Y.-T., Vittur, V., Marquez, M.D. and Lee, T.R. (2018). Bimetallic Nanoparticles: Enhanced Magnetic and Optical Properties for Emerging Biological Applications. *Applied Sciences*, 8(7): 1106.

Stephen, Z.R., Kievit, F.M., Veiseh, O., Chiarelli, P.A., Fang, C., Wang, K., Hatzinger, S.J., Ellenbogen, R.G., Silber, J.R. and Zhang, M. (2014). Redox-responsive magnetic nanoparticle for targeted convection-enhanced delivery of O6-benzylguanine to brain tumors. *ACS nano*, 8(10): 10383–10395.

Tait, S.W.G. and Green, D.R. (2008). Caspase-independent cell death: leaving the set without the final cut. *Oncogene*, 27(50): 6452–6461.

Tang, J., Jiang, X., Wang, L., Zhang, H., Hu, Z., Liu, Y., Wu, X. and Chen, C. T. (2014). Au@Pt nanostructures: a novel photothermal conversion agent for cancer therapy. *Nanoscale*, 6(7): 3670–3678.

Thovhogi, N., Sibuyi, N., Meyer, M., Onani, M. and Madiehe, A. (2015). Targeted delivery using peptide-functionalised gold nanoparticles to white adipose tissues of obese rats. *Journal of Nanoparticle Research*, 17(2): 112.

Uchiyama, M.K., Deda, D.K., Rodrigues, S.F. de P., Drewes, C.C., Bolonheis, S.M., Kiyohara, P.K., Toledo, S.P. de, Colli, W., Araki, K. and Farsky, S.H.P. (2014). In vivo and in vitro toxicity and anti-inflammatory properties of gold nanoparticle bioconjugates to the vascular system. *Toxicological Sciences: An Official Journal of the Society of Toxicology*, 142(2): 497–507.

Valdés-Rives, S.A., Casique-Aguirre, D., Germán-Castelán, L., Velasco-Velázquez, M.A. and González-Arenas, A. (2017). Apoptotic Signaling Pathways in Glioblastoma and Therapeutic Implications. *BioMed Research International*, 2017: 7403747.

van der Zande, M. Undas, A.K., Kramer, E., Monopoli, M.P., Peters, R.J., Garry, D., Antunes, Fernandes, E.C., Hendriksen, P.J., Marvin, H.J., Peijnenburg, A.A. and Bouwmeester, H. (2016). Different responses of Caco-2 and MCF-7 cells to silver nanoparticles are based on highly similar mechanisms of action. *Nanotoxicology*, 10(10): 1431–1441.

Vijayakumar, S. and Ganesan, S. (2012). In Vitro Cytotoxicity Assay on Gold Nanoparticles with Different Stabilizing Agents. *Journal of Nanomaterials*, 2012: e734398.

Visse, R. and Nagase, H. (2003). Matrix Metalloproteinases and Tissue Inhibitors of Metalloproteinases. *Circulation Research*, 92 (8): 827–39.

Wang, K., Kievit, F.M., Chiarelli, P.A., Stephen, Z.R., Lin, G., Silber, J.R., Ellenbogen, R.G. and Zhang, M. (2021). siRNA Nanoparticle Suppresses Drug-Resistant Gene and Prolongs Survival in an Orthotopic Glioblastoma Xenograft Mouse Model. *Advanced Functional Materials*, 31(6): 2007166.

181

Wang, Y., Chen, K., Cai, Yihong, Cai, Yuanxia, Yuan, X., Wang, L., Wu, Z. and Wu, Y. (2017). Annexin A2 could enhance multidrug resistance by regulating NF-κB signaling pathway in pediatric neuroblastoma. *Journal of Experimental & Clinical Cancer Research*, 36(1): 111.

Wang, Y., Li, K., Han, S., Tian, Y., Hu, P., Xu, X., He, Y., Pan, W., Gao, Y., Zhang, Z., Zhang, J. and Wei, L. (2019). Chlorotoxin targets ERα/VASP signaling pathway to combat breast cancer. *Cancer Medicine*, 8(4): 1679–1693.

Welch, D.R. and Hurst, D.R. (2019). Defining the Hallmarks of Metastasis. *Cancer Research*, 79(12): 3011–3027.

Wu, S., Ma, K., Qiao, W.-L., Zhao, L.-Z., Liu, C.-C., Guo, L.-L., Xing, Y., Zhu, M.-L. and Zhao, J.-H. (2018). Anti-metastatic effect of 131I-labeled Buthus martensii Karsch chlorotoxin in gliomas. *International Journal of Molecular Medicine*, 42(6): 3386–3394.

Wu, W., Klockow, J.L., Zhang, M., Lafortune, F., Chang, E., Jin, L., Wu, Y. and Daldrup-Link, H.E. (2021). Glioblastoma multiforme (GBM): An overview of current therapies and mechanisms of resistance. *Pharmacological Research*, 171: 105780.

Wusu, A.D., Sibuyi, N.R.S., Moabelo, K.L., Goboza, M., Madiehe, A. and Meyer, M. (2021). Citrate-capped gold nanoparticles with a diameter of 14 nm alter the expression of genes associated with stress response, cytoprotection and lipid metabolism in CaCo-2 cells. *Nanotechnology*, 33(10): 105101.

Xu, P., Hou, L., Ju, C., Zhang, Z., Sun, W., Zhang, L., Song, J., Lv, Y., Liu, L., Chen, Z. and Wang, Y. (2016). Isatin inhibits the proliferation and invasion of SH-SY5Y neuroblastoma cells. *Molecular Medicine Reports*, 13(3): 2757–2762.

Yang, J.A., Lohse, S.E. and Murphy, C.J. (2014). Tuning cellular response to nanoparticles via surface chemistry and aggregation. *Small (Weinheim an Der Bergstrasse, Germany)*, 10(8): 1642–1651.

Yang, Q., Peng, J., Xiao, Y., Li, W., Tan, L., Xu, X. and Qian, Z. (2018). Porous Au@Pt Nanoparticles: Therapeutic Platform for Tumor Chemo-Photothermal Co-Therapy and Alleviating Doxorubicin-Induced Oxidative Damage. *ACS Applied Materials & Interfaces*, 10(1): 150–164.

Yousaf, M.N., Ehsan, H., Muneeb, A., Wahab, A., Sana, M.K., Neupane, K. and Chaudhary, F.S. (2021). Role of Radiofrequency Ablation in the Management of Unresectable Pancreatic Cancer. *Frontiers in Medicine*, 7: 624997.

Zhang, X., Guo, X., Kang, X., Yang, H., Guo, W., Guan, L., Wu, H. and Du, L. (2020). Surface Functionalization of Pegylated Gold Nanoparticles with Antioxidants Suppresses Nanoparticle-Induced Oxidative Stress and Neurotoxicity. *Chemical Research in Toxicology*, 33(5): 1195–1205.

Zhang, Y., Shen, X., Xiao, X., Liu, M., Li, S., Yan, J., Jin, J., Gao, J., Zhen, C., Hu, N., Zhang, X., Tai, Y., Zhang, L., Bai, Y. and Dong, D. (2016). Mitochondrial uncoupler carbonyl cyanide m-chlorophenylhydrazone induces vasorelaxation without involving KATP channel activation in smooth muscle cells of arteries. *British Journal of Pharmacology*, 173(21): 3145–3158.

Zhang, Y., Chen, X., Gueydan, C. and Han, J. (2018). Plasma membrane changes during programmed cell deaths. *Cell Research*, 28(1): 9–21.

Zhao, L., Ge, X., Yan, G., Wang, X., Hu, P., Shi, L., Wolfbeis, O.S., Zhang, H. and Sun, L. (2017). Double-mesoporous core–shell nanosystems based on platinum nanoparticles functionalized with lanthanide complexes for in vivo magnetic resonance imaging and photothermal therapy. *Nanoscale*, 9(41): 16012–16023.

Zhou, W., Yu, X., Sun, S., Zhang, Xuehai, Yang, W., Zhang, J., Zhang, X. and Jiang, Z. (2019). Increased expression of MMP-2 and MMP-9 indicates poor prognosis in glioma recurrence. *Biomedicine & Pharmacotherapy*, 118: 109369.

Zorov, D.B., Juhaszova, M. and Sollott, S.J. (2014). Mitochondrial reactive oxygen species (ROS) and ROS-induced ROS release. *Physiological Reviews*, 94(3): 909–950.

UNIVERSITY *of the*

WESTERN CAPE

CHAPTER FIVE:

Investigating the early cytotoxic molecular effects of chlorotoxin functionalized bimetallic gold platinum nanoparticles in U87 human glioblastoma cells

Taahirah Boltman[1], Bronwyn Kirby-McCullough[2], Okobi Ekpo[1], Adedoja Dorcas Wusu[3] and Mervin Meyer[3]*

[1] Department of Medical Biosciences, University of the Western Cape, Cape Town, Robert Sobukwe Road, Bellville 7535, South Africa; 2917424@myuwc.ac.za (T.B.)

[2] Institute for Microbial Biotechnology and Metagenomics (IMBM) Department of Biotechnology, University of the Western Cape, Cape Town, Robert Sobukwe Road, Bellville 7535, South Africa

[3] DSI/Mintek Nanotechnology Innovation Centre, Biolabels Node, Department of Biotechnology, University of the Western Cape, Cape Town, Robert Sobukwe Road, Bellville 7535, South Africa

*Correspondence: memeyer@uwc.ac.za (M.M.); Tel.: +27-21-5952032 (M.M.)

Abstract

In recent years, noble bimetallic nanoparticles (BNPs) were shown to be useful for a range of biomedical applications due to their unique physicochemical properties. The BNPs appear to be more advantageous than their monometallic counterparts possibly due to their enhanced properties. Recently, bimetallic gold platinum nanoparticles (AuPtNPs) have generated much interest in applications for the diagnosis and treatment of cancer. These BNPs exhibited improved features for photothermal therapy (PTT) and radiation therapy in comparison to monometallic gold nanoparticles (AuNP) and platinum nanoparticles (PtNPs). Few studies reported on the cytotoxicity of AuPtNPs. In a previous study, we reported for the first time on the cytotoxicity of chlorotoxin functionalized AuPtNPs (CTX-AuPtNPs), which seemed to induce apoptosis in U87 human glioblastoma cells. These NPs can potentially be applied in non-invasive NP-mediated radiofrequency (RF) targeted hyperthermia treatment. The potential risks to human health and the environment should always be

184

evaluated when developing nanoparticles (NPs) for any application. Therefore, in the present work, we investigated the early cytotoxic effects of CTX-AuPtNPs using the WST-1 cell viability assay. The toxicity of CTX-AuPtNPs to U87 cells is dose and time dependent. We identified conditions of treatment (24-hour exposure to 75 µg/ml) that reflect the early stages of cell death and investigated changes in the gene expression profile of 86 genes that are known to be involved in cytotoxicity. Out of the 86 genes studied, 16 genes were differentially expressed. Genes that are involved in cellular stress responses, lipid metabolism endoplasmic reticulum (ER) stress and unfolded protein response (UPR) were more affected than others and resulted in the activation of cytoprotective cellular processes. This study suggests that while low concentrations of CTX-AuPtNPs are not highly toxic to U87 cells as demonstrated by the downregulation of genes involved in cytotoxicity, the NPs induced a stress response in the cells. The concentration (75 µg/ml) of CTX-AuPtNPs and the exposure time (24 hours) may be suitable for use in future NP-mediated RF targeted hyperthermia treatment.

1. Introduction

Monometallic nanoparticles (MNPs) composed of noble metals such as gold and platinum have been intensely investigated for applications in biomedical research (Fahmy *et al.*, 2020; X.-Y. Liu *et al.*, 2021). Gold NPs (AuNPs) and platinum NPs (PtNPs) have been applied in cancer research in areas such as imaging (Zhao *et al.*, 2017; Chan *et al.*, 2021; Luo *et al.*, 2021), target specific drug delivery (Kong *et al.*, 2017; Mukherjee *et al.*, 2020; Siddique and Chow, 2020) and photothermal therapy (Riley and Day, 2017; Depciuch *et al.*, 2019; Yang *et al.*, 2019). Bimetallic NPs (BNPs) constructed of two different metal elements have recently attracted great attention because they present distinct and improved features when compared to their monometallic counterparts with regards to electronic and catalytic activity (Wang, Hao and Li, 2020), optical activity (Nguyen *et al.*, 2020), antimicrobial activity (Arora, Thangavelu and Karanikolos, 2020), and features that make these nanomaterials appropriate for applications in the treatment of cancer (Kotha *et al.*, 2020). However, little is known about the molecular mechanisms by which BNPs exert their anti-cancer effects. The performance of these nanomaterials depends on their composition, shape, size, surface area and due to the synergistic

185

effects of the constituent metals (Srinoi *et al.*, 2018). Among the most studied BNPs are those composed of noble metals (Au, Ag, Pt, and Pd) or transition metals (Ni, Cu, Fe, Co) (Zhang, Yu and Zhang, 2019). Bimetallic AuPtNPs of different sizes and shapes have been shown to exhibit photothermal effects with some exhibiting more enhanced effects when compared to its monometallic counterparts, AuNP and PtNPs (Tang *et al.*, 2014; Liu *et al.*, 2017; Song *et al.*, 2017, 2021; Yang *et al.*, 2018; Depciuch *et al.*, 2019; Fathima and Mujeeb, 2021). AuPtNPs also demonstrated higher radiation effects in comparison with monometallic AuNPs (Salado-Leza *et al.*, 2019) and effective nano-drug delivery models for doxorubicin chemotherapeutic drug (Yang *et al.*, 2018; Oladipo *et al.*, 2020; Song et al., 2021). Moreover, AuPtNPs possess significant computed tomography (CT) imaging signal enhancement, which demonstrates their potential for use in image-guided tumour therapy (Liu *et al.*, 2017). Due to these advantages, AuPtNPs may be effective as multifunctional NPs for cancer theranostics, especially for aggressive brain cancers such as glioblastoma multiforme (GB). However, more research is required into understanding the biological effects and in particular the cytotoxic effects associated with AuPtNPs.

While the toxicity of MNPs have been fairly well studied, very few studies have been done on the toxicity of BNPs, including AuPtNPs. The toxicity of BNPs are affected by the same factors that influence the toxicity of MNPs, such as size, shape, concentrations, time, synthesis methods, surface functionalization and cell type (Sani, Cao and Cui, 2021). Larger AuPtNPs demonstrate negligible toxicity in cells. Tang *et al.* (2014) showed that 60 nm rod shaped AuPtNP caused negligible toxicity to the MDAMB-231 human mammary cancer cells at 10 µg/ml. No acute cytotoxicity to either Human umbilical vein endothelial cells (HUVEC) or 4T1 breast cancer cells was observed with treatment of 30 nm PEGylated AuPtNPs at concentrations as high as 75 µg/ml (Liu *et al.*, 2017). PEG-AuPtNPs in a size range of 40 nm demonstrated low cytotoxicity at concentrations of 0.06-1.5 nM in SKOV3 human ovarian cancer cell line, U8 human glioblastoma cells and noncancerous human hepatic cells (Liang *et al.*, 2017). Treatment of U87 and KMST-6 human fibroblast cells with 14 nm PEG-AuPtNPs at concentrations as high as 300 µg/ml demonstrated low cytotoxicity (Chapter 4). A recent study reported on flower-shaped AuPtNPs which demonstrated cytotoxic effects and apoptotic morphological features in MCF-7 breast cancer cells with a half-maximum inhibitory concentration (IC_{50}) equivalent to 120 µg/ml (Princely *et al.*, 2020). AuPtNPs in the size range of < 10 nm were not toxic to Human fibroblast cell line Hs68 (Formaggio *et al.*, 2019), however caused a significant decrease in cell viability in a dose dependent manner in HepG liver cancer cells (Boomi

et al., 2019) and caused morphological changes suggestive of apoptosis in SH-SY5Y neuroblastoma cancer cells and U87 cancer cells (Chapter 4). A recent study by Chaturvedi *et al.* (2021) reported that 16 nm AuPtNPs caused a dose-dependent decrease in HCT 116 human colon cancer cell viability at concentrations of 100 and 200 µg/ml. Shin *et al.* (2018) showed that AuPt nanoseeds significantly inhibited cell proliferation of EJ bladder cancer cells in a dose-dependent manner inducing G1 phase cell cycle arrest. The accumulation was caused, at least in part, by the downregulation of CDK2, CDK4, cyclin D1, and cyclin E, which was mediated by the upregulation of p21WAF1. In addition, they demonstrated, that AuPt nanoseeds exerted its inhibitory activity by inducing the phosphorylation of p38 and inhibiting the phosphorylation of AKT. In our previous work, we reported on the development of chlorotoxin (CTX) peptide conjugated bimetallic AuPtNPs (CTX-AuPtNPs) for future application in non-invasive radiofrequency (RF) induced thermal therapy of brain tumours (Chapter 3). We demonstrated specific uptake in the glioblastoma (GB) cell line U87, which is known to overexpress receptors for CTX (Soroceanu *et al.*, 1998; Lyons, O'Neal and Sontheimer, 2002; Costa *et al.*, 2013; Dastpeyman *et al.*, 2019). Upon further investigation, we found that these NPs induced apoptosis in U87 cells (Chapter 4). The induction of apoptosis was also associated with increased levels of oxidative stress caused by the elevation of reactive oxygen species (ROS) and impaired mitochondrial function.

Glioblastoma (GB), also referred to glioblastoma multiforme, is the deadliest brain tumour diagnosed in adults with a median survival time of less than 2 years and a 5-year survival rate of less than 7 %, even with current treatment options (Sevastre *et al.*, 2021; Wu *et al.*, 2021). CTX, is a 36 amino acid peptide, isolated from the venom of the deathstalker scorpion (*Leiurus quinquestriatus*) and shown to selectively bind to a broad list of solid tumours, with the highest binding affinity for gliomas without any binding to normal brain tissues (Soroceanu *et al.*, 1998; Lyons, O'Neal and Sontheimer, 2002; Kesavan *et al.*, 2010; McGonigle *et al.*, 2019; Wang *et al.*, 2019). For GB binding, CTX targets the overexpressed matrix metalloproteinase-2 (MMP-2) (Deshane, Garner and Sontheimer, 2003) and chloride channel-3 (ClC-3) (McFerrin and Sontheimer, 2006) both absent in normal brain tissue but overexpressed in glioma cells. ClC-3 and MMP-2 form a protein complex, found on the same membrane domain, to which CTX-peptide binds to inhibit glioma cell invasion (Deshane, Garner and Sontheimer, 2003; Qin et al., 2014). Due to this targeting strategy CTX has been conjugated to a variety of fluorescent molecules and nanoparticles (NPs) and are increasingly being investigated as multifunctional theranostic systems applied in targeted delivery, imaging and enhanced radiotherapy

for the treatment of GB, with some entering clinical trials (Cohen-Inbar and Zaaroor, 2016; Ojeda, Wang and Craik, 2016; Zhao *et al.*, 2020; Yeini *et al.*, 2021). NPs are extensively investigated before entering clinical trials to ensure safety and biocompatibility (Sani, Cao and Cui, 2021). It is evident that NPs cause cell death by various physiochemical properties related to the NPs and cell type (Attarilar *et al.*, 2020). The majority of nanotoxicological evaluations are performed *in vitro* with traditional bioassays due to its simplicity. Though the outcome may not predict the *in vivo* toxicity accurately, it provides the background for understanding the uptake and mechanism of toxicity. The limitations of using traditional bioassays to investigate toxicity of NPs have been described previously (Selck *et al.*, 2016; Nelissen *et al.*, 2020). To understand the underlying mechanisms of cytotoxicity, the use of more sensitive tools such as gene expression technologies, which assess biological responses at a molecular level is suggested as a more suitable technique that must be included when assessing the toxicity of nanomaterials.

The interactions of high-frequency radiowaves (13.56 MHz) of different nanomaterials in biological tissues are currently being investigated as a promising therapeutic platform for non-invasive cancer hyperthermia therapy (Corr *et al.*, 2015). The unique dielectric properties of cancerous tissues allow for radiofrequency (RF) energy absorption and conversion to heat and is increased through the use of RF-energy absorbing nanomaterials such as AuNPs, PtNPs, quantum dots, iron oxide NPs and carbon nanotubes (Glazer and Curley, 2011; San, Moh and Kim, 2013; Corr *et al.*, 2015; Beyk and Tavakoli, 2019). In comparison to other nano-based hyperthermia approaches such as the minimal tissue penetration offered by near-infrared (NIR) light, RF therapy offers the advantage of increased tissue penetration depths (~5–30 cm), which is as a result of long RF wavelengths (~22 m at 13.56 MHz) (Corr *et al.*, 2015). This approach is potentially advantageous for deep-seated tumours such as brain tumours. The novel CTX-AuPtNPs have a potential application in non-invasive RF field-induced targeted hyperthermia treatment of cancers such as GB (Chapter 4), however further toxicological evaluation of these NPs is required. To further evaluate the toxicity of these NPs, this study investigated the cytotoxic effects of CTX-AuPtNPs on U87 cells by assessing the effects of these NPs on the expression of a panel of genes previously linked to toxicity. To the best of our knowledge, this study is the first report on molecular mechanisms involved in AuPtNPs cytotoxicity in a human brain cancer cell line.

188

2. Materials and methods

2.1. Materials

The cell proliferation reagent WST-1 was acquired from Sigma (Roche, United Kingdom). Dulbecco's Modified Eagle's Medium (DMEM), Foetal Bovine Serum (FBS), Phosphate Buffered Saline solution (PBS) and Penicillin-Streptomycin solution was obtained from Gibco, Life Technologies Corporation (Paisley, United Kingdom). Penicillin and 100 µg/ml streptomycin and 0.25 % trypsin EDTA were acquired from Lonza Group Ltd. (Verviers, Belgium). All plasticware including sterile cell culture grade TC25 flasks were acquired from Bio-Smart Scientific (Cape Town, South Africa). RNeasy Mini Kit, RT² First Strand Kit and Human Molecular Toxicology Pathway Finder RT² Profiler real-time polymerase chain reaction (PCR) Array was all acquired from Qiagen (Maryland, USA).

2.2. Synthesis and characterization of CTX-AuPtNPs

The preparation and characterization of CTX-AuPtNPs with a core size of ~ 5 nm was described previously (Chapter 3).

2.3. Cell culture and maintenance

The U87 human malignant glioblastoma cell line was a donation from Professor Sharon Prince, Department of Human Biology, University of Cape Town, South Africa. U87 cells were grown in Dulbecco Modified Eagles Medium (DMEM) supplemented with 10 % foetal bovine serum (FBS, Gibco, Life Technologies Corporation, Paisley, UK) and 1 % 100 U/mL penicillin and 100 µg/mL streptomycin (Lonza Group Ltd. Verviers, Belgium). Phosphate Buffered Saline (PBS) (Gibco, Life Technologies Corporation, Paisley, UK) was also used. U87 cells were grown in an incubator at 37 °C with 5 % CO_2. The cell growth media (DMEM) were replaced every three days. When cells attained 80 % confluency, sub-culturing of cells was performed. The cells were washed with PBS and 0.25 % trypsin EDTA was used for trypsinization procedure (Lonza Group Ltd., Verviers, Belgium).

189

2.4. Cytotoxicity assay

The cell viability assay was performed using WST-1 Cell Proliferation Reagent (Roche, United Kingdom) to determine the suitable time of exposure of 75 µg/ml CTX-AuPtNPs treatment in U87 cells following the manufacturer's instructions and as previously described (Sibuyi *et al.*, 2017) (Chapter 4). Briefly, U87 cells (6 x 10^3 cells/well) were seeded in 96-well cell culture plates and left for 24 hours for attachment in an incubator with a humidified atmosphere of 5 % CO_2 at 37 °C. Thereafter, cells were treated with 100 µl of 75 µg/ml CTX-AuPtNPs prepared in supplemented DMEM; untreated wells (negative control) were replaced with 100 µl fresh DMEM without NPs and 2 % DMSO was used as a positive control (data not shown) and the plates were placed back in the incubator for 3, 6, 12, 24 and 48 hours. After each time point, all wells were replaced with 100 µl DMEM and 10 µl of WST-1 was added to each well and further incubated for 4 hours. For the interference of NPs, interference control was performed as previously described (Thovhogi *et al.*, 2015; van der Zande *et al.*, 2016; Sibuyi *et al.*, 2017; Majoumouo *et al.*, 2020) (Chapter 4). The absorbance was measured using a BMG Labtech Omega® POLARStar multimodal plate reader (BMG, LABTECH, Offenburg, Germany) at 450 nm (620 nm was used as a reference wavelength and subtracted). Cell viability was expressed as a percentage of untreated using the optical density (OD) obtained, where % cell viability = OD treated - OD blank/ OD untreated - OD blank X 100 as previously described (Thovhogi *et al.*, 2015; van der Zande *et al.*, 2016; Sibuyi *et al.*, 2017) (Chapter 4). All experiments were performed in triplicate wells and repeated thrice.

2.5. Cell morphology

Changes in cell morphology after treatments were observed and captured in U87 cells for each time point. U87 cells (6 x 10^3 cells/well) were seeded in 96-well cell culture plates and left for 24 hours for attachment in an incubator with a humidified atmosphere of 5 % CO_2 at 37 °C. Thereafter, cells were treated with 75 µg/ml CTX-AuPtNPs prepared in supplemented DMEM; untreated wells (negative control) were replaced with 100 µl fresh DMEM without NPs and the plates were placed back in the incubator for 12, 24 and 48 hours. Following each treatment timepoint, changes in cell morphology for the untreated and treated were observed using the Carl Zeiss Primo Vert Model 370 Inverted Microscope (Carl Zeiss Microscopy GmbH, Gottingen, Germany) with 10X objective lens.

Images were captured using the Zeiss software version 2.3. Experiments were performed once in triplicate wells.

2.6. Human Molecular Toxicology Pathway RT² PCR Array

2.6.1. Methodology of RNA isolation, reverse transcription, and Real-Time PCR array

The gene expression experiment was performed as previously described with alterations (Wusu *et al.*, 2021). U87 cells were seeded at the density of 4 x 10^5 cells in T25 flask (performed in triplicates) and placed in an incubator with a humidified atmosphere of 5 % CO_2 at 37 ⁰C. After 24 hours of attachment, the medium was replaced with 3 ml DMEM containing 75 µg/ml CTX-AuPtNPs and further incubated for 24 hours. Untreated U87 cells (which were performed in triplicates) were used as the control for gene expression profiling. At the end 24 hours, the DMEM with or without NPs was removed, and cells were washed thrice with PBS, after which the cell lysate was used immediately for RNA extraction.

Using the RNeasy Mini Kit (Qiagen, Maryland, USA) according to the manufacturer's protocol, RNA was extracted from the cell lysate. The concentration of the RNA samples was determined using a Qubit® 2.0 Fluorometer (Invitrogen by Life Technologies, Carlsbad, CA, USA) as described in the manufacturer's protocol. RNA integrity was validated by 1% agarose gel electrophoresis.

The PCR Array analysis was conducted by converting 0.5 µg of RNA to cDNA in a 20 µl reaction volume using the protocol provided for the RT² First Strand Kit (Qiagen, Maryland, USA). PCR was performed and ran on a 1 % agarose gel to confirm cDNA product before proceeding with PCR. The cDNA was then diluted with 91 µl RNase-free water and used for gene expression profiling using the Human Molecular Toxicology Pathway Finder RT² Profiler PCR Array (Qiagen, Maryland, USA) according to the manufacturer's instructions. Briefly, a total volume of 25 µl of PCR master mixture was used, as indicated in the RT² Profiler PCR array 96-well format manufacturer's instructions. The RT² Profiler PCR array contained 86 genes and 6 housekeeping genes (ACTB, B2M, GAPDH, HPRT1, RPLP0 and HGDC). The experiment was done in triplicates. PCR amplification was performed using the LightCycler®480 (Roche, Mannheim, Germany) with an initial 10 min step at 95 °C followed by 45 cycles of 95 °C for 15 seconds, 60 °C for 1 min and 72 °C for 10 seconds. PCR

analysis data was recorded by the LightCycler 480 software (Roche Mannheim, Germany) and analysed at GeneGlobe Data Analysis Center supplied by Qiagen.

2.6.2. Gene expression analysis of real-time PCR array data

The gene expression analysis of real-time PCR array data was carried out as previously described (Wusu *et al.*, 2021). In order to create a table of the cycle threshold (CT) values, the CT values were exported to Microsoft Excel, which was then uploaded to Qiagen GeneGlobe Data Analysis Portal (Bhagwate *et al.*, 2019), where the quality control of the array normalisation was performed. Qiagen GeneGlobe Data Analysis Portal calculated the fold change using the ΔΔCT method (where ΔCT was calculated between the gene of interest and an average of reference genes) which was followed by ΔΔCT calculations (ΔCT (Test Group)- ΔCT (Control Group). By using the $2^{\wedge}$ (-ΔΔCT) formula, the fold change was calculated. Likely experimental biases and outliers were identified and accounted for based on data from GeneGlobe analysis and unsupervised agglomerative hierarchical clustering. GeneGlobe analysis arranges data and group genes according to their similarity in gene expression patterns using pairwise average-linkage cluster analysis. Differentially expressed genes (DEGs) between untreated controls and treated cells, was considered where genes had p values < 0.05 and absolute fold change ≥ 1. These DEGs were then filtered and used for pathway enrichment analysis and protein interaction network analysis.

2.6.3. Pathway enrichment analysis of DEGs

By using the Database for Annotation, Visualization, and Integrated Discovery (DAVID; version 6.7), which is a functional annotation tool for extracting pertinent biological information from gene sets (Huang *et al.*, 2009), Kyoto Encyclopedia of Genes and Genomes (KEGG) pathways enriched with significantly expressed genes were identified (Table 2). Significantly enriched pathways were selected where the p < 0.05.

2.6.4. Protein interaction network analysis of DEGs

To create the protein interaction network for the DEGs, the Search Tool for the Retrieval of Interaction Genes (STRING; https://string-db.org/) database (Szklarczyk *et al.*, 2019) was used.

2.7. Statistical analysis

Cell viability data generated from this study are expressed as mean ± standard error of mean (SEM) of three independent experiments and analysed using GraphPad Prism 6 (GraphPad Software, San Diego, California, United States of America). Significance of differences was determined using one-way analysis of variance (ANOVA) with the level of significance indicated using asterisks, where *** $P \leq 0.001$ and ****$P \leq 0.0001$. QIAGEN GeneGlobe (http://www.qiagen.com/geneglobe), an online software program, was used for the gene expression analysis, and the unpaired Student's T-test was used to compare gene expression data. Statistically significant differences were considered where the p-value was ≤ 0.05.

3. Results and Discussion

Bimetallic AuPtNPs have shown considerable potential for application in biomedicine as agents for CT imaging of tumours (Liu *et al.*, 2017), photothermal therapy (PTT) (Tang *et al.*, 2014; Liu *et al.*, 2017; Song *et al.*, 2017, 2021; Yang *et al.*, 2018; Depciuch *et al.*, 2019; Fathima and Mujeeb, 2021), and radiation (Salado-Leza *et al.*, 2019). The properties of bimetallic AuPtNPs seem to be enhanced when compared to their monometallic counterparts (AuNPs and PtNPs). The use of AuPtNPs for RF-induced hyperthermia treatment has not been explored for aggressive brain tumours such as GB. While these NPs can offer promising novel treatments for cancer, it is very important to evaluate the cytotoxicity of these NPs.

Although inconsistencies on the safety and biological effects of AuNPs have been reported, these apparent discrepancies were shown to be dependent on factors such as the size, shape, composition and concentration of the NPs as well as the specific bioassays used (Sani, Cao and Cui, 2021). Few studies reported on PtNPs causing cytotoxicity in cancer cells in a similar way to platinum-based chemotherapeutic drugs (Jeyaraj *et al.*, 2019; Gurunathan *et al.*, 2020). There is a limited amount of research reported on the cytotoxicity of AuPtNPs in the literature with some studies pointing towards negligible toxicity (Tang *et al.*, 2014; Liu *et al.*, 2017). The premise is that these NPs are not toxic since the NPs requires external activation to exert their heating properties for applications in thermal therapy or coupling to chemotherapeutic drugs for cytotoxic effects (Liu *et al.*, 2017; Song *et al.*, 2017, 2021; Yang *et al.*, 2018; Depciuch *et al.*, 2019; Salado-Leza *et al.*, 2019; Oladipo *et al.*, 2020; Fathima and Mujeeb, 2021), while others reported that the AuPtNPs induced cell death through

193

apoptosis (Chaturvedi *et al.*, 2021). Our own study demonstrated that AuPtNPs are inherently toxic to cancer cell lines including U87 cells, without activation, and that this toxicity is through the activation of apoptosis (Chapter 4).
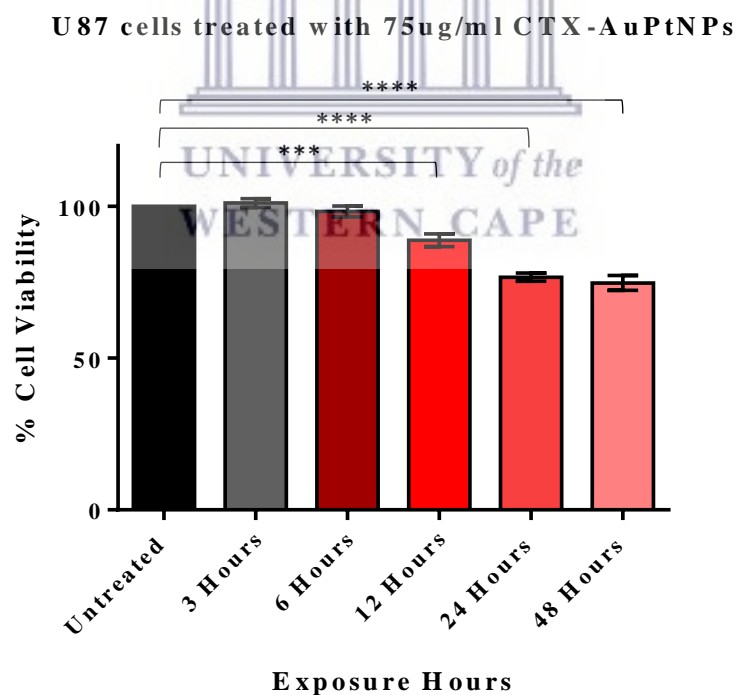
Here we investigated the effects of AuPtNPs on the gene expression profile of the GB cell line, U87. To the best of our knowledge there are no other reports on the effects of AuPtNPs on the gene expression profile of any GB cell line. We set out to investigate the effects of CTX-AuPtNPs with a core size of ~ 5 nm (described in Chapter 3) on U87 GB cell line. The aim of this study was to investigate the cytotoxicity of CTX-AuPtNPs in U87 cells by assessing the effects of the NPs on the expression of a panel of genes that are known to be involved in cell death. It was previously shown that CTX-AuPtNPs are toxic to U87 cells in a dose dependent manner (Chapter 4). To understand which genes and molecular pathways are activated in U87 cells by CTX-AuPtNPs treatment, the study of altered gene expression at the early stages of cell death was required. This meant that the appropriate concentration of CTX-AuPtNPs and time of treatment needed to be established first.

3.1. Cell viability analysis and morphological changes in U87 cell line

A dose response study that was performed previously using the WST-1 assay (Chapter 4) showed that 75 µg/ml CTX-AuPtNPs was the lowest concentration that caused a significant reduction in the cell viability of U87 cells over 48 hours. To determine the optimal concentration and time of treatment for the gene expression study, U87 cells were treated for different time intervals (0, 3, 6, 12, 24 and 48 hours) with 75 µg/ml CTX-AuPtNPs and the viability of the cells were assessed using the WST-1 assay. Figure 1 A shows that the viability of U87 cells were not significantly affected at 3 and 6 hours and that it is only from 12 hours that the viability of these cells were significantly affected. The % cell viability reported at 12, 24 and 48 hours was 88.84 ± 2.07 %, 76.69 ± 1.35 % and 74.79 ± 2.40 % respectively. The toxicity caused by CTX-AuPtNPs was thus time dependent. Figure 1 B shows the morphological changes in U87 cells treated with 75 µg/ml CTX-AuPtNPs at 12, 24 and 48 hours. While the images for the untreated controls show cells with normal astrocyte-shaped morphology, which seem to become more densely populated over time, images of cells treated with the AuPtNPs show the appearance of rounded cells which seem to increase over time. It is also noted that the density of the cells reduced over time. This reduced cell density and rounded shape is due to cell detachment and cell death. The morphological features observed in Figure 1 B, therefore supports the data obtained for the cell viability assay shown in Figure 1 A. The AuPtNPs is functionalized with

PEG and CTX for targeting U87 cells through possible molecular targets ClC-3 and MMP-2 (Deshane, Garner and Sontheimer, 2003; McFerrin and Sontheimer, 2006; Qin *et al.*, 2014). Previous studies report on the biocompatibility and low cytotoxicity of AuPtNPs functionalised with PEG (Liu *et al.*, 2017; Yang *et al.*, 2018) (Chapter 4). A recent study suggested that CTX peptide may not play an important role in cytotoxicity of U87 cells (Ayed *et al.*, 2021), therefore the cytotoxic effects observed may be as a result of intracellular activity of AuPtNPs. These anti-proliferative effects of AuPtNPs is consistent with previous studies, where Boomi *et al.* (2019) showed that 75 µg/ml AuPtNPs of < 10 nm significantly reduced the viability of HepG liver cancer cells and caused morphological changes in the cells that are suggestive of apoptosis. The effects of AuPtNPs on cell viability may be cell line specific, as seen with a recent study by Chaturvedi *et al.* (2021) where 16 nm AuPtNPs significantly reduced the cell viability of HCT 116 human colon cancer at 12.5 µg/ml, with accompanying changes in cell morphology and increasing cell death through the elevation of ROS and apoptosis. A similar observation was made in our previous study, where AuPtNPs significantly decreased cell viability in U87 and SH-SH5Y cells (Chapter 4). Since a 24-hour treatment with 75 µg/ml CTX-AuPtNPs caused significant reduction in the cell viability of U87 cells, this timepoint and concentration was selected for the gene expression study.

A

B

Untreated 12 Hours   75 µg/ml CTX-AuPtNPs 12 Hours

Untreated 24 Hours   75 µg/ml CTX-AuPtNPs 24 Hours

Untreated 48 Hours   75 µg/ml CTX-AuPtNPs 48 Hours
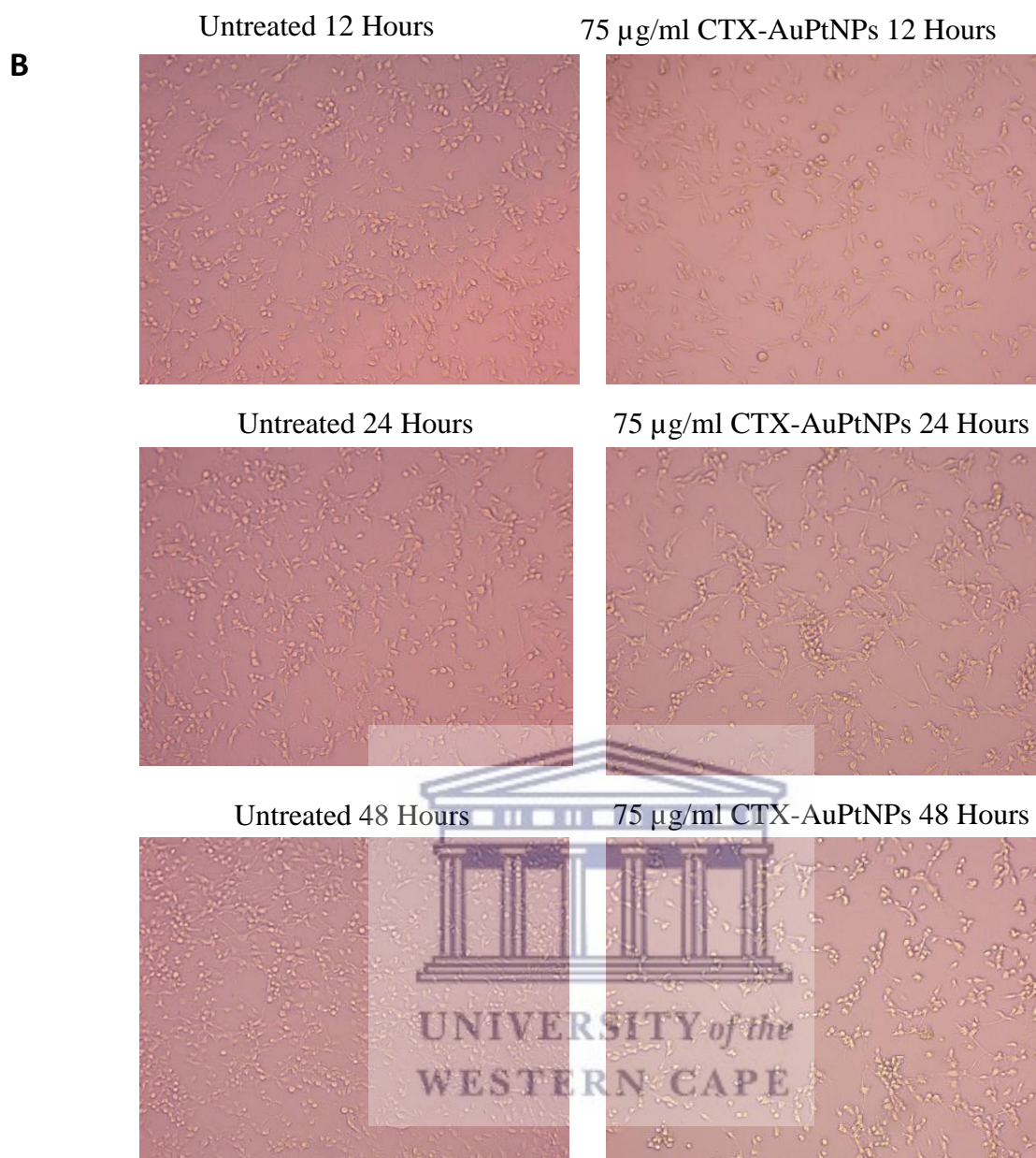
Figure 1. The time-dependent effects of treatment with 75 µg/ml of CTX-AuPtNPs on cell viability and cell morphology in U87 cells. The % cell viability of U87 cells was assessed using WST-1 assay for untreated and treated with 75 µg/ml of CTX-AuPtNPs at 3, 6, 12, 24 and 48 hours (A). Experiments were repeated thrice, and data are presented as bar graphs where mean ± SEM are presented from three independent experiments and *** $P \leq 0.001$ and **** $P \leq 0.0001$ were considered statistically significant. Changes in cell morphology at 12, 24 and 48 hours after treatment with 75µg/ml CTX-AuPtNPs (B) were acquired using Carl Zeiss Primo Vert Model 370 Inverted Microscope (Carl Zeiss Microscopy GmbH, Gottingen, Germany) with a 10X objective lens.

196

3.2. Gene expression profiling after exposure to U87 cells with CTX-AuPtNPs

In this study the Human Molecular Toxicology Pathway RT² PCR Array (Qiagen) was used to assess changes in the gene expression profile of U87 cells after 24-hours exposure to 75 µg/ml CTX-AuPtNPs. This panel consists of 86 selected genes that were previously linked to cytotoxicity. Most of these genes were unaffected by the treatment, while 3 genes (*TRIB3*, *TAGLN* and *ASNS*) were upregulated and 13 (*UHRF1*, *LSS*, *HSPA1A*, *HSPA4*, *MKI67*, *HSPA8*, *CASP8*, *CASP9*, *METAP2*, *PPARA*, *AKT1*, *GCLM* and *ABCC2*) were downregulated (Table 1), compared to the untreated control. STRING analysis revealed that a significant number of the differentially expressed genes (DEGs) were linked in gene networks and that these networks mostly clustered into 1 group (Fig. 3). Except for 5 genes (METAP2, ASNS, LSS, ABCC2 and GCLM), all the other DEGs were connected in functional pathways which formed this cluster. The cluster contained both up and downregulated genes. The two upregulated genes (*TRIB3* and *ASNS*) are involved in endoplasmic reticulum stress (ER) and unfolded protein response (UPR) (Table 1), while the downregulated genes are involved in mitochondrial energy metabolism (*HSPA1A*) and apoptosis (*CASP8, CASP9, AKT1*).

Tribblespseudokinase 3 (*TRIB3*), *Transgelin* (*TAGLN*) and A*sparagine synthetase (ASNS)* were upregulated at 11.56, 3.51 and 2.32-fold, respectively in the treated cells (Table 1). Two of these genes, *TRIB3* and *ASNS* are involved in ER stress and the UPR, while *TAGLN* is involved in phospholipidosis. The ER plays an important role in protein synthesis and processing, lipid synthesis, and cellular homeostasis (Wusu *et al.*, 2021). Disturbances in any of these processes can result in the accumulation of unfolded or misfolded proteins within the ER lumen, and eventually the ER stress triggers the UPR and ER-associated degradation (ERAD) which functions to remove and degrade unfolded proteins (Chadwick and Lajoie, 2019; Wusu *et al.*, 2021). The UPR regulates both cell survival and cell death pathways to either restore cellular homeostasis or induce apoptosis, depending on the severity of the damage caused by ER stress (Boyce and Yuan, 2006; Adams *et al.*, 2019; Sisinni *et al.*, 2019). ERAD is usually considered as a self-rescuing response by which misfolded proteins are removed from the ER into the cytoplasm where they are degraded by the ubiquitin proteasome system and lysosome dependent ERAD system (Neal *et al.*, 2018). When unfolded proteins accumulate in the ER, chaperones such as Binding immunoglobulin protein (BiP) partake in protein folding, leading to a release of transmembrane proteins, Protein kinase RNA-like endoplasmic reticulum kinase (PERK), activating transcription factor-6 (ATF6), and inositol-requiring protein-1

(IRE1) which is responsible for the UPR (Adams *et al.*, 2019). Therefore, depending on the signalling pathway that is triggered, UPR can be either a cell self-rescuing or cell destructive response. For example, the PERK-mediated signalling pathway can either benefit cell survival through autophagy (Bu and Diehl, 2016) or cause apoptosis in cells via the translational upregulation of ATF4/CHOP (Bailey *et al.*, 2015; Rozpedek *et al.*, 2016; Lindner *et al.*, 2020). *TRIB3,* one of the 3 genes that was upregulated in this study, is a negative regulator of CHOP and could be a sensor for ER stress-induced apoptosis; where *TRIB3* functions to block CHOP activity when ER stress levels are not severe (Ohoka *et al.*, 2005). *TRIB3* is a pseudokinase affecting several cell functions, numerous studies suggest that *TRIB3* is upregulated under various stresses, including oxidative stress, ER stress, and metabolic stress (Yokoyama and Nakamura, 2011; Fang *et al.*, 2014; Li *et al.*, 2018; Sisinni *et al.*, 2019; Zhang *et al.*, 2019). Emerging studies have revealed that *TRIB3* can be increased by various stimulations and regulate the signalling pathways of transforming growth factor-β, mitogen-activated protein kinase, and phosphatidylinositol 3-kinase (PI3K), thus playing an important role in glucose/lipid metabolism, cell differentiation, and cell survival (Fang *et al.*, 2014; Tomcik *et al.*, 2016; Zhang *et al.*, 2017; Wang *et al.*, 2021).

When ER stress is severe, excess *TRIB3* is produced, which consequently leads to apoptosis (Shimizu *et al.*, 2012). Under ER stress, ERAD or the self-rescuing UPR signalling pathway is regarded as a means to prevent the worst-case scenario, i.e. cell death. If ER stress persists for long enough, caspase-dependent apoptosis is generally triggered resulting in cell death (Hetz and Papa, 2018). In the current study, *TRIB3* was upregulated which is indicative of ER stress. However, it is possible that ER stress was not severe enough in U87 cells exposed to 75 µg/ml CTX-AuPtNPs for 24-hours to induce apoptosis, as DEGs (*CASP8*, *CASP9* and *AKT1*) that are known to be involved in apoptosis pathways were downregulated (Table 1). This suggests that treatment with 75 µg/ml CTX-AuPtNPs induced stress in the cells and the cells are responding by activating cell survival responses. We demonstrated previously that higher concentrations of CTX-AuPtNPs induced cell death in U87 cells through the activation of apoptosis (Chapter 4). This result is in line with a recent study by Wusu *et al*. (2021) which reported that treatment of Caco-2 cells with 14 nm citrate capped AuNPs (at a concentration of 12.5 nM) resulted in the increased expression of genes involved in oxidative stress and antioxidant response, ER stress and UPR. Wusu *et al*. (2021) also found that *TRIB3* was amongst 13 genes that was upregulated in Caco-2 cells treated with AuNPs. Wusu *et al*. (2021) postulated that the increased expression of genes involved in oxidative stress and antioxidant response, ER stress and

UPR, heat shock response, and lipid metabolism resulted in cytoprotective cellular responses. Another study also showed that *TRIB3* were amongst 9 genes (*Herpud1*, *xbp-1s*, *CHOP/DDIT3*, *ADM2*, *BIP*, *Cas-12*, *ASNS* and *TRIB3*) that were shown to be upregulated in human bronchial epidermal cells (16HBE) treated with silver NPs (Huo *et al.*, 2015). The upregulation of *TRIB3*, *ASNS* and *TAGLN* in U87 cells treated with CTX-AuPtNPs for 24 hours seem to suggest that these cells are experiencing cellular stress (Table 1).

ASNS was previously shown to convert aspartate and glutamine to asparagine and glutamate and its expression is activated by the UPR and the AAR (amino acid response) (Lomelino *et al.*, 2017). A recent study by Karataş *et al.* (2021) showed that *ASNS* was significantly upregulated in PC3 prostate cancer cells after treatment with yttrium oxide NPs (Y_2O_3NPs) as a response to ER stress. Both *TRIB3* and *ASNS* are involved in ER stress and the UPR, and the two genes are upregulated after treatment with CTX-AuPtNP-treated cells. The overexpression of these genes may contribute to protecting the cells against severe ER stress (Yan *et al.*, 2014) and increased levels of oxidative stress (Paredes *et al.*, 2016).

TAGLN is an actin stress fibre binding protein and its expression affects cell survival, migration, and apoptosis of various cancer cells in different ways (Tsui *et al.*, 2019). TAGLN expression and function in cancer biology are dependent on the type and stage of cancer (Dvorakova, Nenutil and Bouchal, 2014; Elsafadi *et al.*, 2020). It was shown that the overexpression of *TAGLN* causes a significant increase in cell invasion and proliferation in U87 cells and primary GBM30 glioma neurospheres (Beyer *et al.*, 2018) and silencing of *TAGLN-2* decreased proliferation and invasion in gliomas (Han *et al.*, 2017). The downregulation of *TAGLN-2* expression significantly decreases cell invasion, proliferation, and colony formation in the human malignant meningioma cell line CH157, while significantly increasing the apoptosis rate of the cells (Pei *et al.*, 2018; Lei-Miao, Luis and Yong-Qing, 2019). A common feature of cancer cell invasion, metastasis, and cancer drug resistance is the rearrangement of actin filaments (Caswell and Zech, 2018; Lei-Miao, Luis and Yong-Qing, 2019) which can in part be attributed to the overexpression of *TAGLN*. This gene is also involved in phospholipidosis, which is a lysosomal storage disorder that is characterized by excessive intracellular accumulation of phospholipids within lamellar bodies (Breiden and Sandhoff, 2020). Phospholipidosis can be induced by cationic amphiphilic drugs (CAD). Several mechanisms for this effect of CADs were proposed, where these CADs may either block phospholipase activity directly, or form a complex with phospholipids preventing its access to the digestive enzyme (Shayman and

Abe, 2013). *TAGLN* is generally downregulated by compounds known to induce phospholipidosis (Atienzar *et al*., 2007).

In this study, 13 genes (*UHRF1*, *LSS*, *HSPA1A*, *HSPA4*, *MKI67*, *HSPA8*, *CASP8*, *CASP9*, *METAP2*, *PPARA*, *AKT1*, *GCLM*, *ABCC2*) were downregulated (Table 1). Some (e.g., *LSS*) are involved in molecular pathways such as lipid metabolism in particular phospholipidosis, cholestasis (*ABCC2*) and steatosis (*PPARA)*. Others are involved in ER stress and UPR (*UHRF1*), heat shock response (*HSPA4* and *HSPA8*), stress and antioxidant response (*GCLM*), immunotoxicity (*MKI67* and *METAP2*), mitochondrial energy metabolism (*HSPA1A*) and apoptosis (*CASP8*, *CASP9* and *AKT1*). Interestingly, while *TRIB3* and *ASNS* which is involved in ER stress and the UPR, and *TAGLN* which is involved in phospholipidosis were upregulated some other genes that were also involved in these processes were downregulated. Examples include *Ubiquitin-like with PHD and ring finger domains (UHRF1)* and *Lanosterol synthase* (*LSS*) (Table 1). Phospholipidosis and steatosis may occur as a result of altered lipid metabolism due to prolonged exposure to certain drugs and xenobiotics (Dash *et al.*, 2017; Klaunig, Li and Wang, 2018). Steatosis, cholestasis and phospholipidosis are considered markers of liver toxicity and can be used to assess the safety of drug candidates (Satapathy *et al.*, 2015).

UHRF1 is a 90-kDa nuclear protein that plays an important role in cancer progression through epigenetic regulation (Ashraf *et al.*, 2017). *UHRF1* plays a role in cancer cells by keeping these cells in a proliferated state (Kent *et al*., 2016). The expression of *UHRF1* was more significantly reduced (5.66-fold) than any other gene after treatment with 75 µg/ml of CTX-AuPtNPs. This is in line with a previous study reporting on the downregulation of *UHRF1* in U87 cells after treatment with Y$_2$O$_3$NPs (Karataş *et al.*, 2021). Pogribna *et al.* (2020) recently reported on the effect of titanium dioxide NPs (TiO$_2$NPs) on DNA methylation in multiple human cell lines, with a decrease in *UHRF1* expression in Caco-2 cells, HepG2 cells, and A-431 cells and an increase in NL20 cells, indicating that the aberrant expression of epigenetic regulatory genes involved in DNA methylation including *UHRF1* in TiO$_2$NP exposed cells, was cell type dependent. *UHRF1* plays an important role in the inheritance of the DNA epigenetic marks from the mother cell to the daughter cells (Bronner, Krifa and Mousli, 2013). It also appears that preventing the transmission of these marks via knock-down of *UHRF1*, leads to an activation of pro-apoptotic pathways (Avvakumov *et al.*, 2008; Karambataki *et al.*, 2010). Therefore, inhibiting *UHRF1* expression would be an efficient way to block the development of a tumour by blocking the transformation and the proliferation of the cells, as well as

200

the vascularization of the tumour (Alhosin *et al.*, 2011). A previous study demonstrated that the pro-apoptotic activity of anti-cancer compounds in U373 human GB astrocytoma cells is linked to a repression of *UHRF1* (Krifa, 2014). *UHRF1* not only plays an important role in carcinogenesis, but also in toxoplasmosis, by effectively stopping the proliferation of the parasites, which is occasionally fatal to people with a weakened immune system and can cause blindness in the major pathology of ocular toxoplasmosis (Unoki, Brunet and Mousli, 2009). Interestingly, toxoplasmosis was one of the enriched pathways identified when the interactions networks between the DEGs was analysed showing that 5 genes (*AKT1, CASP8, CASP9, HSPA1A* and *HSPA8*) are functionally connected (Table 2). These genes can be associated with cytoprotective mechanism of the U87 cells after treatment with 75 µg/ml CTX-AuPtNPs for 24-hour exposure.

A number of *in vitro* and *in vivo* studies showed that treatments with AuNPs can alter the lipid metabolism in cells and in animals (Chen *et al.*, 2018a). As a result these treatments have been proposed as a possible way to reverse obesity (Lai *et al.*, 2015; Chen *et al.*, 2018b). In this study, *LSS*, *Peroxisome proliferator-activated receptor alpha* (*PPARA*) which is involved in steatosis and *ABCC2* which is involved in cholestasis were downregulated. *LSS* is responsible for the biosynthesis of cholesterol, steroid hormones, and vitamin D (Wada *et al.*, 2020). The downregulation of *LSS* in this study indicated disruption of cholesterol homeostasis. *LSS* has also been linked to the prognosis of GB patients and may be a potential therapeutic target (Phillips *et al.*, 2019; Han *et al.*, 2020), as the upregulation of cholesterol associated genes is implicated in novel resistance mechanism in U87 cells after treatment with Archazolid B compound (Hamm *et al.*, 2014). *PPARA* is a transcription factor and a key regulator of lipid metabolism peroxisome through β-oxidation of fatty acids (Zhao *et al*., 2018). The decreased expression of *PPARA* suggests that de novo lipogenesis is inhibited in ER stressed cells as previously reported where the *PPARA* was downregulated in Caco-2 cells after treatment with citrate AuNPs (Wusu *et al.*, 2021). Other studies reported that ER stress increased lipogenesis (Kammoun *et al.*, 2009; Yu *et al.*, 2013; Choi *et al.*, 2014). However, the effect of ER stress on lipid metabolism may be cell type specific (Chiappisi *et al.*, 2017; Sun *et al.*, 2018; Lemmer *et al.*, 2021). The *ABCC2* gene provides instructions for producing a protein called multidrug resistance protein 2 (MRP2) (Zhang *et al.*, 2015). This protein is one of a family of multidrug resistance proteins involved in the transport of substances out of cells. For example, MRP2 clears certain drugs from organs and tissues, playing a part in drug metabolism (Jedlitschky, Hoffmann and Kroemer, 2006). In the current study, the *ABCC2* gene was downregulated which may suggest that

CTX-AuPtNPs interferes with the production of MRP2, which was in line with a previous study where C3A cells was exposed to 40 nm PEG-AuNP (Choi and Joo, 2018).

Three genes (*CASP8, CASP9* and *AKT1*) that are involved in the apoptosis pathway were also downregulated in this study (Table 1). While CASP*8* and *CASP9* are pro-apoptotic genes, *AKT1* is an anti-apoptotic gene. A previous study which demonstrated the dose-dependent cytotoxicity of 40 nm PEG-AuNP over 24 hours also showed the differential expression of these 3 genes in C3A cells (Choi and Joo, 2018). In another study treatments of MCF-7 cells with AuNPs at concentrations as high as 200 µg/ml for 24 hours exerted concentration-dependent cytotoxicity and significant upregulation of *p53*, *Bax*, *CASP3* and *CASP9* (Selim and Hendi, 2012). The downregulation of *CASP8* is in line with the treatment of low dose citrate AuNPs treatment to Caco-2 cells (Wusu *et al.*, 2021). Several studies showed that treatment with PtNPs causes an increase in intracellular ROS production, which results in oxidative damage and apoptosis through CASP3 activation (Alshatwi, Athinarayanan and Vaiyapuri Subbarayan, 2015; Kutwin *et al.*, 2017; Almeer *et al.*, 2018; Almarzoug *et al.*, 2020). Apoptosis is stimulated by intrinsic and extrinsic pathways that merge through the activation of caspase 3, leading to apoptosis (Solano-Gálvez *et al.*, 2018). Caspase 8 and caspase 9 activate caspase 3 by proteolytic cleavage and caspase 3 then cleaves vital cellular proteins or other caspases. The expression of Fas Ligand (*FASLG*), which causes apoptosis by activating the caspase 8 cascade, was shown to increase in U87 and PC3 cells treated with Y_2O_3NPs (Karataş *et al.*, 2021). The downregulation of *AKT* in this study is in line with the findings of other published reports which studied similar bimetallic NPs. In a study by Shin *et al.* (2018), AKT phosphorylation was downregulated in the EJ human bladder carcinoma cell line after treatment with low doses of AuPtNPs. Fernández-Gallardo *et al.* (2015) demonstrated that heterometallic NPs made with titanium and gold could inhibit the growth of renal cancers significantly, both *in vitro* and *in vivo* studies, by suppressing the activity of *AKT*. The downregulation of these genes which are known to play a role in the control of apoptosis seem to support the notion that U87 cells treated with 75 µg/ml of CTX-AuPtNPs over 24 hours is under stress, but that the cells have activated cytoprotective mechanisms to prevent the activation of cell death.

Three heat shock proteins (HSPs), which include *HSPA1A, HSPA4* and *HSPA8* were also downregulated in U87 cells (Table 1). HSP70 is encoded by the HSPA1A gene and interacts with several other heat shock proteins to mediate protein refolding and acts as molecular chaperones when cells are exposed to stressors (Radons, 2016). It directly impairs the activation of initiator caspases (caspase-8 and -9), effector caspases (caspase-3) and pro-apoptotic proteins (such as Bax and Bak) (Parrish, Freel and

202

Kornbluth, 2013). At a mitochondrial level, HSP70 prevents mitochondrial membrane permeabilization through inhibition of Bax activity to block the release of cytochrome c, SMAC, AIF, and Endo-G (Wang *et al.*, 2014). Also, HSP70 protects cells from apoptosis by interacting with and inhibiting AIF and Apaf-1 proapoptotic activity, thereby impairing apoptosis downstream to mitochondria (Guo *et al.*, 2020). It is possible that the downregulation of these heat shock proteins could be due to cellular stress not being severe enough.

Glutathione (GSH) is a tripeptide that scavenges excess ROS produced by tumour cells owing to their increased metabolic activity (Mohapatra, Sathiyamoorthy and Park, 2021). The synthesis of GSH in cells is a two-step ATP-mediated biosynthesis process. The first step is the catalysis of glutamate-cysteine ligase (GSH) by γ-glutamyl cysteine ligase (GCL), which is composed of two micro-units, namely, GCLC (a highly catalytic unit) and glutamate-cysteine ligase, modifier subunit (*GCLM*) (a modifier unit) (Mohapatra, Sathiyamoorthy and Park, 2021). GSH is an important hydrophilic intracellular antioxidant that protects cells against different stressors such as ROS, xenobiotics and metal exposure (Gaucher *et al.*, 2018; Kwon *et al.*, 2019; Wusu *et al.*, 2021). *GCLM* was downregulated in this study suggesting that CTX-AuPtNPs did not cause any antioxidant stress response, which is in accordance with a previous study where *GCLM* was downregulated in U87 cells after treatment with bimetallic NPs (Karataş *et al.*, 2021), suggesting that ROS activity in cells was not significant. This is in contrast with other studies which showed the upregulation of *GCLM*, as a result of ROS after treatment with other metallic NPs including gold, silver and iron oxide NPs (Bouwmeester *et al.*, 2011; Luo *et al.*, 2020; Wusu *et al.*, 2021). Other studies reported that increased ROS caused decreased levels of GSH in cells following incubation with AuNPs (Gao *et al.*, 2011; Rizwan *et al.*, 2017; M. Liu *et al.*, 2021). The reduction in GSH by metallic NPs, via the formation of a metal-GSH thiolate, induces the generation of excess ROS at the tumour site, thereby increasing inflammation and severe immune response (Mohapatra, Sathiyamoorthy and Park, 2021).

Two genes involved in immunotoxicity *MKI67* and *METAP2* were downregulated, which is in line with a previous study where *MKI67* was one of the genes that was downregulated in U87 cells treated with Y$_2$O$_3$NPs (Karataş *et al.*, 2021). *MKI67* is a nuclear protein that plays a role in cell proliferation and is also considered as an immune toxicity marker (Scholzen and Gerdes, 2000). It is reported that *METAP2* is upregulated during cell proliferation and previous studies showed that that knocking down *METAP2* in GB and other cancer types slowed the tumour cell proliferation and had anti-

angiogenic activity (Selvakumar *et al.*, 2004; Bernier *et al.*, 2005; Chun *et al.*, 2005; Selvakumar *et al.*, 2009; Lin *et al.*, 2018).

In this study, the low concentration, exposure time and the specific physicochemical properties of CTX-AuPtNPs all contributed to the cellular response of U87 cells. A 24-hour treatment with CTX-AuPtNPs, seem to induce cellular stress in the U87 cells, however genes implicated in cell death pathways was not upregulated. Therefore, the specific conditions used here to treat U87 cells can be considered in the future for hyperthermia studies. To the best of our knowledge this is the first report on bimetallic AuPtNPs investigating the expression levels of genes involved in brain cancer cell line and provides insight into low dose AuPtNPs cytotoxicity.

Table 1. Differentially expressed genes (DEGs) in U87 cells treated with CTX-AuPtNPs at 75 µg/ml for 24 hours treatment

DEGs	Gene Symbol	Fold Regulation	P-value	Gene Function
Upregulated				
Tribbles homolog 3 (Drosophila)	*TRIB3*	11.56	0.000042	Endoplasmic Reticulum Stress & Unfolded Protein Response
Transgelin	*TAGLN*	3.51	0.041508	Phospholipidosis
Asparagine synthetase (glutamine-hydrolyzing)	*ASNS*	2.23	0.003107	Endoplasmic Reticulum Stress & Unfolded Protein Response
Downregulated				
Ubiquitin-like with PHD and ring finger domains 1	*UHRF1*	-5.66	0.044809	Endoplasmic Reticulum Stress & Unfolded Protein Response
Lanosterol synthase (2,3-oxidosqualene-lanosterol cyclase)	*LSS*	-3.78	0.029725	Phospholipidosis
Heat shock 70kDa protein 1A	*HSPA1A*	-2.36	0.000297	Mitochondrial Energy Metabolism
Heat shock 70kDa protein 4	*HSPA4*	-2.04	0.023754	Heat Shock Response

204

Antigen identified by monoclonal antibody Ki-67	*MKI67*	-1.78	0.048524	Immunotoxicity
Heat shock 70kDa protein 8	HSPA8	-1.77	0.033042	Heat Shock Response
Caspase 8, apoptosis-related cysteine peptidase	CASP8	-1.68	0.038765	Apoptosis
Cytochrome P450, family 2, subfamily D, polypeptide 6	CASP9	-1.59	0.042728	Apoptosis
Methionyl aminopeptidase 2	METAP2	-1.52	0.024686	Immunotoxicity
Peroxisome proliferator-activated receptor alpha	PPARA	-1.48	0.015455	Steatosis
V-akt murine thymoma viral oncogene homolog 1	AKT1	-1.42	0.038168	Apoptosis
Glutamate-cysteine ligase, modifier subunit	GCLM	-1.32	0.041377	Stress & Antioxidant Response
ATP-binding cassette, sub-family C (CFTR/MRP), member 2	*ABCC2*	-1.32	0.007740	Cholestasis

Fold changes in differentailly expressed genes (DEGs)

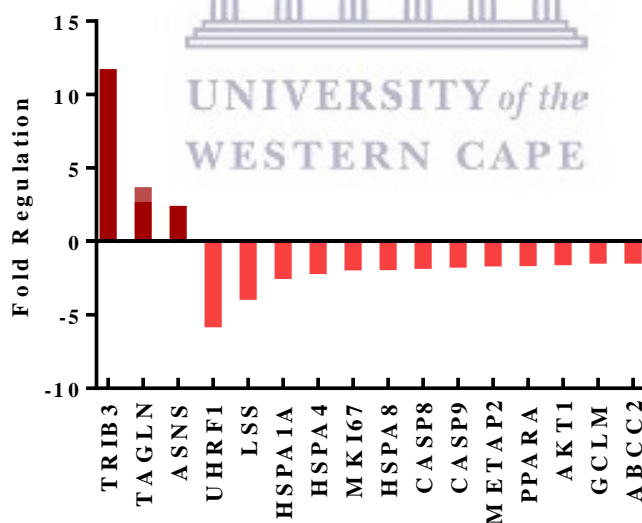**Figure 2. Bar chart demonstrating the fold changes in DEGs in U87 cells after treatment with CTX-AuPtNPs at 75 µg/ml for 24 hours**. Genes with p values < 0.05 and absolute fold change ≥ 1

were considered DEGs. Bars in red denote fold changes of upregulated genes and bars in pink indicates downregulated genes.

3.3. Functional interactions of proteins encoded by DEGs

Using STRING version 11.5 analysis, the interactions of proteins encoded by the DEGs were investigated through text-mining, curated databases, experimentally determined and co-expression studies as previously reported (Wusu *et al*., 2021). As shown in Figure 3., DEGs are grouped into one cluster. The cluster shows 11 interactions of proteins of DEGs (*AKT1*, *CASP8*, *CASP9*, *HSPA1A*, *HSPA8*, *HSPA4*, *MK167*, *PPARA*, *TAGLN*, *TRIB3* and *UHFR1*), while 4 DEGs (*ABCC2*, *GCLM*, *METAP2* and *LSS*) can be considered independent of these protein interactions.

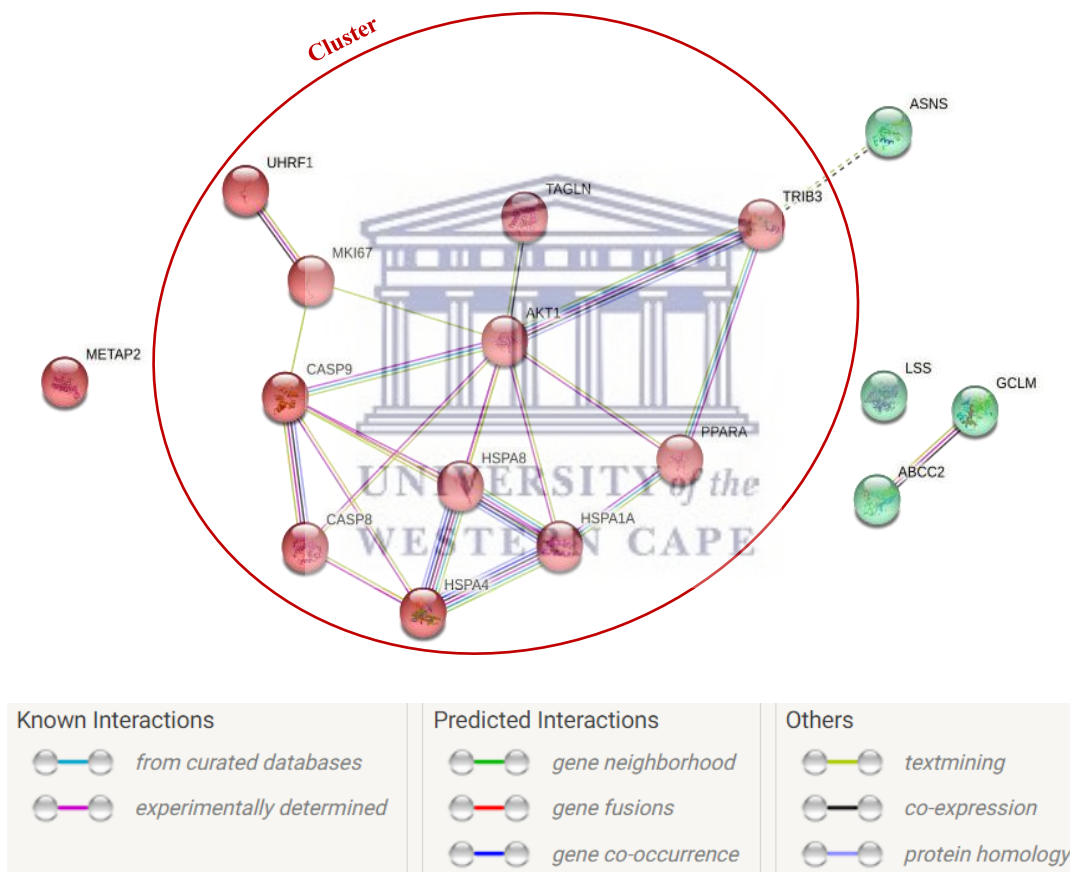

Figure 3. Protein networks established from the interactions between DEGs as reported from STRING database. The protein networks were searched against *Homo sapiens*. Each of the lines are protein interactions from known, predicted or other interactions. Dotted lines refer to undetermined interactions between the proteins and similar colours represent proteins with related functions.

206

Table 2. Enriched pathways involved in the network interaction between DEGs

Biological Processes	P-Value	Genes
Toxoplasmosis	0.000019	*AKT1, CASP8, CASP9, HSPA1A, HSPA8*
Legionellosis	0.000072	*CASP8, CASP9, HSPA1A, HSPA8*
Influenza A	0.0023	*AKT1, CASP9, HSPA1A, HSPA8*
Apoptosis	0.0042	*AKT1, CASP8, CASP9*
Antigen processing and presentation	0.0062	*HSPA1A, HSPA4, HSPA8*
Estrogen signalling pathway	0.010	*AKT1, HSPA1A, HSPA8*
Insulin resistance	0.012	*AKT1, PPARA, TRIB3*
Measles	0.018	*AKT1, HSPA1A, HSPA8*
Hepatitis B	0.021	*AKT1, CASP8, CASP9*
Non-alcoholic fatty liver disease (NAFLD)	0.023	*AKT1, CASP8, PPARA*
Tuberculosis	0.013	*AKT1, CASP8, CASP9*

4. Conclusion

BNPs such as AuPtNPs have attracted much interest in recent years due to their application in catalytic processes, electronics, and nanomedicine (Formaggio *et al.*, 2019; Oladipo *et al.*, 2020; Wang, Hao and Li, 2020; Chaturvedi *et al.*, 2021). AuPtNPs have diverse biological activities and have been developed as novel diagnostic and therapeutic agents to manage cancer. We previously demonstrated the synthesis of AuPtNP that was functionalized with the cancer targeting peptide, CTX (Chapter 3). CTX-AuPtNPs can potentially be applied in RF induced ablation of deep-seated cancer cells. However, although there are many studies related to the efficacy of other BNPs, there are limited published reports on the cytotoxic potential of AuPtNP, not to mention the molecular effects of these NPs. Therefore, this study aimed to investigate the early cytotoxicity of CTX-AuPtNPs in U87 cells by assessing the effects of the NPs on the expression of a panel of genes that are known to be involved in cell death.

The appropriate concentration of CTX-AuPtNPs and exposure time to assess changes in gene expression in U87 cells was established at 75 µg/ml and 24-hours, respectively. The gene expression studies suggests that under these conditions the U87 cells are experiencing ER stress and that the cells

207

activated cytoprotective responses. At this stage the damage to the cells is not severe enough to trigger cell death pathways. It is very likely that if the cells were treated for a period longer than 24 hours that the damage to the cells will be more severe resulting in the increased expression of genes that will result in the death of the cells, as was observed in our previous study (Chapter 4).

In conclusion, the findings provide guidance in the evaluation of possible mechanisms related to early cytotoxicity of CTX-AuPtNPs at 24 hours exposure to brain cancer cells and this information will be useful for future experiments investigating the hyperthermia potential of target specific CTX-AuPtNPs using RF field-induced hyperthermia treatment and as promising candidates for clinical applications in brain cancer. Future work will also investigate the changes in gene expression in U87 cells at increasing treatment durations with 75 µg/ml CTX-AuPtNPs.

5. References

Adams, C.J., Kopp, M.C., Larburu, N., Nowak, P.R. and Ali, M.M.U. (2019). Structure and Molecular Mechanism of ER Stress Signaling by the Unfolded Protein Response Signal Activator IRE1. *Frontiers in Molecular Biosciences*, 6: 11.

Alhosin, M., Sharif, T., Mousli, M., Etienne-Selloum, N., Fuhrmann, G., Schini-Kerth, V.B., and Bronner, C. (2011). Down-regulation of UHRF1, associated with re-expression of tumor suppressor genes, is a common feature of natural compounds exhibiting anti-cancer properties. *Journal of Experimental & Clinical Cancer Research: CR*, 30(1): 41.

Almarzoug, M.H.A., Ali, D., Alarifi, S., Alkahtani, S. and Alhadheq, A.M. (2020). Platinum nanoparticles induced genotoxicity and apoptotic activity in human normal and cancer hepatic cells via oxidative stress-mediated Bax/Bcl-2 and caspase-3 expression. *Environmental Toxicology*, 35(9): 930–941.

Almeer, R.S., Ali, D., Alarifi, S., Alkahtani, S. and Almansour, M. (2018). Green Platinum Nanoparticles Interaction With HEK293 Cells: Cellular Toxicity, Apoptosis, and Genetic Damage. *Dose-Response*, 16(4): 1559325818807382.

Alshatwi, A.A., Athinarayanan, J. and Vaiyapuri Subbarayan, P. (2015). Green synthesis of platinum nanoparticles that induce cell death and G2/M-phase cell cycle arrest in human cervical cancer cells. *Journal of Materials Science. Materials in Medicine*, 26(1): 5330.

Arora, N., Thangavelu, K. and Karanikolos, G.N. (2020). Bimetallic Nanoparticles for Antimicrobial Applications. *Frontiers in Chemistry*, 8: 412.

Ashraf, W., Ibrahim, A., Alhosin, M., Zaayter, L., Khalid, O., Papin, C., Ahmad, T., Hamiche, A., Mély, Y., Bronner, C. and Mousli, M. (2017). The epigenetic integrator UHRF1: On the road to become a universal biomarker for cancer. *Oncotarget*, 8(31): 51946-51962.

Atienzar, F., Gerets, H., Dufrane, S., Tilmant, K., Cornet, M., Dhalluin, S., Ruty, B., Rose, G. and Canning, M. (2007). Determination of Phospholipidosis Potential Based on Gene Expression Analysis in HepG2 Cells. *Toxicological Sciences: An Official Journal of the Society of Toxicology* 96 (1): 101–14.

Attarilar, S., Yang, Jinfan, Ebrahimi, M., Wang, Q., Liu, J., Tang, Y. and Yang, J. (2020). The Toxicity Phenomenon and the Related Occurrence in Metal and Metal Oxide Nanoparticles: A Brief Review From the Biomedical Perspective. *Frontiers in Bioengineering and Biotechnology*, 8: 822.

Avvakumov, G.V., Walker, J.R., Xue, S., Li, Y., Duan, S., Bronner, C., Arrowsmith, C.H. and Dhe-Paganon, S. (2008). Structural basis for recognition of hemi-methylated DNA by the SRA domain of human UHRF1. *Nature*, 455(7214): 822–825.

Ayed, A.S., Omran, M.A.A.A., Nabil, Z., Strong, P., Newton, K. and Abdel Rahman, M. A. (2021). C-Terminal Amidation of Chlorotoxin Does Not Affect Tumour Cell Proliferation and Has No Effect on Toxin Cytotoxicity. *International Journal of Peptide Research and Therapeutics*, 27(1): 659-667.

Bailey, C.M., Kamaloo, E., Waterman, K.L., Wang, K.F., Nagarajan, R. and Camesano, T.A. (2015). Size dependence of gold nanoparticle interactions with a supported lipid bilayer: A QCM-D study. *Biophysical Chemistry*, 203–204: 51–61.

Bernier, S.G., Taghizadeh, N., Thompson, C.D., Westlin, W.F. and Hannig, G. (2005). Methionine aminopeptidases type I and type II are essential to control cell proliferation. *Journal of Cellular Biochemistry*, 95(6): 1191–1203.

Beyer, S.J., Bell, E.H., McElroy, J.P., Fleming, J.L., Cui, T., Becker, A., Bassett, E., Johnson, B., Gulati, P., Popp, I., Staszewski, O., Prinz, M., Grosu, A.L., Haque, S.J. and Chakravarti, A. (2018). Oncogenic transgelin-2 is differentially regulated in isocitrate dehydrogenase wild-type vs. mutant gliomas. *Oncotarget*, 9(98): 37097–37111.

Beyk, J. and Tavakoli, H. (2019). Selective radiofrequency ablation of tumor by magnetically targeting of multifunctional iron oxide–gold nanohybrid. *Journal of Cancer Research and Clinical Oncology*, 145(9): 2199–2209.

Bhagwate, A.V., Liu, Y., Winham, S.J., McDonough, S.J., Stallings-Mann, M.L., Heinzen, E.P., Davila, J.I., Vierkant, R.A., Hoskin, T.L., Frost, M., Carter, J.M., Radisky, D.C., Cunningham, J.M., Degnim, A.C. and Wang, C. (2019). Bioinformatics and DNA-extraction strategies to reliably detect genetic variants from FFPE breast tissue samples. *BMC Genomics*, 20(1): 689.

Boomi, P., Poorani, G.P., Palanisamy, S., Selvam, S., Ramanathan, G., Ravikumar, S., Barabadi, H., Prabu, H.G., Jeyakanthan, J. and Saravanan, M. (2019). Evaluation of Antibacterial and Anticancer Potential of Polyaniline-Bimetal Nanocomposites Synthesized from Chemical Reduction Method. *Journal of Cluster Science*, 30(3): 715–726.

Bouwmeester, H., Poortman, J., Peters, R.J., Wijma, E., Kramer, E., Makama, S., Puspitaninganindita, K., Marvin, H.J.P., Peijnenburg, A.A.C.M. and Hendriksen, P.J.M. (2011). Characterization of translocation of silver nanoparticles and effects on whole-genome gene expression using an in vitro intestinal epithelium coculture model. *ACS nano*, 5(5): 4091–4103.

Boyce, M. and Yuan, J. (2006). Cellular response to endoplasmic reticulum stress: a matter of life or death. *Cell Death & Differentiation*, 13(3): 363–373.

Breiden, B. and Sandhoff, K. (2020). Emerging mechanisms of drug-induced phospholipidosis. *Biological Chemistry*, 401(1): 31–46.

Bronner, C., Krifa, M. and Mousli, M. (2013). Increasing role of UHRF1 in the reading and inheritance of the epigenetic code as well as in tumorogenesis. *Biochem Pharmacology*, 86(12): 1643–1649.

Bu, Y. and Diehl, J.A. (2016). PERK integrates oncogenic signaling and cell survival during cancer development. *Journal of cellular physiology*, 231(10): 2088–2096.

Caswell, P.T. and Zech, T. (2018). Actin-Based Cell Protrusion in a 3D Matrix. *Trends in Cell Biology*, 28(10): 823–834.

Chadwick, S.R. and Lajoie, P. (2019). Endoplasmic Reticulum Stress Coping Mechanisms and Lifespan Regulation in Health and Diseases. *Frontiers in Cell and Developmental Biology*, 7: 84.

Chan, M.-H., Lu, C.-N., Chung, Y.-L., Chang, Y.-C., Li, C.-H., Chen, C.-L., Wei, D.-H. and Hsiao, M. (2021). Magnetically guided theranostics: montmorillonite-based iron/platinum nanoparticles for enhancing in situ MRI contrast and hepatocellular carcinoma treatment. *Journal of Nanobiotechnology*, 19(1): 08.

Chaturvedi, V.K., Yadav, N., Rai, N.K., Bohara, R.A., Rai, S.N., Aleya, L. and Singh, M.P. (2021). Two birds with one stone: oyster mushroom mediated bimetallic Au-Pt nanoparticles for agro-waste management and anticancer activity. *Environmental Science and Pollution Research International*, 28(11): 13761–13775.

Chen, H., Ng, J.P.M., Bishop, D.P., Milthorpe, B.K. and Valenzuela, S.M. (2018a). Gold nanoparticles as cell regulators: beneficial effects of gold nanoparticles on the metabolic profile of mice with pre-existing obesity. *Journal of Nanobiotechnology*, 16(1): 88.

Chen, H., Ng, J.P.M., Tan, Y., McGrath, K., Bishop, D.P., Oliver, B., Chan, Y.L., Cortie, M.B., Milthorpe, B.K. and Valenzuela, S.M. (2018b). Gold nanoparticles improve metabolic profile of mice fed a high-fat diet. *Journal of Nanobiotechnology*, 16(1): 11.

Chiappisi, E., Ringseis, R., Eder, K. and Gessner, D.K. (2017). Effect of endoplasmic reticulum stress on metabolic and stress signaling and kidney-specific functions in Madin-Darby bovine kidney cells. *Journal of Dairy Science*, 100(8): 6689–6706.

Choi, K. and Joo, H. (2018). Assessment of Gold Nanoparticles-Inhibited Cytochrome P450 3A4 Activity and Molecular Mechanisms Underlying Its Cellular Toxicity in Human Hepatocellular Carcinoma Cell Line C3A. *Nanoscale Research Letters*, 13(1): 279.

Choi, Y.-J., Shin, H.-S., Choi, H.S., Park, J.-W., Jo, I., Oh, E.-S., Lee, K.-Y., Lee, B.-H., Johnson, R.J. and Kang, D.-H. (2014). Uric acid induces fat accumulation via generation of endoplasmic reticulum stress and SREBP-1c activation in hepatocytes. *Laboratory Investigation; a Journal of Technical Methods and Pathology*, 94(10): 1114–1125.

Chun, E., Han, C.K., Yoon, J.H., Sim, T.B., Kim, Y.-K. and Lee, K.-Y. (2005). Novel inhibitors targeted to methionine aminopeptidase 2 (MetAP2) strongly inhibit the growth of cancers in xenografted nude model. *International Journal of Cancer*, 114(1): 124–130.

Cohen-Inbar, O. and Zaaroor, M. (2016). Glioblastoma multiforme targeted therapy: The Chlorotoxin story. *Journal of Clinical Neuroscience: Official Journal of the Neurosurgical Society of Australasia*, 33: 52–58.

Corr, S.J., Shamsudeen, S., Vergara, L.A., Ho, J.C.-S., Ware, M.J., Keshishian, V., Yokoi, K., Savage, D.J., Meraz, I.M., Kaluarachchi, W., Cisneros, B.T., Raoof, M., Nguyen, D.T., Zhang, Y., Wilson, L.J., Summers, H., Rees, P., Curley, S.A. and Serda, R.E. (2015). A New Imaging Platform for Visualizing Biological Effects of Non-Invasive Radiofrequency Electric-Field Cancer Hyperthermia. *PLOS ONE*, 10(8): e0136382.

Costa, P.M., Cardoso, A.L., Mendonça, L.S., Serani, A., Custódia, C., Conceição, M., Simões, S., Moreira, J.N., Pereira de Almeida, L. and Pedroso de Lima, M.C. (2013). Tumor-targeted Chlorotoxin-coupled Nanoparticles for Nucleic Acid Delivery to Glioblastoma Cells: A Promising System for Glioblastoma Treatment. *Molecular Therapy. Nucleic Acids*, 2(6): e100.

Dash, A., Figler, R.A., Sanyal, A.J. and Wamhoff, B. (2017). Drug-induced steatohepatitis. *Expert opinion on drug metabolism & toxicology*, 13(2): 193–204.

Dastpeyman, M., Giacomin, P., Wilson, D., Nolan, M.J., Bansal, P.S. and Daly, N.L. (2019). A C-Terminal Fragment of Chlorotoxin Retains Bioactivity and Inhibits Cell Migration. *Frontiers in Pharmacology*, 10: 250.

Depciuch, J., Stec, M., Klebowski, B., Baran, J. and Parlinska-Wojtan, M. (2019). Platinum–gold nanoraspberries as effective photosensitizer in anticancer photothermal therapy. *Journal of Nanobiotechnology*, 17(1): 107.

Deshane, J., Garner, C.C. and Sontheimer, H. (2003). Chlorotoxin Inhibits Glioma Cell Invasion via Matrix Metalloproteinase-2. *Journal of Biological Chemistry*, 278(6): 4135–4144.

Dvorakova, M., Nenutil, R. and Bouchal, P. (2014). Transgelins, cytoskeletal proteins implicated in different aspects of cancer development. *Expert Review of Proteomics*, 11(2): 149–165.

Elsafadi, M., Manikandan, M., Almalki, S., Mahmood, A., Shinwari, T., Vishnubalaji, R., Mobarak, M., Alfayez, M., Aldahmash, A., Kassem, M. and Alajez, N.M. (2020). Transgelin is a poor prognostic factor associated with advanced colorectal cancer (CRC) stage promoting tumor growth and migration in a TGFβ-dependent manner. *Cell Death & Disease*, 11(5): 1–13.

Fahmy, S.A., Preis, E., Bakowsky, U. and Azzazy, H.M.E.-S. (2020). Platinum Nanoparticles: Green Synthesis and Biomedical Applications. *Molecules*, 25(21): 4981.

Fang, N., Zhang, W., Xu, S., Lin, H., Wang, Z., Liu, H., Fang, Q., Li, C., Peng, L. and Lou, J. (2014). TRIB3 alters endoplasmic reticulum stress-induced β-cell apoptosis via the NF-κB pathway. *Metabolism: Clinical and Experimental*, 63(6): 822–830.

Fathima, R. and Mujeeb, A. (2021). Enhanced nonlinear and thermo optical properties of laser synthesized surfactant-free Au-Pt bimetallic nanoparticles. *Journal of Molecular Liquids*, 343: 117711.

Fernández-Gallardo, J., T. Elie, B., Sadhukha, T., Prabha, S., Sanaú, M., A. Rotenberg, S., W. Ramos, J. and Contel, M. (2015). Heterometallic titanium–gold complexes inhibit renal cancer cells in vitro and in vivo. *Chemical Science*, 6(9): 5269–5283.

Formaggio, D.M.D., de Oliveira Neto, X.A., Rodrigues, L.D.A., de Andrade, V.M., Nunes, B.C., Lopes-Ferreira, M., Ferreira, F.G., Wachesk, C.C., Camargo, E.R., Conceição, K. and Tada, D.B. (2019). In vivo toxicity and antimicrobial activity of AuPt bimetallic nanoparticles. *Journal of Nanoparticle Research*, 21(11): 244.

Gao, W., Xu, K., Ji, L. and Tang, B. (2011). Effect of gold nanoparticles on glutathione depletion-induced hydrogen peroxide generation and apoptosis in HL7702 cells. *Toxicology Letters*, 205(1): 86–95.

Gaucher, C., Boudier, A., Bonetti, J., Clarot, I., Leroy, P. and Parent, M. (2018). Glutathione: Antioxidant Properties Dedicated to Nanotechnologies. *Antioxidants*, 7(5): 62.

Glazer, E.S. and Curley, S.A. (2011). Non-invasive radiofrequency ablation of malignancies mediated by quantum dots, gold nanoparticles and carbon nanotubes. *Therapeutic Delivery*, 2(10): 1325–1330.

Guo, Z., Song, T., Wang, Z., Lin, D., Cao, K., Liu, P., Feng, Y., Zhang, X., Wang, P., Yin, F., Dai, J., Zhou, S. and Zhang, Z. (2020). The chaperone Hsp70 is a BH3 receptor activated by the pro-apoptotic Bim to stabilize anti-apoptotic clients. *Journal of Biological Chemistry*, 295(37): 12900–12909.

Gurunathan, S., Jeyaraj, M., Kang, M.-H. and Kim, J.-H. (2020). Anticancer Properties of Platinum Nanoparticles and Retinoic Acid: Combination Therapy for the Treatment of Human Neuroblastoma Cancer. *International Journal of Molecular Sciences*, 21(18): E6792.

Hamm, R., Zeino, M., Frewert, S. and Efferth, T. (2014). Up-regulation of cholesterol associated genes as novel resistance mechanism in glioblastoma cells in response to archazolid B. *Toxicology and Applied Pharmacology*, 281(1): 78–86.

Han, M.-Z., Xu, R., Xu, Y.-Y., Zhang, X., Ni, S.-L., Huang, B., Chen, A.-J., Wei, Y.-Z., Wang, S., Li, W.-J., Zhang, Q., Li, G., Li, X.-G. and Wang, J. (2017). TAGLN2 is a candidate prognostic biomarker promoting tumorigenesis in human gliomas. *Journal of experimental & clinical cancer research: CR*, 36(1): 155.

Han, X., Wang, D., Zhao, P., Liu, C., Hao, Y., Chang, L., Zhao, J., Zhao, W., Mu, L., Wang, J., Li, H., Kong, Q. and Han, J. (2020). Inference of Subpathway Activity Profiles Reveals Metabolism Abnormal Subpathway Regions in Glioblastoma Multiforme. *Frontiers in Oncology*, 10: 1549.

Hetz, C. and Papa, F.R. (2018). The Unfolded Protein Response and Cell Fate Control. *Molecular Cell*, 69(2): 169–181.

Huang, D.W., Sherman, B.T., Zheng, X., Yang, J., Imamichi, T., Stephens, R. and Lempicki, R.A. (2009). Extracting biological meaning from large gene lists with DAVID. *Current protocols in bioinformatics* 27(13.11): 11-13

Huo, L., Chen, R., Zhao, L., Shi, X., Bai, R., Long, D., Chen, F., Zhao, Y., Chang, Y.-Z. and Chen, C. (2015). Silver nanoparticles activate endoplasmic reticulum stress signaling pathway in cell and mouse models: The role in toxicity evaluation. *Biomaterials*, 61: 307–315.

Jedlitschky, G., Hoffmann, U. and Kroemer, H.K. (2006). Structure and function of the MRP2 (ABCC2) protein and its role in drug disposition. *Expert Opinion on Drug Metabolism & Toxicology*, 2(3): 351–366.

Jeyaraj, M., Gurunathan, S., Qasim, M., Kang, M.-H. and Kim, J.-H. (2019). A Comprehensive Review on the Synthesis, Characterization, and Biomedical Application of Platinum Nanoparticles. *Nanomaterials*, 9(12): 1719.

Kammoun, H.L., Chabanon, H., Hainault, I., Luquet, S., Magnan, C., Koike, T., Ferré, P. and Foufelle, F. (2009). GRP78 expression inhibits insulin and ER stress-induced SREBP-1c activation and reduces hepatic steatosis in mice. *The Journal of Clinical Investigation*, 119(5): 1201–1215.

Karambataki, M., Malousi, A., Maglaveras, N. and Kouidou, S. (2010). Synonymous polymorphisms at splicing regulatory sites are associated with CpGs in neurodegenerative disease-related genes. *Neuromolecular Medicine*, 12(3): 260–269.

Karataş, E.A., Bayindirli, K., Tozlu, Ö.Ö., Sönmez, E., Kerli, S., Türkez, H. and Yazici, A. (2021). Investigating the Effect of Yttrium Oxide Nanoparticle in U87MG Glioma and PC3 Prostate Cancer: Molecular Approaches. *Journal of the Institute of Science and Technology*, 11(3): 2307–2318.

Kent, B., Magnani, E., Walsh, M.J. and Sadler, K.C. (2016). UHRF1 Regulation of Dnmt1 Is Required for Pre-Gastrula Zebrafish Development. *Developmental Biology* 412 (1): 99–113

Kesavan, K., Ratliff, J., Johnson, E.W., Dahlberg, W., Asara, J.M., Misra, P., Frangioni, J.V. and Jacoby, D.B. (2010). Annexin A2 is a molecular target for TM601, a peptide with tumor-targeting and anti-angiogenic effects. *The Journal of Biological Chemistry*, 285(7): 4366–4374.

Klaunig, J.E., Li, X. and Wang, Z. (2018). Role of xenobiotics in the induction and progression of fatty liver disease. *Toxicology Research*, 7(4): 664–680.

Kong, F.-Y., Zhang, J.-W., Li, R.-F., Wang, Z.-X., Wang, W.-J. and Wang, W. (2017). Unique Roles of Gold Nanoparticles in Drug Delivery, Targeting and Imaging Applications. *Molecules (Basel, Switzerland)*, 22(9): E1445.

Kotha, R., Fernandes, G., Nikam, A.N., Kulkarni, S., Pandey, A., Pandey, S. and Mutalik, S. (2020). Surface engineered bimetallic nanoparticles based therapeutic and imaging platform: recent advancements and future perspective. *Materials Science and Technology*. 36(16): 1729–1748.

Krifa, M. (2014). Limoniastrum guyonianum extracts induce apoptosis via DNA damage, PARP cleavage and UHRF1 down-regulation in human glioma U373 cells. *Journal of Natural Products*, 7 (2014): 79-86

Kutwin, M., Sawosz, E., Jaworski, S., Hinzmann, M., Wierzbicki, M., Hotowy, A., Grodzik, M., Winnicka, A. and Chwalibog, A. (2017). Investigation of platinum nanoparticle properties against U87 glioblastoma multiforme. *Archives of medical science: AMS*, 13(6): 1322–1334.

Kwon, D.H., Cha, H.-J., Lee, H., Hong, S.-H., Park, C., Park, S.-H., Kim, G.-Y., Kim, S., Kim, H.-S., Hwang, H.-J. and Choi, Y.H. (2019). Protective Effect of Glutathione against Oxidative Stress-induced Cytotoxicity in RAW 264.7 Macrophages through Activating the Nuclear Factor Erythroid 2-Related Factor-2/Heme Oxygenase-1 Pathway. *Antioxidants*, 8(4): 82.

Lai, S.-F., Ko, B.-H., Chien, C.-C., Chang, C.-J., Yang, S.-M., Chen, H.-H., Petibois, C., Hueng, D.-Y., Ka, S.-M., Chen, A., Margaritondo, G. and Hwu, Y. (2015). Gold nanoparticles as multimodality imaging agents for brain gliomas. *Journal of Nanobiotechnology*, 13(1): 85.

Lei-Miao, Y., Luis, U. and Yong-Qing, Y. (2019). Transgelin-2: Biochemical and Clinical Implications in Cancer and Asthma. *Trends in biochemical sciences*, 44(10): 885–896.

Lemmer, I.L., Willemsen, N., Hilal, N. and Bartelt, A. (2021). A guide to understanding endoplasmic reticulum stress in metabolic disorders. *Molecular Metabolism*, 47: 101169.

Li, Y., Zhu, D., Hou, L., Hu, B., Xu, M. and Meng, X. (2018). TRB3 reverses chemotherapy resistance and mediates crosstalk between endoplasmic reticulum stress and AKT signaling pathways in MHCC97H human hepatocellular carcinoma cells. *Oncology Letters*, 15(1): 1343–1349.

Liang, H., Wu, Y., Ou, X.-Y., Li, J.-Y. and Li, J. (2017). Au@Pt nanoparticles as catalase mimics to attenuate tumor hypoxia and enhance immune cell-mediated cytotoxicity. *Nanotechnology*, 28(46): 465702.

Lin, M., Zhang, X., Jia, B. and Guan, S. (2018). Suppression of glioblastoma growth and angiogenesis through molecular targeting of methionine aminopeptidase-2. *Journal of Neuro-Oncology*, 136(2): 243–254.

Lindner, P., Christensen, S.B., Nissen, P., Møller, J.V. and Engedal, N. (2020). Cell death induced by the ER stressor thapsigargin involves death receptor 5, a non-autophagic function of MAP1LC3B, and distinct contributions from unfolded protein response components. *Cell Communication and Signaling*, 18(1): 12.

Liu, M., Li, W., Xu, R., Jiang, X. and Liu, A. (2021). Hollow Gold Nanoparticles Loaded with L-Buthionine-Sulfoximine as a Novel Nanomedicine for In Vitro Cancer Cell Therapy. *Journal of Nanomaterials*, 2021: e3595470.

Liu, X., Zhang, X., Zhu, M., Lin, G., Liu, J., Zhou, Z., Tian, X. and Pan, Y. (2017). PEGylated Au@Pt Nanodendrites as Novel Theranostic Agents for Computed Tomography Imaging and Photothermal/Radiation Synergistic Therapy. *ACS Applied Materials & Interfaces*, 9(1): 279–285.

Liu, X.-Y., Wang, J.-Q., Ashby, C.R., Zeng, L., Fan, Y.-F. and Chen, Z.-S. (2021). Gold nanoparticles: synthesis, physiochemical properties and therapeutic applications in cancer. *Drug Discovery Today*, 26(5): 1284–1292.

Lomelino, C.L., Andring, J.T., McKenna, R. and Kilberg, M.S. (2017). Asparagine synthetase: Function, structure, and role in disease. *The Journal of Biological Chemistry*, 292(49): 19952–19958.

Luo, D., Wang, X., Burda, C. and Basilion, J.P. (2021). Recent Development of Gold Nanoparticles as Contrast Agents for Cancer Diagnosis. *Cancers*, 13(8): 1825.

Luo, T., Gao, J., Lin, N. and Wang, J. (2020). Effects of Two Kinds of Iron Nanoparticles as Reactive Oxygen Species Inducer and Scavenger on the Transcriptomic Profiles of Two Human Leukemia Cells with Different Stemness. *Nanomaterials*, 10(10): 1951.

Lyons, S.A., O'Neal, J. and Sontheimer, H. (2002). Chlorotoxin, a scorpion-derived peptide, specifically binds to gliomas and tumors of neuroectodermal origin. *Glia*, 39(2): 162–173.

Majoumouo, M.S., Sharma, J.R., Sibuyi, N.R.S., Tincho, M.B., Boyom, F.F. and Meyer, M. (2020). Synthesis of Biogenic Gold Nanoparticles from Terminalia mantaly Extracts and the Evaluation of Their In Vitro Cytotoxic Effects in Cancer Cells. *Molecules*, 25(19): 4469.

McFerrin, M.B. and Sontheimer, H. (2006). A role for ion channels in glioma cell invasion. *Neuron Glia Biology*, 2(1): 39–49.

McGonigle, S., Majumder, U., Kolber-Simonds, D., Wu, J., Hart, A., Noland, T., TenDyke, K., Custar, D., Li, D., Du, H., Postema, M.H.D., Lai, W.G., Twine, N.C., Woodall-Jappe, M. and Nomoto, K. (2019). Neuropilin-1 drives tumor-specific uptake of chlorotoxin. *Cell communication and signaling: CCS*, 17(1): 67.

Mohapatra, A., Sathiyamoorthy, P. and Park, I.-K. (2021). Metallic Nanoparticle-Mediated Immune Cell Regulation and Advanced Cancer Immunotherapy. *Pharmaceutics*, 13(11): 1867.

Mukherjee, S., Kotcherlakota, R., Haque, S., Bhattacharya, D., Kumar, J.M., Chakravarty, S. and Patra, C.R. (2020). Improved delivery of doxorubicin using rationally designed PEGylated platinum nanoparticles for the treatment of melanoma. *Materials Science and Engineering: C*, 108: 110375.

Neal, S., Jaeger, P.A., Duttke, S.H., Benner, C., K Glass, C., Ideker, T. and Hampton, R.Y. (2018). The Dfm1 Derlin Is Required for ERAD Retrotranslocation of Integral Membrane Proteins. *Molecular Cell*, 69(2): 306-320.e4.

Nelissen, I., Haase, A., Anguissola, S., Rocks, L., Jacobs, A., Willems, H., Riebeling, C., Luch, A., Piret, J.-P., Toussaint, O., Trouiller, B., Lacroix, G., Gutleb, A.C., Contal, S., Diabaté, S., Weiss, C., Lozano-Fernández, T., González-Fernández, Á., Dusinska, M., Huk, A., Stone, V., Kanase, N., Nocuń, M., Stępnik, M., Meschini, S., Ammendolia, M.G., Lewinski, N., Riediker, M., Venturini, M., Benetti, F., Topinka, J., Brzicova, T., Milani, S., Rädler, J., Salvati, A. and Dawson, K.A. (2020). Improving Quality in Nanoparticle-Induced Cytotoxicity Testing by a Tiered Inter-Laboratory Comparison Study. *Nanomaterials (Basel, Switzerland)*, 10(8): E1430.

Nguyen, L., Dass, M., Ober, M.F., Besteiro, L.V., Wang, Z.M., Nickel, B., Govorov, A.O., Liedl, T. and Heuer-Jungemann, A. (2020). Chiral Assembly of Gold–Silver Core–Shell Plasmonic Nanorods on DNA Origami with Strong Optical Activity. *ACS Nano*, 14(6): 7454–7461

Ohoka, N., Yoshii, S., Hattori, T., Onozaki, K. and Hayashi, H. (2005). TRB3, a novel ER stress-inducible gene, is induced via ATF4-CHOP pathway and is involved in cell death. *The EMBO journal*, 24: 1243–55.

Ojeda, P.G., Wang, C.K. and Craik, D.J. (2016). Chlorotoxin: Structure, activity, and potential uses in cancer therapy. *Biopolymers*, 106(1): 25–36.

Oladipo, A.O., Iku, S.I.I., Ntwasa, M., Nkambule, T.T.I., Mamba, B.B. and Msagati, T.A.M. (2020). Doxorubicin conjugated hydrophilic AuPt bimetallic nanoparticles fabricated from Phragmites australis: Characterization and cytotoxic activity against human cancer cells. *Journal of Drug Delivery Science and Technology*, 57: 101749.

Paredes, F., Parra, V., Torrealba, N., Navarro-Marquez, M., Gatica, D., Bravo-Sagua, R., Troncoso, R., Pennanen, C., Quiroga, C., Chiong, M., Caesar, C., Taylor, W.R., Molgó, J., San Martin, A., Jaimovich, E. and Lavanderos, S. (2016). HERPUD1 protects against oxidative stress-induced apoptosis through downregulation of the inositol 1,4,5-trisphosphate receptor. *Free Radical Biology & Medicine*, 90: 206–218.

Parrish, A.B., Freel, C.D. and Kornbluth, S. (2013). Cellular Mechanisms Controlling Caspase Activation and Function. *Cold Spring Harbor Perspectives in Biology*, 5(6): a008672.

Pei, J., Li, P., Zhang, Z.-Y., Zhang, H.-L., Gao, Y.-H., Wang, D.-Y., Zheng, Y., Xu, X. and Cui, J.-Z. (2018). Effect of TAGLN2 in the regulation of meningioma tumorigenesis and development. *European Review for Medical and Pharmacological Sciences*, 22(2): 307–313.

Phillips, R.E., Yang, Y., Smith, R.C., Thompson, B.M., Yamasaki, T., Soto-Feliciano, Y.M., Funato, K., Liang, Y., Garcia-Bermudez, J., Wang, X., Garcia, B.A., Yamasaki, K., McDonald, J.G., Birsoy, K., Tabar, V. and Allis, C.D. (2019). Target identification reveals lanosterol synthase as a vulnerability in glioma. *Proceedings of the National Academy of Sciences of the United States of America*, 116(16): 7957–7962.

Pogribna, M., Koonce, N.A., Mathew, A., Word, B., Patri, A.K., Lyn-Cook, B. and Hammons, G. 2020. Effect of titanium dioxide nanoparticles on DNA methylation in multiple human cell lines. *Nanotoxicology*, 14(4): 534–553.

Princely, S.X., Puja, P., Vinita, M.N., Devan, U., Velangani, A.J., Sunita, S., Yuvakkumar, R., Velmurugan, P., Ravi, A.V., Govarthanan, M. and Kumar, P. (2020). Anti-proliferative and anti-migratory effects of flower-like bimetallic (Au@Pt) nanoparticles. *Materials Letters*, 267: 127491.

Qin, C., He, B., Dai, W., Lin, Z., Zhang, H., Wang, X., Wang, J., Zhang, X., Wang, G., Yin, L. and Zhang, Q. (2014). The impact of a chlorotoxin-modified liposome system on receptor MMP-2 and the receptor-associated protein ClC-3. *Biomaterials*, 35(22): 5908–5920.

Radons, J. (2016). The human HSP70 family of chaperones: where do we stand?. *Cell Stress & Chaperones*, 21(3): 379–404.

Riley, R.S. and Day, E.S. (2017). Gold nanoparticle-mediated photothermal therapy: applications and opportunities for multimodal cancer treatment. *Wiley Interdisciplinary Reviews. Nanomedicine and Nanobiotechnology*, 9(4): 1-25.

Rizwan, H., Mohanta, J., Si, S. and Pal, A. (2017). Gold nanoparticles reduce high glucose-induced oxidative-nitrosative stress regulated inflammation and apoptosis via tuberin-mTOR/NF-κB pathways in macrophages. *International Journal of Nanomedicine*, 12: 5841–5862.

Rozpedek, W., Pytel, D., Mucha, B., Leszczynska, H., Diehl, J.A. and Majsterek, I. (2016). The Role of the PERK/eIF2α/ATF4/CHOP Signaling Pathway in Tumor Progression During Endoplasmic Reticulum Stress. *Current Molecular Medicine*, 16(6): 533–544.

Salado-Leza, D., Traore, A., Porcel, E., Dragoe, D., Muñoz, A., Remita, H., García, G. and Lacombe, S. (2019). Radio-Enhancing Properties of Bimetallic Au:Pt Nanoparticles: Experimental and Theoretical Evidence. *International Journal of Molecular Sciences*, 20(22): E5648.

San, B.H., Moh, S.H. and Kim, K.K. (2013). Investigation of the heating properties of platinum nanoparticles under a radiofrequency current. *International Journal of Hyperthermia: The Official Journal of European Society for Hyperthermic Oncology, North American Hyperthermia Group*, 29(2): 99–105.

Sani, A., Cao, C. and Cui, D. (2021). Toxicity of gold nanoparticles (AuNPs): A review. *Biochemistry and Biophysics Reports*, 26: 100991.

Satapathy, S.K., Kuwajima, V., Nadelson, J., Atiq, O. and Sanyal, A.J. (2015). Drug-induced fatty liver disease: An overview of pathogenesis and management. *Annals of Hepatology*, 14(6): 789–806.

Scholzen, T. and Gerdes, J. (2000). The Ki-67 protein: from the known and the unknown. *Journal of Cellular Physiology*, 182(3): 311–322.

Selck, H., Handy, R.D., Fernandes, T.F., Klaine, S.J. and Petersen, E.J. (2016). Nanomaterials in the aquatic environment: A European Union-United States perspective on the status of ecotoxicity testing, research priorities, and challenges ahead. *Environmental Toxicology and Chemistry*, 35(5): 1055–1067.

Selim, M.E. and Hendi, A.A. (2012). Gold nanoparticles induce apoptosis in MCF-7 human breast cancer cells. *Asian Pacific journal of cancer prevention: APJCP*, 13(4): 1617–1620.

Selvakumar, P., Lakshmikuttyamma, A., Kanthan, R., Kanthan, S.C., Dimmock, J.R. and Sharma, R.K.S (2004). High Expression of Methionine Aminopeptidase 2 in Human Colorectal Adenocarcinomas. *Clinical Cancer Research*, 10(8): 2771–2775.

Selvakumar, P., Lakshmikuttyamma, A., Das, U., Pati, H.N., Dimmock, J.R. and Sharma, R.K. (2009). NC2213: a novel methionine aminopeptidase 2 inhibitor in human colon cancer HT29 cells. *Molecular Cancer*, 8: 65.

Sevastre, A., Costachi, A., Tataranu, L. G., Brandusa, C., Artene, S. A., Stovicek, O., Alexandru, O., Danoiu, S., Sfredel, V. and Dricu, A. (2021). Glioblastoma Pharmacotherapy: A Multifaceted Perspective of Conventional and Emerging Treatments (Review). *Experimental and Therapeutic Medicine*, 22 (6): 1–18.

217

Shayman, J.A. and Abe, A. (2013). Drug induced phospholipidosis: an acquired lysosomal storage disorder. *Biochimica et biophysica acta*, 1831(3): 602–611.

Shimizu, K., Takahama, S., Endo, Y. and Sawasaki, T. (2012). Stress-Inducible Caspase Substrate TRB3 Promotes Nuclear Translocation of Procaspase-3. *PLOS ONE*, 7(8): e42721.

Shin, S.-S., Noh, D.-H., Hwang, B., Lee, J.-W., Park, S.L., Park, S.-S., Moon, B., Kim, W.-J. and Moon, S.-K. (2018). Inhibitory effect of Au@Pt-NSs on proliferation, migration, and invasion of EJ bladder carcinoma cells: involvement of cell cycle regulators, signaling pathways, and transcription factor-mediated MMP-9 expression. *International Journal of Nanomedicine*, 13: 3295–3310.

Sibuyi, N.R.S., Thovhogi, N., Gabuza, K.B., Meyer, M.D., Drah, M., Onani, M.O., Skepu, A., Madiehe, A.M. and Meyer, M. (2017). Peptide-functionalized nanoparticles for the selective induction of apoptosis in target cells. *Nanomedicine (London, England)*, 12(14): 1631–1645.

Siddique, S. and Chow, J.C.L. (2020). Gold Nanoparticles for Drug Delivery and Cancer Therapy. *Applied Sciences*, 10(11): 3824.

Sisinni, L., Pietrafesa, M., Lepore, S., Maddalena, F., Condelli, V., Esposito, F. and Landriscina, M. (2019). Endoplasmic Reticulum Stress and Unfolded Protein Response in Breast Cancer: The Balance between Apoptosis and Autophagy and Its Role in Drug Resistance. *International Journal of Molecular Sciences*, 20(4): 857.

Solano-Gálvez, S.G., Abadi-Chiriti, J., Gutiérrez-Velez, L., Rodríguez-Puente, E., Konstat-Korzenny, E., Álvarez-Hernández, D.-A., Franyuti-Kelly, G., Gutiérrez-Kobeh, L. and Vázquez-López, R. (2018). Apoptosis: Activation and Inhibition in Health and Disease. *Medical Sciences*, 6(3): 54.

Song, Y., Shi, Q., Zhu, C., Luo, Y., Lu, Q., Li, H., Ye, R., Du, D. and Lin, Y. (2017). Mitochondrial Reactive Oxygen Species Burst for Cancer Therapy Triggered by Near-Infrared Light. *Nanoscale*, 2017.

Song, Y., Qu, Z., Li, J., Shi, L., Zhao, W., Wang, H., Sun, T., Jia, T. and Sun, Y. (2021). Fabrication of the biomimetic DOX/Au@Pt nanoparticles hybrid nanostructures for the combinational chemo/photothermal cancer therapy. *Journal of Alloys and Compounds*, 881: 160592.

Soroceanu, L., Gillespie, Y., Khazaeli, M.B. and Sontheimer, H. (1998). Use of chlorotoxin for targeting of primary brain tumors. *Cancer Research*, 58(21): 4871–4879.

Srinoi, P., Chen, Y.-T., Vittur, V., Marquez, M.D. and Lee, T.R. (2018). Bimetallic Nanoparticles: Enhanced Magnetic and Optical Properties for Emerging Biological Applications. *Applied Sciences*, 8(7): 1106.

Sun, Y., Zhang, D., Liu, X., Li, X., Liu, F., Yu, Y., Jia, S., Zhou, Y. and Zhao, Y. (2018). Endoplasmic Reticulum Stress Affects Lipid Metabolism in Atherosclerosis Via CHOP Activation and Over-Expression of miR-33. *Cellular Physiology and Biochemistry*, 48(5): 1995–2010.

Szklarczyk, D., Gable, A.L., Lyon, D., Junge, A., Wyder, S., Huerta-Cepas, J., Simonovic, M., Doncheva, N.T., Morris, J.H., Bork, P., Jensen, L.J. and Mering, C.V. (2019). STRING v11: protein-

protein association networks with increased coverage, supporting functional discovery in genome-wide experimental datasets. *Nucleic Acids Research*, 47(D1): D607–D613.

Tang, J., Jiang, X., Wang, L., Zhang, H., Hu, Z., Liu, Y., Wu, X. and Chen, C. (2014). Au@Pt nanostructures: a novel photothermal conversion agent for cancer therapy. *Nanoscale*, 6(7): 3670–3678.

Thovhogi, N., Sibuyi, N., Meyer, M., Onani, M. and Madiehe, A. (2015). Targeted delivery using peptide-functionalised gold nanoparticles to white adipose tissues of obese rats. *Journal of Nanoparticle Research*, 17(2): 112.

Tomcik, M., Palumbo-Zerr, K., Zerr, P., Sumova, B., Avouac, J., Dees, C., Distler, A., Becvar, R., Distler, O., Schett, G., Senolt, L. and Distler, J.H.W. (2016). Tribbles homologue 3 stimulates canonical TGF-β signalling to regulate fibroblast activation and tissue fibrosis. *Annals of the Rheumatic Diseases*, 75(3): 609–616.

Tsui, K.-H., Lin, Y.-H., Chang, K.-S., Hou, C.-P., Chen, P.-J., Feng, T.-H. and Juang, H.-H. (2019). Transgelin, a p53 and PTEN-Upregulated Gene, Inhibits the Cell Proliferation and Invasion of Human Bladder Carcinoma Cells In Vitro and In Vivo. *International Journal of Molecular Sciences*, 20(19): 4946.

Unoki, M., Brunet, J. and Mousli, M. (2009). Drug discovery targeting epigenetic codes: The great potential of UHRF1, which links DNA methylation and histone modifications, as a drug target in cancers and toxoplasmosis. *Biochemical Pharmacology*, 78(10): 1279–1288.

Wada, Y., Kikuchi, A., Kaga, A., Shimizu, N., Ito, J., Onuma, R., Fujishima, F., Totsune, E., Sato, R., Niihori, T., Shirota, M., Funayama, R., Sato, K., Nakazawa, T., Nakayama, K., Aoki, Y., Aiba, S., Nakagawa, K. and Kure, S. (2020). Metabolic and pathologic profiles of human LSS deficiency recapitulated in mice. *PLOS Genetics*, 16(2): e1008628.

Wang, H., Hao, H. and Li, Y. (2020). Size-Dependent Electrochemistry and Electrocatalysis at Single Au@Pt Bimetallic Nanoparticles. *The Journal of Physical Chemistry C*, 124(45): 24740–24746.

Wang, R.-Q., He, F.-Z., Meng, Q., Lin, W.-J., Dong, J.-M., Yang, H.-K., Yang, Y., Zhao, M., Qiu, W.-T., Xin, Y.-J. and Zhou, Z.-L. (2021). Tribbles pseudokinase 3 (TRIB3) contributes to the progression of hepatocellular carcinoma by activating the mitogen-activated protein kinase pathway. *Annals of Translational Medicine*, 9(15): 1253.

Wang, X., Chen, M., Zhou, J. and Zhang, X. (2014). HSP27, 70 and 90, anti-apoptotic proteins, in clinical cancer therapy (Review). *International Journal of Oncology*, 45(1): 18–30.

Wang, Y., Li, K., Han, S., Tian, Y., Hu, P., Xu, X., He, Y., Pan, W., Gao, Y., Zhang, Z., Zhang, J. and Wei, L. (2019). Chlorotoxin targets ERα/VASP signaling pathway to combat breast cancer. *Cancer Medicine*, 8(4): 1679–1693.

Wu, W., Klockow, J.L., Zhang, M., Lafortune, F., Chang, E., Jin, L., Wu, Y. and Daldrup-Link, H.E. (2021). Glioblastoma multiforme (GBM): An overview of current therapies and mechanisms of resistance. *Pharmacological Research*, 171: 105780.

219

Wusu, A.D. Sibuyi, N.R.S., Moabelo, K.L., Goboza, M., Madiehe, A. and Meyer, M. (2021). Citrate-capped gold nanoparticles with a diameter of 14 nm alter the expression of genes associated with stress response, cytoprotection and lipid metabolism in CaCo-2 cells. *Nanotechnology*, 33(10): 105101.

Yan, L., Liu, W., Zhang, H., Liu, C., Shang, Y., Ye, Y., Zhang, X. and Li, W. (2014). Ube2g2-gp78-mediated HERP polyubiquitylation is involved in ER stress recovery. *Journal of Cell Science*, 127(Pt 7): 1417–1427.

Yang, Q., Peng, J., Xiao, Y., Li, W., Tan, L., Xu, X. and Qian, Z. (2018). Porous Au@Pt Nanoparticles: Therapeutic Platform for Tumor Chemo-Photothermal Co-Therapy and Alleviating Doxorubicin-Induced Oxidative Damage. *ACS Applied Materials & Interfaces*, 10(1): 150–164.

Yang, Q., Peng, J., Xiao, Y., Li, W., Tan, L., Xu, X. and Qian, Z. (2019). Gold nanoparticle based photothermal therapy: Development and application for effective cancer treatment. *Sustainable Materials and Technologies*, 22: e00109.

Yeini, E., Ofek, P., Albeck, N., Rodriguez Ajamil, D., Neufeld, L., Eldar-Boock, A., Kleiner, R., Vaskovich, D., Koshrovski-Michael, S., Dangoor, S.I., Krivitsky, A., Burgos Luna, C., Shenbach-Koltin, G., Goldenfeld, M., Hadad, O., Tiram, G. and Satchi-Fainaro, R. (2021). Targeting Glioblastoma: Advances in Drug Delivery and Novel Therapeutic Approaches, *Advanced Therapeutics*, 4(1): 2000124.

Yokoyama, T. and Nakamura, T. (2011). Tribbles in disease: Signaling pathways important for cellular function and neoplastic transformation: *Cancer Science*, 102(6): 1115–1122.

Yu, Y., Pierciey, F.J., Maguire, T.G.and Alwine, J.C. (2013). PKR-like endoplasmic reticulum kinase is necessary for lipogenic activation during HCMV infection. *PLoS pathogens*, 9(4): e1003266.

van der Zande, M. Undas, A.K., Kramer, E., Monopoli, M.P., Peters, R.J., Garry, D., Antunes, Fernandes, E.C., Hendriksen, P.J., Marvin, H.J., Peijnenburg, A.A. and Bouwmeester, H. (2016). Different responses of Caco-2 and MCF-7 cells to silver nanoparticles are based on highly similar mechanisms of action. Nanotoxicology, 10(10): 1431–1441.

Zhang, C., Hong, F.-F., Wang, C.-C., Li, L., Chen, J.-L., Liu, F., Quan, R.-F. and Wang, J.-F. (2017). TRIB3 inhibits proliferation and promotes osteogenesis in hBMSCs by regulating the ERK1/2 signaling pathway. *Scientific Reports*, 7(1): 10342.

Zhang, J., Han, Y., Zhao, Y., Li, Q.-R., Jin, H.-F., Du, J.-B. and Qin, J. (2019). Role of endoplasmic reticulum stress-associated gene TRIB3 in rats following kainic acid-induced seizures. *International Journal of Clinical and Experimental Pathology*, 12(2): 599–605.

Zhang, J., Yu, Y. and Zhang, B. (2019). Synthesis and characterization of size controlled alloy nanoparticles. *Physical Sciences Reviews*, 5(3): 1-19.

Zhang, Y.-K., Wang, Y.-J., Gupta, P. and Chen, Z.-S. (2015). Multidrug Resistance Proteins (MRPs) and Cancer Therapy. *The AAPS Journal*, 17(4): 802–812.

Zhao, L., Ge, X., Yan, G., Wang, X., Hu, P., Shi, L., Wolfbeis, O.S., Zhang, H. and Sun, L. (2017). Double-mesoporous core–shell nanosystems based on platinum nanoparticles functionalized with lanthanide complexes for in vivo magnetic resonance imaging and photothermal therapy. *Nanoscale*, 9(41): 16012–16023.

Zhao, L., Zhu, J., Gong, J., Song, N., Wu, S., Qiao, W., Yang, J., Zhu, M. and Zhao, J. (2020). Polyethylenimine-based theranostic nanoplatform for glioma-targeting single-photon emission computed tomography imaging and anticancer drug delivery. *Journal of Nanobiotechnology*, 18(1): 143.

Zhao, Z., Xu, D., Wang, Zheng, Wang, L., Han, R., Wang, Zhenzhen, Liao, L. and Chen, Y. (2018). Hepatic PPARα function is controlled by polyubiquitination and proteasome-mediated degradation through the coordinated actions of PAQR3 and HUWE1. *Hepatology*, 68 (1): 289–303.

UNIVERSITY *of the*

WESTERN CAPE

CHAPTER SIX:

Catalytic reduction of 4-nitrophenol to 4-aminophenol with bimetallic gold platinum nanoparticles

Taahirah Boltman[1], Abram Madiehe[2], Okobi Ekpo[1] and Mervin Meyer [2]*

[1] Department of Medical Biosciences, University of the Western Cape, Cape Town, Robert Sobukwe Road, Bellville 7535, South Africa; 2917424@myuwc.ac.za (T.B.)

[2] DSI/Mintek Nanotechnology Innovation Centre, Biolabels Node, Department of Biotechnology, University of the Western Cape, Cape Town, Robert Sobukwe Road, Bellville 7535, South Africa

*Correspondence: memeyer@uwc.ac.za (M.M.); Tel.: +27-21-5952032 (M.M.)

Abstract

In recent years, noble or transition metals are being combined with other metals to form bimetallic nanostructures or alloys which enhance the catalytic activity of nanoparticles (NPs) when compared to their monometallic counterparts. This is primarily achieved through exploiting the synergistic effects of combined metals and creating new surface and catalytic properties, which are different from their monometallic counterparts. In our previous study, we reported on the synthesis of small citrate capped bimetallic gold-platinum nanoparticles (AuPtNPs) with a roughly spherical shape and a core size average of approximately 5 nm. The catalytic activity of AuPtNPs was assessed using 4-nitrophenol (4-NP) and sodium borohydride (NaBH$_4$). AuPtNPs successfully reduced the 4-NP to 4-aminophenol (4-AP) at a catalytic rate constant (k_{cat}) of 3.2 x 10^{-3}/sec and for diluted AuPtNPs (1:2) and AuPtNPs (1:5) the k_{cat} was reported at 2.2 x 10^{-3}/sec and 1.2 x 10^{-3}/sec, respectively. Therefore, citrate capped AuPtNPs have a potential application in catalysis.

Keywords: Bimetallic nanoparticles, Catalytic activity, Gold-platinum nanoparticles (AuPtNPs), 4-Nitrophenol (4-NP) and 4-Aminophenol (4-AP).

1. Introduction

Nitro-phenolic compounds are amongst the most common substances that contribute to water pollution (Al Bakain *et al.*, 2015). 4-Nitrophenol (4-NP) is a toxic substance that is often present in industrial and agricultural wastewaters and has also been found in marine and fresh water and their reduction presents a major challenge (Yahya *et al.*, 2021). It can be found in the manufacturing of certain drugs (e.g., acetaminophen), dyes, fungicides, methyl and ethyl parathion insecticides and processes involved in the darkening of leather and poses a threat to the environment and to human beings (Abdollahi and Mohammadirad, 2014). The USA Environmental Protection Agency (EPA) has listed 4-NP in a list of priority pollutants due to its high toxicity (Yahya *et al.*, 2021). It is a known mutagen, teratogen, and carcinogen, and is more specifically linked to certain skin diseases (Harrison *et al.*, 2005). It is therefore important to monitor the presence of 4-NP in the environment and to find solutions for its remediation. The removal of 4-NP from wastewater and the development of efficient eco-friendly wastewater removal routes is vital in maintaining a balanced eco-system and an overall healthier environment. However, the process of removing it is tedious and involves specific physical, chemical, and biological treatments. Many methods have been proposed for the degradation of nitrophenols, however, most of the common methods for the removal of nitrophenols involve techniques such as adsorption, electrochemical removal, and chemical reduction (Din *et al.*, 2020). Such methods are not only expensive, but can also contribute to pollution (Din *et al.*, 2020). Therefore, more eco-friendly, and cost-effective routes are required for the removal of 4-NP from the environment.

Alternative methods using metallic nanoparticles (MNPs) as catalysts for the reduction of nitrophenols are being explored (Din *et al.*, 2020). Favourable features of using MNPs include that these nanomaterials can be synthesised using relatively simple methodologies and can be produced in a variety of shapes and sizes. The small size of the MNPs have increased surface area which enhance their catalytic performances (Zhu and Xu, 2016; Teimouri *et al.*, 2018). Monometallic NPs, generally, noble- and transition metals have shown remarkable catalytic activity because of their adjustable size and shape (Li *et al.*, 2021). One of the most popular and simple methods for the reduction of 4-NP is to introduce sodium borohydride ($NaBH_4$) as a reductant and a metal catalyst such as MNPs (Din *et al.*, 2020). The reduction of 4-NP by $NaBH_4$ is thermodynamically possible but without a catalyst this reaction is unfavorable (Saha *et al.*, 2010). Various monometallic NPs, which include gold (AuNPs) (Seoudi and Said, 2011;

223

Lim, Ahn and Park, 2016; Seoudi and Al-Marhaby, 2016; Saira *et al.*, 2021) silver (AgNPs) (Al-Marhaby and Seoudi, 2016; Kästner and Thünemann, 2016; Kaur, Singh and Rawat, 2019), palladium (PdNPs) (Chatterjee, Diagaradjane and Krishnan, 2011; Islam *et al.*, 2018; Baran, 2019; Lee *et al.*, 2021), copper (CuNPs) (Deka, Deka and Bharali, 2014; Garba *et al.*, 2021) and platinum (PtNPs) (Pandey and Mishra, 2014; You *et al.*, 2017) have been studied as catalysts for the reduction of 4-NP.

The Langmuir–Hinshelwood (L-H) adsorption model, as seen in Figure 1, has been proposed for the catalytic reduction reaction of 4-NP, where NPs are used as a catalyst for the reaction, as previously explained (Wunder *et al.*, 2010; Din *et al.*, 2020). At the start of the reaction 4-NP (dye) and NaBH$_4$ (reductant) are introduced into the reaction medium containing the NPs. These reactants are adsorbed on the surface of the NPs. As the reaction is following the L-H mechanism, both the 4-NP and NaBH$_4$ are adsorbed on the surface of NPs. The nitrophenol molecule will be adsorbed but the NaBH$_4$ molecule will be converted into its respective ions and the borohydride ion (BH$_4^{-1}$) will be adsorbed on the surface of the NPs. The BH$_4^{-1}$ performs as an electron donating species and will release an electron. This electron, via electron-transferring surface from the NPs, will travel to the 4-NP molecules, which consequently results in the acceptance of this electron and conversion into the 4-aminophenol (4-AP).

Combining metals to produce bimetallic NPs (BNPs) can be used to develop new nano-materials that may produce greater technological usefulness than their starting substances. BNPs usually metallic alloys, are composed of two different types of metals (Zaleska-Medynska *et al.*, 2016). BNPs, have elicited much attraction in recent years for improved catalytic performances when compared to monometallic NPs, due to the synergistic effects of the individual metals (Petkar, Kadu and Chikate, 2014; Zaleska-Medynska *et al.*, 2016). This is the result of electronic interactions between the atomic orbitals of different metals which results in synergistic effects (Petkar, Kadu and Chikate, 2014; Zhang *et al.*, 2019).The extra electrons in the outer orbitals of the metallic sources which have higher activity can be transferred to the adjacent metallic atoms with a relatively lower activity, resulting in an organized action between the different metallic elements. Consequently, the formed electron-rich metallic atoms facilitate electron transfer from the adsorbed NaBH$_4$ to the 4-NP, improving the efficiency of reduction. BNPs have greatly improved catalytic properties, selectivity features, long-term stability and better resistance potential to poisoning than monometallic NPs (Petkar, Kadu and Chikate, 2014).

224

Several different types of bimetallic NPs have been used as catalysts for the reduction of 4-NP to 4-AP using aqueous $NaBH_4$ as the reductant and demonstrated higher catalytic activity in comparison to monometallic NPs. An extensive review of different types of bimetallic NPs reducing 4-NP can be found in recent literature (Din *et al.*, 2020). Au is very often used in combination with other metals to produce bimetallic NPs. Examples include AuAgNPs (Berahim *et al.*, 2018; Liang *et al.*, 2019) AuPd (Srisombat *et al.*, 2017; Zhao *et al.*, 2017; Alshammari *et al.*, 2020), AuCu (Pozun *et al.*, 2013) and AuPtNPs (Chu and Su, 2014; Fu *et al.*, 2014; Zhang *et al.*, 2014) amongst others. Chu and Su, (2014) reported that polyelectrolyte multi-layered supported AuPt alloy NPs exhibit higher catalytic activity than Au and Pt monometallic catalysts for the reduction of 4-NP by $NaBH_4$. Fu *et al.* (2014) reported on the reduction of 4-NP to 4-AP within 33 minutes using Pt–Au alloy nanocubes as a catalyst, which is reportedly shorter than that of the commercial Pt black (51 minutes). Rod shaped bimetallic AuPtNPs double-walled nanotubes proved to be an efficient catalyst for 4-NP breakdown (Lu *et al.*, 2010). Zhang *et al.* (2014) suggested that bare AuPtNPs produced using pulsed laser ablation in liquid outperform most of the reported Pt or Au based catalysts for 4-NP reduction and was likely due to their unique "bare" surface and structure. They also reported on one of the highest rate constants for AuPtNPs when compared to similar AuPtNPs for reduction of 4-NP to 4-AP using aqueous $NaBH_4$.

Since there is growing interest in the use of BNPs for catalysis applications, the current study investigated the potential catalytic activity of citrate capped AuPtNPs (~ 5 nm) using 4-NP reduction method.
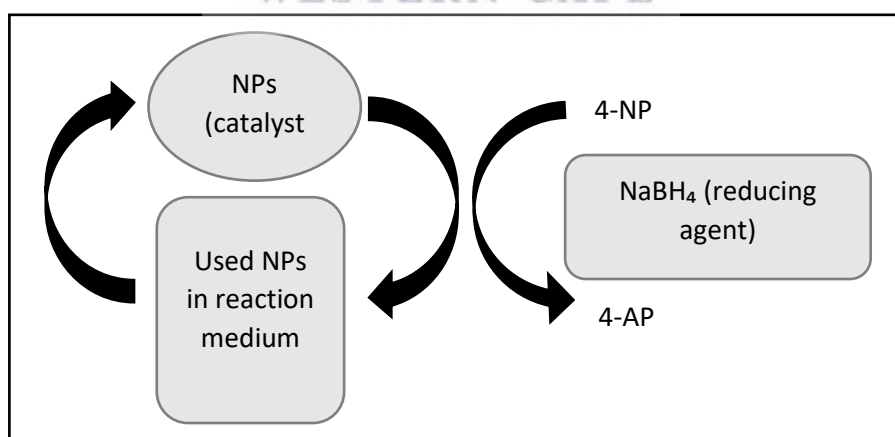

Figure 1. Langmuir–Hinshelwood (L-H) mechanism for catalytic reduction of 4-NP

[Figure adapted with permission from Din *et al.*, (2020), Taylor & Francis Online]

225

2. Materials and methods

2.1. Chemicals

Gold (III) chloride trihydrate (≥99.9% trace metals basis), chloroplatinic acid hydrate (≥99.9% trace metals basis), sodium citrate, sodium borohydride (ReagentPlus®, 99%) and 4-Nitrophenol (reagent grade) were purchased from Sigma-Aldrich (Sigma-Aldrich,St Louis, Missouri, United States of America). Double distilled water (DDW) was used throughout the experiments. Greiner bio-one 96 well flat bottom polystyrene microplates were acquired from Sigma-Aldrich.

2.2. Preparation of citrate capped AuPtNPs

The synthesis of citrate capped AuPtNPs was previously described (Chapter 3).

2.3. Catalytic reduction method of 4-NP to 4-AP using citrate capped AuPtNPs

The photo-catalytic reduction of 4-NP was performed as previously described with a few modifications (Seoudi and Said, 2011; Seoudi and Al-Marhaby, 2016). The photocatalysis reactions were carried out in a 96 well plate, with a 1-cm path length containing the reaction mixture, 140 µl of double distilled water (DDW) and 30 µl of 2 mM 4-NP (Table 1) were taken. The addition and mixing of 100 µl of 0.3 M $NaBH_4$ and 30 µl of AuPtNPs (either diluted by the dilution factor or undiluted) caused a decrease in the intensity of the peak of 4-NP. The progress of the reduction of 4-NP was monitored in situ using a POLARstar Omega UV-Vis spectrophotometer (BMG, Labtech, Germany). The UV-Vis spectra were measured at different time points. The reaction temperature was kept constant at room temperature (25˚C) to decrease thermal effects on the catalytic rate.

Table 1. Catalytic reduction of 4-NP using AuPtNPs

Reactants	Blank	4-NP	4-NP + NaBH₄	4-NP+NaBH₄ +AuPtNPs
DDW (µl)	300	270	170	140
4-NP (2 mM) (µl)	0	30	30	30
NaBH₄ (0.3 M) (µl)	0	0	100	100
AuPtNPs (µl)	0	0	0	30
Total (µl)	300	300	300	300

226

3. Statistical analysis

UV-Vis spectra were constructed in Microsoft Excel. The reaction was designed in such a way that pseudo first order rate kinetics can be used to model the reaction as previously described (Seoudi and Said, 2011). Pseudo first order law:

K'(A)= -dA/dt. where K'=k[B$_0$].

The rate constant was calculated from the decrease of the peak intensity of nitrophenol at 400 nm (the slope of the curve) (Seoudi and Said, 2011).

4. Results and discussion

4.1. Physiochemical characterization of citrate capped AuPtNP

The characterization results of citrate AuPtNPs were previously reported (Chapter 3)

4.2. Catalytic reduction of 4-NP to 4-AP using citrate AuPtNPs

The reduction of 4-NP to 4-AP with sodium borohydride (NaBH$_4$) in aqueous media is by far the most widely used reaction for testing the catalytic performance of a large variety of MNPs. The reduction of 4-NP to 4-AP using NaBH$_4$ as a reducing agent is typically monitored by measuring changes in the UV-Vis absorption spectrum of the reaction medium (Seoudi and Said, 2011; Al-Marhaby and Seoudi, 2016; Ravi *et al.*, 2019; Chatterjee *et al.*, 2021). Figure 2 (i) shows the UV-Vis absorption spectrum of 4-NP in the absence and presence of NaBH$_4$. Upon addition of NaBH$_4$, the absorption peak of 4-NP shifted from ± 320 nm to ± 400 nm [Figure 2 (ii)]. The peak formed at ± 400 nm is due to the formation of the nitrophenolate ion (Seoudi and Said, 2011; Chatterjee *et al.*, 2021)**.** Figure 3 also showed that in the absence of NaBH$_4$, the spectra of 4-NP does not change, even for an extended period of up to 180 minutes. Similarly, Figure 4 showed that the spectra of 4-NP in the presence of NaBH$_4$, also does not change for a period up to 180 minutes. This indicated that the reducing agent NaBH$_4$ by itself cannot reduce the 4-nitrophenolate ions over this time period. These results are in agreement with results reported in literature (Seoudi and Said, 2011; Seoudi and Al-Marhaby, 2016). However, the addition of bimetallic AuPtNPs to the reaction containing 4-NP and NaBH$_4$, resulted in a time-dependent decrease in absorbance peak at ± 400 nm, which indicated that the concentration of 4-NP is continuously decreasing (Figure 5). This decrease in the absorbance of the nitrophenolate peak accompanied by the appearance of an absorbance peak at ± 300 nm,

227

which represented the 4-AP. The bimetallic AuPtNPs therefore acted as a catalyst for the reduction of 4-NP to 4-AP. This is corroborated by previous studies demonstrating different types of AuPtNPs successfully reducing 4-NP to 4-AP (Pozun *et al.*, 2013; Chu and Su, 2014; Fu *et al.*, 2014; Zhang *et al.*, 2014). Figures 5, 6 and 7 show the time dependent reduction of 4-NP to 4-AP using $NaBH_4$ as the reducing agent in the presence of decreasing concentrations of AuPtNPs, i.e., the AuPtNPs are used either as undiluted or diluted 1 in 2 times or diluted 1 in 5 times, respectively. While all these concentrations of AuPtNPs used were able to catalyse the reduction of 4-NP to 4-AP, the kinetics of the reduction reaction are affected by the concentration of the AuPtNPs. Figure 5 shows that when highly concentrated AuPtNP are used, all the 4-NP is reduced within 90 minutes. In comparison, Figures 6 and 7 showed that lower concentrations of AuPtNP are less effective in catalysing the reduction of 4-NP, with significant amounts of 4-NP remaining even at 180 minutes. The catalytic rate constant (k_{cat}), for the undiluted AuPtNPs (1:0) and AuPtNPs (1:2) and AuPtNPs (1:5) decreased from 3.2 x 10^{-3}/sec to 2.2 x 10^{-3}/sec and 1.2 x 10^{-3}/sec, respectively (Table 2 and Figure 8). The reduction of 4-NP by AuPtNPs can be attributed to the Langmuir-Hinshelwood model and the kinetic analysis of all three concentrations was carried out using first order kinetics as previously described (Seoudi and Said, 2011). Figure 9 shows the UV-Vis absorbance of AuPtNPs did not change over a period of 2 hours, while Figure 10 shows the addition of AuPtNPs to 4-NP had no effect on 4-NP stability over 2 hours.

As seen in Table 3, the k_{cat} in the current study can be compared to previous studies where, it was higher when compared to the k_{cat} derived from studies using AuNPs (Seoudi and Said, 2011; Seoudi and Al-Marhaby, 2016) and PtNPs (Maji *et al.*, 2014; Zhang *et al.*, 2014) for reduction of 4-NP to 4-AP in the presence of $NaBH_4$. This is supported by other studies that suggested bimetallic NPs are more effective as catalysts for the reduction of 4-NP to 4-AP when compared to its monometallic counterparts based on properties relating to combined metal atoms and unique surface areas (Peng *et al.*, 2013; Chu and Su, 2014; Zhang *et al.*, 2014). The reaction rate for the reduction of 4-NP with $NaBH_4$ is proportional to the exposed surface area of the catalyst and smaller NPs are known to have larger surface areas potentially contributing to enhanced catalytic activity (Panigrahi *et al.*, 2007; Al-Marhaby and Seoudi, 2016). Interestingly, the rate constant of the small AuPtNPs (1:0) reported in this study was equivalent to that of carbon PtAuNPs reported in a previous study (Peng *et al.*, 2013). When compared to other spherical PtAuNP alloy structures using different molar ratios of Au and Pt during the synthesis procedure, it is evident that these rate constant values were either lower or

higher than the k_{cat} reported in this study (Table 3) (Fu *et al.*, 2014; Zhang *et al.*, 2014). In another study, the use of PtAu dendrimer-like NPs on the surface of polydopamine (PDA)-wrapped reduced graphene oxide (RGO) with different starting molar ratios of Au and Pt used during NP synthesis demonstrated high k_{cat} (Ye *et al.*, 2016), however using equal molar ratios to produce the Pt1Au1-RGO NPs had a rate constant lower than our reported rate constant for undiluted AuPtNPs (1:0). Though, the rate constant reported in this study is mostly observed to be lower than previous studies for other bimetallic NPs constructed using Au and Pt, this is primarily due to the capping agents on NPs, the sizes and initial molar ratios of Au and Pt used in NP synthesis and the concentrations of NaBH$_4$ used in the catalytic reaction as previously described (Seoudi and Said, 2011; Petrucci *et al.*, 2013; Zhang *et al.*, 2014; Seo *et al.*, 2017). Nonetheless, successful reduction of the 4-NP to 4-AP was observed with citrate-capped AuPtNPs, which was concentration dependent and demonstrated higher rate constants than AuNPs and PtNPs reported previously (Table 3). To the best of our knowledge, this type of citrate capped AuPtNPs (~ 5 nm) has not been previously reported for the reduction of 4-NP to 4-AP using NaBH$_4$. This enhanced catalytic activity may be attributed to the synergistic effects between Au and Pt atoms in AuPtNPs as previously described (Peng *et al.*, 2013; Chu and Su, 2014; Zhang *et al.*, 2014).
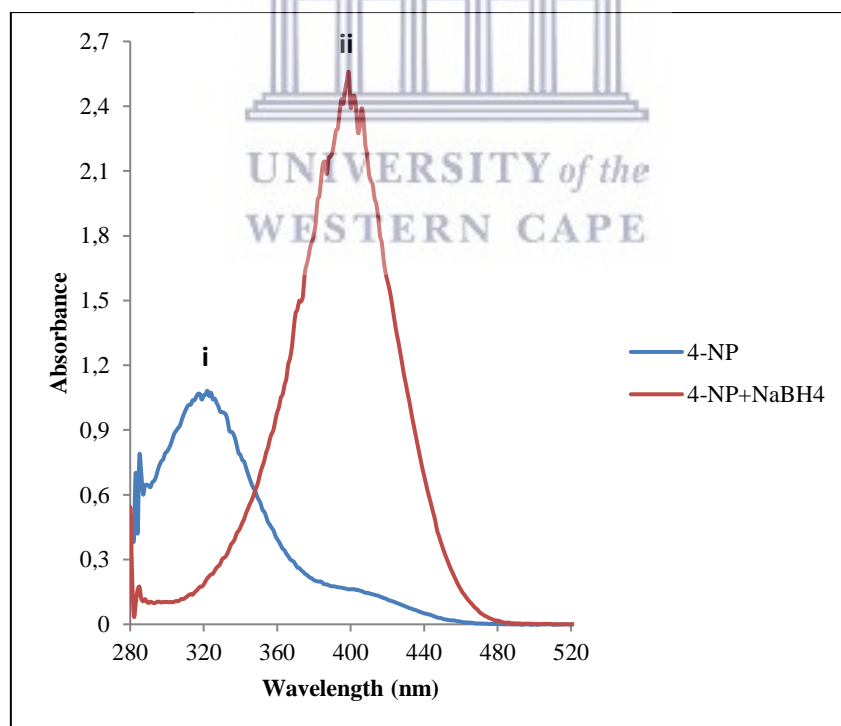

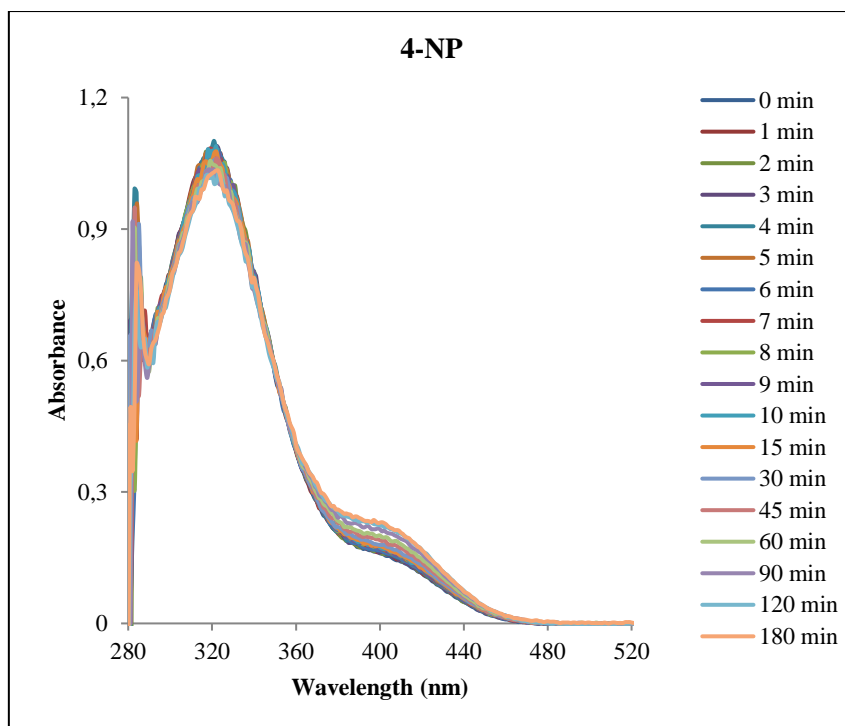Figure 2. UV-Vis spectra of 4-NP before (i) and after (ii) the addition of NaBH$_4$

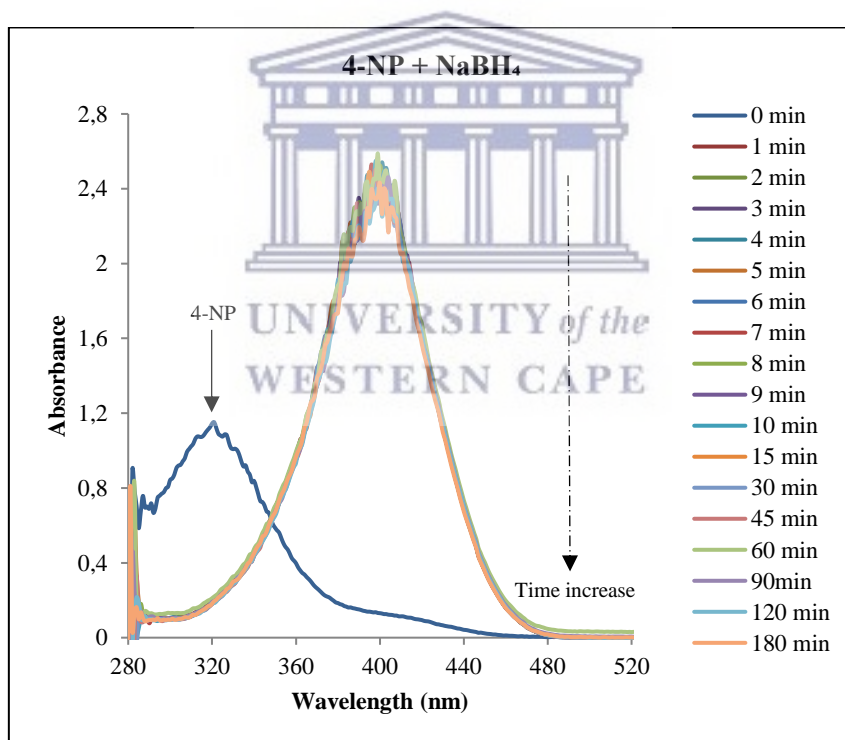Figure 3. UV-Vis spectra of 4-NP over a 180 min period

Figure 4. UV-Vis spectrum of 4-NP over 180 min period in the presence of NaBH₄
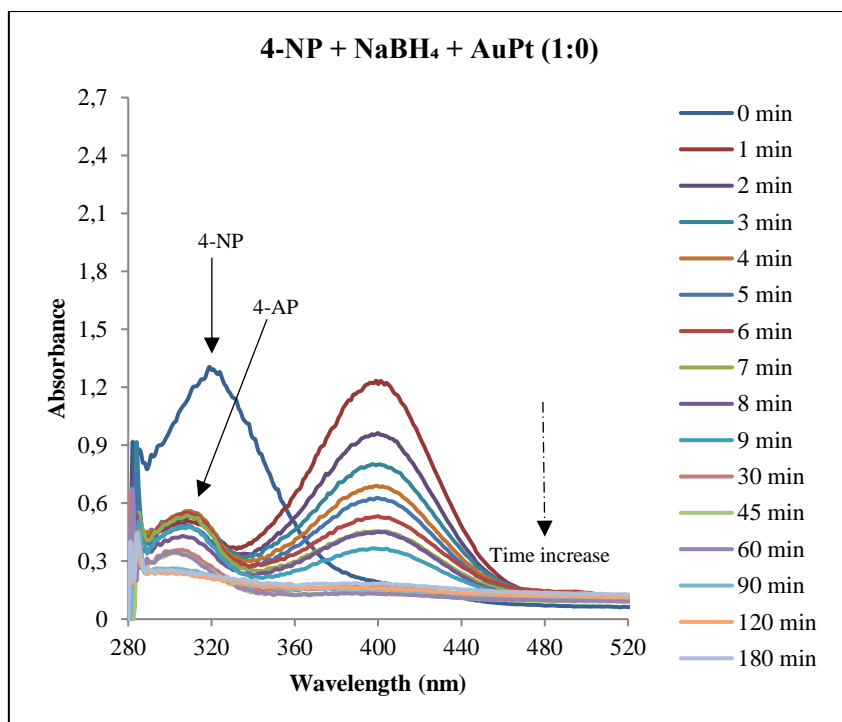
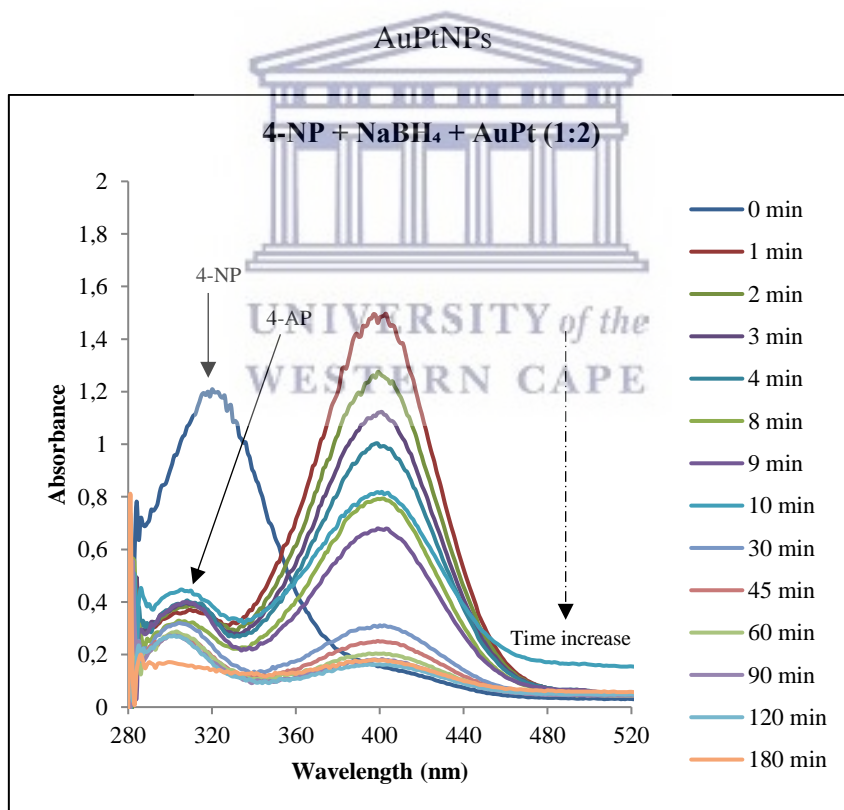Figure 5. UV-Vis spectrum of 4-NP in the presence of NaBH$_4$ and undiluted citrate-capped AuPtNPs

Figure 6. UV-Vis spectrum of 4-NP in the presence of NaBH$_4$ and a 1 in 2 dilution of citrate-capped AuPtNPs
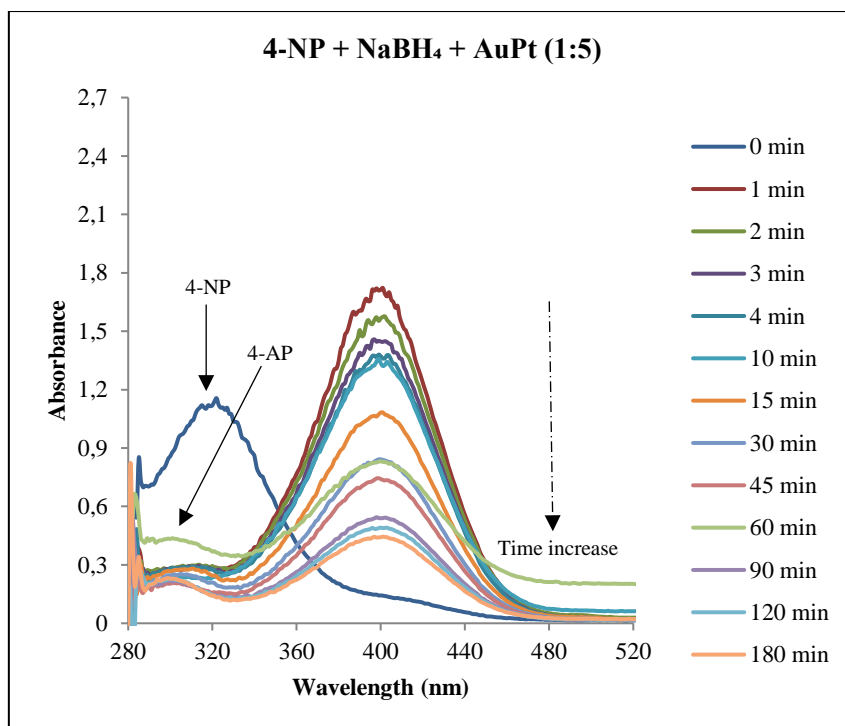
231

Figure 7. UV-Vis spectrum of 4-NP in the presence of NaBH$_4$ and a 1 in 5 dilution of citrate-capped AuPtNPs
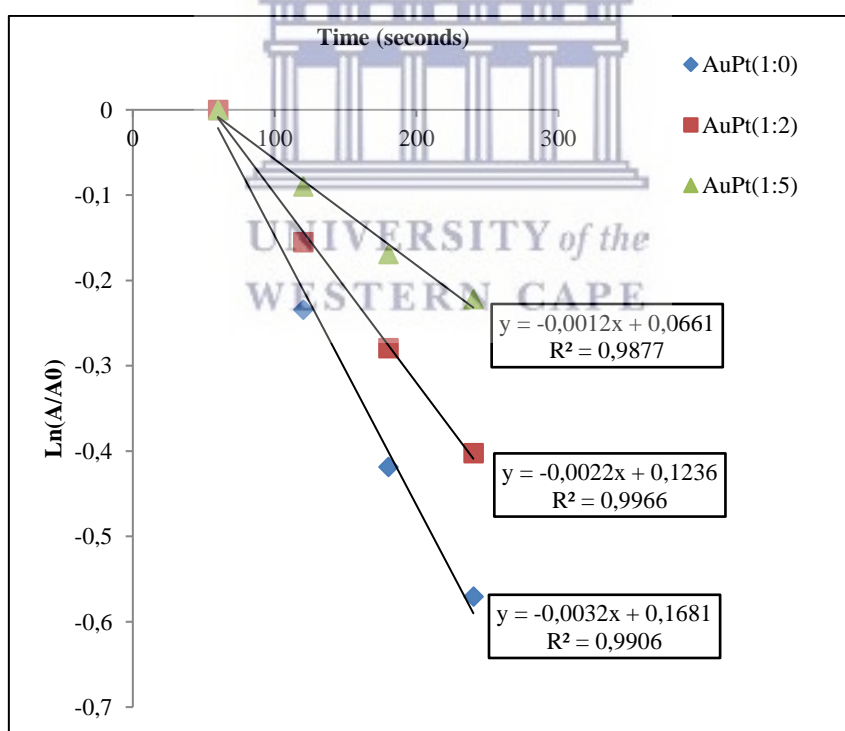
Figure 8. UV-Vis absorption changes vs. time in seconds for the disappearance of 4-NP absorption at 400 nm

232

Table 2: Calculated rate constants (k_{cat}) of undiluted and diluted AuPtNPs

Nanoparticles	kcat
AuPtNPs (1:0)	3.2×10^{-3}/sec
AuPtNPs (1:2)	2.2×10^{-3}/sec
AuPtNPs (1:5)	1.2×10^{-3}/sec

Figure 9. UV-Vis spectrum of AuPtNPs (1:0) over 120 min period

Figure 10. UV-Vis absorption of 4NP in the absence of AuPt (1:0) and in the presence of AuPtNPs (1:0) at different times

233

Table 3. Summary of the catalytic rate constants (k_{cat}) obtained from AuPtNPs from the current work compared to k_{cat} of similar studies reported in literature

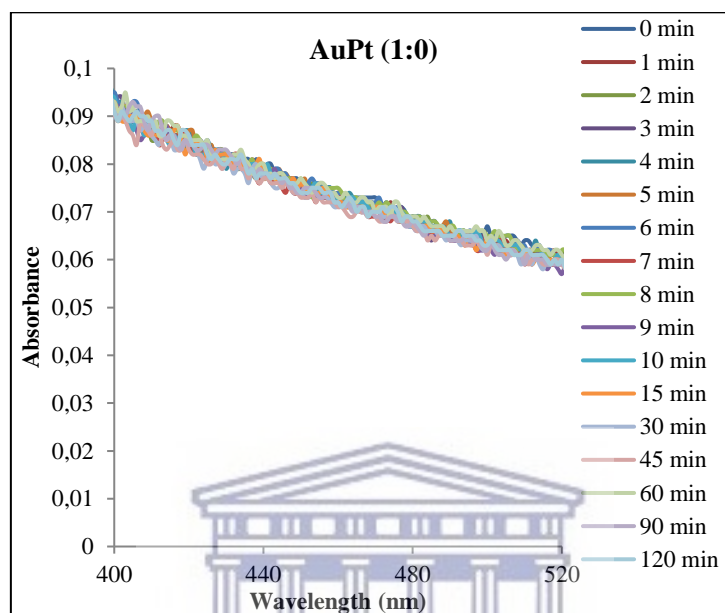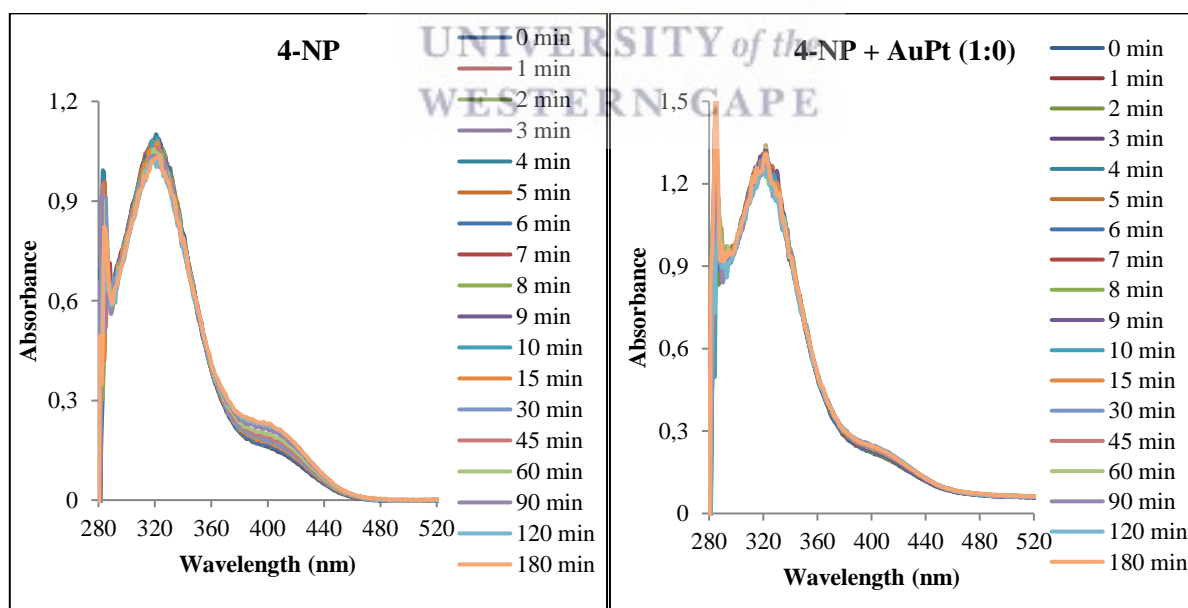| Nanoparticles	Rate constant (kcat)	References
AuPtNPs (1:0)	3.2×10^{-3}/sec	Current work
AuPtNPs (1:2)	2.2×10^{-3}/sec	Current work
AuPtNPs (1:5)	1.2×10^{-3}/sec	Current work
Citrate AuNPs	0.6×10^{-3}/sec	(Seoudi and Said, 2011)
CTAB AuNPs	1.9×10^{-3}/sec	
Chitosan AuNPs	2.4×10^{-3}/sec	
AuNPs (4 nm)	1.4×10^{-2}/sec	(Seoudi and Al-Marhaby, 2016)
AuNPs (7 nm)	9.1×10^{-3}/sec	
AuNPs (10 nm)	3×10^{-3}/sec	
PtNPs	3.5×10^{-2}/sec	(Zhang *et al.*, 2014)
Bare PtNPs	1.51×10^{-3}/sec	(Maji *et al.*, 2014)
PVPh–PtBH$_4$	2.1×10^{-3}/sec	
PVPh–Pt1.3	1.08×10^{-3}/sec	
Pt$_{50}$Au$_{50}$NPs	10.87×10^{-2}/sec	(Zhang *et al.*, 2014)
Pt$_{70}$Au$_{30}$NPs	5.5×10^{-2}/sec	
Pt$_{30}$Au$_{70}$NPs	10.14×10^{-2}/sec	
AuPtNPs (nanotubes)	1.3×10^{-3}/sec	(Fu *et al.*, 2014)
Carbon-PtAuNPs	3.2×10^{-3}/sec	(Peng *et al.*, 2013)

*Abbreviations: Au: gold; Pt: platinum; NPs: nanoparticles; Pt$_{50}$Au$_{50}$; Pt$_{70}$Au$_{30}$ and Pt$_{30}$Au$_{70}$: molar ratios of precursor metallic salts used in synthesis; PVPh: poly(4-vinyl phenol): PVPh; PVPh–PtBH$_4$: poly(4-vinyl phenol) platinum nanoparticles (PtNPs) synthesized using sodium borohydride and PVPh–Pt1.3: poly(4-vinyl phenol) platinum nanoparticles synthesized using 1.3 mM H$_2$PtCl$_6$ concentration

5. Conclusion

Citrate-capped AuPtNPs were shown to successfully reduce 4-NP to 4-AP. The rate of reduction was dependent on the concentration of AuPtNPs. The k_{cat} is 3.2×10^{-3}/sec for the undiluted AuPtNPs (1:0) and for diluted AuPtNPs (1:2) and AuPtNPs (1:5) reduced the k_{cat} to 3.2×10^{-3}/sec; 2.2×10^{-3}/sec and 1.2×10^{-3}/sec respectively. This was in line with previous reported rate constants for similar bimetallic AuPtNPs and demonstrated higher k_{cat} when

234

compared to some of the monometallic AuNPs and PtNPs reported in literature. Therefore, citrate-capped AuPtNPs have a potential application in catalysis and may provide hope in the management of 4-NP removal in the environment.

6. References

Abdollahi, M. and Mohammadirad, A. (2014). Nitrophenol, in Wexler, P. (ed.). *Encyclopedia of Toxicology (Third Edition)*. Oxford: Academic Press, 575–577.

Al Bakain, R.Z., Abu-Zurayk, R.A., Hamadneh, I., Khalili, F.I. and Al-Dujaili, A.H. (2015). A study on removal characteristics of o-, m-, and p-nitrophenol from aqueous solutions by organically modified diatomaceous earth. *Desalination and Water Treatment*, 56(3): 826–838.

Al-Marhaby, F.A. and Seoudi, R. (2016). Preparation and Characterization of Silver Nanoparticles and Their Use in Catalytic Reduction of 4-Nitrophenol. *World Journal of Nano Science and Engineering*, 6(1): 29–37.

Alshammari, K., Niu, Y., Palmer, R.E. and Dimitratos, N. (2020). Optimization of sol-immobilized bimetallic Au–Pd/TiO2 catalysts: reduction of 4-nitrophenol to 4-aminophenol for wastewater remediation. *Philosophical Transactions of the Royal Society A: Mathematical, Physical and Engineering Sciences*, 378(2176): 20200057.

Baran, T. (2019). Biosynthesis of Highly Retrievable Magnetic Palladium Nanoparticles Stabilized on Bio-composite for Production of Various Biaryl Compounds and Catalytic Reduction of 4-Nitrophenol. *Catalysis Letters*, 149(6): 1721–1729.

Berahim, N., Basirun, W.J., Leo, B.F. and Johan, M.R. (2018). Synthesis of Bimetallic Gold-Silver (Au-Ag) Nanoparticles for the Catalytic Reduction of 4-Nitrophenol to 4-Aminophenol. *Catalysts*, 8(10): 412.

Chatterjee, D.K., Diagaradjane, P. and Krishnan, S. (2011). Nanoparticle-mediated hyperthermia in cancer therapy. *Therapeutic Delivery*, 2(8): 1001–1014.

Chatterjee, S., Chakraborty, M., Bera, K.K., Mahajan, A., Banik, S., Roy, P.S. and Bhattacharya, S.K. (2021). Catalytic reduction of 4-nitrophenol to 4-aminophenol using an efficient Pd nanoparticles. *IOP Conference Series: Materials Science and Engineering*, 1080(1): 012010.

Chu, C. and Su, Z. (2014). Facile synthesis of AuPt alloy nanoparticles in polyelectrolyte multilayers with enhanced catalytic activity for reduction of 4-nitrophenol. *Langmuir: the ACS journal of surfaces and colloids*, 30(50): 15345–15350.

Deka, P., Deka, R.C. and Bharali, P. (2014). In situ generated copper nanoparticle catalyzed reduction of 4-nitrophenol. *New Journal of Chemistry*, 38(4): 1789–1793.

Din, M.I., Khalid, R., Hussain, Z., Hussain, T., Mujahid, A., Najeeb, J. and Izhar, F. (2020). Nanocatalytic Assemblies for Catalytic Reduction of Nitrophenols: A Critical Review. *Critical Reviews in Analytical Chemistry*, 50(4): 322–338.

Fu, G., Ding, L., Chen, Y., Lin, J., Tang, Y. and Lu, T. (2014). Facile water-based synthesis and catalytic properties of platinum–gold alloy nanocubes. *CrystEngComm*, 16(9): 1606–1610.

Garba, H.W., Abdullahi, M.S., Jamil, M.S.S. and Endot, N.A. (2021). Efficient Catalytic Reduction of 4-Nitrophenol Using Copper(II) Complexes with N,O-Chelating Schiff Base Ligands. *Molecules*, 26(19): 5876.

Harrison, M.A.J., Barra, S., Borghesi, D., Vione, D., Arsene, C. and Olariu, R.I. (2005). Nitrated phenols in the atmosphere: a review. *Atmospheric Environment*, 2(39): 231–248.

Islam, M.T., Saenz-Arana, R., Wang, H., Bernal, R. and Noveron, J.C. (2018). Green synthesis of gold, silver, platinum, and palladium nanoparticles reduced and stabilized by sodium rhodizonate and their catalytic reduction of 4-nitrophenol and methyl orange. *New Journal of Chemistry*, 42(8): 6472–6478.

Kästner, C. and Thünemann, A.F. (2016). Catalytic Reduction of 4-Nitrophenol Using Silver Nanoparticles with Adjustable Activity. *Langmuir*, 32(29): 7383–7391.

Kaur, J., Singh, J. and Rawat, M. (2019). An efficient and blistering reduction of 4-nitrophenol by green synthesized silver nanoparticles. *SN Applied Sciences*, 1(9): 1060.

Lee, S.J., Yu, Y., Jung, H.J., Naik, S.S., Yeon, S. and Choi, M.Y. (2021). Efficient recovery of palladium nanoparticles from industrial wastewater and their catalytic activity toward reduction of 4-nitrophenol. *Chemosphere*, 262: 128358.

Li, G., Zhang, W., Luo, N., Xue, Z., Hu, Q., Zeng, W. and Xu, J. (2021). Bimetallic Nanocrystals: Structure, Controllable Synthesis and Applications in Catalysis, Energy and Sensing. *Nanomaterials*, 11(8): 1926.

Liang, M., Zhang, G., He, Y., Hou, P., Li, M. and Lv, B. (2019). Lysimachia christinae polysaccharide mediated facile synthesis of gold-silver alloy nanoparticles for catalytic reduction of 4-nitrophenol. *IOP Conference Series: Earth and Environmental Science*, 330(4): 042053.

Lim, S.H., Ahn, E.-Y. and Park, Y. (2016). Green Synthesis and Catalytic Activity of Gold Nanoparticles Synthesized by Artemisia capillaris Water Extract. *Nanoscale Research Letters*, 11(1): 474.

Lu, Y., Yuan, J., Polzer, F., Drechsler, M. and Preussner, J. (2010). In situ growth of catalytic active Au-Pt bimetallic nanorods in thermoresponsive core-shell microgels. *ACS nano*, 4(12): 7078–7086.

Maji, T., Banerjee, S., Biswas, M. and Mandal, T.K. (2014). In situ synthesis of ultra-small platinum nanoparticles using a water soluble polyphenolic polymer with high catalytic activity. *RSC Advances*, 4(93): 51745–51753.

Pandey, S. and Mishra, S.B. (2014). Catalytic reduction of p-nitrophenol by using platinum nanoparticles stabilised by guar gum. *Carbohydrate Polymers*, 113: 525–531.

Panigrahi, S., Basu, S., Praharaj, S., Pande, S., Jana, S., Pal, A., Ghosh, S.K. and Pal, T. (2007). Synthesis and Size-Selective Catalysis by Supported Gold Nanoparticles: Study on Heterogeneous and Homogeneous Catalytic Process. *The Journal of Physical Chemistry C*, 111(12): 4596–4605.

Peng, Y., Wu, X., Qiu, L., Liu, C., Wang, S. and Yan, F. (2013). Synthesis of carbon–PtAu nanoparticle hybrids originating from triethoxysilane-derivatized ionic liquids for methanol electrooxidation and the catalytic reduction of 4-nitrophenol. *Journal of Materials Chemistry A*, 1(32): 9257–9263.

Petkar, D.R., Kadu, B.S. and Chikate, R.C. (2014). Highly efficient and chemoselective transfer hydrogenation of nitroarenes at room temperature over magnetically separable Fe–Ni bimetallic nanoparticles. *RSC Advances*, 4(16): 8004–8010.

Petrucci, O.D., Buck, D.C., Farrer, J.K. and Watt, R.K. (2013). A ferritin mediated photochemical method to synthesize biocompatible catalytically active gold nanoparticles: size control synthesis for small (∼2 nm), medium (∼7 nm) or large (∼17 nm) nanoparticles. *RSC Advances*, 4(7): 3472–3481.

Pozun, Z.D., Rodenbusch, S.E., Keller, E., Tran, K., Tang, W., Stevenson, K.J. and Henkelman, G. (2013). A Systematic Investigation of p-Nitrophenol Reduction by Bimetallic Dendrimer Encapsulated Nanoparticles. *The Journal of Physical Chemistry. C, Nanomaterials and Interfaces*, 117(15): 7598–7604.

Ravi, G., Sarasija, M., Ayodhya, D., Kumari, L.S., Ashok, D. and Ravi, G. (2019). Facile synthesis, characterization and enhanced catalytic reduction of 4-nitrophenol using NaBH4 by undoped and Sm3+, Gd3+, Hf3+ doped La2O3 nanoparticles. *Nano Convergence*, 6(1): 12.

Saha, S., Pal, A., Kundu, S., Basu, S. and Pal, T. (2010). Photochemical Green Synthesis of Calcium-Alginate-Stabilized Ag and Au Nanoparticles and Their Catalytic Application to 4-Nitrophenol Reduction. *Langmuir*, 26(4): 2885–2893.

Saira, F., Saleemi, S., Razzaq, H. and Qureshi, R. (2021). Spectrophotometric analysis of stability of gold nanoparticles during catalytic reduction of 4-nitrophenol. *Turkish Journal of Chemistry*, 45(1): 82–91.

Seo, Y.S., Ahn, E.-Y., Park, J., Kim, T.Y., Hong, J.E., Kim, K., Park, Yohan, P. and Youmie, P. (2017). Catalytic reduction of 4-nitrophenol with gold nanoparticles synthesized by caffeic acid. *Nanoscale Research Letters*, 12:7.

Seoudi, R. and Al-Marhaby, F.A. (2016). Synthesis, Characterization and Photocatalytic Application of Different Sizes of Gold Nanoparticles on 4-Nitrophenol. *World Journal of Nano Science and Engineering*, 06(03): 120.

Seoudi, R. and Said, D.A. (2011). Studies on the Effect of the Capping Materials on the Spherical Gold Nanoparticles Catalytic Activity. *World Journal of Nano Science and Engineering*, 1(2): 51–61.

Srisombat, L., Nonkumwong, J., Suwannarat, K., Kuntalue, B. and Ananta, S. (2017). Simple preparation Au/Pd core/shell nanoparticles for 4-nitrophenol reduction. *Colloids and Surfaces A: Physicochemical and Engineering Aspects*, C (512): 17–25.

Teimouri, M., Khosravi-Nejad, F., Attar, F., Saboury, A.A., Kostova, I., Benelli, G. and Falahati, M. (2018). Gold nanoparticles fabrication by plant extracts: synthesis, characterization, degradation of 4-nitrophenol from industrial wastewater, and insecticidal activity – A review. *Journal of Cleaner Production*, 184: 740–753.

Wunder, S., Polzer, F., Lu, Y., Mei, Y. and Ballauff, M. (2010). Kinetic Analysis of Catalytic Reduction of 4-Nitrophenol by Metallic Nanoparticles Immobilized in Spherical Polyelectrolyte Brushes. *The Journal of Physical Chemistry C*, 114(19): 8814–8820.

Yahya, A.A., Rashid, K.T., Ghadhban, M.Y., Mousa, N.E., Majdi, H.S., Salih, I.K. and Alsalhy, Q.F. (2021). Removal of 4-Nitrophenol from Aqueous Solution by Using Polyphenylsulfone-Based Blend Membranes: Characterization and Performance. *Membranes*, 11(3): 171.

Ye, W., Yu, J., Zhou, Y., Gao, D., Wang, D., Wang, C. and Xue, D. (2016). Green synthesis of Pt–Au dendrimer-like nanoparticles supported on polydopamine-functionalized graphene and their high performance toward 4- nitrophenol reduction. *Applied Catalysis B: Environmental*, 181: 71–378.

You, J.-G., Shanmugam, C., Liu, Y.-W., Yu, C.-J. and Tseng, W.-L. (2017). Boosting catalytic activity of metal nanoparticles for 4-nitrophenol reduction: Modification of metal naoparticles with poly(diallyldimethylammonium chloride). *Journal of Hazardous Materials*, 324(Pt B): 420–427.

Zaleska-Medynska, A., Marchelek, M., Diak, M. and Grabowska, E. (2016). Noble metal-based bimetallic nanoparticles: the effect of the structure on the optical, catalytic and photocatalytic properties. *Advances in Colloid and Interface Science*, 229: 80–107.

Zhang, J., Chen, G., Guay, D., Chaker, M. and Ma, D. (2014). Highly active PtAu alloy nanoparticle catalysts for the reduction of 4-nitrophenol. *Nanoscale*, 6(4): 2125–2130.

Zhang, K., Suh, J.M., Choi, J.-W., Jang, H.W., Shokouhimehr, M. and Varma, R.S. (2019). Recent Advances in the Nanocatalyst-Assisted NaBH4 Reduction of Nitroaromatics in Water. *ACS Omega*, 4(1): 483–495.

Zhao, Y., Wu, Z., Wang, Y., Yang, C. and Yunxing, L. (2017). Facile fabrication of polystyrene microsphere supported gold-palladium alloy nanoparticles with superior catalytic performance for the reduction of 4-nitrophenol in water. *Colloids and Surfaces A: Physicochemical and Engineering Aspects*, 529: 417–424.

Zhu, Q.-L. and Xu, Q. (2016). Immobilization of Ultrafine Metal Nanoparticles to High-Surface-Area Materials and Their Catalytic Applications. *Chem*, 1(2): 220–245.

CHAPTER SEVEN: CONCLUSION

7.1. General discussion and conclusions

The current treatment options for glioblastoma multiforme (GB) and neuroblastoma (NB) are largely unsatisfactory and there have been no significant improvements in effectiveness of therapeutic strategies for these two cancers in recent years. Standard chemotherapeutic drugs and radiation treatments have severe side effects, drug resistance, poor targeted delivery efficiency and a highly selective blood-brain barrier (BBB) which restricts drug delivery of most chemotherapeutic drugs into the brain (Smith and Foster, 2018; Bastiancich, Da Silva and Estève, 2021). This necessitates the development of novel therapeutic strategies that encompass high specificity and demonstrates the potential to cross the BBB. Chlorotoxin (CTX) is a scorpion venom derived peptide, which has been a cancer cell targeting peptide of intense focus recently, due to its high selectivity and binding affinity to a broad-spectrum of cancer cells, especially GB and tumours of neuroectodermal origin such as NB cancer (Lyons, O'Neal and Sontheimer, 2002). Given the potential of nanotechnology, within neuroscience for its favourable size in targeting tumours and bypassing the blood brain barrier (BBB), CTX-based NPs is a promising area of research for developing therapeutic approaches that combine target specific drug delivery and diagnostics, to address the many challenges still posed by these cancers. CTX thus holds promise for the development of novel and effective multi-functional nano-based applications for cancer. Therefore, the principal aim of this study was to develop two new target-specific metallic nano-systems for the *in vitro* investigation into GB and NB cells, with the potential to be used for future non-invasive RF field-induced targeted hyperthermia.

The review (Chapter 2) highlights the challenges associated with GB and NB cancers and describes the characteristics of CTX as a promising targeting peptide for these cancers and discusses CTX-based nanotechnology applications that could serve diagnostic and therapeutic purposes in the management of GB and potentially for NB. There is substantial evidence that demonstrated the BBB crossing potential of CTX as well as its high tumour-binding function mediated by the molecular targets namely, chloride channels, matrix metalloproteinase MMP-2 (MMP-2), annexin A2 and recently, estrogen receptor alpha (Erα) and Neuropilin-1 (NRP-1) in different cancer cells (Kesavan *et al.*, 2010; Cohen, Burks and Frank, 2018; Ayomide *et al.*, 2018; Sharma *et al.*, 2021). However, CTX has the highest binding affinity for GB. It is

239

widely reported and accepted that MMP-2 and chloride channel-3 (CIC-3) form a protein complex located within the same membrane domain in GB cells and is targeted by CTX which inhibits glioma cell migration and invasion (Deshane, Garner and Sontheimer, 2003; Qin *et al.*, 2014). Although CTX has been shown in several *in vivo* studies to demonstrate considerable potential for crossing the BBB (Chapter 2), the specific mechanism of action is still not well understood in literature, and more research is required to fully elucidate the mechanisms involved in crossing of the BBB. CTX-NPs may function by improving localization of chemotherapeutic and genotherapeutic drugs to diseased cells specifically, enhancing imaging modalities like magnetic resonance imaging (MRI), single-photon emission computed tomography (SPECT), optical imaging techniques and image-guided surgery, as well as improving the sensitization of radio-resistant cells to radiotherapy treatment. While recent studies demonstrated combined diagnostic and therapeutic applications (theranostic approaches), few studies report on the hyperthermia applications of CTX-NPs using near-infrared (NIR) light triggered photothermal therapy (PTT) (Locatelli *et al.*, 2014; Pandey *et al.*, 2020). However, NIR PTT is limited to subcutaneous malignant tumours because of minimal tissue penetration which may not be suitable for deep-seated brain tumours whereas radiofrequency (RF) waves are shown to penetrate more deeply located tumours and are considered generally safer (Nasseri *et al.*, 2016; Corr and Curley, 2017; Chang *et al.*, 2018). Additionally, the use of bimetallic NPs such as gold platinum NPs (AuPtNPs) exhibits photothermal effects with some studies showing better effects than the respective monometallic NPs (Tang *et al.*, 2014; Liu *et al.*, 2017; Song *et al.*, 2017, 2021; Yang *et al.*, 2018; Depciuch *et al.*, 2019; Fathima and Mujeeb, 2021), possibly due to the synergistic effects of the two composite metallic atoms and new surface properties that are different in their monometallic NPs. Therefore, the use of CTX-AuPtNPs incorporating RF waves for targeted hyperthermia was recommended as one of the prospective applications for GB and NB treatment as it has not been investigated previously and may yield promising results that could offer new hope for the effective treatment and management of these tumours.

In this study we aimed to develop two novel types of CTX functionalised metallic NPs not previously reported in literature, to add to the growing variety of CTX-NPs being developed and investigated for GB and other cancers with the potential for future targeted non-invasive radiofrequency-induced thermal therapy. We demonstrated in Chapter 3, using a facile three-step preparation method, the synthesis of CTX functionalized monometallic gold NPs (CTX-AuNPs) and CTX functionalized bimetallic gold platinum NPs (CTX-AuPtNPs). The first step

240

was the preparation of citrate capped AuNPs and AuPtNPs which were then PEGylated using PEG-OH and PEG-biotin to produce PEG-AuNPs and PEG-AuPtNPs and finally conjugated with biotinylated CTX onto the surface of NPs via streptavidin to produce CTX-AuNPs and CTX-AuPtNPs. UV-Vis absorbance spectra showed a redshift in the SPR peaks from citrate AuNPs (508 nm) after PEGylation (518) and CTX functionalization (521), while the absence of an SPR peak for AuPtNPs confirmed the formation of bimetallic NPs. This was in line with the increase in mean hydrodynamic size and changes in surface charges of NPs as reported from DLS analysis. Both citrate capped AuNPs and AuPtNPs had a hydrodynamic size of approximately 7 nm and doubled in size to approximately 14 nm after PEGylation and further increased after CTX conjugation to 16.71 ± 2.48 nm and 21.13 ± 1.62 nm, for CTX-AuNPs and CTX-AuPtNPs, respectively. The shift in ζ-potential values from approximately - 30 mV for citrate capped NPs to more neutral charges after PEGylation (PEG-AuNPs: -16.92 ± 0.76 mV and PEG-AuPtNPs: -20.08 ± 1.64 mV) and CTX functionalization (CTX-Au: -11.04 ± 2.12 mV and CTX-AuPtNPs: -14.53 ± 2.74 mV) also confirmed changes in surface modification of NPs and suggests successful surface functionalization. This was further confirmed by FTIR analysis. The co-stabilization method of using two PEG molecules, PEG-OH and PEG-Biotin and CTX bimolecular immobilization via streptavidin added to the greater stability and dispersibility that was observed for these NPs in DMEM supplemented with 10 % FBS over a 48- hour incubation period at 37 ⁰C when compared to citrate capped NPs. TEM analysis also confirmed that the NPs did not aggregate. All NPs had an average core size of approximately 5 nm, were monodispersed and mostly spherical with almost equidistant arrangement of NPs after surface functionalization. This observation was in good agreement with the PDI values (< 0.5) reported by DLS analysis, which is indicative of a monodisperse distribution of the NPs in solution. EDX confirmed the presence of Au in all AuNPs and both Au and Pt in all AuPtNPs. Using a simple competitive binding assay and FITC-tagged CTX (FITC-CTX), the binding efficiency of CTX to U87 human GB cell line was more pronounced than in SH-SY5Y human NB cell line as determined by flow cytometry. This did not only demonstrate the target specific binding of CTX but also suggests that the expression levels of the target surface proteins are higher in U87 cells than in SH-SY5Y cells. We also demonstrated uptake of NPs by U87 and SH-SY5Y cells using dark field microscopy.

We then proceeded to investigate the effects of the CTX-NPs on the viability of the cancerous U87 and SH-SY5Y cell lines as well as the non-cancerous KMST-6 cell line (Chapter 4). Using the WST-1 Cell Proliferation Assay, cell viability was assessed after 48 hours treatment with

241

citrate AuNPs, citrate AuPtNPs, PEG-AuNPs, PEG-AuPtNPs, CTX-AuNPs and CTX-AuPtNPs at a concentration range of 75-300 µg/ml. The responses of the different cell lines varied significantly, with the viability of the KMST-6 cells being less affected by the treatment with the NPs, since the IC_{50} values were significantly higher for this cell line compared to the U87 and SH-SY5 cell lines. The U87 cell line appeared to be the most sensitive to the effects of the NPs, since the IC_{50} values for all the NPs were lower for this cell line. Based on the IC_{50} values, the bimetallic citrate AuPtNPs were more toxic than the monometallic citrate AuNPs in U87 and SH-SY5Y cells and the addition of PEG onto NPs reduced the observed toxicity in these cell lines. The higher cytotoxic effects of AuPtNPs as compared to AuNPs may potentially be due to synergistic effects of the 2 metals (Au and Pt) or due to Pt as previously reported in different cell lines (Kutwin *et al.*, 2017; Almeer *et al.*, 2018; Shin *et al.*, 2018; Boomi *et al.*, 2019; Gurunathan *et al.*, 2020; Chaturvedi *et al.*, 2021). The selective toxicity of CTX-NPs to U87 and SH-SY5Y cells, and negligible toxicity to KMST-6 cells may be attributed to CTX binding to target recognition sites which is more abundantly expressed in the cancer cell lines (Soroceanu *et al.*, 1998; Lyons, O'Neal and Sontheimer, 2002). Treatments with the NPs was accompanied with distinct morphological changes where the normal astrocyte-like shape of untreated U87 and SH-SY-5Y cells became spherical in shape and detached from the growth plate after exposure to the different NPs (at a concentration of 225 µg/ml) for 48 hours, which was in line with the viability experiments and is indicative of cellular stress and cell death caused by the NPs. Based on the morphology of the cells and the density of the cells, it was apparent that treatments with CTX-AuPtNP was more toxic in both U87 and SH-SY-5Y cells. The established IC_{50} concentration value for CTX-AuPtNPs (166 µg/ml) in U87 cells was the lowest reported value and was used to assess the induction of apoptosis, oxidative stress, and mitochondrial depolarization in these cells using the Cell-APOPercentage™ assay, CM-H_2DCFDA fluorogenic molecular probe and TMRE assay, respectively. The results revealed that the mechanism of toxicity of the CTX-AuPtNP in U87 cells is associated with increased oxidative stress, mitochondrial depolarization, and the eventual induction of apoptosis. To determine the effect of NPs on cell survival and clonogenicity, a clonogenic assay was performed over a 20-day period by treating U87 cells with citrate AuNPs, citrate AuPtNPs, CTX-AuNPs and CTX-AuPtNPs with the established IC_{50} values obtained from the cell viability assay. CTX-AuNPs and CTX-AuPtNPs showed a near complete inhibition in colony formation in U87 cells when compared to untreated and citrate capped NPs, highlighting the inhibitory properties of CTX in cell lines known to overexpress surface proteins involved in cell migration. In addition to cell viability, cell

migration is also an important factor for tumour enlargement and therefore a wound healing assay using U87 cells were performed to further investigate the anti-migratory properties of the CTX-NPs. CTX-NPs significantly inhibited the closure of the wounds, with CTX-AuPtNPs displaying a slightly more efficient inhibitory effect than CTX-AuNPs. The results reported in clonogenic assay and wound healing assay raised the possibility that CTX-NPs inhibits U87 cell migration through the MMP-2/ClC-3 protein complex or A2 interaction or both as previously described (Deshane, Garner and Sontheimer, 2003; Kesavan *et al.*, 2010; Qin *et al.*, 2014). To the best of our knowledge, this is the first report on the evaluation of the cytotoxicity of the PEG-NPs (using a ratio of PEG-OH and PEG-biotin) and CTX-NPs as synthesized in Chapter 3, as well as treatment with small citrate AuPtNPs (~5 nm) at concentrations as high as 300 µg/ml in these cell lines.

Nanotoxicological evaluations are usually performed *in vitro* with traditional bioassays owing to its simplicity. The outcome may not predict the *in vivo* toxicity accurately; however, it does provide important information for understanding the uptake and mechanism of toxicity. Using traditional bioassays to investigate toxicity of NPs does have some limitations which have been described previously (Nelissen *et al.*, 2020). To better understand the underlying mechanisms of cytotoxicity, the use of gene expression technologies, which assess biological responses at a molecular level is often recommended in addition to the use of bioassays. Therefore, in Chapter 5, to further evaluate the cytotoxic effects of CTX-AuPtNPs on U87 cells, genes involved in cytotoxicity was investigated using the RT² First Strand Kit and Human Molecular Toxicology Pathway Finder RT² Profiler PCR Array from Qiagen. A dose response study that was performed previously using the WST-1 assay (Chapter 4) showed that 75 µg/ml CTX-AuPtNPs was the lowest concentration that caused a significant reduction in the cell viability of U87 cells over 48 hours.To determine the optimal timepoint to use for gene expression studies, U87 cells were treated with 75 µg/ml CTX-AuPtNPs and the cell viability was determined using the WST-1 Cell Proliferation Assay for exposure timepoints of: 0; 3; 6; 12; 24; 48 hours. Based on this, 24-hour treatment with 75 µg/ml CTX-AuPtNPs was selected for the gene expression profiling experiments. A total of 16 genes out of 86 that were differentially expressed in U87 cells treated with 75 µg/ml of CTX-AuPtNPs for 24 hours. Three of these genes were upregulated (*TRIB3*, *TAGLN* and *ASNS*) while sixteen were downregulated (*UHRF1*, *LSS*, *HSPA1A*, *HSPA4*, *MKI67*, *HSPA8*, *CASP8*, *CASP9*, *METAP2*, *PPARA*, *AKT1*, *GCLM* and *ABCC2*). The expression of the upregulated genes is involved in endoplasmic reticulum stress (ER) and unfolded protein response (UPR), which was more significantly

243

affected than the other differentially expressed genes (DEGs), while genes involved in mitochondrial energy metabolism and apoptosis were downregulated. While 24-hour treatment with 75 µg/ml CTX-AuPtNPs was not cytotoxic and genotoxic in U87 cells, these cells experienced some form of cellular stress and interference with protein synthesis and that cytoprotective cellular pathways were activated as a response to this cellular stress. To the best of our knowledge, this is the first ever gene expression study which investigated the effects of bimetallic AuPtNPs on the expression levels of genes in a brain cancer cell line.

Bimetallic NPs (BNPs) constructed of two different metal elements have not only attracted great attention for improved anti-cancer applications but are widely investigated for applications in catalysis. AuPtNPs have attracted much attention because they present distinct and improved features when compared to their monometallic counterparts for enhancing catalytic activity (Seoudi and Said, 2011; Peng *et al.*, 2013; Maji *et al.*, 2014; Zhang *et al.*, 2014). This is achieved primarily through exploiting the synergistic effects of the combined metals. While an investigation into the application of the NPs in catalysis is outside the scope of the initial study, there is a growing interest in the use of BNPs for applications in catalysis, and we therefore investigated the catalytic activity of citrate capped AuPtNPs (Chapter 6). In this study we investigated the potential of citrate capped AuPtNPs to catalyse the reduction of 4-nitrophenol (4-NP). 4-NP is a toxic substance that is often present in industrial and agricultural wastewaters and has also been found in marine and fresh water (Yahya *et al.*, 2021). The removal of 4-NP from water bodies and the development of efficient eco-friendly wastewater removal routes is vital to maintain a balanced eco-system and an overall healthier environment. AuPtNPs were used in the reduction of 4-NP to 4-aminophenol (4-AP) in the presence of sodium borohydride ($NaBH_4$). Citrate-capped AuPtNPs successfully reduced the 4-NP to 4-AP at a k_{cat} (catalytic rate constant) of 3.2×10^{-3}/sec and was in line with a previous study reporting on similar AuPtNPs (Peng *et al.*, 2013). Although the k_{cat} was lower than most previously reported k_{cat} for similar bimetallic AuPtNPs (Lu *et al.*, 2010; Zhang *et al.*, 2014), the AuPtNPs used in this study demonstrated higher k_{cat} when compared to monometallic AuNPs and PtNPs previously reported in literature (Seoudi and Said, 2011; Maji *et al.*, 2014; Seoudi and Al-Marhaby, 2016). This enhanced catalytic activity may be attributed to the synergistic effects between Au and Pt atoms in AuPtNPs as previously described (Peng *et al.*, 2013; Chu and Su, 2014; Zhang *et al.*, 2014). To the best of our knowledge, the use of this type of citrate AuPtNPs for the reduction of 4-NP to 4-AP was not previously reported. Therefore,

244

these citrate AuPtNPs may have a potential application in catalysis and provide hope in the management of 4-NP removal from the environment.

In conclusion, the findings of this study provide two novel CTX metallic NPs, that demonstrated uptake and targeting to cells known to overexpress molecular targets of interest. The uptake of these NPs resulted in cell death as a result of apoptosis, increase in oxidative stress and mitochondrial depolarization as well as inhibition of cell migration and invasion. Gene expression studies revealed that cells experienced some form of cellular stress and interference with protein synthesis and that cytoprotective cellular pathways were activated as a response to this cellular stress when treated with low concentrations of CTX-AuPtNPs. In addition to the anti-cancer activity reported with AuPtNPs, they also demonstrated a promising application in catalysis. These results indicate that the developed nanosystems have the potential for application in hyperthermia treatment and therefore can be investigated in future for non-invasive RF-induced targeted hyperthermia treatment for GB and NB *in vitro* and *in vivo*.

7.2. Future recommendations

In this study we designed stable small PEG-AuNPs and PEG-AuPtNPs using a ratio of PEG-OH and PEG-Biotin, streptavidin was used for linking the PEG-biotin to the biotinylated CTX (Chapter 3). The same approach can be used to design multi-layered nanoconjugates for other biotinylated molecules for applications involving imaging and cell tracking investigations. For future imaging and cell tracking investigations, biotinylated fluorescent molecules will be attached to the CTX-NPs due to the versatility of PEG-biotin used in this study.

Darkfield microscopy was used to confirm the uptake of metallic NPs in cells (Chapter 3), however it could not be used to quantify uptake, therefore inductively coupled plasma optical emission spectrometry (ICP-OES) is needed in the future to quantitatively assess the cellular uptake of CTX-NPs compared to CTX-void NPs.

The production of intracellular ROS was evaluated using the fluorogenic molecular CM-H$_2$DCFDA (Chapter 4). The experiment was conducted once in triplicate wells and revealed highly comparable results and raised the possibility that the ROS activity is due to cellular internalization of CTX-AuPtNPs, especially when considered with the results reported from

245

the other assays assessing apoptosis and mitochondrial function. However, in future, the experiments will be repeated thrice to conclusively report on the induction of ROS.

U87 cells treated CTX-AuPtNPs induced changes in cell morphology reminiscent of cells undergoing apoptosis (Chapter 4). We then confirmed apoptosis was induced by CTX-AuPtNPs using IC_{50} concentrations in U87 and quantified using APOPercentage™ assay (Chapter 4). Caspases are known as important molecular biomarkers for assessing apoptosis and executioner caspases, caspase 3 and 7, are frequently used as markers of apoptosis (Bressenot *et al.*, 2009). Therefore, to further validate the apoptotic effects of these NPs, in future studies we will assess Caspase-3/7 activation using the Caspase-3/7 GloTM assay kit.

CTX does not bind to human skin fibroblast cell lines (Lyons, O'Neal and Sontheimer, 2002). Therefore, we selected KMST-6 Human skin fibroblasts as a non-cancerous control cell line. In future, NPs will also be assessed in a non-cancerous control cell line that is derived from human brain tissues such as Normal Human Astrocytes (NHA).

The gene expression analysis study reported in chapter 5, provides insight into the molecular mechanisms involved in early cytotoxicity in U87 cell lines after treatment with CTX-AuPtNPs by analysing 86 genes involved in cytotoxicity. Future studies will also evaluate the differentially expressed genes after increasing the treatment times to 48 and 72 hours. We will also employ the use of additional bioinformatics tools or in silico tools to further investigate and explain CTX-AuPtNPs biological function at the molecular level.
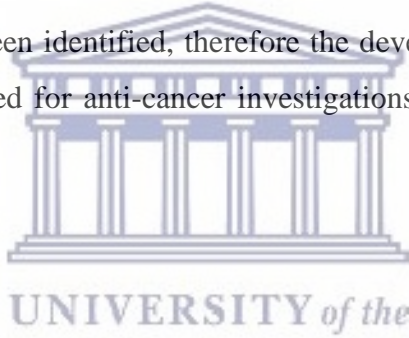
In order to investigate the permeability of CTX across the BBB *in vitro*, future work will make use of an *in vitro* BBB model (with specific tight junction proteins) for assessing transendothelial electrical resistance (TEER) measurements (Bagchi *et al.*, 2019). Animal models of GB and NB are recommended to investigate the *in vivo* effects of NPs, in terms of targeting brain tumours and monitoring the clearance and biodistribution to determine whether there is an association with the *in vitro* findings reported in this study.

Hyperthermia treatment is one of the oldest treatments for cancer and combining it with the characteristics of metallic NPs has recently generated a renewed sense of excitement for novel thermal therapies. The CTX-NPs were constructed with the intention of future applications using radiofrequency field-based targeted hyperthermia treatment. The use of MNPs to induce

246

localized hyperthermia ablation within cancer cells has recently gained momentum in cancer nanotechnology research but has not been fully exploited for brain and other nervous system tumours. Therefore, we are encouraged to explore this as an alternative therapeutic option for the treatment of GB and NB resistant tumours in future. Due to the highly sophisticated set up of some RF-generators for research based purposes (e.g. The Kanzius non-invasive radio-frequency hyperthermia system) for NP-mediated thermal ablation *in vitro* and *in vivo*, these types of experiments are recommended to be performed in a medical research facility that houses this equipment and is currently not available in South Africa, but in countries such as the United States of America, Russia and China (Corr and Curley, 2017; Gongalsky *et al.*, 2019; Li *et al.*, 2020; Mocan *et al.*, 2021). In addition to the two CTX-AuNPs and CTX-AuPtNPs that was developed in this study, in our future work, we will develop and optimize CTX conjugated to platinum NPs (CTX-PtNPs), for further investigation of all three CTX-NPs *in vitro* and *in vivo* mice models for GB using RF-induced hyperthermia treatment.

Finally, CTX targets a broad list of cancer cells of neuroectodermal origin and in recent years more molecular targets have been identified, therefore the developed CTX-NPs in this work has the potential to be expanded for anti-cancer investigations *in vitro* and *in vivo* in other cancer types.

7.3. References

Almeer, R.S., Ali, D., Alarifi, S., Alkahtani, S. and Almansour, M. (2018). Green Platinum Nanoparticles Interaction With HEK293 Cells: Cellular Toxicity, Apoptosis, and Genetic Damage. *Dose-Response*, 16(4): 1559325818807382.

Ayomide, S.O., Oko, G.E., Chukwu, C.C., Vo, K.T.K. and Okoi, E.P. (2018). Effects of Chlorotoxin on Matrix Metalloproteinase-2 (MMP-2) in Melanoma and Breast Cancer Cell Lines. *Journal of Advances in Medical and Pharmaceutical Sciences*, 17(2): 1–11.

Bagchi, S., Chhibber, T., Lahooti, B., Verma, A., Borse, V. and Jayant, R.D. (2019). In-vitro blood-brain barrier models for drug screening and permeation studies: an overview. *Drug Design, Development and Therapy*, 13: 3591–3605.

Bastiancich, C., Da Silva, A. and Estève, M.-A. (2021). Photothermal Therapy for the Treatment of Glioblastoma: Potential and Preclinical Challenges. *Frontiers in Oncology*, 10: 610356.

Boomi, P., Poorani, G.P., Palanisamy, S., Selvam, S., Ramanathan, G., Ravikumar, S., Barabadi, H., Prabu, H.G., Jeyakanthan, J. and Saravanan, M. (2019). Evaluation of

Antibacterial and Anticancer Potential of Polyaniline-Bimetal Nanocomposites Synthesized from Chemical Reduction Method. *Journal of Cluster Science*, 30(3): 715–726.

Bressenot, A., Marchal, S., Bezdetnaya, L., Garrier, J., Guillemin, F. and Plénat, F. (2009). Assessment of Apoptosis by Immunohistochemistry to Active Caspase-3, Active Caspase-7, or Cleaved PARP in Monolayer Cells and Spheroid and Subcutaneous Xenografts of Human Carcinoma. *Journal of Histochemistry & Cytochemistry*, 57(4): 289–300.

Chang, D., Lim, M., Goos, J.A.C.M., Davis, T.P. and Kavallaris, M. (2018). Biologically Targeted Magnetic Hyperthermia: Potential and Limitations. *Frontiers in Pharmacology*, 9: 831.

Chaturvedi, V.K., Yadav, N., Rai, N.K., Bohara, R.A., Rai, S.N., Aleya, L. and Singh, M.P. (2021). Two birds with one stone: oyster mushroom mediated bimetallic Au-Pt nanoparticles for agro-waste management and anticancer activity. *Environmental Science and Pollution Research International*, 28(11): 13761–13775.

Chu, C. and Su, Z. (2014). Facile synthesis of AuPt alloy nanoparticles in polyelectrolyte multilayers with enhanced catalytic activity for reduction of 4-nitrophenol. *Langmuir: the ACS journal of surfaces and colloids*, 30(50): 15345–15350.

Cohen, G., Burks, S.R. and Frank, J.A. (2018). Chlorotoxin-A Multimodal Imaging Platform for Targeting Glioma Tumors. *Toxins*, 10(12): E496.

Corr, S.J. and Curley, S.A. (2017). Chapter 1 - Gold nanoparticles for noninvasive radiofrequency cancer hyperthermia', in Mathur, A.B. (ed.). *Nanotechnology in Cancer*. William Andrew Publishing (Micro and Nano Technologies), 1–18.

Dardevet, L., Rani, D., Abd El Aziz, T., Bazin, I., Sabatier, J.-M., Fadl, M., Brambilla, E. and De Waard, M. (2015). Chlorotoxin: A Helpful Natural Scorpion Peptide to Diagnose Glioma and Fight Tumor Invasion. *Toxins*, 7(4): 1079–1101.

Depciuch, J., Stec, M., Klebowski, B., Baran, J. and Parlinska-Wojtan, M. (2019). Platinum–gold nanoraspberries as effective photosensitizer in anticancer photothermal therapy. *Journal of Nanobiotechnology*, 17(1): 107.

Deshane, J., Garner, C.C. and Sontheimer, H. (2003). Chlorotoxin Inhibits Glioma Cell Invasion via Matrix Metalloproteinase-2. *Journal of Biological Chemistry*, 278(6): 4135–4144.

Fathima, R. and Mujeeb, A. (2021). Enhanced nonlinear and thermo optical properties of laser synthesized surfactant-free Au-Pt bimetallic nanoparticles. *Journal of Molecular Liquids*, 343: 117711.

Fu, G., Ding, L., Chen, Y., Lin, J., Tang, Y. and Lu, T. (2014). Facile water-based synthesis and catalytic properties of platinum–gold alloy nanocubes. *CrystEngComm*, 16(9): 1606–1610.

Gongalsky, M., Gvindzhiliia, G., Tamarov, K., Shalygina, O., Pavlikov, A., Solovyev, V., Kudryavtsev, A., Sivakov, V. and Osminkina, L.A. (2019). Radiofrequency Hyperthermia of Cancer Cells Enhanced by Silicic Acid Ions Released During the Biodegradation of Porous Silicon Nanowires. *ACS Omega*, 4(6): 10662–10669.

Gurunathan, S., Jeyaraj, M., Kang, M.-H. and Kim, J.-H. (2020). Anticancer Properties of Platinum Nanoparticles and Retinoic Acid: Combination Therapy for the Treatment of Human Neuroblastoma Cancer. *International Journal of Molecular Sciences*, 21(18): E6792.

Kesavan, K., Ratliff, J., Johnson, E.W., Dahlberg, W., Asara, J.M., Misra, P., Frangioni, J.V. and Jacoby, D.B. (2010). Annexin A2 is a molecular target for TM601, a peptide with tumor-targeting and anti-angiogenic effects. *The Journal of Biological Chemistry*, 285(7): 4366–4374.

Khanyile, S., Masamba, P., Oyinloye, B.E., Mbatha, L.S., Kappo, A.P. and Khanyile, S. (2019). Current Biochemical Applications and Future Prospects of Chlorotoxin in Cancer Diagnostics and Therapeutics. *Advanced Pharmaceutical Bulletin*, 9(4): 510–520.

Kutwin, M., Sawosz, E., Jaworski, S., Hinzmann, M., Wierzbicki, M., Hotowy, A., Grodzik, M., Winnicka, A. and Chwalibog, A. (2017). Investigation of platinum nanoparticle properties against U87 glioblastoma multiforme. *Archives of medical science: AMS*, 13(6): 1322–1334.

Li, L., Guo, X., Peng, X., Zhang, H., Liu, Y., Li, H., He, X., Shi, D., Xiong, B., Zhao, Y., Zheng, C. and Yang, X. (2020). Radiofrequency-responsive dual-valent gold nanoclusters for enhancing synergistic therapy of tumor ablation and artery embolization. *Nano Today*, 35: 100934.

Liu, X., Zhang, X., Zhu, M., Lin, G., Liu, J., Zhou, Z., Tian, X. and Pan, Y. (2017). PEGylated Au@Pt Nanodendrites as Novel Theranostic Agents for Computed Tomography Imaging and Photothermal/Radiation Synergistic Therapy. *ACS Applied Materials & Interfaces*, 9(1): 279–285.

Loan, T.T., Do, L.T. and Yoo, H. (2018). Platinum Nanoparticles Induce Apoptosis on Raw 264.7 Macrophage Cells. *Journal of Nanoscience and Nanotechnology*, 18(2): 861–864.

Locatelli, E., Bost, W., Fournelle, M., Llop, J., Gil, L., Arena, F., Lorusso, V. and Comes Franchini, M. (2014a). Targeted polymeric nanoparticles containing gold nanorods: a therapeutic approach against glioblastoma. *Journal of Nanoparticle Research*, 16(3): 2304

Lu, Y., Yuan, J., Polzer, F., Drechsler, M. and Preussner, J. (2010). In situ growth of catalytic active Au-Pt bimetallic nanorods in thermoresponsive core-shell microgels. *ACS nano*, 4(12): 7078–7086.

Lyons, S.A., O'Neal, J. and Sontheimer, H. (2002). Chlorotoxin, a scorpion-derived peptide, specifically binds to gliomas and tumors of neuroectodermal origin. *Glia*, 39(2): 162–173.

Maji, T., Banerjee, S., Biswas, M. and Mandal, T.K. (2014). In situ synthesis of ultra-small platinum nanoparticles using a water soluble polyphenolic polymer with high catalytic activity. *RSC Advances*, 4(93): 51745–51753.

Mocan, T., Stiufiuc, R., Popa, C., Nenu, I., Pestean, C., Nagy, A.L., Mocan, L.P., Leucuta, D.C., Hajjar, N.A. and Sparchez, Z. (2021). Percutaneous ultrasound guided PEG-coated gold nanoparticles enhanced radiofrequency ablation in liver. *Scientific Reports*, 11(1): 1316.

Nasseri, B., Yilmaz, M., Turk, M., Kocum, I.C. and Piskin, E. (2016). Antenna-type radiofrequency generator in nanoparticle-mediated hyperthermia. *RSC Advances*, 6(54): 48427–48434.

Nelissen, I., Haase, A., Anguissola, S., Rocks, L., Jacobs, A., Willems, H., Riebeling, C., Luch, A., Piret, J.-P., Toussaint, O., Trouiller, B., Lacroix, G., Gutleb, A.C., Contal, S., Diabaté, S., Weiss, C., Lozano-Fernández, T., González-Fernández, Á., Dusinska, M., Huk, A., Stone, V., Kanase, N., Nocuń, M., Stępnik, M., Meschini, S., Ammendolia, M.G., Lewinski, N., Riediker, M., Venturini, M., Benetti, F., Topinka, J., Brzicova, T., Milani, S., Rädler, J., Salvati, A. and Dawson, K.A. (2020). Improving Quality in Nanoparticle-Induced Cytotoxicity Testing by a Tiered Inter-Laboratory Comparison Study. *Nanomaterials (Basel, Switzerland)*, 10(8): E1430.

Pandey, A., Singh, K., Subramanian, S., Korde, A., Singh, R. and Sawant, K. (2020). Heterogeneous surface architectured pH responsive Metal-Drug Nano-conjugates for mitochondria targeted therapy of Glioblastomas: A multimodal intranasal approach. *Chemical Engineering Journal*, 394: 124419.

Peng, Y., Wu, X., Qiu, L., Liu, C., Wang, S. and Yan, F. (2013). Synthesis of carbon–PtAu nanoparticle hybrids originating from triethoxysilane-derivatized ionic liquids for methanol electrooxidation and the catalytic reduction of 4-nitrophenol. *Journal of Materials Chemistry A*, 1(32): 9257–9263.

Petkar, D.R., Kadu, B.S. and Chikate, R.C. (2014). Highly efficient and chemoselective transfer hydrogenation of nitroarenes at room temperature over magnetically separable Fe–Ni bimetallic nanoparticles. *RSC Advances*, 4(16): 8004–8010.

Qin, C., He, B., Dai, W., Lin, Z., Zhang, H., Wang, X., Wang, J., Zhang, X., Wang, G., Yin, L. and Zhang, Q. (2014). The impact of a chlorotoxin-modified liposome system on receptor MMP-2 and the receptor-associated protein ClC-3. *Biomaterials*, 35(22): 5908–5920

Seoudi, R. and Al-Marhaby, F.A. (2016). Synthesis, Characterization and Photocatalytic Application of Different Sizes of Gold Nanoparticles on 4-Nitrophenol. *World Journal of Nano Science and Engineering*, 06(03): 120.

Seoudi, R. and Said, D.A. (2011). Studies on the Effect of the Capping Materials on the Spherical Gold Nanoparticles Catalytic Activity. *World Journal of Nano Science and Engineering*, 1(2): 51–61.

Sharma, G., Braga, C.B., Chen, K.-E., Jia, X., Ramanujam, V., Collins, B.M., Rittner, R. and Mobli, M. (2021). Structural basis for the binding of the cancer targeting scorpion toxin, ClTx, to the vascular endothelia growth factor receptor neuropilin-1. *Current Research in Structural Biology*, 3: 179–186.

Shin, S.-S., Noh, D.-H., Hwang, B., Lee, J.-W., Park, S.L., Park, S.-S., Moon, B., Kim, W.-J. and Moon, S.-K. (2018). Inhibitory effect of Au@Pt-NSs on proliferation, migration, and invasion of EJ bladder carcinoma cells: involvement of cell cycle regulators, signaling pathways, and transcription factor-mediated MMP-9 expression. *International Journal of Nanomedicine*, 13: 3295–3310.

Smith, V. and Foster, J. (2018). High-Risk Neuroblastoma Treatment Review. *Children*, 5(9): 114.

Song, Y., Qu, Z., Li, J., Shi, L., Zhao, W., Wang, H., Sun, T., Jia, T. and Sun, Y. (2021). Fabrication of the biomimetic DOX/Au@Pt nanoparticles hybrid nanostructures for the

combinational chemo/photothermal cancer therapy. *Journal of Alloys and Compounds*, 881: 160592.

Song, Y., Shi, Q., Zhu, C., Luo, Y., Lu, Q., Li, H., Ye, R., Du, D. and Lin, Y. (2017). Mitochondrial Reactive Oxygen Species Burst for Cancer Therapy Triggered by Near-Infrared Light. *Nanoscale*, 2017.

Soroceanu, L., Gillespie, Y., Khazaeli, M.B. and Sontheimer, H. (1998). Use of chlorotoxin for targeting of primary brain tumors. *Cancer Research*, 58(21): 4871–4879.

Tang, J., Jiang, X., Wang, L., Zhang, H., Hu, Z., Liu, Y., Wu, X. and Chen, C. (2014). Au@Pt nanostructures: a novel photothermal conversion agent for cancer therapy. *Nanoscale*, 6(7): 3670–3678.

Wang, K., Kievit, F.M., Chiarelli, P.A., Stephen, Z.R., Lin, G., Silber, J.R., Ellenbogen, R.G. and Zhan, M. (2021). siRNA Nanoparticle Suppresses Drug-Resistant Gene and Prolongs Survival in an Orthotopic Glioblastoma Xenograft Mouse Model. *Advanced Functional Materials*, 31(6): 2007166.

Yahya, A.A., Rashid, K.T., Ghadhban, M.Y., Mousa, N.E., Majdi, H.S., Salih, I.K. and Alsalhy, Q.F. (2021). Removal of 4-Nitrophenol from Aqueous Solution by Using Polyphenylsulfone-Based Blend Membranes: Characterization and Performance. *Membranes*, 11(3): 171.

Yang, Q., Peng, J., Xiao, Y., Li, W., Tan, L., Xu, X. and Qian, Z. (2018). Porous Au@Pt Nanoparticles: Therapeutic Platform for Tumor Chemo-Photothermal Co-Therapy and Alleviating Doxorubicin-Induced Oxidative Damage. *ACS Applied Materials & Interfaces*, 10(1): 150–164.

Zhang, J., Chen, G., Guay, D., Chaker, M. and Ma, D. (2014). Highly active PtAu alloy nanoparticle catalysts for the reduction of 4-nitrophenol. *Nanoscale*, 6(4): 2125–2130.